

*Midwest State's Regional Pooled Fund Research Program
Fiscal Years 1996-1997 (Year 7) and 1997-1998 (Year 8)
Research Project Number SPR-3(017)*

PHASE III DEVELOPMENT OF A BULLNOSE GUARDRAIL SYSTEM FOR MEDIAN APPLICATIONS

Submitted by

Bob W. Bielenberg, M.S.M.E., E.I.T.
Research Associate Engineer

John D. Reid, Ph.D.
Associate Professor

Ronald K. Faller, Ph.D., P.E.
Research Assistant Professor

John R. Rohde, Ph.D., P.E.
Associate Professor

Dean L. Sicking, Ph.D., P.E.
Associate Professor and MwRSF Director

Eric A. Keller, B.S.M.E., E.I.T.
Research Associate Engineer

James C. Holloway, M.S.C.E., E.I.T.
Research Associate Engineer

Lora Supencheck
Undergraduate Assistant

MIDWEST ROADSIDE SAFETY FACILITY

University of Nebraska-Lincoln
1901 "Y" Street, Building "C"
Lincoln, Nebraska 68588-0601
(402) 472-6864

Submitted to

MIDWEST STATE'S REGIONAL POOLED FUND PROGRAM

Nebraska Department of Roads
1500 Nebraska Highway 2
Lincoln, Nebraska 68502

MwRSF Research Report No. TRP-03-95-00

June 1, 2000

Technical Report Documentation Page

1. Report No. SPR-3(017)	2.	3. Recipient's Accession No.	
4. Title and Subtitle Phase II Development of a Bullnose Guardrail System for Median Applications		5. Report Date June 1, 2000	
		6.	
7. Author(s) Bielenberg, B.W., Reid, J.D., Faller, R.K., Rohde, J.R., Sicking, D.L., Keller, E.A., Holloway, J.C., and Supencheck, L. L.		8. Performing Organization Report No. TRP-03-95-00	
9. Performing Organization Name and Address Midwest Roadside Safety Facility (MwRSF) University of Nebraska-Lincoln 1901 Y St., Bldg. C Lincoln, NE 68588-0601		10. Project/Task/Work Unit No.	
		11. Contract © or Grant (G) No. SPR-3(017)	
12. Sponsoring Organization Name and Address Midwest States Regional Pooled Fund Program Nebraska Department of Roads 1500 Nebraska Highway 2 Lincoln, Nebraska 68502		13. Type of Report and Period Covered Final Report 1997-1999	
		14. Sponsoring Agency Code	
15. Supplementary Notes Prepared in cooperation with U.S. Department of Transportation, Federal Highway Administration			
16. Abstract (Limit: 200 words) <p>The research study consisted of Phase III of the development and full-scale vehicle crash testing of a bullnose barrier concept for the treatment of median hazards. The bullnose guardrail consisted of a 12-gauge thrie beam rail supported by twenty-two wood posts, eleven posts on each side of the system. Horizontal slots were cut in the valleys of selected thrie beam sections to aid in vehicle capture as well as to reduce the buckling and bending capacities of the rail.</p> <p>Five full-scale crash tests were performed, using both a 2000-kg pickup truck and a 820-kg small car. The first crash test, consisting of a 2000-kg pickup truck impacting at a speed of 103.0 km/h and an angle of 13.4 degrees, was successful. The results of that test led to the system being redefined as a non-gating rather than a gating terminal. The second and third tests of the series were unsuccessful tests of an impact of a 2000-kg pickup truck on the critical impact point at an angle of 20 degrees and a speed of 100 km/h. The failure of both of these tests was due to a combination of a lack of lateral stiffness and guardrail tension that led to vaulting of the vehicle. Computer simulation was used to investigate the failed tests and aid in making design changes. Analysis of the simulation and full-scale test results led to the addition of six new posts to the system as well as the use of double, tapered blockouts. LS-DYNA computer simulation modeling of the modified design demonstrated successful containment of the pickup truck. The fourth test, impacting at a speed of 99.8 km/h and an angle of 22.3 degrees on the critical impact point was determined to be successful according to the safety standards set forth by the Test Level 3 (TL-3) evaluation criteria described in the NCHRP Report No. 350, <i>Recommended Procedures for the Safety Performance Evaluation of Highway Features</i>. A final test, impacting the nose of the barrier at 105.0 km/h and an angle of 15.7 degrees, was also judged successful. Based on the performance of the system under these NCHRP Report No. 350 tests as well as those previously reported, it is recommended that the bullnose barrier be approved for use on federal highway systems. Recommendations for the application of the new design were also provided.</p>			
17. Document Analysis/Descriptors Highway Safety, Guardrail Longitudinal Barrier, Bullnose Barrier, Median Protection		18. Availability Statement No restrictions. Document available from: National Technical Information Services, Springfield, Virginia 22161	
19. Security Class (this report) Unclassified	20. Security Class (this page) Unclassified	21. No. of Pages 240	22. Price

DISCLAIMER STATEMENT

The contents of this report reflect the views of the authors who are responsible for the facts and the accuracy of the data presented herein. The contents do not necessarily reflect the official views or policies of the state highway departments participating in the Midwest State's Regional Pooled Fund Program nor the Federal Highway Administration. This report does not constitute a standard, specification, or regulation.

ACKNOWLEDGMENTS

The authors wish to acknowledge the following organizations that made this project possible:

(1) the Midwest States Regional Pooled Fund Program funded by the Iowa Department of Transportation, Kansas Department of Transportation, Minnesota Department of Transportation, Missouri Department of Transportation, Nebraska Department of Roads, Ohio Department of Transportation, South Dakota Department of Transportation, and Wisconsin Department of Transportation for sponsoring this project; (2) MwRSF personnel for constructing the barriers and conducting the crash tests; (4) Center for Infrastructure Research, Engineering Research Center, for matching support; (5) the Federal Highway Administration for matching support; (6) Daniel Mushett, Highway Timber Products Co. - a division of Cox Industries, for donating timber posts and blockouts; and (7) Martin Snow and Jim Fowers of Universal Industrial Sales for donating the slotted sections of thrie beam rail.

A special thanks is also given to the following individuals who made a contribution to the completion of this research project.

Midwest Roadside Safety Facility

Kenneth L. Krenk, Field Operations Manager
Mike Hanau, Laboratory Mechanic I
Ken Addink, Field Technician
David McBride, Laboratory Mechanic I
Undergraduate and Graduate Assistants

Iowa Department of Transportation

David Little, P.E., Deputy Director, Engineering Division
Jay Chiglo, P.E., Design Methods Engineer

Missouri Department of Transportation

Vince Imhoff, P.E., Contract Administration Engineer
Tom Allen, P.E., Research and Development Engineer

Nebraska Department of Roads

Leona Kolbet, Research Coordinator
Ken Sieckmeyer, Transportation Planning Manager
Phil TenHulzen, P.E., Design Standards Engineer

Kansas Department of Transportation

Ron Seitz, P.E., Road Design Squad Leader

Minnesota Department of Transportation

Ron Cassellius, Research Program Coordinator

Ohio Department of Transportation

Monique Evans, P.E., Roadway Standards Engineer

South Dakota Department of Transportation

David Huft, Research Engineer

Wisconsin Department of Transportation

Rory Rhinesmith, P.E., Chief Roadway Development Engineer
Peter Amakobe, Standards Development Engineer

Federal Highway Administration

Martin Hargrave, P.E., Research Engineer

Dunlap Photography

James Dunlap, President and Owner

Universal Industrial Sales

Martin Snow, President
Jim Fowers

TABLE OF CONTENTS

	Page
TECHNICAL DOCUMENTATION PAGE	i
DISCLAIMER STATEMENT	ii
ACKNOWLEDGMENTS	iii
TABLE OF CONTENTS	v
List of Figures	viii
List of Tables	xii
1 INTRODUCTION	1
2 BARRIER DESIGN	7
2.1 Phase II Barrier Design	7
2.2 Nose Section Design	7
2.3 Barrier Design Details	7
3 TEST REQUIREMENTS AND PERFORMANCE EVALUATION CRITERIA	20
3.1 Test Requirements	20
3.2 Evaluation Criteria	22
4 TEST CONDITIONS	24
4.1 Test Facility	24
4.2 Vehicle Tow and Guidance System	24
4.3 Test Vehicles	24
4.4 Data Acquisition Systems	36
4.4.1 Accelerometers	36
4.4.2 Rate Transducers	36
4.4.3 High Speed Photography	37
4.4.4 Pressure Tape Switches	42
5 CRASH TEST MBN-5	45
5.1 Test MBN-5	45
5.2 Test Description	45
5.3 Vehicle Damage	46
5.4 Barrier Damage	47
5.5 Occupant Risk Values	47
5.6 Discussion	48

6 REVISED TEST REQUIREMENTS AND PERFORMANCE EVALUATION CRITERIA .	60
6.1 Test Requirements	60
6.2 Evaluation Criteria	61
7 CRASH TEST MBN-6	64
7.1 Test MBN-6	64
7.2 Test Description	64
7.3 Vehicle Damage	65
7.4 Barrier Damage	65
7.5 Occupant Risk Values	66
7.6 Discussion	66
8 BARRIER MODIFICATIONS (DESIGN FOR MBN-7)	78
8.1 Modification of Bullnose Design	78
9 CRASH TEST MBN-7	82
9.1 Test MBN-7	82
9.2 Test Description	82
9.3 Vehicle Damage	83
9.4 Barrier Damage	83
9.5 Occupant Risk Values	84
9.6 Discussion	85
10 COMPUTER SIMULATION	96
10.1 Introduction	96
10.2 Transition from Frontal to CIP	96
10.3 MBN-6 Simulation and Analysis	96
10.4 Design Modifications	98
10.5 Final Design Simulation	98
11 BARRIER MODIFICATIONS (DESIGN FOR MBN-8)	106
11.1 Modification of Bullnose Design	106
12 CRASH TEST MBN-8	111
12.1 Test MBN-8	111
12.2 Test Description	111
12.3 Vehicle Damage	112
12.4 Barrier Damage	112
12.5 Occupant Risk Values	113
12.6 Discussion	114
13 CRASH TEST MBN-9	125
13.1 Test MBN-9	125

13.2 Test Description	125
13.3 Vehicle Damage	126
13.4 Barrier Damage	126
13.5 Occupant Risk Values	127
13.6 Discussion	127
14 SUMMARY AND CONCLUSIONS	138
15 RECOMMENDATIONS	144
16 REFERENCES	151
17 APPENDICES	154
APPENDIX A - ACCELEROMETER DATA ANALYSIS TEST MBN-5	155
APPENDIX B - ACCELEROMETER DATA ANALYSIS TEST MBN-6	163
APPENDIX C - ACCELEROMETER DATA ANALYSIS TEST MBN-7	170
APPENDIX D - ADDITIONAL COMPUTER SIMULATION DISCUSSION AND RESULTS	178
APPENDIX E - ACCELEROMETER DATA ANALYSIS TEST MBN-8	194
APPENDIX F - ACCELEROMETER DATA ANALYSIS TEST MBN-9	202
APPENDIX G - FINAL PHASE III BULLNOSE MEDIAN BARRIER DESIGN DETAILS	210
APPENDIX H - BULLNOSE MEDIAN BARRIER DESIGN NO. 2 DETAILS	227
APPENDIX I - BULLNOSE MEDIAN BARRIER DESIGN NO. 3 DETAILS	234

LIST OF FIGURES

	Page
Figure 1. Final Phase II Bullnose Median Barrier Design	6
Figure 2. Bullnose Barrier Design Layout	8
Figure 3. Modified Ground line Strut	10
Figure 4. Layout of Bullnose Rails No. 1 and 2	12
Figure 5. Rail Section No. 1 Detail	13
Figure 6. Rail Section No. 2 Detail	14
Figure 7. Rail Section No. 3 Detail	15
Figure 8. Cable Detail and Cable Plate	17
Figure 9. Bullnose Barrier Design, Test MBN-5	18
Figure 10. Bullnose Barrier Design, Test MBN-5	19
Figure 11. Proposed Full Scale Crash Tests for Bullnose Barrier Evaluation	21
Figure 12. Vehicle Dimensions, Test MBN-5	25
Figure 13. Vehicle Dimensions, Test MBN-6	27
Figure 14. Vehicle Dimensions, Test MBN-7	28
Figure 15. Vehicle Dimensions, Test MBN-8	29
Figure 16. Vehicle Dimensions, Test MBN-9	30
Figure 17. Vehicle Target Locations, Test MBN-5	31
Figure 18. Vehicle Target Locations, Test MBN-6	32
Figure 19. Vehicle Target Locations, Test MBN-7	33
Figure 20. Vehicle Target Locations, Test MBN-8	34
Figure 21. Vehicle Target Locations, Test MBN-9	35
Figure 22. Location of High-Speed Cameras, Test MBN-5	38
Figure 23. Location of High-Speed Cameras, Test MBN-6	40
Figure 24. Location of High-Speed Cameras, Test MBN-7	41
Figure 25. Location of High-Speed Cameras, Test MBN-8	43
Figure 26. Location of High-Speed Cameras, Test MBN-9	44
Figure 27. Impact Location, Test MBN-5	50
Figure 28. Summary and Sequential Photos, Test MBN-5	51
Figure 29. Additional Sequential Photographs, Test MBN-5	52
Figure 30. Full-Scale Crash Test MBN-5	53
Figure 31. Full-Scale Crash Test MBN-5	54
Figure 32. Vehicle Trajectory, MBN-5	55
Figure 33. Vehicle Damage, Test MBN-5	56
Figure 34. Barrier Damage, Test MBN-5	57
Figure 35. Barrier Damage, Test MBN-5	58
Figure 36. Barrier Damage, Test MBN-5	59
Figure 37. NCHRP 350 Test Matrix for a Non-Gating System	62
Figure 38. Impact Location, Test MBN-6	68
Figure 39. Summary and Sequential Photographs, Test MBN-6	69

Figure 40. Additional Sequential Photographs, Test MBN-6	70
Figure 41. Full-Scale Crash Test, Test MBN-6	71
Figure 42. Full-Scale Crash Test, Test MBN-6	72
Figure 43. Vehicle Trajectory, Test MBN-6	73
Figure 44. Vehicle Damage, Test MBN-6	74
Figure 45. Barrier Damage, Test MBN-6	75
Figure 46. Barrier Damage, Test MBN-6	76
Figure 47. Barrier Damage, Test MBN-6	77
Figure 48. Bullnose Barrier Design, Test MBN-7	79
Figure 49. Modified Rail Section No. 3, Test MBN-7	80
Figure 50. Bullnose Design, Test MBN-7	81
Figure 51. Impact Location, Test MBN-7	87
Figure 52. Summary and Sequential Photographs, Test MBN-7	88
Figure 53. Additional Sequential Photographs, Test MBN-7	89
Figure 54. Full-Scale Crash Test, Test MBN-7	90
Figure 55. Vehicle Trajectory, Test MBN-7	91
Figure 56. Vehicle Damage, Test MBN-7	92
Figure 57. Barrier Damage, Test MBN-7	93
Figure 58. Barrier Damage, Test MBN-7	94
Figure 59. Barrier Damage, Test MBN-7	95
Figure 60. MBN-6 Simulation	97
Figure 61. Ground Strut Influences Tire Behavior	99
Figure 62. MBN-6 Top View - Test and Simulation	100
Figure 63. No Strut Simulation - Rail Does Not Roll Over	101
Figure 64. Chamfered Blockout Allows Rail to Wrap Around Tire	102
Figure 65. Double Blockout Reduces Tire Snag	103
Figure 66. Model of Modified Design for Test MBN-8	104
Figure 67. Modified Design Indicates Capture of Vehicle	105
Figure 68. Bullnose Barrier Design, Test MBN-8	107
Figure 69. Bullnose Design, Test MBN-8	108
Figure 70. Bullnose Design, Test MBN-8	109
Figure 71. Impact Location, Test MBN-8	115
Figure 72. Summary and Sequential Photos, Test MBN-8	116
Figure 73. Additional Sequential Photographs, Test MBN-8	117
Figure 74. Full-Scale Crash Test MBN-8	118
Figure 75. Full-Scale Crash Test MBN-8	119
Figure 76. Vehicle Trajectory, MBN-8	120
Figure 77. Vehicle Damage, Test MBN-8	121
Figure 78. Barrier Damage, Test MBN-8	122
Figure 79. Barrier Damage, Test MBN-8	123
Figure 80. Barrier Damage, Test MBN-8	124
Figure 81. Impact Location, Test MBN-9	129
Figure 82. Summary and Sequential Photos, Test MBN-9	130

Figure 83. Additional Sequential Photographs, Test MBN-9	131
Figure 84. Full-Scale Crash Test, Test MBN-9	132
Figure 85. Full-Scale Crash Test, Test MBN-9	133
Figure 86. Vehicle Trajectory, Test MBN-9	134
Figure 87. Vehicle Damage, Test MBN-9	135
Figure 88. Barrier Damage, Test MBN-9	136
Figure 89. Barrier Damage, Test MBN-9	137
Figure 90. Typical Bullnose Installation for Protection of Median Hazards	146
Figure 91. Schematic of Double Bridge Rail Installation	149
Figure A-1. Graph of Longitudinal Deceleration - Filtered Data, Test MBN-5	156
Figure A-2. Graph of Longitudinal Occupant Impact Velocity - Filtered Data, Test MBN-5 ..	157
Figure A-3. Graph of Longitudinal Occupant Displacement - Filtered Data, Test MBN-5 ...	158
Figure A-4. Graph of Lateral Deceleration - Filtered Data, Test MBN-5	159
Figure A-5. Graph of Lateral Occupant Impact Velocity - Filtered Data, Test MBN-5	160
Figure A-6. Graph of Lateral Occupant Displacement - Filtered Data, Test MBN-5	161
Figure A-7. Rate Transducer Data, Test MBN-5	162
Figure B-1. Graph of Longitudinal Deceleration - Filtered Data, Test MBN-6	164
Figure B-2. Graph of Longitudinal Occupant Impact Velocity - Filtered Data, Test MBN-6 ..	165
Figure B-3. Graph of Longitudinal Occupant Displacement - Filtered Data, Test MBN-6 ...	166
Figure B-4. Graph of Lateral Deceleration - Filtered Data, Test MBN-6	167
Figure B-5. Graph of Lateral Occupant Impact Velocity - Filtered Data, Test MBN-6	168
Figure B-6. Graph of Lateral Occupant Displacement - Filtered Data, Test MBN-6	169
Figure C-1. Graph of Longitudinal Deceleration - Filtered Data, Test MBN-7	171
Figure C-2. Graph of Longitudinal Occupant Impact Velocity - Filtered Data, Test MBN-7 ..	172
Figure C-3. Graph of Longitudinal Occupant Displacement - Filtered Data, Test MBN-7 ...	173
Figure C-4. Graph of Lateral Deceleration - Filtered Data, Test MBN-7	174
Figure C-5. Graph of Lateral Occupant Impact Velocity - Filtered Data, Test MBN-7	175
Figure C-6. Graph of Lateral Occupant Displacement - Filtered Data, Test MBN-7	176
Figure C-7. Rate Transducer Data, Test MBN-7	177
Figure E-1. Graph of Longitudinal Deceleration - Filtered Data, Test MBN-8	195
Figure E-2. Graph of Longitudinal Occupant Impact Velocity - Filtered Data, Test MBN-8 ..	196
Figure E-3. Graph of Longitudinal Occupant Displacement - Filtered Data, Test MBN-8 ...	197
Figure E-4. Graph of Lateral Deceleration - Filtered Data, Test MBN-8	198
Figure E-5. Graph of Lateral Occupant Impact Velocity - Filtered Data, Test MBN-8	199
Figure E-6. Graph of Lateral Occupant Displacement - Filtered Data, Test MBN-8	200
Figure E-7. Rate Transducer Data, Test MBN-8	201
Figure F-1. Graph of Longitudinal Deceleration - Filtered Data, Test MBN-9	203
Figure F-2. Graph of Longitudinal Occupant Impact Velocity - Filtered Data, Test MBN-9 ..	204
Figure F-3. Graph of Longitudinal Occupant Displacement - Filtered Data, Test MBN-9 ...	205
Figure F-4. Graph of Lateral Deceleration - Filtered Data, Test MBN-9	206
Figure F-5. Graph of Lateral Occupant Impact Velocity - Filtered Data, Test MBN-9	207
Figure F-6. Graph of Lateral Occupant Displacement - Filtered Data, Test MBN	208
Figure F-7. Rate Transducer Data, Test MBN-9	209

Figure G-1. Final Bullnose Barrier Design	211
Figure G-2. Layout of Bullnose Rails No. 1 and 2	212
Figure G-3. Rail Section No. 1 Detail	213
Figure G-4. Rail Section No. 2 Detail	214
Figure G-5. Rail Section No. 3 Detail	215
Figure G-6. Post Details	216
Figure G-7. Bullnose Cable Assembly	217
Figure G-8. Cable Detail and Cable Plate	218
Figure G-9. Final Bullnose Barrier Design , English Units	219
Figure G-10. Layout of Bullnose Rails No. 1 and 2, English Units	220
Figure G-11. Rail Section No. 1 Detail, English Units	221
Figure G-12. Rail Section No. 2 Detail, English Units	222
Figure G-13. Rail Section No. 3 Detail, English Units	223
Figure G-14. Post Details, English Units Bullnose Cable Assembly, English Units	224
Figure G-15. Bullnose Cable Assembly, English Units	225
Figure G-16. Cable Detail and Cable Plate, English Units	226
Figure H-1. Bullnose Design No. 2	228
Figure H-2. Rail Section No. 1, Bullnose Design No. 2	229
Figure H-3. Nose Cable, Bullnose Design No. 2	230
Figure H-4. Bullnose Design No. 2, English Units	231
Figure H-5. Rail Section No. 1, Bullnose Design No. 2, English Units	232
Figure H-6. Nose Cable, Bullnose Design No. 2, English Units	233
Figure I-1. Bullnose Design No. 3	235
Figure I-2. Rail Section No. 1, Bullnose Design No. 3	236
Figure I-3. Nose Cable, Bullnose Design No. 3	237
Figure I-4. Bullnose Design No. 3, English Units	238
Figure I-5. Rail Section No. 1, Bullnose Design No. 3, English Units	239
Figure I-6. Nose Cable, Bullnose Design No. 3, English Units	240

LIST OF TABLES

	Page
Table 1. Summary of Safety Performance Evaluation for Tests MBN-1 and MBN-2 (Phase I)	3
Table 2. Summary of Safety Performance Evaluation for Tests MBN-3 and MBN-4 (Phase II)	5
Table 3. NCHRP Report 350 Evaluation Criteria for 2000P Pickup Truck and 820C Small Car Tests	23
Table 4. NCHRP Report 350 Evaluation Criteria for 2000P Pickup Truck and 820C Small Car Tests	63
Table 5. Summary of Safety Performance Evaluation	139

1 INTRODUCTION

The use of the divided highway separated by a median area has been a valuable safety feature in modern roadway design. The median allows a safe recovery area for errant vehicles to come to rest without impeding upon oncoming traffic. It is possible, however, that the median is not always a safe zone for vehicle recovery. Many roadway structures are built in the median such as bridge supports, drainage structures, and large sign supports. These structures present undue hazards to errant vehicles traveling in the median area.

The three main treatments that have been used in the protection against median hazards are crash cushions, open guardrails, and closed guardrail envelopes. Bridge piers are often treated by surrounding them with rigid barriers and placing crash cushions on each end. This alternative is very short and therefore reduces the number of run-off-road accidents to a minimum. Unfortunately, this type of treatment is very costly and therefore is hard to justify for most median situations. Another popular treatment involves using open guardrail envelopes. This design incorporates long runs of guardrail upstream from the hazards. Although this alternative is less expensive than crash cushion designs, the long runs of guardrail generate many guardrail related accidents, and when used in narrow medians, the backside of the guardrails can become a major hazard. Enclosed guardrail envelopes, commonly called bullnose systems, involve wrapping a semi-rigid guardrail system completely around the hazards. These designs are smaller and therefore generate fewer guardrail accidents. Further, bullnose designs are generally the least costly alternatives. Unfortunately, bullnose guardrail designs have never met current safety standards. This report describes the continued effort to develop a new bullnose guardrail design that will meet modern safety standards.

The objective of this research project was to continue development and evaluation of a

bullnose guardrail system that meets the Test Level 3 (TL-3) safety performance criteria provided in National Cooperative Highway Research Program (NCHRP) Report No. 350, *Recommended Procedures for the Safety Performance Evaluation of Highway Features* (1). Phases I and II of the design process were covered in previous reports (2,3). Phase I included two full-scale crash tests which provided information for redesign and computer simulation of the bullnose barrier system. The initial design concept from Phase I was subjected to two full-scale crash tests, tests MBN-1 and MBN-2. Test MBN-1 was a head-on impact involving a 2000-kg pickup truck, while test MBN-2 was a one-quarter offset, head-on impact using an 820-kg small car. The results of those tests are shown in Table 1. Although only one of the two tests was successful, these tests demonstrated that the bullnose barrier concept had potential but required further development to meet the impact safety standards.

Phase II of the bullnose barrier system design consisted of the continued development of the bullnose barrier through computer simulation and testing to meet the NCHRP Report No. 350 requirements for test 3-31, a head-on impact of a 2000-kg pickup truck. Two full-scale tests, test MBN-3 and MBN-4, were performed for a head-on impact of a 2000-kg pickup truck with the bullnose at a target speed and angle of 100 km/h and 0 degrees, respectively. Test MBN-3 failed due to fracture of the guardrail. A successful computer simulation model of test MBN-3 was created in LS-DYNA and was used to investigate the failure in greater detail. Results of the simulation paired with other information led to the bullnose design being changed by the addition of a pair of steel cables behind the nose section to contain the impact vehicle. The modified bullnose design was then simulated in LS-DYNA with positive results which cleared the way for a repeat of the previous failed test. Test MBN-4 was run successfully with controlled containment of the impact vehicle. The

Table 1. Summary of Safety Performance Evaluation for Tests MBN-1 and MBN-2 (Phase I)

Evaluation Factors	Evaluation Criteria	Test MBN-1	Test MBN-2						
Structural Adequacy	C. Acceptable test article performance may be by redirection, controlled penetration, or controlled stopping of the vehicle.	U	S						
Occupant Risk	D. Detached elements, fragments or other debris from the test article should not penetrate or show potential for penetrating the occupant compartment, or present an undue hazard to other traffic, pedestrians, or personnel in a work zone. Deformations of, or intrusions into, the occupant compartment that could cause serious injuries should not be permitted.	S	S						
	F. The vehicle should remain upright during and after collision although moderate roll, pitching, and yawing are acceptable.	S	S						
	H. Occupant impact velocities should satisfy the following: Occupant Impact Velocity Limits (m/s) <table border="1" style="margin-left: 20px;"> <thead> <tr> <th>Component</th> <th>Preferred</th> <th>Maximum</th> </tr> </thead> <tbody> <tr> <td>Longitudinal and Lateral</td> <td>9</td> <td>12</td> </tr> </tbody> </table>	Component	Preferred	Maximum	Longitudinal and Lateral	9	12	S	S
Component	Preferred	Maximum							
Longitudinal and Lateral	9	12							
Vehicle Trajectory	I. Occupant ride down accelerations should satisfy the following: Occupant Ride down Acceleration Limits (G's) <table border="1" style="margin-left: 20px;"> <thead> <tr> <th>Component</th> <th>Preferred</th> <th>Maximum</th> </tr> </thead> <tbody> <tr> <td>Longitudinal and Lateral</td> <td>15</td> <td>20</td> </tr> </tbody> </table>	Component	Preferred	Maximum	Longitudinal and Lateral	15	20	S	S
	Component	Preferred	Maximum						
Longitudinal and Lateral	15	20							
	K. After collision it is preferable that the vehicle's trajectory not intrude into adjacent traffic lanes.	S	S						
	N. Vehicle trajectory behind the test article is acceptable.	U	S						

S - (Satisfactory)

U - (Unsatisfactory)

results of tests MBN-3 and MBN-4 are shown in Table 2. Completion of Phase II of the bullnose project finished with test MBN-4; however, there remained a large amount of development before a successful design could be realized. The final design from Phase II is shown in Figure 1.

Phase III of the bullnose median barrier development continued the progression of the barrier design through a series of five additional full-scale crash tests and a parallel simulation effort. These full-scale crash tests followed the NCHRP Report No. 350 requirements for tests 3-32, 3-33, and 3-38. Data from all five crash tests was collected, analyzed, and documented. Conclusions and recommendations were then made with regards to the safety performance of the bullnose barrier terminal. Computer simulation of the testing using LS-DYNA was successfully used to analyze and predict the performance of the bullnose design. The following sections of this report document the Phase III development, computer simulation modeling, testing, and evaluation of the bullnose barrier terminal concept.

Table 2. Summary of Safety Performance Evaluation for Tests MBN-3 and MBN-4 (Phase II)

Evaluation Factors	Evaluation Criteria	Test MBN-3	Test MBN-4						
Structural Adequacy	C. Acceptable test article performance may be by redirection, controlled penetration, or controlled stopping of the vehicle.	U	S						
Occupant Risk	D. Detached elements, fragments or other debris from the test article should not penetrate or show potential for penetrating the occupant compartment, or present an undue hazard to other traffic, pedestrians, or personnel in a work zone. Deformations of, or intrusions into, the occupant compartment that could cause serious injuries should not be permitted.	S	S						
	F. The vehicle should remain upright during and after collision although moderate roll, pitching, and yawing are acceptable.	S	S						
	H. Occupant impact velocities should satisfy the following: Occupant Impact Velocity Limits (m/s) <table border="1" style="margin-left: 20px;"> <thead> <tr> <th>Component</th> <th>Preferred</th> <th>Maximum</th> </tr> </thead> <tbody> <tr> <td>Longitudinal and Lateral</td> <td>9</td> <td>12</td> </tr> </tbody> </table>	Component	Preferred	Maximum	Longitudinal and Lateral	9	12	S	S
Component	Preferred	Maximum							
Longitudinal and Lateral	9	12							
Vehicle Trajectory	I. Occupant ride down accelerations should satisfy the following: Occupant Ride down Acceleration Limits (G's) <table border="1" style="margin-left: 20px;"> <thead> <tr> <th>Component</th> <th>Preferred</th> <th>Maximum</th> </tr> </thead> <tbody> <tr> <td>Longitudinal and Lateral</td> <td>15</td> <td>20</td> </tr> </tbody> </table>	Component	Preferred	Maximum	Longitudinal and Lateral	15	20	S	S
	Component	Preferred	Maximum						
Longitudinal and Lateral	15	20							
	K. After collision it is preferable that the vehicle's trajectory not intrude into adjacent traffic lanes.	S	S						
	N. Vehicle trajectory behind the test article is acceptable.	U	S						

S - (Satisfactory)

U - (Unsatisfactory)

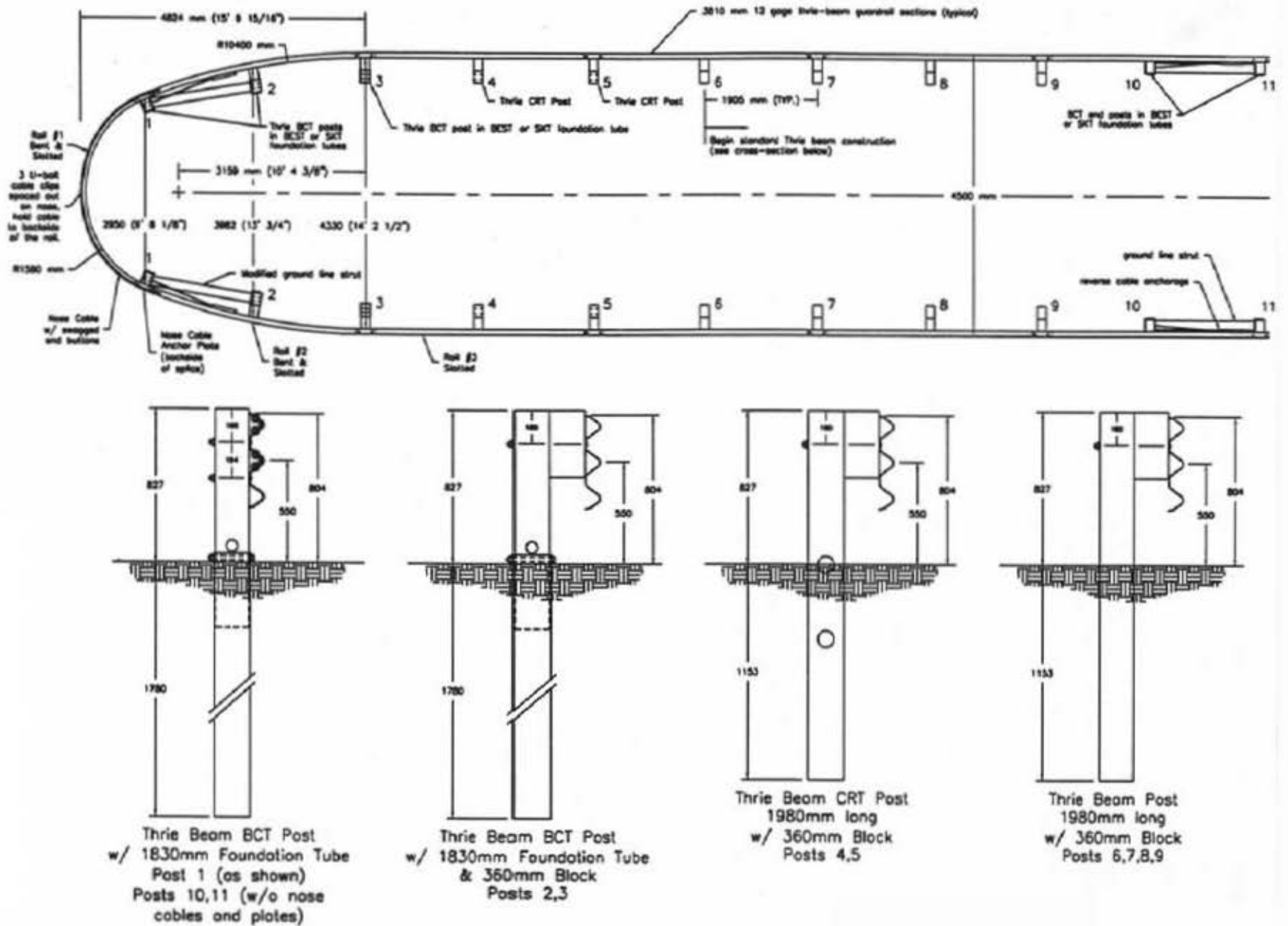


Figure 1. Final Phase II Bullnose Median Barrier Design

2 BARRIER DESIGN

2.1 Phase III Barrier Design

The design layout for test MBN-5 was unchanged from the final design developed in Phase II. A detailed discussion of the entire bullnose barrier as it was used for test MBN-5 is presented below.

2.2 Nose Section Design

After reviewing the Pooled Fund member states' bullnose standards, a 4,500-mm wide design was selected for use in the current study. The shape of the nose section was chosen after an analysis of prior bullnose (4-8) and short radius guardrail designs (9-14). The nose section was formed using one 1,580-mm radius curved section of guardrail with one 10,400-mm radius curved section attached to each end of the nose section. The overall shape was chosen using simple curves to simplify the design and fabrication of the rail. The curve radii were sized based on ease of fabrication as well as to maintain the design width of the system.

The front-end section of the bullnose barrier was designed without a post at the centerline of the nose since the end post tends to rotate back after impact, often creating a potential for the vehicle to vault over the rail. It was determined that a nose section without the centerline post would have sufficient structural strength to maintain the shape of the rail without sagging while not causing a vehicle vaulting hazard.

2.3 Barrier Design Details

The complete layout of the bullnose barrier system used for the test MBN-5 is shown in Figure 2. A one-half barrier system was designed for testing purposes to limit costs and time of construction. The bullnose barrier was 4,500-mm wide by 20,144-mm long. The bullnose system

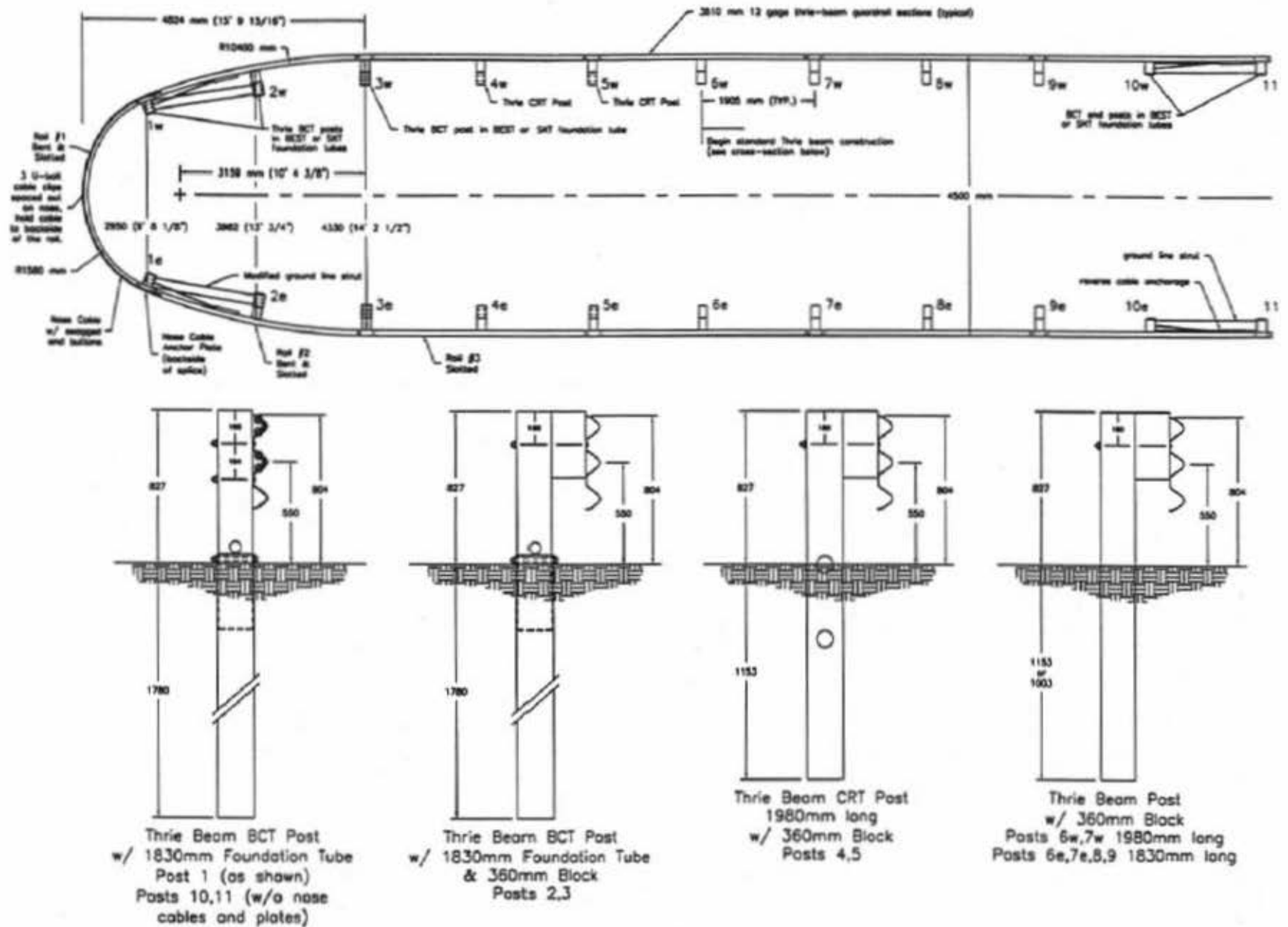
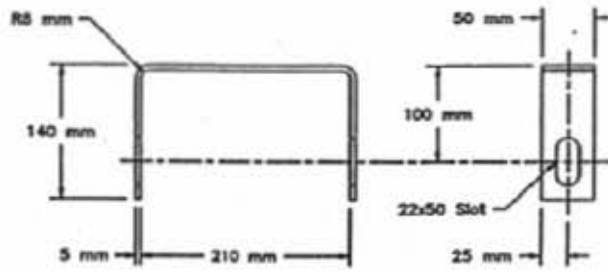


Figure 2. Bullnose Barrier Design Layout

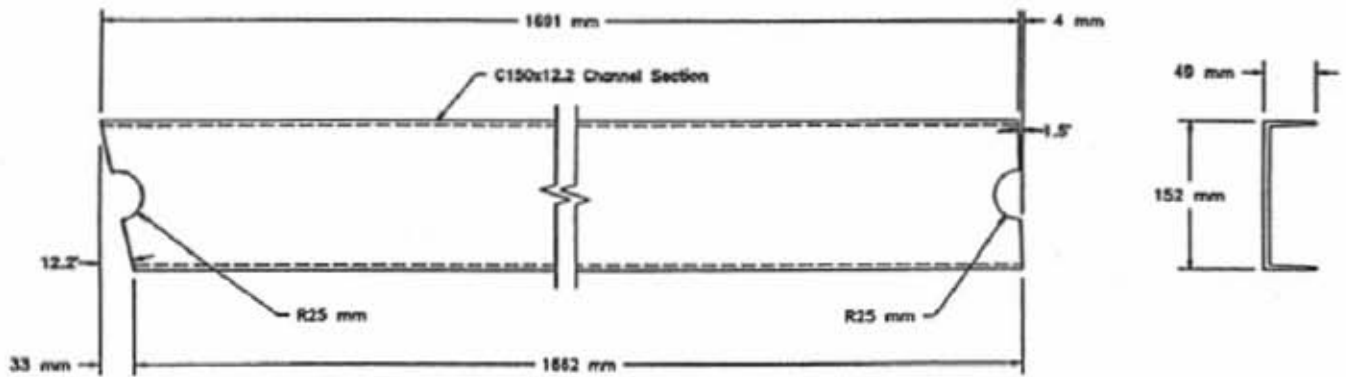
was constructed with twenty-two wood posts with eleven posts positioned on each side of the system. The first two posts on each side of the system were 140-mm wide by 190.5-mm deep by 1830-mm long Breakaway Cable Terminal (BCT) posts set in Sequential Kinking Terminal (SKT) (15) foundation tubes with soil plates and ground line channel strut. Post no. 1 on each side of the barrier used no blockout while post no. 2 on each side used a 150-mm wide by 200-mm deep by 360-mm long thrie blockout. Post no. 3 on each side of the system was a BCT post set in a SKT foundation tube without a bearing plate. Posts nos. 4 and 5 on each side of the barrier were 1980-mm long CRT posts. The next four posts along both sides of the bullnose barrier were standard 150-mm wide by 200-mm deep by 1,980-mm long wood posts spaced 1,905-mm apart, as shown in Figure 2. Each of these posts uses a 150-mm wide by 200-mm deep by 360-mm long thrie blockout to space the rail away from the post. The top mounting height of the rail was 804 mm, as measured from the ground surface. Posts nos. 3 through 9 had a soil embedment depth of 1,153 mm. The last two posts on each side of the bullnose barrier were 140-mm wide by 190.5-mm deep BCT posts set in foundation tubes without soil plates but with a ground line channel strut.

A modified ground strut, as shown in Figure 3 and positioned between post nos. 1 and 2 on each side of the system, was designed to compensate for the curve of the nose section. The ground strut was altered by angling the upstream yoke of the strut 12.2 degrees.

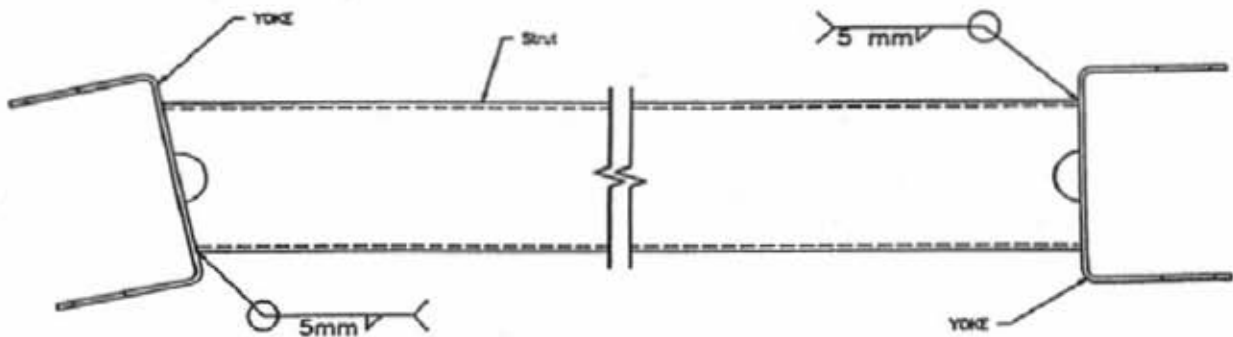
A cable anchor system was used between post nos. 1 and 2 on each side of the system in order to develop the tensile strength of the thrie beam guardrail downstream of the post no. 2. A reverse cable anchor system was used between post nos. 11 and 12 to replicate the rail strength of an actual installation. This setup was used for testing purposes only in order to simulate the effects of a complete bullnose barrier system with both halves connected. All guardrail used in the bullnose



Yoke



Strut



Assembly

NOTE: Strut as shown for one side of the system, for other side the mirror image is required.

Figure 3. Modified Ground line Strut

barrier consisted of 12-gauge steel thrie beam. Eleven 3,810-mm long sections of thrie beam were spliced together with a standard lap splice on each interior end. The first three rail sections were cut with slots in the valleys. The nose section of the rail consisted of a 3,810-mm long section bent into a 1,580-mm radius, as shown in Figure 4. The nose section bends were prefabricated with the these radii. The nose section was cut with slots in the valleys to aid in vehicle capture, as shown in Figure 5. There were six primary 700-mm long slots centered about the midspan of the rail, three in each valley. The primary slots were divided from one another by 25-mm wide slot tabs. Eight additional smaller 230-mm long slots, four on each end of the rail section, were also cut with a 50-mm wide slot tab between them. All slots were 25-mm wide. The second rail section on each side was bent to form a 10,400-mm radius curve, as shown in Figure 4. These sections were cut with a different pattern of slots, as shown in Figure 6. There were nine 290-mm long slots in each valley. A 100-mm wide slot tab separated each slot. The slot pattern for the third rail section on each side consisted of two sets of six 300-mm long slots centered between post slots, as shown in Figure 7. The slots were separated by 250-mm wide slot tabs, which provided three slots per valley between posts.

The Phase II development of the bullnose barrier system found that it was necessary to add a set of steel cable retention devices to contain impacting vehicles in the event of rail fracture. A 4.38-m long by 15.9-mm diameter cable was added behind the top and middle humps of the nose section of thrie beam rail. A 7 x 19 cable was chosen such that one of the two cables was capable of containing the impacting vehicle. Cables were only placed behind the first rail section because it was the only section that had failed in previous testing. It was believed that the rail sections after the nose section would be active in containing the vehicle, and therefore, the use of longer cable lengths was deemed unnecessary. The cables were attached to the guardrail using three U-bolts per cable to

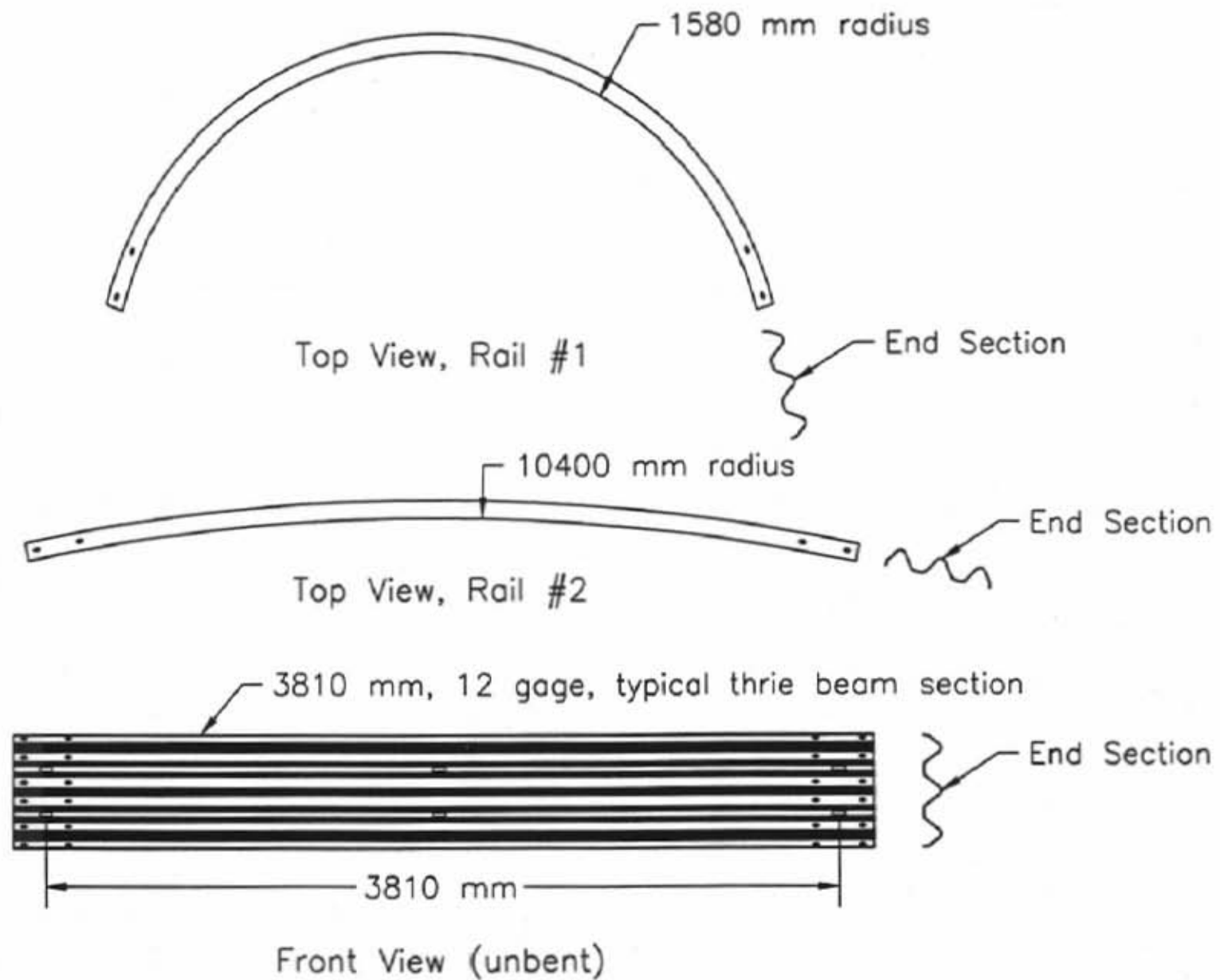
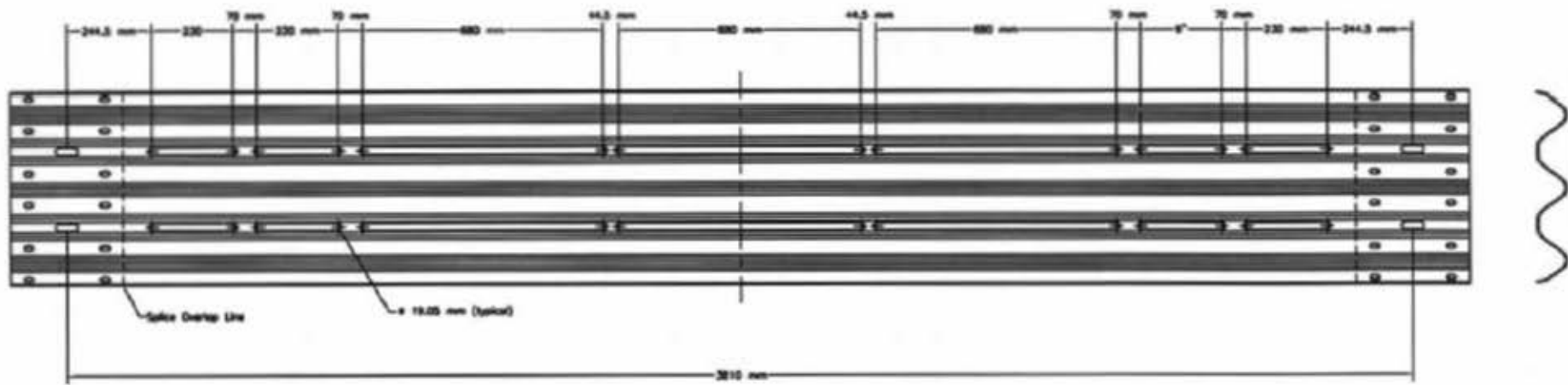
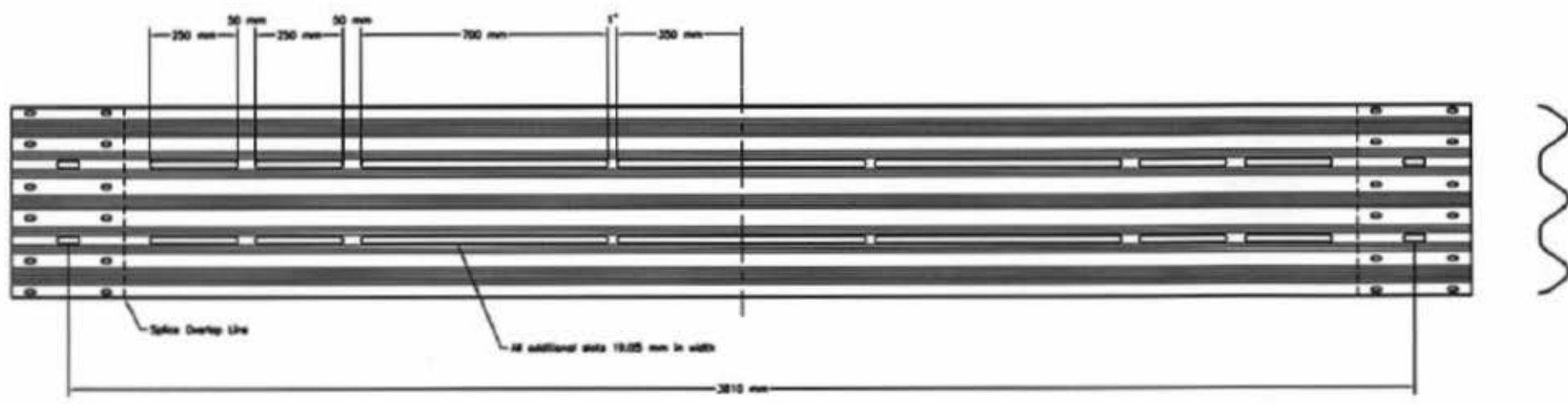


Figure 4. Layout of Bullnose Rails No. 1 and 2



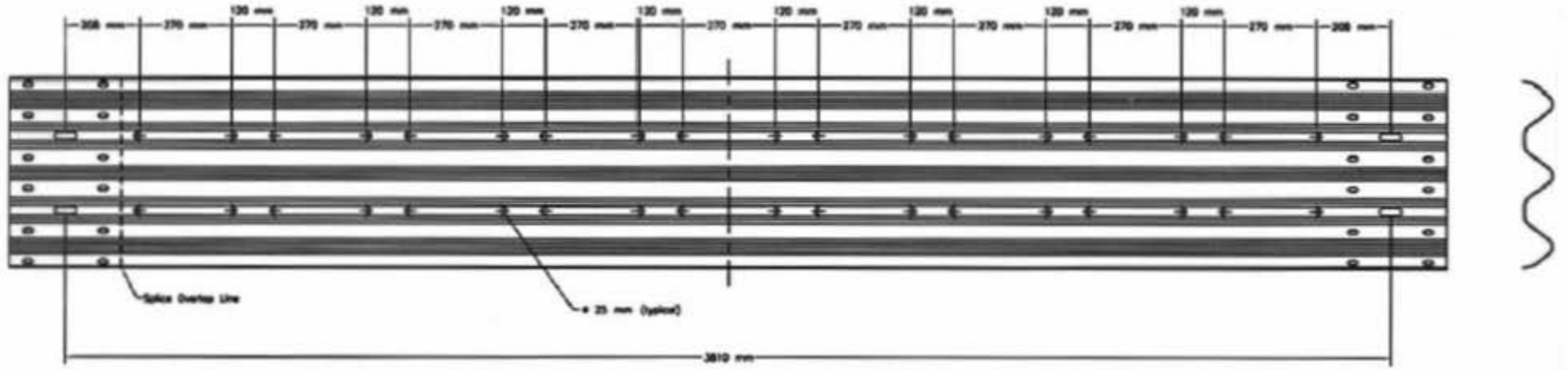
Rail Section 1 ("Nose" Section)

13

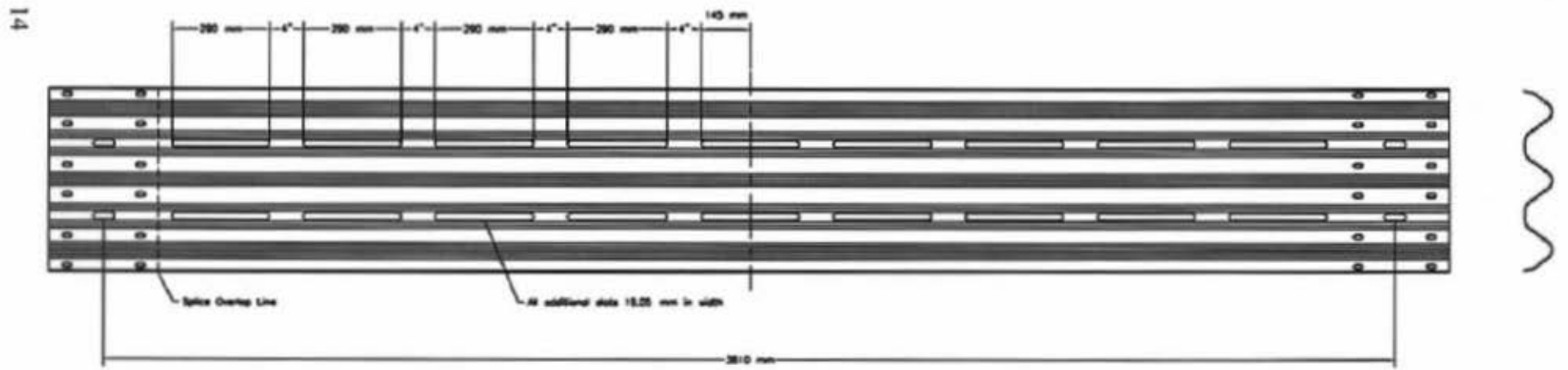


Rail Section 1 ("Nose" Section)

Figure 5. Rail Section No. 1 Detail

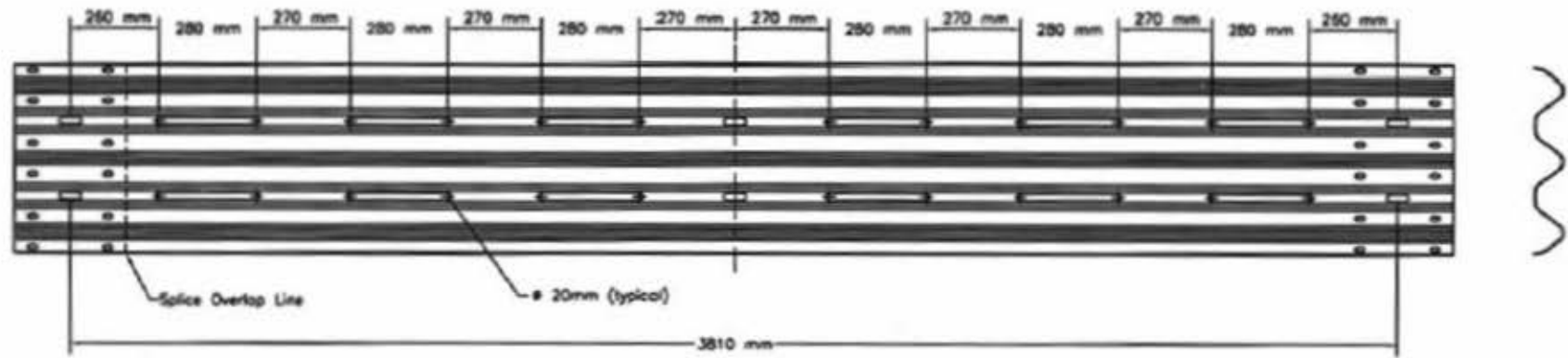


Rail Section 2



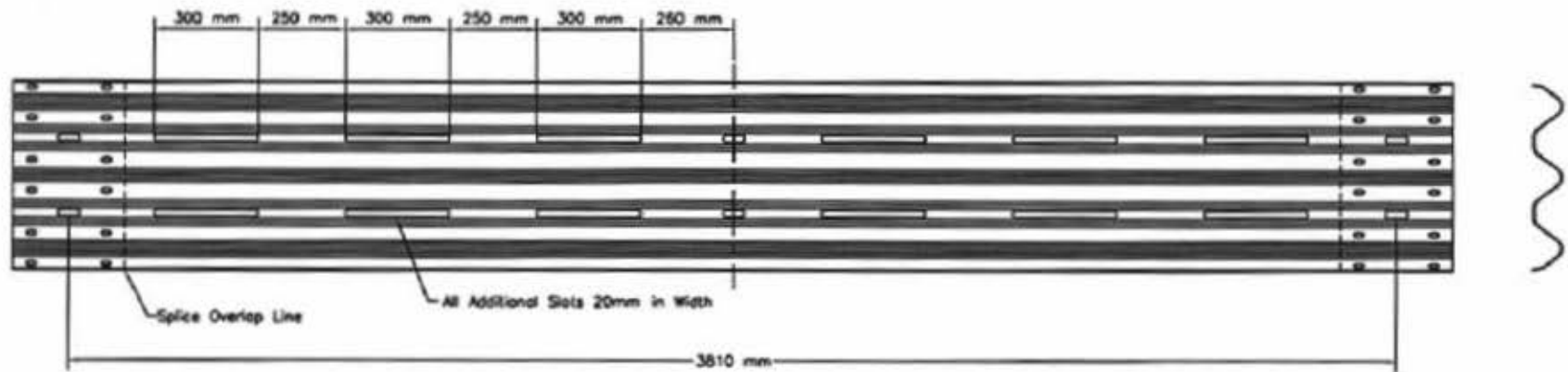
Rail Section 2

Figure 6. Rail Section No. 2 Detail



Rail Section 3 (MBN-3)

15

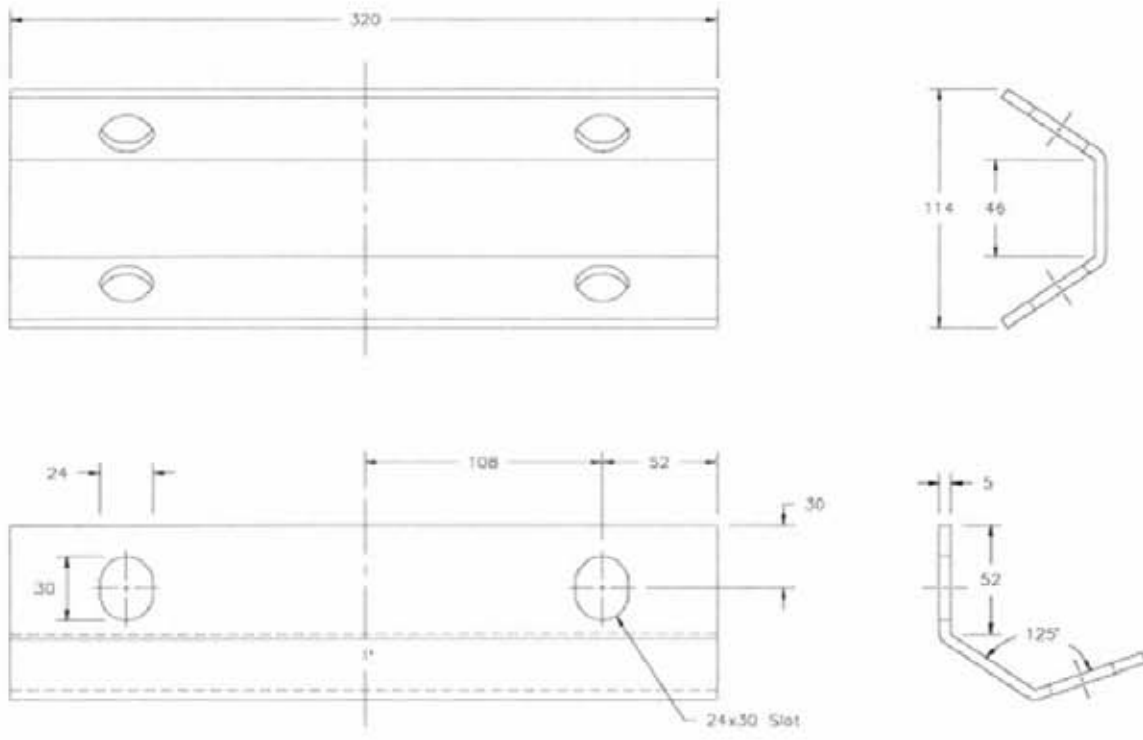
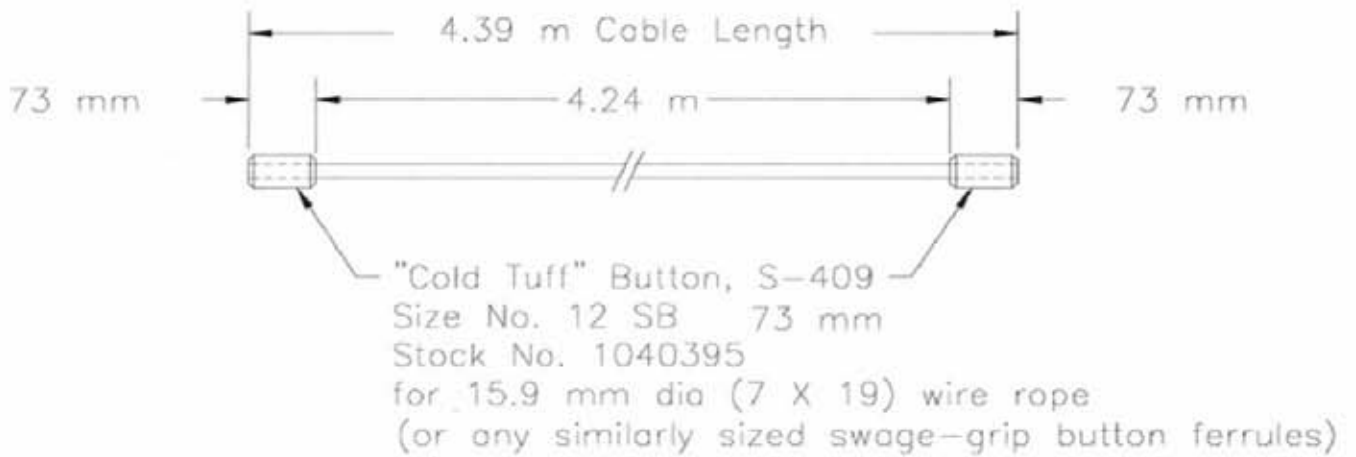


Rail Section 3 (MBN-3)

Figure 7. Rail Section No. 3 Detail

fix the cables behind the top and middle humps of the thrie beam. The ends of each cable were fitted with 73-mm diameter "Cold Tuff" buttons and clamped between formed steel plates located at the guardrail splice at post no. 1 on each side. The "Cold Tuff" buttons are swaged-grip button ferrules. As such, any similarly sized swaged-grip button ferrule could be substituted into the design. The cable plate and the cable assembly detail are shown in Figure 8.

Photographs of the assembled bullnose median barrier for test MBN-5 are shown in Figures 9 through 10.



Steel Plate, A306
 320mm x 150mm x 5mm

Figure 8. Cable Detail and Cable Plate



Figure 9. Bullnose Barrier Design, Test MBN-5

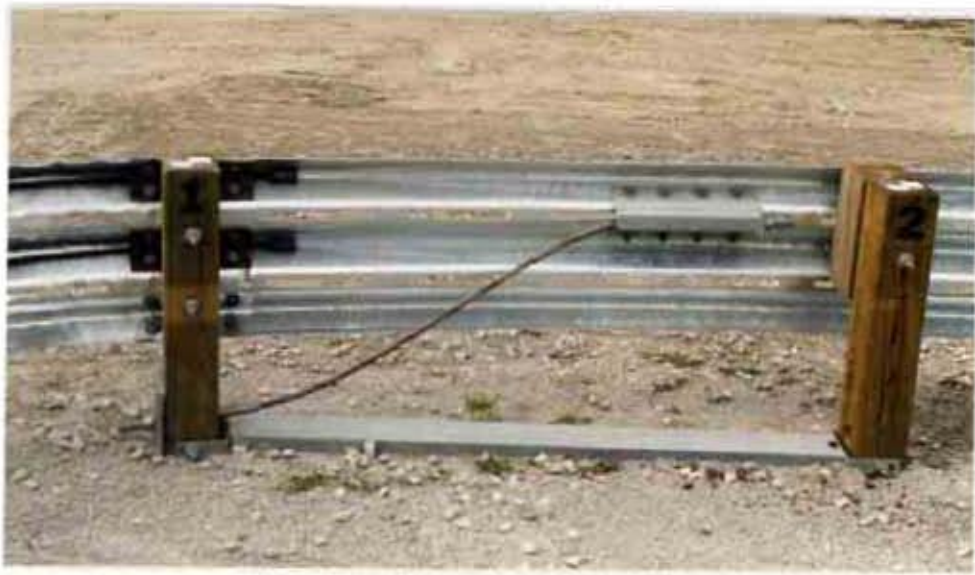


Figure 10. Bullnose Barrier Design, Test MBN-5

3 TEST REQUIREMENTS AND PERFORMANCE EVALUATION CRITERIA

3.1 Test Requirements

Terminals and crash cushions, such as bullnose barriers, must satisfy the requirements provided in NCHRP Report No. 350 (1) in order to be accepted for use on new construction projects or as a replacement for existing barriers not meeting current safety standards. The bullnose barrier is defined as a gated barrier and must fulfill the requirements for gated barriers. A gating device is one designed to allow controlled penetration of the vehicle when impacted between the beginning and the end of the length of need. According to NCHRP Report No. 350, terminals and crash cushions must be subjected to seven full-scale vehicle crash tests, four using a 2000-kg pickup truck and three using an 820-kg small car. The required 2000-kg pickup truck crash tests are: (1) Test 3-31, a 100 km/h impact at a nominal angle of 0 degrees on the tip of the barrier nose; (2) Test 3-33, a 100 km/h impact at a nominal angle of 15 degrees on the tip of the barrier nose; (3) Test 3-35, a 100 km/h impact at a nominal angle of 20 degrees on the beginning of the Length-of-Need (LON); and (4) Test 3-39, a 100 km/h impact at a nominal angle of 20 degrees on a point at the length of the terminal divided by two. The required 820-kg small car crash tests are: (1) Test 3-30, a 100 km/h impact at a nominal angle of 0 degrees on the tip of the barrier nose with a 1/4 point offset; (2) Test 3-32, a 100 km/h impact at a nominal angle of 15 degrees on the tip of the barrier nose; (3) Test 3-34, a 100 km/h impact at a nominal angle of 15 degrees on the Critical Impact Point (CIP). A diagram showing the impact location for the seven crash tests is shown in Figure 11.

Tests nos. 3-30 and 3-31 were successfully completed in the course of Phase I and Phase II of the bullnose median barrier project. During Phase III, full-scale crash tests of test designations nos. 3-32, 3-33, 3-34, and 3-35 were planned for this report. These tests were planned to further

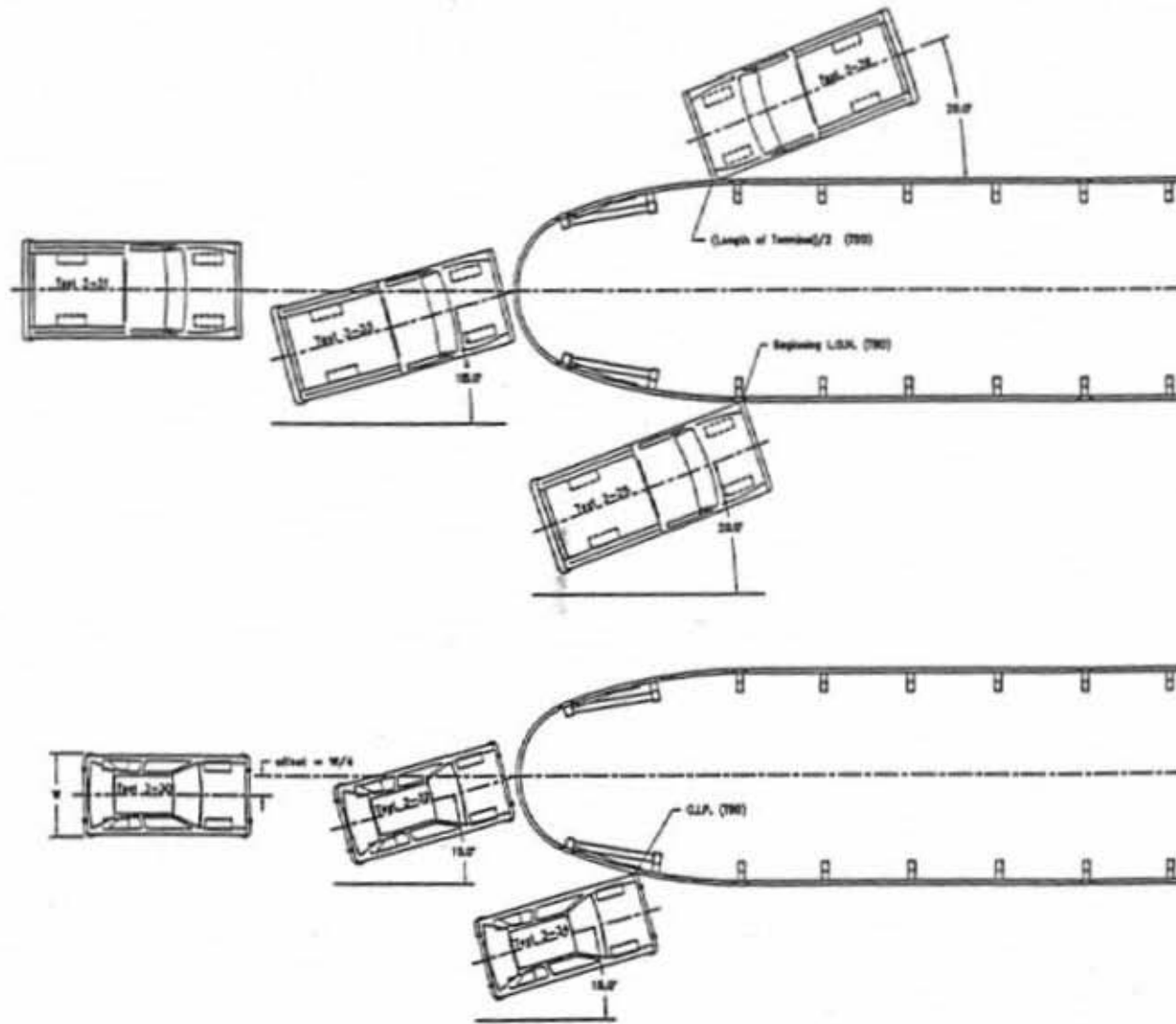


Figure 11. Proposed Full Scale Crash Tests for Bullnose Barrier Evaluation

develop the bullnose design concept from Phase II as well as to fulfill the safety requirements set forth in NCHRP Report No. 350. The results of these tests would be used to obtain information for calibrating computer models, evaluating the feasibility of the design concept for the other required impact conditions, and obtaining information for future design modifications and improvements.

3.2 Evaluation Criteria

Evaluation criteria for full-scale vehicle crash testing are based on three appraisal areas: (1) structural adequacy; (2) occupant risk; and (3) vehicle trajectory after collision. Criteria for structural adequacy are intended to evaluate the ability of the barrier to contain, redirect, or allow controlled vehicle penetration in a predictable manner. Occupant risk evaluates the degree of hazard to occupants in the impacting vehicle. Vehicle trajectory after collision is a measure of the potential for the post-impact trajectory of the vehicle to cause subsequent multi-vehicle accidents, thereby subjecting occupants of other vehicles to an undue hazard or to subject the occupants of the impacting vehicle to secondary collisions with other fixed objects. These three evaluation criteria are defined in Table 3. The full-scale vehicle crash tests were conducted and reported in accordance with the procedures provided in NCHRP Report No. 350.

Table 3. NCHRP Report 350 Evaluation Criteria for 2000P Pickup Truck and 820C Small Car Tests

Evaluation Factors	Evaluation Criteria	Applicable Tests						
Structural Adequacy	A. Test article should contain and redirect the vehicle; the vehicle should not penetrate, underride, or override the installation although controlled lateral deflection of the test article is acceptable.	3-35						
	C. Acceptable test article performance may be by redirection, controlled penetration, or controlled stopping of the vehicle.	3-30 3-31 3-32 3-33 3-34 3-39						
Occupant Risk	D. Detached elements, fragments or other debris from the test article should not penetrate or show potential for penetrating the occupant compartment, or present an undue hazard to other traffic, pedestrians, or personnel in a work zone. Deformations of, or intrusions into, the occupant compartment that could cause serious injuries should not be permitted.	ALL						
	F. The vehicle should remain upright during and after collision although moderate roll, pitching, and yawing are acceptable.	ALL						
	H. Occupant impact velocities should satisfy the following: Occupant Impact Velocity Limits (m/s) <table border="1" data-bbox="347 1010 1279 1108"> <thead> <tr> <th>Component</th> <th>Preferred</th> <th>Maximum</th> </tr> </thead> <tbody> <tr> <td>Longitudinal and Lateral</td> <td>9</td> <td>12</td> </tr> </tbody> </table>	Component	Preferred	Maximum	Longitudinal and Lateral	9	12	3-30 3-31 3-32 3-33 3-34
	Component	Preferred	Maximum					
Longitudinal and Lateral	9	12						
I. Occupant ridedown accelerations should satisfy the following: Occupant Ridedown Acceleration Limits (G's) <table border="1" data-bbox="347 1199 1279 1318"> <thead> <tr> <th>Component</th> <th>Preferred</th> <th>Maximum</th> </tr> </thead> <tbody> <tr> <td>Longitudinal and Lateral</td> <td>15</td> <td>20</td> </tr> </tbody> </table>	Component	Preferred	Maximum	Longitudinal and Lateral	15	20	3-30 3-31 3-32 3-33 3-34	
Component	Preferred	Maximum						
Longitudinal and Lateral	15	20						
Vehicle Trajectory	K. After collision it is preferable that the vehicle's trajectory not intrude into adjacent traffic lanes.	ALL						
	L. The occupant impact velocity in the longitudinal direction should not exceed 12 m/sec and the occupant ridedown acceleration in the longitudinal direction should not exceed 20 G's.	3-35 3-39						
	M. The exit angle from the test article preferably should be less than 60 percent of the test impact angle, measured at the time the vehicle lost contact with the device.	3-35 3-39						
	N. Vehicle trajectory behind the test article is acceptable.	3-30 3-31 3-32 3-33 3-34 3-39						

4 TEST CONDITIONS

4.1 Test Facility

The testing facility is located at the Lincoln Air-Park on the NW end of the Lincoln Municipal Airport and is approximately 8.0 km NW of the University of Nebraska-Lincoln. The site is protected by a 2.44-m high chain-link security fence.

4.2 Vehicle Tow and Guidance System

A reverse cable tow system with a 1:2 mechanical advantage was used to propel the test vehicles. The distance traveled and the speed of the tow vehicle are one-half that of the test vehicle. The test vehicle was released from the tow cable before impact with the guardrail system. A digital speedometer was located in the tow vehicle to increase the accuracy of the test vehicle impact speed.

A vehicle guidance system developed by Hinch (16) was used to steer the test vehicle. A guide-flag, attached to the front-left wheel and the guide cable, was sheared off before impact. The 9.5-mm diameter guide cable was tensioned to approximately 13.3 kN, and supported laterally and vertically every 30.48 m by hinged stanchions. The hinged stanchions stood upright while holding up the guide cable, but as the vehicle was towed down the line, the guide-flag struck and knocked each stanchion to the ground. The vehicle guidance system was approximately 457.2-m long for the 2000-kg pickup tests and 313.9-m long for the small car tests.

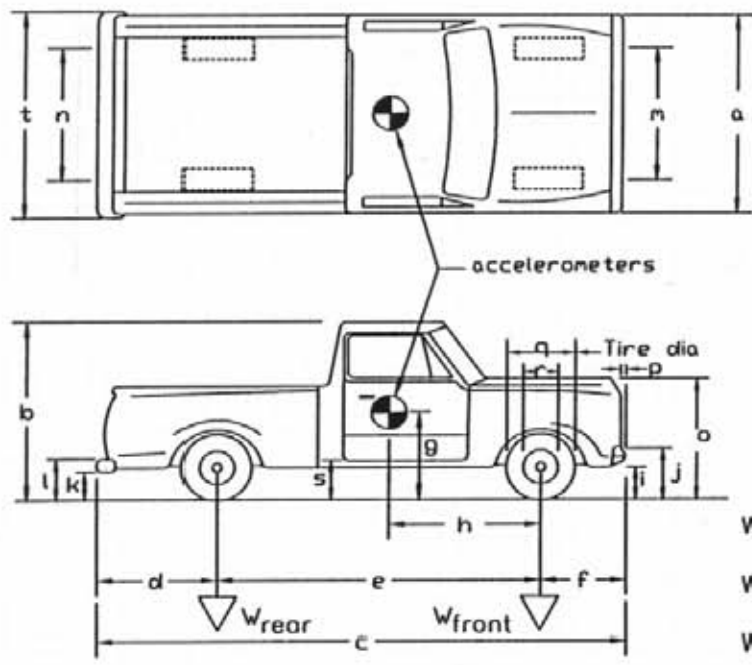
4.3 Test Vehicles

For test MBN-5, a 1993 Chevy 2500 ¾-ton pickup truck was used as the test vehicle. The test inertial and gross static weights were 2039 kg. The test vehicle and vehicle dimensions are shown in Figure 12.

For test MBN-6, a 1992 GMC 2500 ¾-ton pickup truck was used. The test inertial and gross

Date: 8/12/98 Test Number: MBN-5 Model: 2000P
 Make: Chevy Vehicle I.D.#: 1GBGC34K3PE202772
 Tire Size: LT245/75R16 Year: 1993 Odometer: 103500

*(All Measurements Refer to Impacting Side)



Vehicle Geometry - mm

a	<u>1892</u>	b	<u>1842</u>
c	<u>5531</u>	d	<u>1321</u>
e	<u>3327</u>	f	<u>813</u>
g	<u>738</u>	h	<u>1414</u>
i	<u>470</u>	j	<u>692</u>
k	<u>527</u>	l	<u>730</u>
m	<u>1575</u>	n	<u>1626</u>
o	<u>1092</u>	p	<u>102</u>
q	<u>762</u>	r	<u>445</u>
s	<u>489</u>	t	<u>1835</u>

Wheel Center Height Front	<u>375</u>
Wheel Center Height Rear	<u>368</u>
Wheel Well Clearance (FR)	<u>940</u>
Wheel Well Clearance (RR)	<u>940</u>

Engine Type V-6 gasoline
 Engine Size 5.7 L

Transmission Type:
 Automatic or Manual
 FWD or RWD or 4WD

Weights - kg	Curb	Test Inertial	Gross Static
W_{front}	<u>1188</u>	<u>1173</u>	<u>1173</u>
W_{rear}	<u>904</u>	<u>866</u>	<u>866</u>
W_{total}	<u>2092</u>	<u>2039</u>	<u>2039</u>

Note any damage prior to test:
 rear drivers well small dent, dented tailgate, drivers door small dent/scratch

Figure 12. Vehicle Dimensions, Test MBN-5

static weights were 2031 kg. The test vehicle and vehicle dimensions are shown in Figure 13.

For test MBN-7, a 1992 Chevy 2500 ¾-ton pickup truck was used. The test inertial and gross static weights were 2036 kg. The test vehicle and vehicle dimensions are shown in Figure 14.

For test MBN-8, a 1992 GMC 2500 ¾-ton pickup truck was used. The test inertial and gross static weights were 2033 kg. The test vehicle and vehicle dimensions are shown in Figure 15.

For test MBN-9, a 1996 Ford Festiva small car was used. The test inertial and gross static weights were 829 kg and 904 kg, respectively. The test vehicle and vehicle dimensions are shown in Figure 16.

The Suspension Method was used to determine the vertical component of the center of gravity for the test vehicles. This method is based on the principle that the center of gravity of any freely suspended body is in the vertical plane through the point of suspension. The vehicle was suspended successively in three positions, and the respective planes containing the center of gravity were established. The intersection of these planes pinpointed the location of the center of gravity. The longitudinal component of the center of gravity was determined using the measured axle weights. The locations of the final centers of gravity are shown in Figures 12 through 21.

Square, black and white-checked targets were placed on the vehicle to aid in the analysis of the high-speed film, as shown in Figures 17 through 21. One target was placed on the center of gravity on the driver's side door, the passenger's side door, and on the roof of the vehicle. The remaining targets were located for reference so that they could be viewed from the high-speed cameras for film analysis.

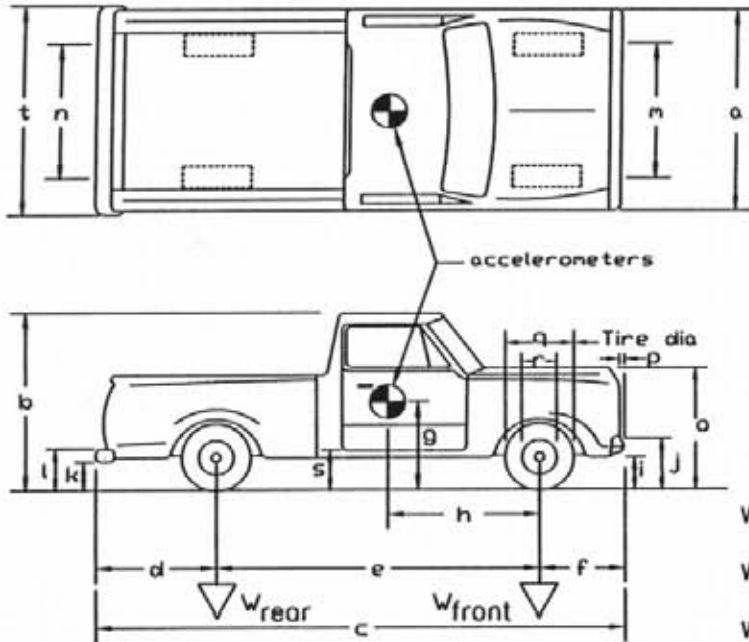
The front wheels of the test vehicle were aligned for camber, caster, and toe-in values of zero so that the vehicles would track properly along the guide cable. Two 5B flash bulbs were mounted

Date: 9/4/98 Test Number: MBN-6 Model: 2000P

Make: GMC Vehicle I.D.#: 1GDGC24K7PE531492

Tire Size: 245/75/R16 Year: 1992 Odometer: 209008

*(All Measurements Refer to Impacting Side)



Vehicle Geometry - mm

a	<u>1854</u>	b	<u>1810</u>
c	<u>5563</u>	d	<u>1308</u>
e	<u>3327</u>	f	<u>927</u>
g	<u>738</u>	h	<u>1439</u>
i	<u>446</u>	j	<u>673</u>
k	<u>565</u>	l	<u>762</u>
m	<u>1549</u>	n	<u>1629</u>
o	<u>1092</u>	p	<u>64</u>
q	<u>749</u>	r	<u>438</u>
s	<u>483</u>	t	<u>1848</u>

Wheel Center Height Front	<u>368</u>
Wheel Center Height Rear	<u>365</u>
Wheel Well Clearance (FR)	<u>902</u>
Wheel Well Clearance (RR)	<u>943</u>

Weights - kg	Curb	Test Inertial	Gross Static
W _{front}	<u>9325</u>	<u>1153</u>	<u>1153</u>
W _{rear}	<u>894</u>	<u>878</u>	<u>878</u>
W _{total}	<u>2055</u>	<u>2031</u>	<u>2031</u>

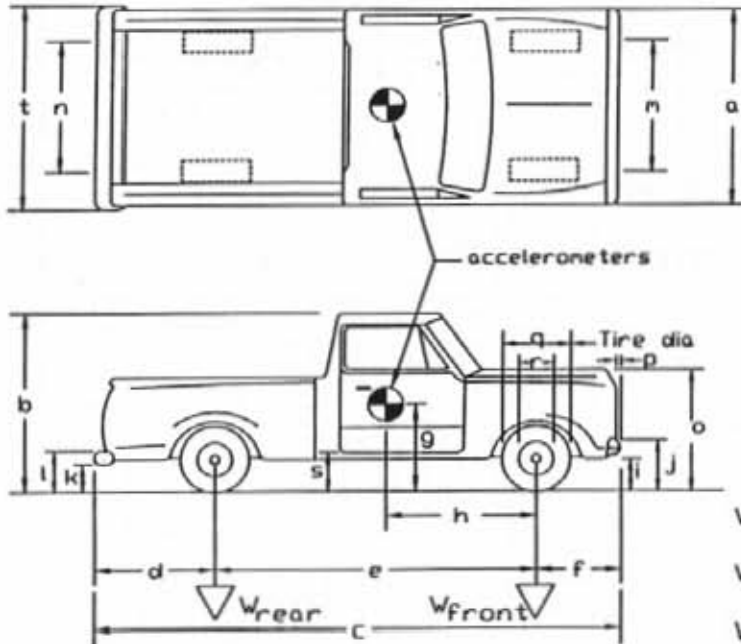
Engine Type V-8
 Engine Size 5.7L
 Transmission Type:
 Automatic or Manual
 FWD or RWD or 4WD

Note any damage prior to test: _____

Figure 13. Vehicle Dimensions, Test MBN-6

Date: 5/24/99 Test Number: MBN-7 Model: 2000P
 Make: Chevy 2500 Vehicle I.D.#: 1GCGC24J3NE207125
 Tire Size: 245/75R16 Year: 1992 Odometer: 139602

*(All Measurements Refer to Impacting Side)



Vehicle Geometry - mm

a 1861 b 1854
 c 5563 d 1308
 e 3327 f 914
 g 738 h 1354
 i 483 j 641
 k 610 l 800
 m 1600 n 1616
 o 1010 p 114
 q 775 r 445
 s 464 t 1873

Wheel Center Height Front 362
 Wheel Center Height Rear 371
 Wheel Well Clearance (FR) 895
 Wheel Well Clearance (RR) 959

Engine Type 8 Cyl. Diesel

Engine Size 6.2 L

Transmission Type:

Automatic or Manual

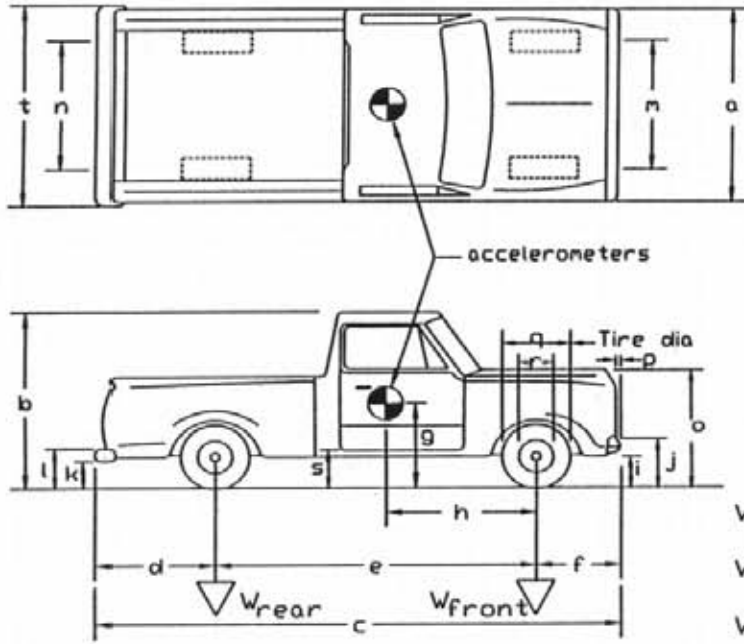
FWD or RWD or 4WD

Weights - kg	Curb	Test Inertial	Gross Static
W_{front}	<u>1287</u>	<u>1207</u>	<u>1207</u>
W_{rear}	<u>855</u>	<u>828</u>	<u>828</u>
W_{total}	<u>2142</u>	<u>2036</u>	<u>2036</u>

Note any damage prior to test: Rust

Figure 14. Vehicle Dimensions, Test MBN-7

Date: 9/24/99 Test Number: MBN-8 Model: 2500/2000P
 Make: GMC Vehicle I.D.#: 1GDGC24J2NE541514
 Tire Size: 245/75R16 Year: 1992 Odometer: 207260
 *(All Measurements Refer to Impacting Side)



Vehicle Geometry - mm

a	<u>1921</u>	b	<u>1842</u>
c	<u>5512</u>	d	<u>1308</u>
e	<u>3327</u>	f	<u>876</u>
g	<u>738</u>	h	<u>1342</u>
i	<u>508</u>	j	<u>679</u>
k	<u>578</u>	l	<u>768</u>
m	<u>1591</u>	n	<u>1613</u>
o	<u>1029</u>	p	<u>89</u>
q	<u>762</u>	r	<u>445</u>
s	<u>476</u>	t	<u>1854</u>

Wheel Center Height Front 365
 Wheel Center Height Rear 371
 Wheel Well Clearance (FR) 902
 Wheel Well Clearance (RR) 949

Weights

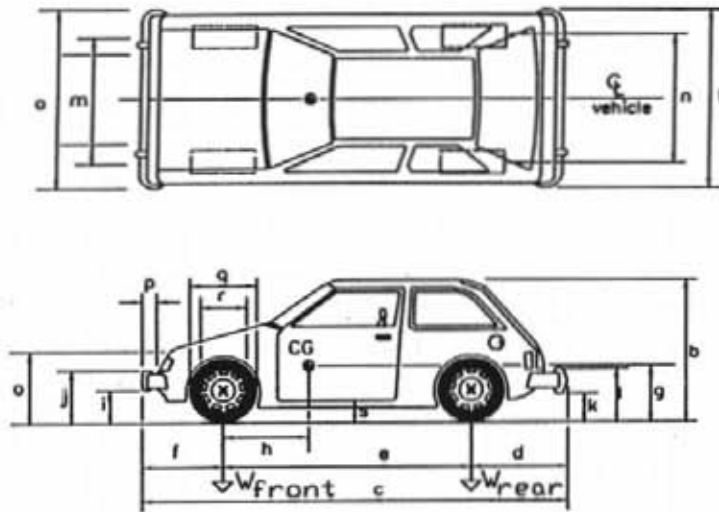
- kg	Curb	Test Inertial	Gross Static
W_{front}	<u>1280</u>	<u>1213</u>	<u>1213</u>
W_{rear}	<u>826</u>	<u>820</u>	<u>820</u>
W_{total}	<u>2106</u>	<u>2033</u>	<u>2033</u>

Engine Type 8 Cyl. Diesel
 Engine Size 6.2 L
 Transmission Type:
 Automatic or Manual
 FWD or RWD or 4WD

Note any damage prior to test: _____
 D.Side box damg-Rear/P.Side dent front fender-by light

Figure 15. Vehicle Dimensions, Test MBN-8

Dates: 10/29/99 Test Numbers: MBN-9 Model: Festiva
 Make: Ford Vehicle I.D.#: KNJPT06H1L6103459
 Tire Size: 155 R12 Year: 1990 Odometer: 132834



Vehicle Geometry - mm

a 1588 b 1461
 c 3569 d 584
 e 2299 f 686
 g 546 h 746
 i 362 j 514
 k 406 l 572
 m 1403 n 1391
 o 711 p 102
 q 540 r 330
 s 318 t 1588

height of wheel center 251

Engine Type 4 cyl. gas

Engine size 1.3 L

Transmission Type:

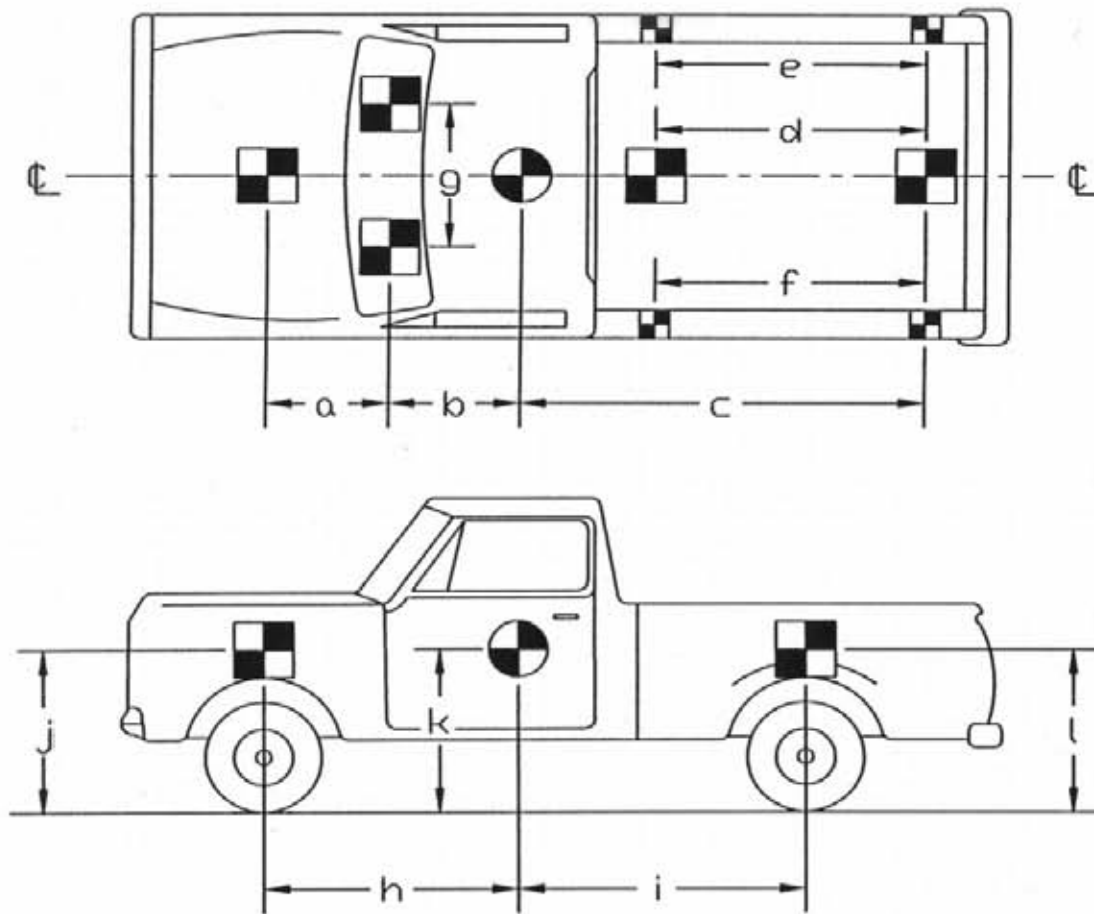
Automatic or Manual

FWD or RWD or 4WD

Weight - kg	Curb	Test Inertial	Gross Static
W_{front}	<u>566</u>	<u>560</u>	<u>595</u>
W_{rear}	<u>290</u>	<u>269</u>	<u>309</u>
W_{total}	<u>856</u>	<u>829</u>	<u>904</u>

Damage prior to test: _____

Figure 16. Vehicle Dimensions, Test MBN-9

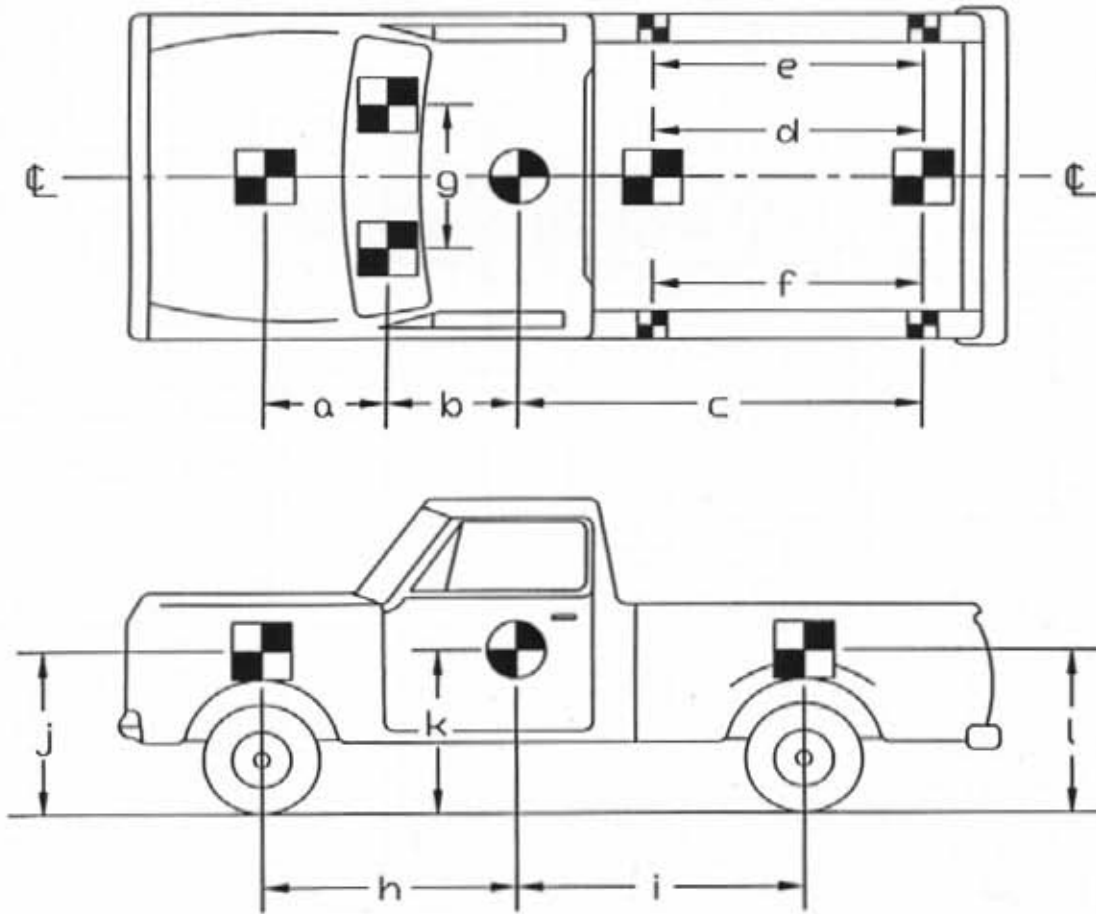


TEST #: MBN-5

TARGET GEOMETRY (mm)

a	<u>1359</u>	b	<u>616</u>	c	<u>2718</u>	d	<u>1826</u>
e	<u>2032</u>	f	<u>2013</u>	g	<u>978</u>	h	<u>1414</u>
i	<u>1943</u>	j	<u>1032</u>	k	<u>738</u>	l	<u>1048</u>

Figure 17. Vehicle Target Locations, Test MBN-5

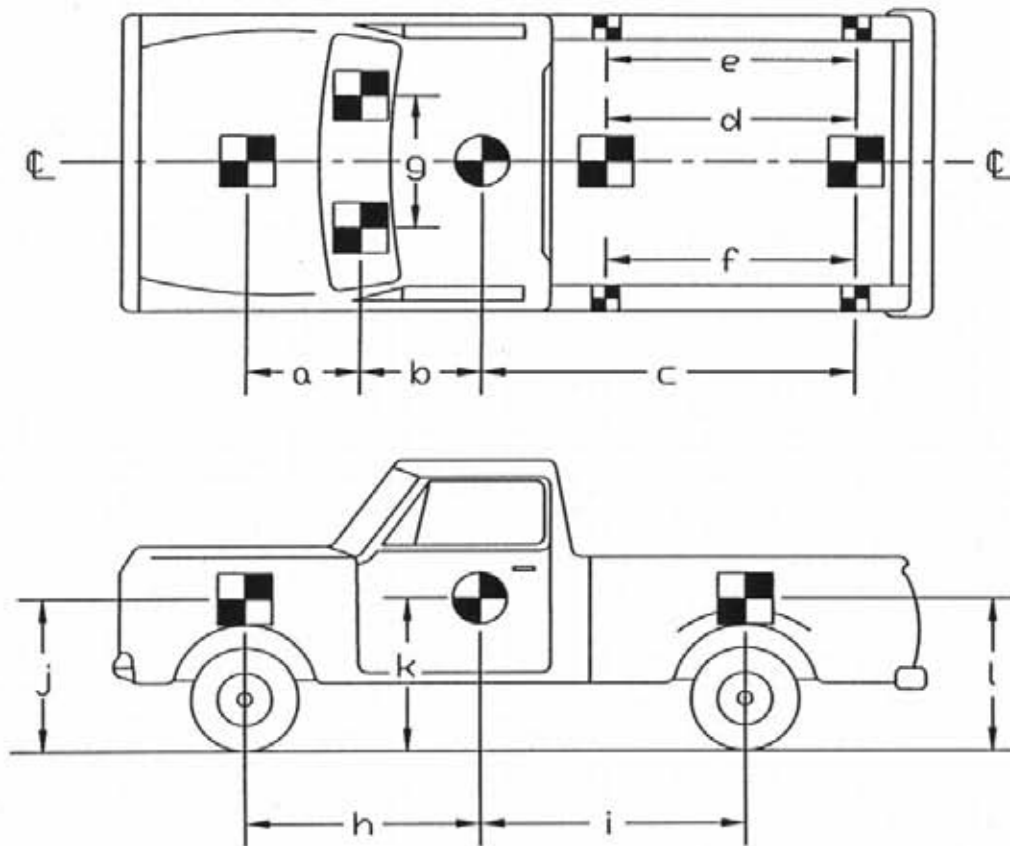


TEST #: MBN-6

TARGET GEOMETRY (mm)

a	<u>1016</u>	b	<u>699</u>	c	<u>2845</u>	d	<u>2048</u>
e	<u>2146</u>	f	<u>2153</u>	g	<u>934</u>	h	<u>1439</u>
i	<u>1915</u>	j	<u>1003</u>	k	<u>738</u>	l	<u>1048</u>

Figure 18. Vehicle Target Locations, Test MBN-6

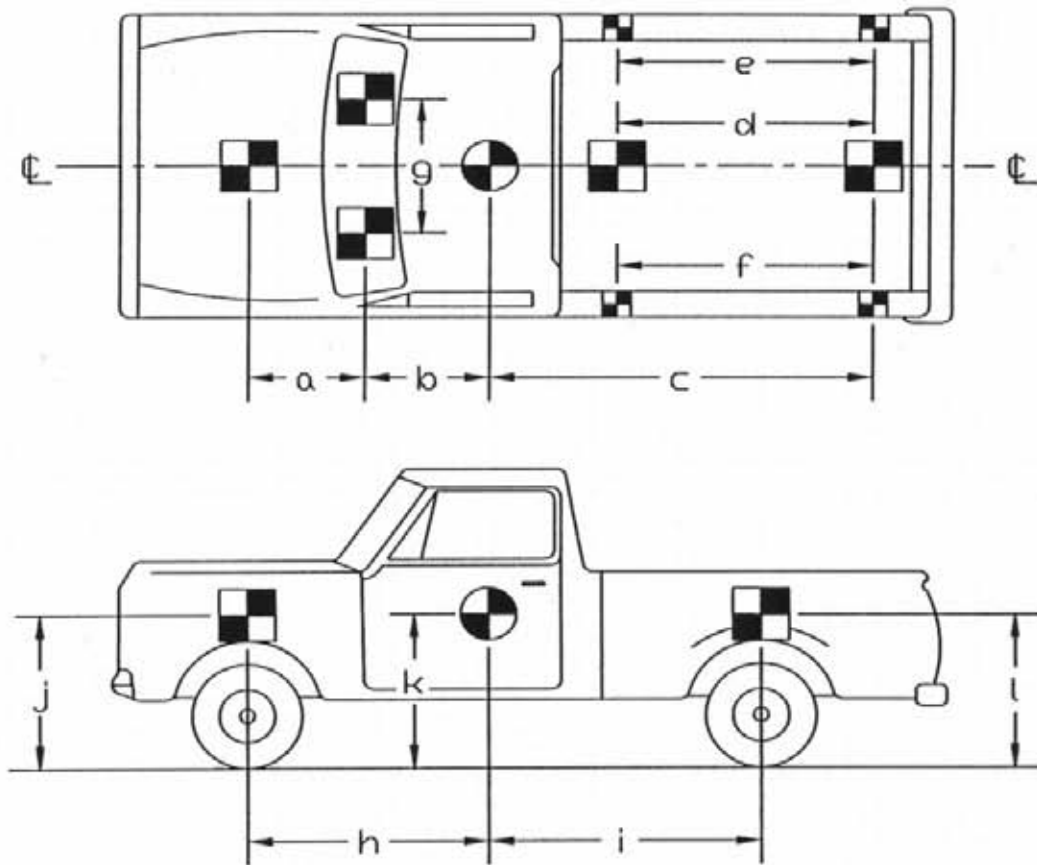


TEST #: MBN-7

TARGET GEOMETRY (mm)

a	<u>1080</u>	b	<u>622</u>	c	<u>2940</u>	d	<u>1559</u>
e	<u>2152</u>	f	<u>2153</u>	g	<u>978</u>	h	<u>1354</u>
i	<u>1994</u>	j	<u>997</u>	k	<u>738</u>	l	<u>1060</u>

Figure 19. Vehicle Target Locations, Test MBN-7

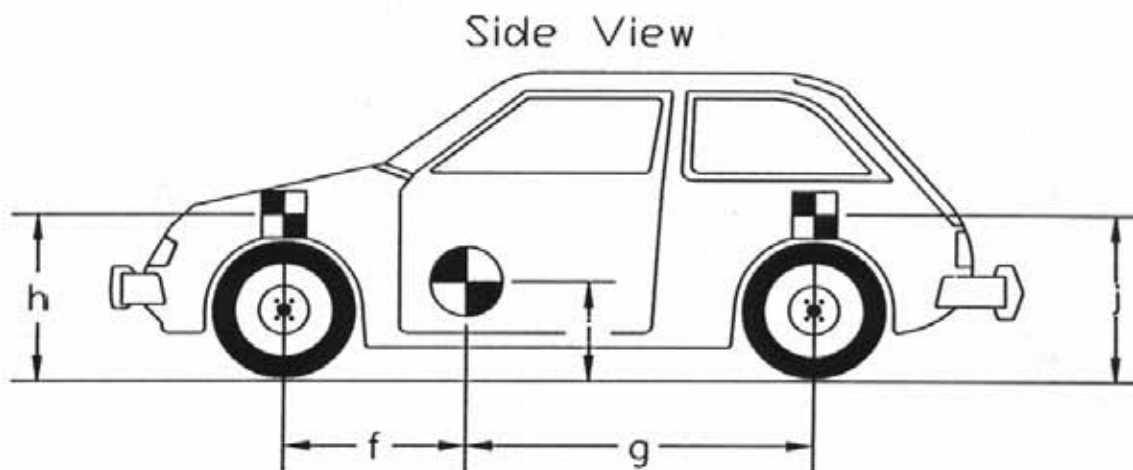
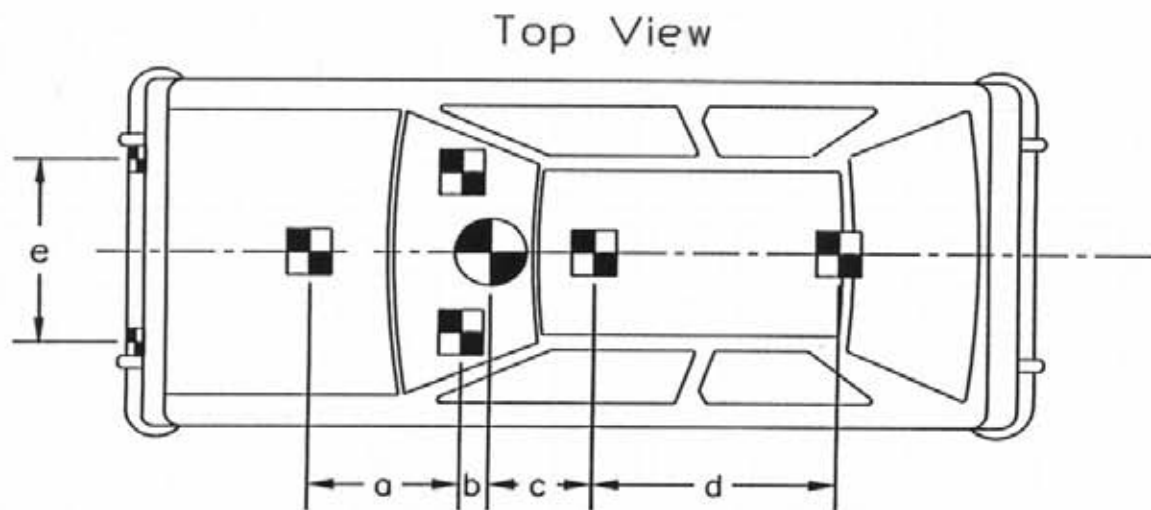


TEST #: MBN-8

TARGET GEOMETRY (mm)

a	<u>972</u>	b	<u>641</u>	c	<u>2903</u>	d	<u>1981</u>
e	<u>2153</u>	f	<u>2153</u>	g	<u>940</u>	h	<u>1342</u>
i	<u>1981</u>	j	<u>1003</u>	k	<u>738</u>	l	<u>1054</u>

Figure 20. Vehicle Target Locations, Test MBN-8



TEST #: <u>MBN-9</u>			
TARGET GEOMETRY (mm)			
a	<u>813</u>	b	<u>203</u>
c	<u>445</u>	d	<u>921</u>
e	<u>927</u>	f	<u>746</u>
g	<u>1553</u>	h	<u>711</u>
i	<u>546</u>	j	<u>730</u>

Figure 21. Vehicle Target Locations, Test MBN-9

on both the hood and roof of the vehicles to pinpoint on high-speed film the time of impact with the guardrail system. The flash bulbs were fired by a pressure tape switch mounted on the front face of the bumper. A remote-controlled brake system was installed in the test vehicle so the vehicle could be brought safely to a stop after the test.

4.4 Data Acquisition Systems

4.4.1 Accelerometers

One triaxial piezoresistive accelerometer system with a range of ± 200 G's was used to measure the acceleration in the longitudinal, lateral, and vertical directions at a sample rate of 10,000 Hz. The environmental shock and vibration sensor/recorder system, Model EDR-4M6, was developed by Instrumented Sensor Technology (IST) of Okemos, Michigan and includes three differential channels as well as three single-ended channels. The EDR-4 was configured with 6 Mb of RAM memory and a 1,500 Hz lowpass filter. Computer software, "DynaMax 1 (DM-1)" and "DADiSP" were used to digitize, analyze, and plot the accelerometer data.

A backup triaxial piezoresistive accelerometer system with a range of ± 200 G's was also used to measure the acceleration in the longitudinal, lateral, and vertical directions at a sample rate of 3,200 Hz. The environmental shock and vibration sensor/recorder system, Model EDR-3, was developed by Instrumented Sensor Technology (IST) of Okemos, Michigan. The EDR-3 was configured with 256 Kb of RAM memory and a 1,120 Hz lowpass filter. Computer software, "DynaMax 1 (DM-1)" and "DADiSP" were used to digitize, analyze, and plot the accelerometer data.

4.4.2 Rate Transducers

A Humphrey 3-axis rate transducer with a range of 250 deg/sec in each of the three directions (pitch, roll, and yaw) was used to measure the rates of motion of the test vehicle for test MBN-5. For

tests MBN-6 through MBN-9, a Humphrey 3-axis rate transducer with a range of 360 deg/sec in each of the three directions (pitch, roll, and yaw) was used. The rate transducers were rigidly attached to the vehicles near the center of gravity of the test vehicle. Rate transducer signals, excited by a 28 volt DC power source, were received through the three single-ended channels located externally on the EDR-4M6 and stored in the internal memory. The raw data measurements were then downloaded for analysis and plotting. Computer software, "DynaMax 1 (DM-1)" and "DADiSP" were used to digitize, analyze, and plot the rate transducer data.

4.4.3 High Speed Photography

For test MBN-5, five high-speed 16-mm Red Lake Locam cameras, with operating speeds of approximately 500 frames/sec, were used to film the crash test. A Locam with a wide angle 12.5-mm lens was placed 17.09-m above the test installation to provide a field of view perpendicular to the ground. A Locam with a zoom lens was placed 59.35-m downstream from the impact point and had a field of view parallel to the barrier. Another Locam with a zoom lense was placed 35.16-m downstream and offset 24.2 m to the left of the barrier to provide an additional viewing angle of the crash test. A fourth Locam was placed 7.68-m downstream of the nose of the barrier and offset 8.23 m to the right with a field of view perpendicular to the barrier. The final Locam was placed 5.82-m downstream and offset 15.45 m to the left with a field of view perpendicular to the installation. A schematic of the five high speed camera locations for test MBN-5 is shown in Figure 22.

For test MBN-6, four high-speed 16-mm Red Lake Locam cameras, with operating speeds of approximately 500 frames/sec, were used to film the crash test. A Locam with a wide angle 12.5-mm lens was placed 18.81-m above the test installation to provide a field of view perpendicular to the ground. A Locam with a zoom lens was placed 38.41-m downstream from the impact point

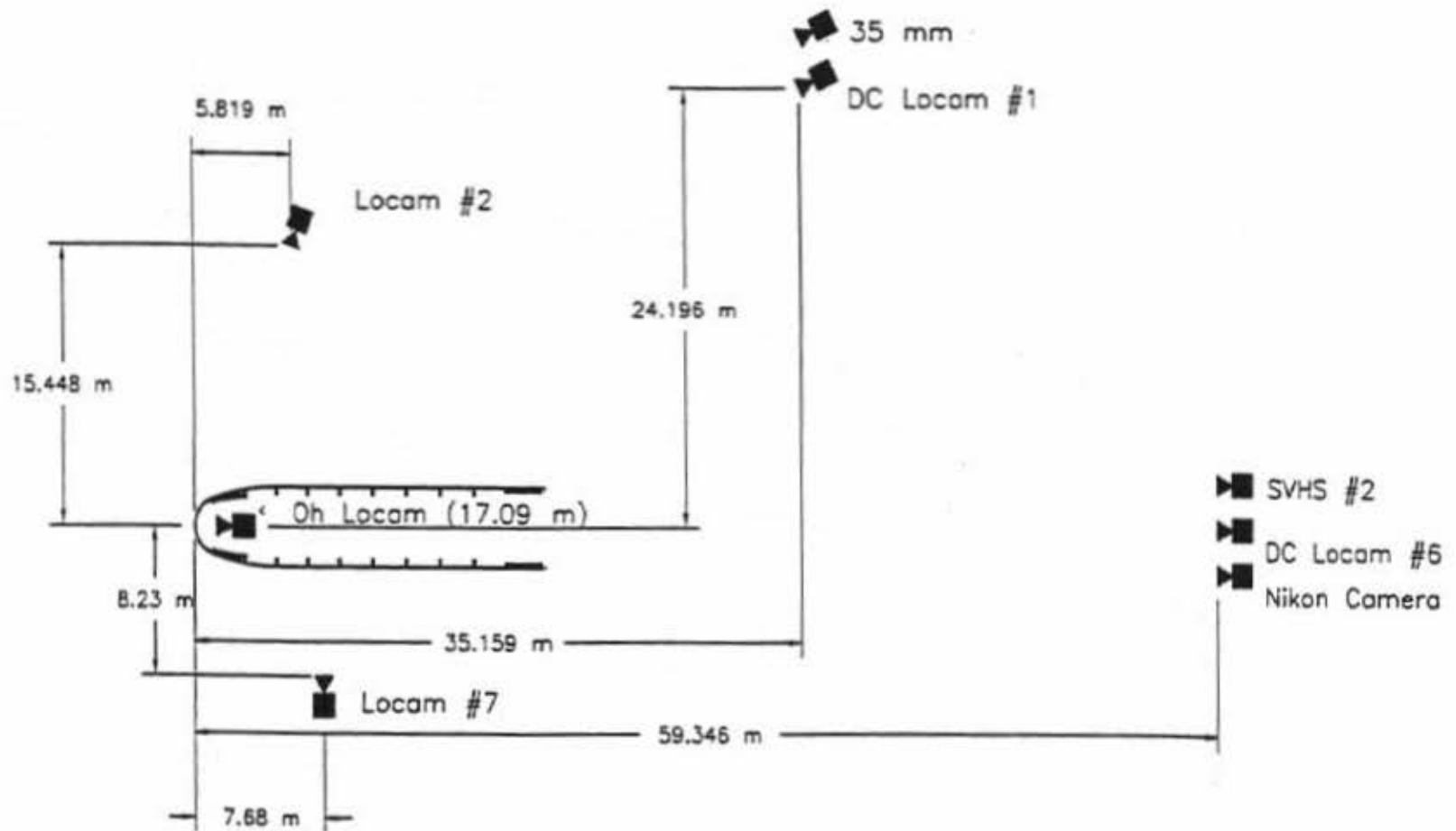


Figure 22. Location of High-Speed Cameras, Test MBN-5

and had a field of view parallel to the barrier. Another Locam was placed 17.07-m upstream and offset 12.19 m to the left of the barrier to provide an additional viewing angle of the crash test. The fourth Locam was placed 11.5-m downstream of the nose of the barrier and offset 16.15 m to the right with a field of view perpendicular to the barrier. A schematic of the four high speed camera locations for test MBN-6 is shown in Figure 23.

For test MBN-7, four high-speed 16-mm Red Lake Locam cameras, with operating speeds of approximately 500 frames/sec, were used to film the crash test. A Locam with a wide angle 12.5-mm lens was placed 18.81-m above the test installation to provide a field of view perpendicular to the ground. A Locam with a zoom lens was placed 38.41-m downstream from the impact point and had a field of view parallel to the barrier. Another Locam was placed 17.07-m upstream and offset 12.19 m to the left of the barrier to provide an additional viewing angle of the crash test. The fourth Locam was placed 11.5-m downstream of the nose of the barrier and offset 16.15 m to the right with a field of view perpendicular to the barrier. A schematic of the four high speed camera locations for test MBN-7 is shown in Figure 24.

For test MBN-8, six high-speed 16-mm Red Lake Locam cameras, with operating speeds of approximately 500 frames/sec, were used to film the crash test. A Locam with a wide angle 12.5-mm lens was placed 18.64-m above the test installation to provide a field of view perpendicular to the ground. A Locam with a zoom lens was placed 40.23-m downstream from the impact point and had a field of view parallel to the barrier. Another Locam was placed 17.07-m upstream and offset 12.19 m to the left of the barrier to provide an additional viewing angle of the crash test. The fourth Locam was placed 11.5-m downstream of the nose of the barrier and offset 13.72 m to the right with a field of view perpendicular to the barrier. A fifth and sixth Locam were placed 3.87-m and 7.11-m

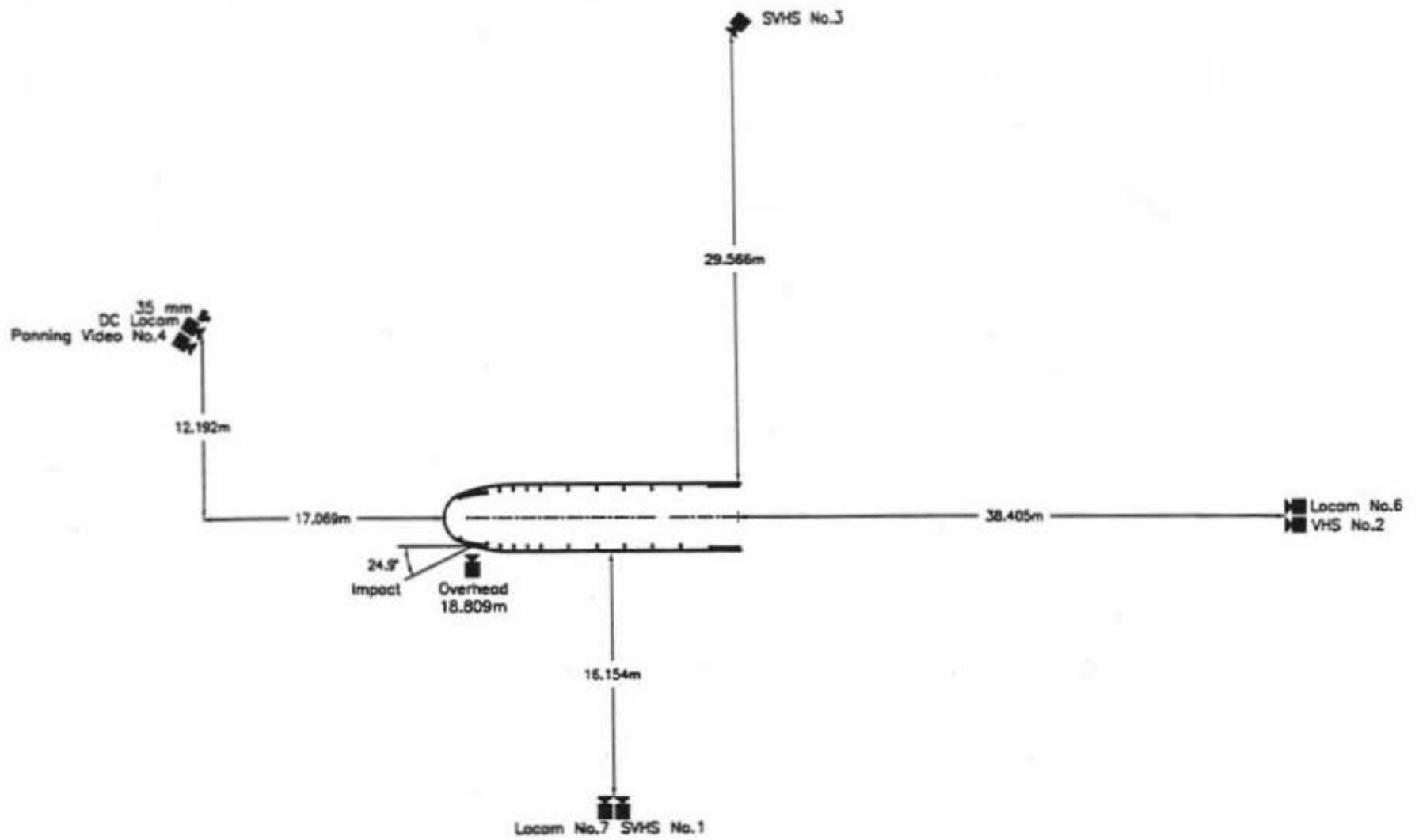


Figure 23. Location of High-Speed Cameras, Test MBN-6

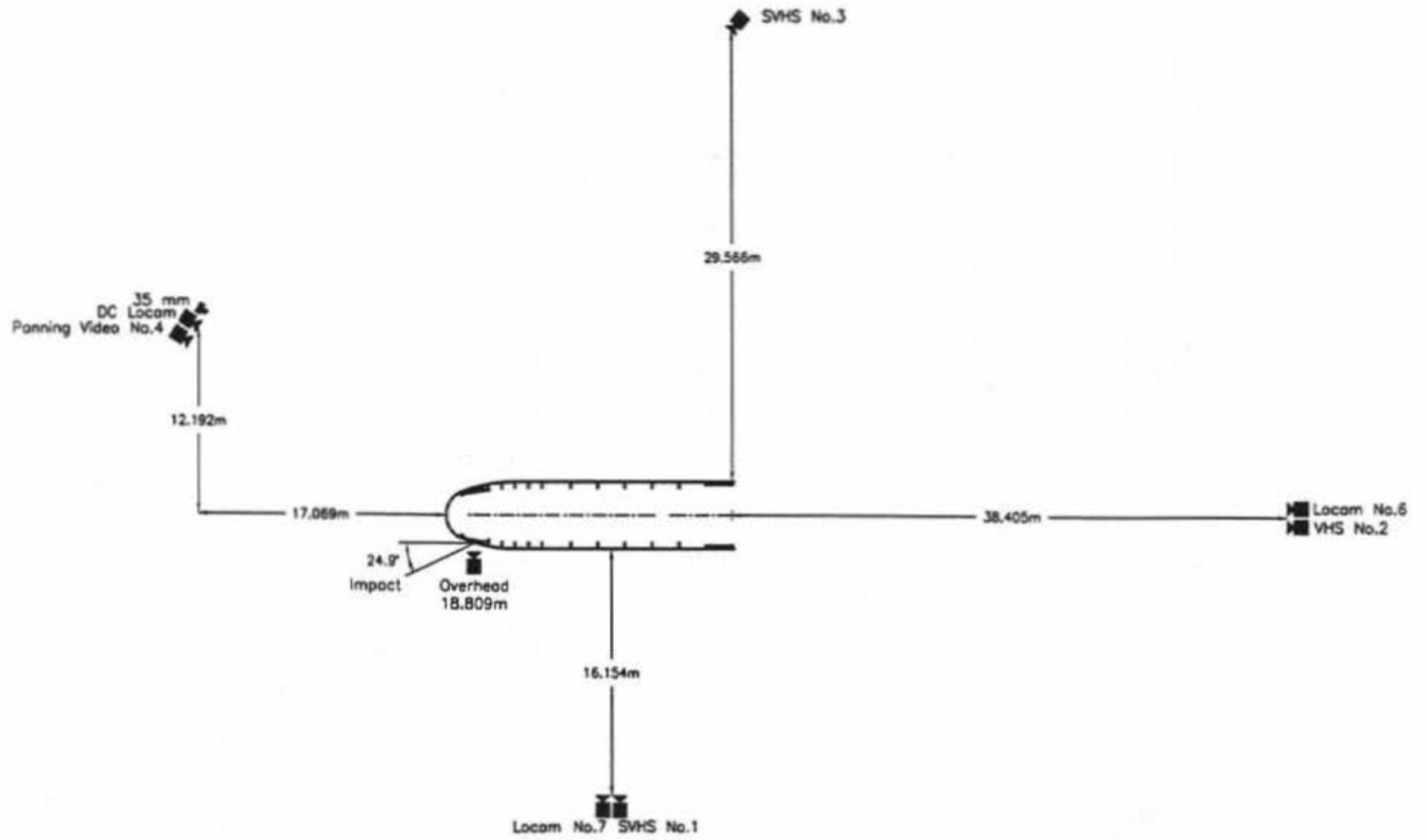


Figure 24. Location of High-Speed Cameras, Test MBN-7

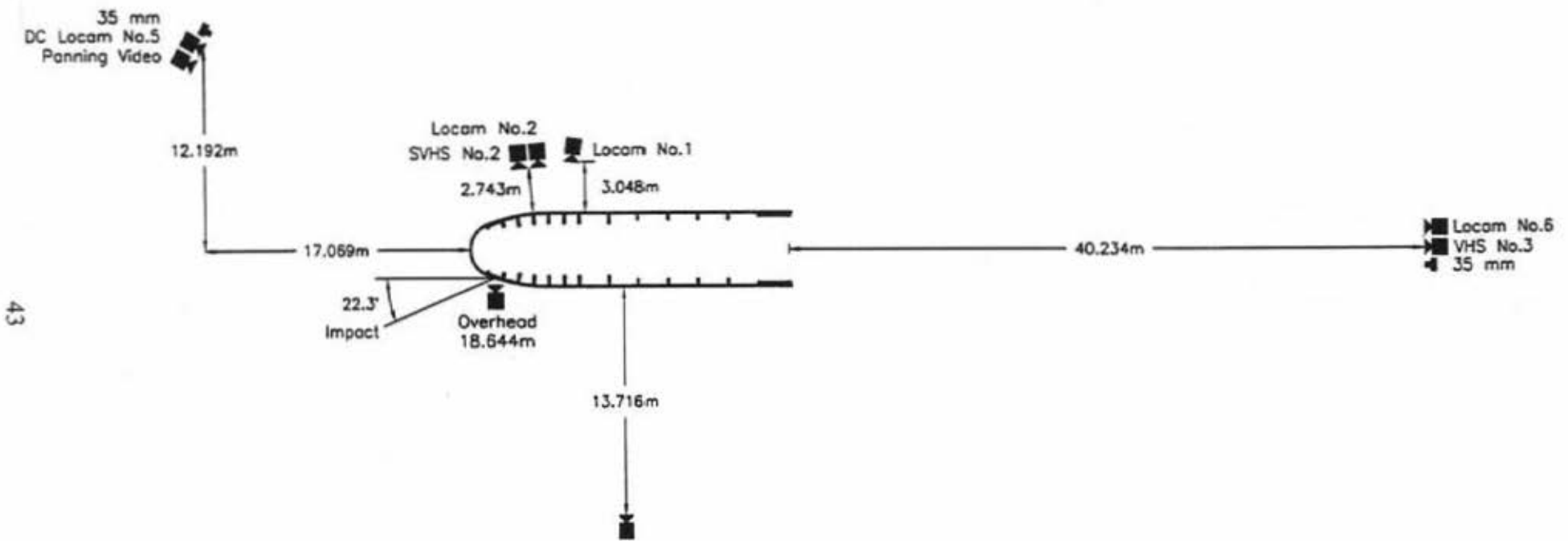
downstream and offset 2.74 m and 3.05 m to the right, respectively, with a field of view perpendicular to the installation. A schematic of the six high speed camera locations for test MBN-8 is shown in Figure 25.

For test MBN-9, five high-speed 16-mm Red Lake Locam cameras, with operating speeds of approximately 500 frames/sec, were used to film the crash test. A Locam with a wide angle 12.5-mm lens was placed 18.29-m above the test installation to provide a field of view perpendicular to the ground. A Locam with a zoom lens was placed 61.83-m downstream and offset 16.57 m to the left from the impact point and had a field of view parallel to the barrier. Another Locam was placed 17.07-m upstream and offset 12.19 m to the left of the barrier to provide an additional viewing angle of the crash test. A fourth Locam was placed 6.71 m to the right of the impact point with a field of view perpendicular to the barrier. The final Locam was placed 36.58-m to the left of the impact point with a field of view perpendicular to the installation. A schematic of the five high speed camera locations for test MBN-9 is shown in Figure 26.

The film was analyzed using the Vanguard Motion Analyzer. Actual camera speed and camera divergence factors were considered in the analysis of the high-speed film.

4.4.4 Pressure Tape Switches

For tests MBN-5 through MBN-9, five pressure-activated tape switches, spaced at 2-m intervals, were used to determine the speed of the vehicle before impact. Each tape switch fired a strobe light which sent an electronic timing signal to the data acquisition system as the left-front tire of the test vehicle passed over it. Test vehicle speeds were determined from electronic timing mark data recorded on "Test Point" software. Strobe lights and high-speed film analysis are used only as a backup in the event that vehicle speeds cannot be determined from the electronic data.



43

Figure 25. Location of High-Speed Cameras, Test MBN-8

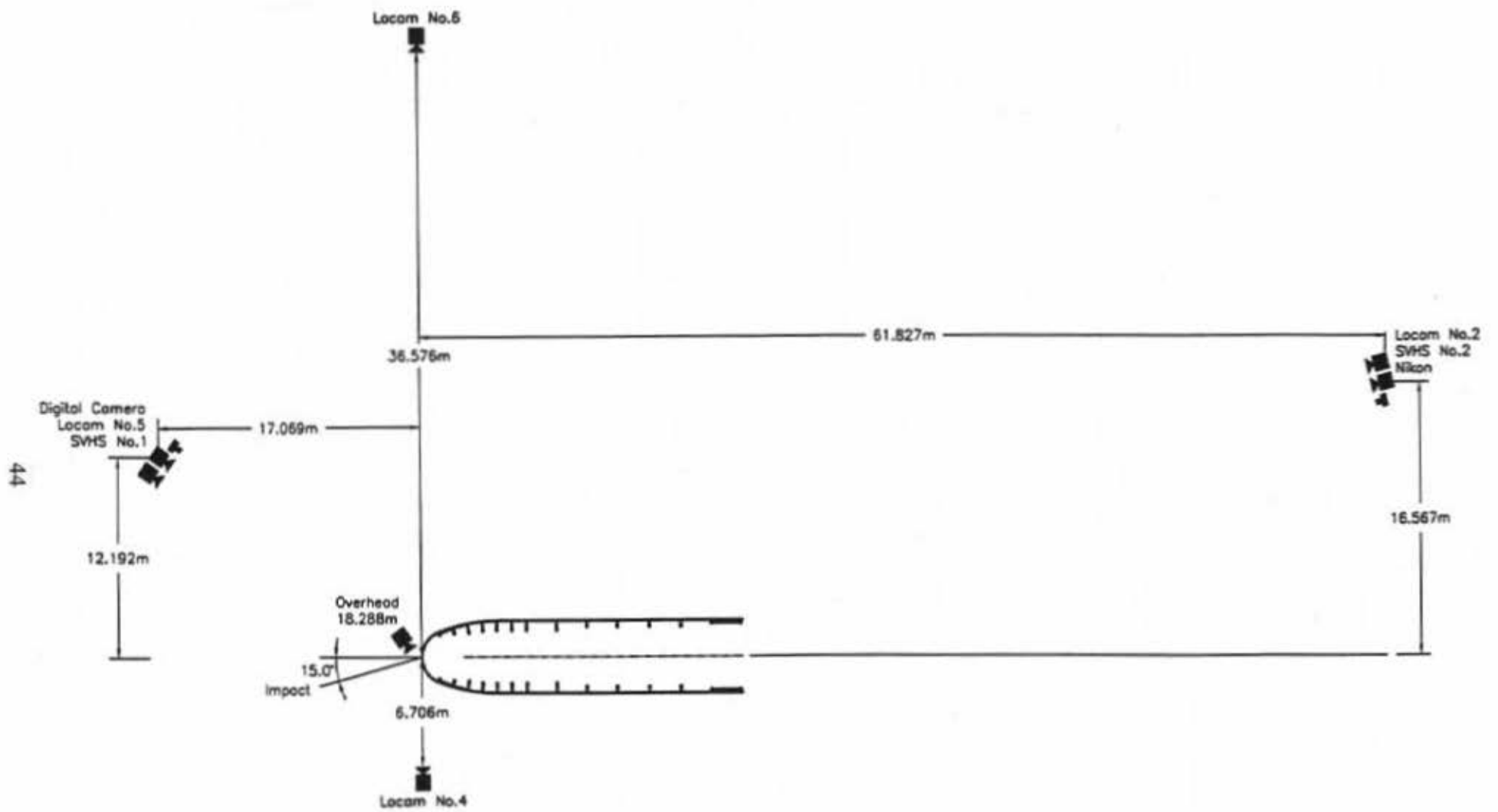


Figure 26. Location of High-Speed Cameras, Test MBN-9

5 CRASH TEST MBN-5

5.1 Test MBN-5

Test MBN-5 was conducted according to the NCHRP Report No. 350 test 3-33 impact conditions. The 2,039-kg pickup truck impacted the bullnose barrier with the centerline of the vehicle aligned with the nose, as shown in Figure 27, and at a speed of 103.0 km/h and at an angle of 13.4 degrees. A summary of the test results and the sequential photographs are shown in Figure 28. Additional sequential photographs are shown in Figure 29. Full-scale crash documentary photographs are shown in Figures 30 and 31.

5.2 Test Description

Following the initial impact with the pickup truck, the three beam rail immediately began to flatten across the front of the pickup truck and deform inward. At 0.068 sec after impact, the left front of the truck impacted post no. 1 on the right side. At the same time, the bottom hump of the three beam guardrail was pushed under the front wheels of the truck. As the pickup penetrated further into the barrier, post no. 1 on the right side fractured, as the beam wrapped around the post at 0.093 sec. At 0.110 sec, post no. 1 on the left side fractured and the guardrail on the left side bowed outward, pulling away from post no. 2. The pickup truck then continued to penetrate into the system, impacting post no. 2 on the left side and breaking it, thus causing the front grill of the truck to detach. After post no. 2 fractured, a buckle in the guardrail formed at the location of post no. 2 on the left side due to the bowing of the guardrail. The rail continued to bow outward as the truck penetrated into the system. At 0.210 sec, post no. 3 on the left side was broken as it was impacted by the left-front corner of the pickup truck. Post no. 2 on the right side was subsequently broken as the guardrail wrapped around the post. At 0.307 sec, post no. 4 on the left was broken after impact

with the front of the pickup truck. Shortly afterward, the pickup truck impacted the back side of the three beam guardrail near post no. 4 on the left side and pushed it outward. At 0.569 sec, the pickup truck continued to decelerate, hitting and breaking post no. 5 on the left side. The motion of the truck continued to push a large section of the guardrail outward and to the left, thus forming a large kink in the rail near post no. 4 on the left side. This action formed a sizeable wedge of guardrail on the left side of the barrier. The pickup truck continued to move forward, breaking post nos. 6 and 7 on the left side and coming to a stop as the front of the vehicle reached post no. 8 at 0.906 sec after impact. At this time, the wedge of guardrail had been pushed perpendicular to the centerline of the guardrail. The trajectory of the pickup truck during the crash test and the final position of the vehicle are provided in Figure 32.

5.3 Vehicle Damage

Vehicle damage was moderate, as shown in Figure 33. The front bumper and the front of the pickup truck were crushed inward across the entire front width of the vehicle. The bumper crushed inward at the center and was folded around the supports at the end of the frame rails. The radiator of the truck was flattened. There was very little engine movement which occurred during the impact. The left-front fender of the pickup truck was bent down and forward. The lower section of the left door was dented and scratched and was slightly ajar. The left-front tire was cut and deflated. There was no significant rim damage. The front tire on the right side was not damaged and remained inflated. The right-front fender was crushed down and forward due to the barrier impact. A small amount of buckling and gouging occurred at the lower rear of the fender and the lower front of the right-side door. A quarter sized hole and scrape were made on the right side of the pickup truck box slightly in front of and above the wheel well. There was no crushing of the pickup truck's interior

occupant compartment.

5.4 Barrier Damage

Barrier damage was extensive, as shown in Figures 34 through 36. Most of the post damage occurred on the left side of the system. A total of ten posts in the system were fractured. Six of the BCT posts fractured at the hole near the base of the post. Post nos. 1 through 3 on both sides of the barrier were broken in this manner. On the left side of the barrier, CRT post no. 4 was broken at the top hole while post no. 5 was broken at the bottom hole. Posts nos. 6 and 7 on the left side were also broken at ground level.

The damage to the three beam guardrail in the system consisted of buckling and tearing of the guardrail. Major buckles in the rail were formed around post nos. 4 and 7 on the left side of the barrier. Minor tearing of the rail occurred around post nos. 1 and 2 on both sides of the barrier. Additional tearing was observed 508-mm upstream of post no. 2 on the left side of the system. Major tearing was also observed in the nose section of the system. The top hump of the rail was ripped through the entire hump in the nose section beginning 330-mm right of the centerline of the nose, while the bottom hump of the rail in the nose was completely disengaged from the main piece of guardrail. No damage of the cables or the cable plates was found. The maximum longitudinal permanent set deflection of the rail was 11.3-m downstream of the nose of the barrier.

5.5 Occupant Risk Values

The longitudinal and lateral occupant impact velocities (OIV) were determined to be 6.22 m/s and 1.03 m/s, respectively. The maximum 0.010-sec average occupant ridedown deceleration (ORD) in the longitudinal and lateral directions were 10.53 g's and 7.06 g's, respectively. It is noted that the occupant impact velocities and occupant ridedown decelerations were within the suggested

limits provided in NCHRP Report No. 350. The results of the occupant risk data are summarized in Figure 28. Results are shown graphically in Appendix A. The results from the rate transducer are also shown graphically in Appendix A.

5.6 Discussion

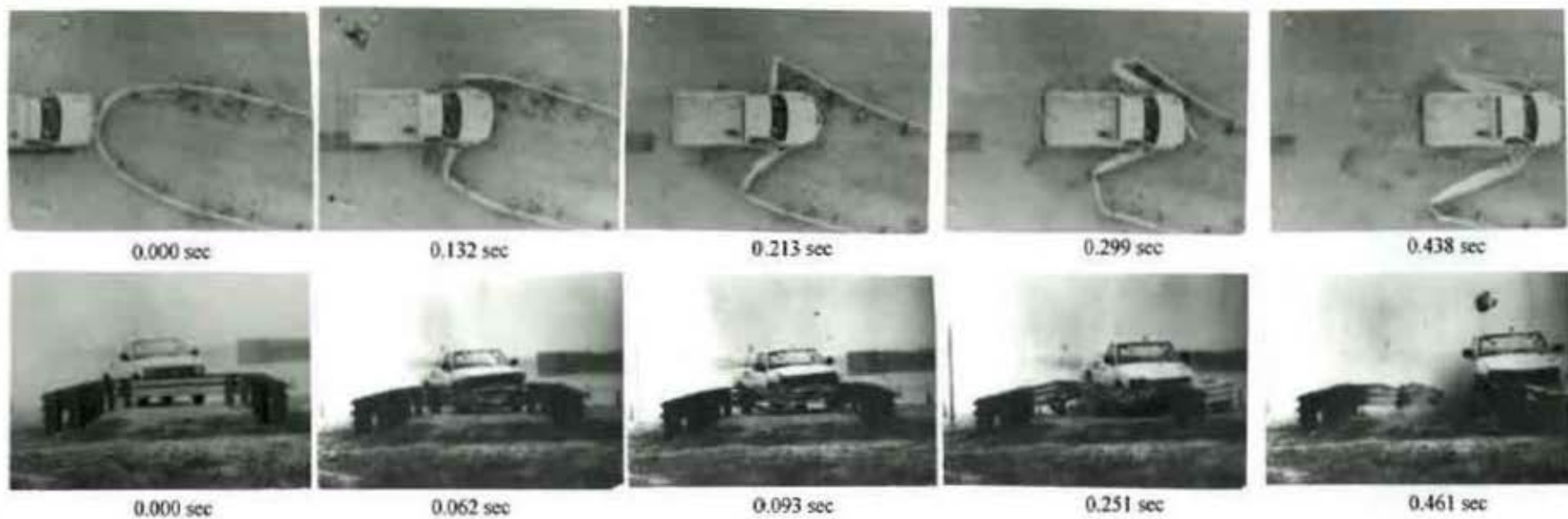
Following test MBN-5, a safety performance evaluation was conducted, and the bullnose barrier design was determined to be acceptable for the test 3-33 impact condition according to NCHRP Report No. 350 criteria. The bullnose barrier successfully contained and stopped the test vehicle in a controlled manner. Detached elements and debris from the test article did not penetrate or show potential for penetrating the occupant compartment. There was no deformation of, or intrusion into, the occupant compartment that could have caused serious injury. The vehicle remained upright during and after collision and the vehicle's trajectory did not intrude into adjacent traffic lanes. Vehicle trajectory behind the test article was acceptable as the test vehicle was captured in the median area behind the bullnose. The occupant impact velocities and ridedown accelerations were within the suggested limits imposed by NCHRP Report No. 350.

The results of this test were cause for redefining the gating/non-gating status of the barrier as well as adjustment of the appropriate test matrix for evaluation of the design. Originally, the bullnose barrier had been defined as a gating system. A gating device is one that is designed to allow controlled penetration of the vehicle when impacted between the beginning and the end of the length of need. Test MBN-5 showed that the bullnose is actually a non-gating terminal as it captured and contained the impacting pickup truck rather than allowing it to penetrate through the barrier. Based on this result, the bullnose barrier system was redefined as a non-gating system. By definition, a non-gating device is one that is designed to contain and redirect a vehicle when impacted

downstream from the nose of the device. Due to the reclassification of the barrier, the NCHRP Report No. 350 test matrix was revised. The modified test matrix is discussed in Section 6.



Figure 27. Impact Location, Test MBN-5



51

- Test Number MBN-5
- Date 8/12/98
- Appurtenance Bullnose Median Barrier
- Total Length 20,144 mm
- Steel Thrie Beam
 - Thickness 12 gauge (2.66 mm)
 - Top Mounting Height 804 mm
- Wood Posts
 - Post Nos. 1 - 3, 10 - 11 140 mm x 190.5 mm x 1080-mm long BCT
 - Post Nos. 4 - 5 150 mm x 200 mm x 1980-mm long CRT
 - Post Nos. 6 - 9 150 mm x 200 mm x 1980-mm long
- Wood Spacer Blocks
 - Post Nos. 2 - 9 150 mm x 200 mm x 360-mm long
- Soil Type Grading B - AASHTO M 147-65 (1990)
- Vehicle Model 1993 Chevy 2500 2WD
 - Curb 2,092 kg
 - Test Inertial 2,039 kg
 - Gross Static 2,039 kg
- Vehicle Speed
 - Impact 103.0 km/hr
 - Exit 0.0 km/hr

- Vehicle Angle
 - Impact 13.4 deg
 - Exit NA
- Vehicle Snagging None
- Vehicle Stability Satisfactory
- Occupant Ridedown Deceleration (10 msec avg.)
 - Longitudinal 10.53 g's
 - Lateral (not required) 7.06 g's
- Occupant Impact Velocity
 - Longitudinal 6.22 m/s
 - Lateral (not required) 1.03 m/s
- Vehicle Damage Moderate
 - TAD⁽¹⁾ 11-FD-3
 - SAE⁽²⁾ 11FDEW2
- Vehicle Stopping Distance 11.26 m downstream
2.66 m left of centerline
- Barrier Damage Extensive rail damage and
ten fractured posts
- Maximum Deflections
 - Permanent Set 11.3-m downstream
 - Dynamic NA

Figure 28. Summary and Sequential Photos, Test MBN-5



0.000 sec



0.074 sec



0.252 sec



0.288 sec



0.454 sec

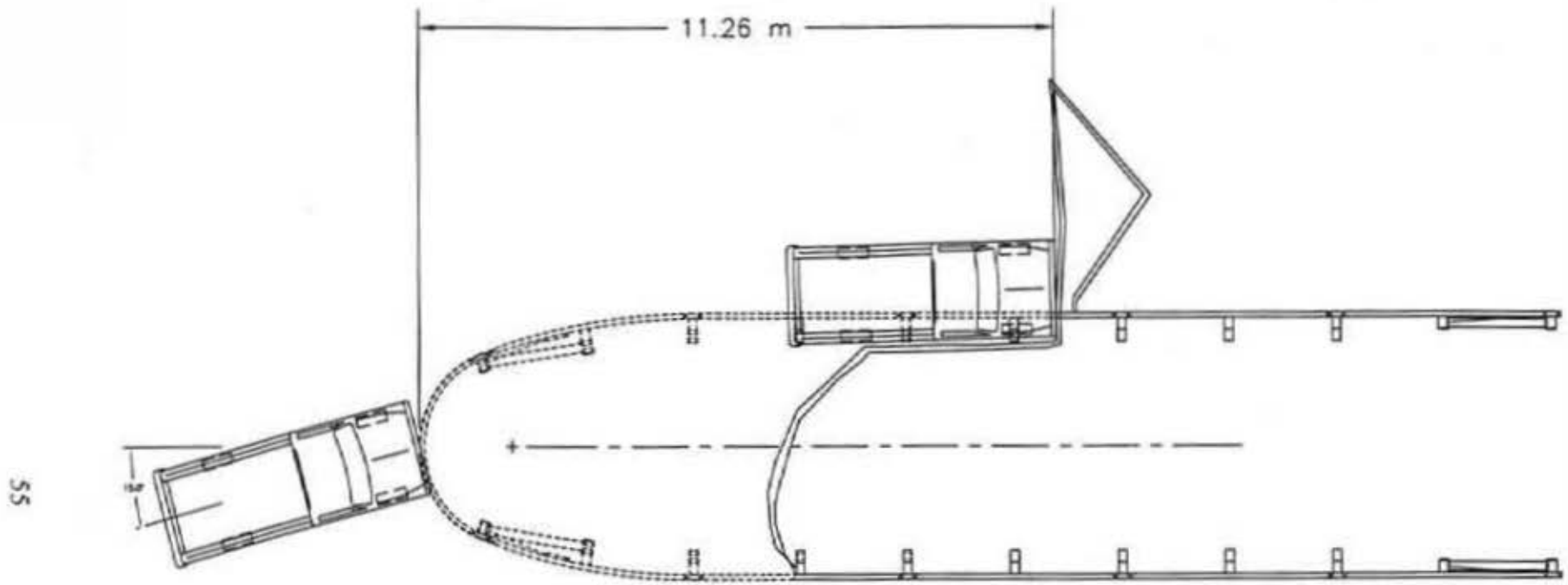
Figure 29. Additional Sequential Photographs, Test MBN-5



Figure 30. Full-Scale Crash Test MBN-5



Figure 31. Full-Scale Crash Test MBN-5



MBN-5 TRAJECTORY

Figure 32. Vehicle Trajectory, MBN-5



Figure 33. Vehicle Damage, Test MBN-5



Figure 34. Barrier Damage, Test MBN-5



Figure 35. Barrier Damage, Test MBN-5



Figure 36. Barrier Damage, Test MBN-5

6 REVISED TEST REQUIREMENTS AND PERFORMANCE EVALUATION

CRITERIA

6.1 Test Requirements

Due to the results from test MBN-5, the bullnose median barrier system was redefined as a non-gating design and therefore must fulfill the NCHRP Report No. 350 evaluation criteria for a non-gating device. As mentioned previously, a non-gating device is one that is designed to contain and redirect a vehicle when impacted downstream from the end of the device. Terminals and crash cushions must satisfy the requirements provided in NCHRP Report No. 350 (1) in order to be accepted for use on new construction projects or as a replacement for existing barriers not meeting current safety standards.

According to NCHRP Report No. 350, terminals and crash cushions must be subjected to eight full-scale vehicle crash tests, five using a 2000-kg pickup truck and three using an 820-kg small car. The required 2000-kg pickup truck crash tests for a Test Level 3 (TL-3) device are: (1) Test 3-31, a 100 km/h impact at a nominal angle of 0 degrees on the tip of the barrier nose; (2) Test 3-33, a 100 km/h impact at a nominal angle of 15 degrees on the tip of the barrier nose; (3) Test 3-37, a 100 km/h impact at a nominal angle of 20 degrees on the beginning of the LON (Length-of-Need); (4) Test 3-38, a 100 km/h impact at a nominal angle of 20 degrees on the Critical Impact Point (CIP); and (5) Test 3-39, a 100km/h reverse direction impact at an angle of 20 degrees one half of the LON from the end of the terminal. The required 820-kg small car crash tests for a TL-3 device are: (1) Test 3-30, a 100 km/h impact at a nominal angle of 0 degrees on the tip of the barrier nose with a ¼-point offset; (2) Test 3-32, a 100 km/h impact at a nominal angle of 15 degrees on the tip of the barrier nose; and (3) Test 3-36, a 100 km/h impact at a nominal impact angle of 15 degrees on the

beginning of the LON. A diagram showing the impact location for the eight crash tests is shown in Figure 37. It is noted that the Critical Impact Point (CIP) mentioned above is defined for non-gating terminals as the point along the installation where it unknown whether the guardrail will capture the impacting vehicle or redirect it.

Previous testing in Phases I and II of this research successfully completed tests 3-30, 3-31, and 3-33. The remainder of Phase III testing was focused on tests 3-32 and 3-38. The next full-scale test of the bullnose median barrier, test MBN-6, was chosen to be NCHRP 350 test 3-38. This test consists of a 2000-kg pickup truck impact at 100 km/h and 20 degrees and at the CIP of the system.

6.2 Evaluation Criteria

Evaluation criteria for full-scale vehicle crash testing are based on three appraisal areas: (1) structural adequacy; (2) occupant risk; and (3) vehicle trajectory after collision. Criteria for structural adequacy are intended to evaluate the ability of the terminal to contain, redirect, or allow controlled vehicle penetration in a predictable manner. Occupant risk evaluates the degree of hazard to occupants in the impacting vehicle. Vehicle trajectory after collision is a measure of the potential for the post-impact trajectory of the vehicle to cause subsequent multi-vehicle accidents, thereby subjecting occupants of other vehicles to undue hazard or to subject the occupants of the impacting vehicle to secondary collisions with other fixed objects. These three evaluation criteria are defined in Table 4.

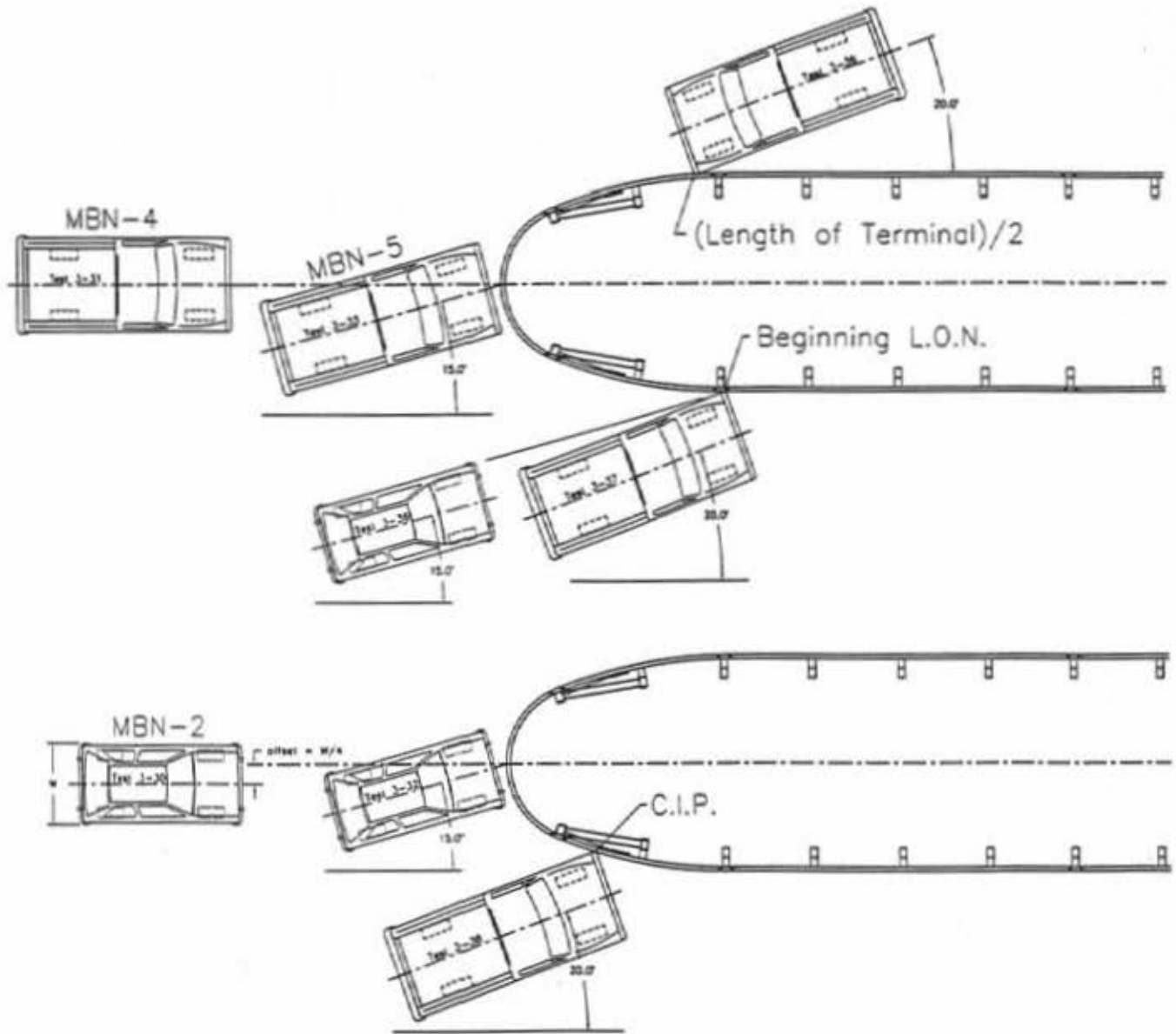


Figure 37. NCHRP 350 Test Matrix for Non-Gating Systems

Table 4. NCHRP Report 350 Evaluation Criteria for 2000P Pickup Truck and 820C Small Car Tests

Evaluation Factors	Evaluation Criteria	Applicable Tests
Structural Adequacy	A. Test article should contain and redirect the vehicle; the vehicle should not penetrate, underide, or override the installation although controlled lateral deflection of the test article is acceptable.	3-36 3-37 3-38
	C. Acceptable test article performance may be by redirection, controlled penetration, or controlled stopping of the vehicle.	3-30 3-31 3-32 3-33 3-39
Occupant Risk	D. Detached elements, fragments or other debris from the test article should not penetrate or show potential for penetrating the occupant compartment, or present an undue hazard to other traffic, pedestrians, or personnel in a work zone. Deformations of, or intrusions into, the occupant compartment that could cause serious injuries should not be permitted.	ALL
	F. The vehicle should remain upright during and after collision although moderate roll, pitching, and yawing are acceptable.	ALL
	H. Occupant impact velocities should satisfy the following: Occupant Impact Velocity Limits (m/s) <u>Component</u> Longitudinal and Lateral	3-30 3-31 3-32 3-33 3-36
	I. Occupant ridedown accelerations should satisfy the following: Occupant Ridedown Acceleration Limits (G's) <u>Component</u> Longitudinal and Lateral	3-30 3-31 3-32 3-33 3-36
Vehicle Trajectory	K. After collision it is preferable that the vehicle's trajectory not intrude into adjacent traffic lanes.	ALL
	L. The occupant impact velocity in the longitudinal direction should not exceed 12 m/sec and the occupant ridedown acceleration in the longitudinal direction should not exceed 20 G's.	3-37 3-38 3-39
	M. The exit angle from the test article preferably should be less than 60 percent of the test impact angle, measured at the time the vehicle lost contact with the device.	3-36 3-37 3-38 3-39
	N. Vehicle trajectory behind the test article is acceptable.	3-30 3-31 3-32 3-33 3-39

7 CRASH TEST MBN-6

7.1 Test MBN-6

Test MBN-6 was conducted according to NCHRP Report No. 350 test 3-38 impact conditions. The 2,031-kg pickup truck impacted the bullnose barrier with the left-front corner of the vehicle aligned midway between posts nos. 1 and 2 on the right-side of the barrier, as shown in Figure 38, at a speed of 101.5 km/h and an angle of 20.4 degrees. A summary of the test results and the sequential photographs are shown in Figure 39. Additional sequential photographs are shown in Figure 40. Full-scale crash documentary photographs are shown in Figures 41 and 42. It is noted that the bullnose system design used for test MBN-6 remained unchanged from the configuration used in test MBN-5.

7.2 Test Description

Following the initial impact with the pickup truck, the thrie beam rail immediately began to deform inward. At 0.041 sec after impact, post no. 2 on the right side fractured due to the impact with the left front of the pickup truck, thus allowing the guardrail to deflect inward considerably. Subsequently, the left-front tire of the pickup truck rode up and over the ground line strut and snagged on post no. 2, causing the tire to rotate counter clockwise into the guardrail. As the pickup penetrated farther into the barrier, it impacted and fractured post no. 3 on the right side at 0.089 sec. However, post no. 3 did not detach from the guardrail but instead remained attached to the rail, pulling the guardrail downward as it fractured. The top of the guardrail displaced back laterally farther than the bottom of the rail, thus forming a ramp for the tire to climb up and over. The left-front tire began to ride up the ramp formed by the deformation of the rail at 0.105 sec. By 0.153 sec, the left-front tire was on top of the thrie beam. Subsequently, post no. 4 on the right side fractured;

however, it remained attached to the guardrail and pulled it downward in a similar manner to post no. 3. The right-front tire rode up the broken post no. 4 and onto the rail. At 0.253 sec, the entire front of the pickup truck had ridden up and over the top of the rail. The back wheel then traveled up and over the guardrail near post no. 2 on the right side. The pickup truck became completely airborne and lost contact with the guardrail at 0.384 sec. At 1.110 sec after impact, the truck returned to the ground, just clearing the installation and landing on its side. The truck slid to a stop 35.1-m downstream of the end of the installation. The trajectory of the pickup truck during the crash test and the final position of the vehicle are provided in Figure 43.

7.3 Vehicle Damage

The extensive vehicle damage, occurring as a result of the vehicle vaulting over the system upon impact, is shown in Figure 44. Significant undercarriage damage was observed on the vehicle along with extensive body damage. There was also considerable crushing of the pickup truck's interior occupant compartment. It is noted that it is difficult to determine the amount and extent of the damage caused by interaction with the guardrail as opposed to damage caused with vehicle vaulting and subsequent rollover of the vehicle.

7.4 Barrier Damage

Barrier damage was moderate, as shown in Figures 45 through 47. All of the post damage occurred to the right side of the system. The first five posts on the right side of the system were fractured. Although post no. 1 was split down the centerline, starting at the top and ending at the top of the foundation tube, it did not break away completely. BCT post nos. 2 and 3 fractured through the holes at ground level. CRT post no. 4 was broken at the bottom hole. The fracture of post no. 5 was observed at both the top and bottom holes in the post. The bolts attaching post no. 4 and 5 to the

guardrail did not pull through the rail and remained in place during the impact.

The damage to the three beam guardrail in the system was moderate due to the limited interaction of the impact vehicle with the system prior to vaulting. No major tearing of the guardrail was observed. Buckles in the rail were formed 279-mm upstream of post no. 1 and at post no. 6 on the right side of the barrier. The three beam between post nos. 1 through 6 was deformed and pushed down. No damage of the cables or the cable plates was found.

7.5 Occupant Risk Values

The longitudinal and lateral occupant impact velocities (OIV) were determined to be 6.22 m/s and 2.41 m/s, respectively. The maximum 0.010-sec average occupant ridedown deceleration (ORD) in the longitudinal and lateral directions was 2.08 g's and 4.46 g's, respectively. It is noted that the occupant impact velocities and occupant ridedown decelerations, as determined by the vehicle contact with the barrier before rollover, were within the suggested limits provided in NCHRP Report No. 350. The results of the occupant risk data are summarized in Figure 39. Results are shown graphically in Appendix B. A rate transducer malfunction prevented rate transducer data from being collected in test MBN-6.

7.6 Discussion

Following test MBN-6, a safety performance evaluation was conducted, and the bullnose barrier design was determined to be unacceptable for the test 3-38 impact condition according to the NCHRP Report No. 350 criteria. The bullnose barrier failed to contain and stop the test vehicle in a controlled manner due to the vehicle override and vaulting. Detached elements and debris from the test article did not penetrate or show potential for penetrating the occupant compartment. As a result of vehicle rollover, there was significant deformation of, or intrusion into, the occupant compartment

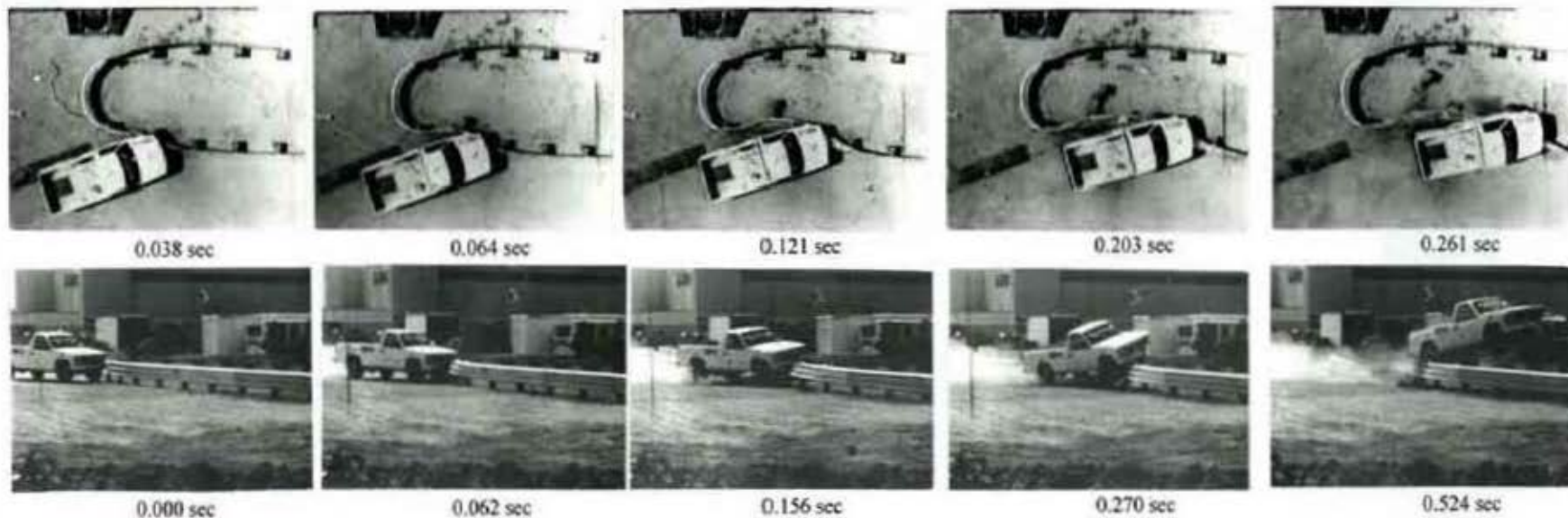
that could have caused serious injury. The vehicle did not remain upright during and after collision, and the vehicle's trajectory likely intruded into adjacent traffic lanes. Vehicle trajectory behind the test article was unacceptable as the test vehicle vaulted and became airborne in the median area behind the bullnose.

The failure of test MBN-6 to meet all of the safety performance criteria was directly attributed to the vaulting of the pickup truck. The pickup truck rode up the guardrail between post nos. 2 through 4 on the right side of the system. Two factors were believed to have attributed to the vehicle climbing and vaulting over the system. The first contributing factor which led to the failure of the system was a lack of sufficient guardrail tension developed upstream of the impact point. A second factor was that little lateral resistance was provided by the posts as post nos. 3 and 4 fractured on the right side. As these posts rotated and fractured, they remained bolted to the guardrail and pulled it down towards the ground.¹ The lack of tension and lateral resistance allowed the pickup truck to penetrate into the guardrail with increased rail deflection and rotation and without the vehicle being captured or redirected. This combination turned the guardrail into an effective ramp for the impacting pickup truck to climb up and vault over.

As a result of the failed test, design changes were necessary to allow the successful containment or redirection of the pickup truck. This meant that the three beam rail would need to remain upright and functional long enough in order to capture the front of the impacting vehicle, thus preventing vehicle climbing, vaulting, and rollover. These changes required that the rail tension and lateral stiffness be increased without adversely affecting the head-on impact performance of either the pickup truck or small car impacts.



Figure 38. Impact Location, Test MBN-6



- Test Number MBN-6
- Date 9/16/98
- Appurtenance Bullnose Median Barrier
- Total Length 20,144 m
- Steel Thrie Beam
 - Thickness 12 gauge (2.66 mm)
 - Top Mounting Height 804 mm
- Wood Posts
 - Post Nos. 1 - 3, 10 - 11 140 mm x 190.5 mm x 1080-mm long BCT
 - Post Nos. 4 - 5 150 mm x 200 mm x 1980-mm long CRT
 - Post Nos. 6 - 9 150 mm x 200 mm x 1980-mm long
- Wood Spacer Blocks
 - Post Nos. 2 - 9 150 mm x 200 mm x 360-mm long
- Soil Type Grading B - AASHTO M 147-65 (1990)
- Vehicle Model 1991 Chevy 2500 2WD
 - Curb 2,055 kg
 - Test Inertial 2,031 kg
 - Gross Static 2,031 kg
- Vehicle Speed
 - Impact 101.5 km/hr
 - Exit NA

- Vehicle Angle
 - Impact 20.4 deg
 - Exit NA
- Vehicle Snagging None
- Vehicle Stability Unsatisfactory/Rollover
- Occupant Ridedown Deceleration (10 msec avg.)
 - Longitudinal 2.08 g's
 - Lateral (not required) 4.46 g's
- Occupant Impact Velocity
 - Longitudinal 6.22 m/s
 - Lateral (not required) 2.41 m/s
- Vehicle Damage Extensive (Rollover)
 - TAD^(L) NA
 - SAE^(L) NA
- Vehicle Stopping Distance 52.29 m downstream
5.98 m left of centerline
- Barrier Damage Moderate rail damage and five fractured posts
- Maximum Deflections
 - Permanent Set NA
 - Dynamic NA

Figure 39. Summary and Sequential Photographs, Test MBN-6



0.000 sec



0.041 sec



0.099 sec



0.169 sec



0.232 sec

Figure 40. Additional Sequential Photographs, Test MBN-6



Figure 41. Full-Scale Crash Test, Test MBN-6



Figure 42. Full-Scale CrashTest, Test MBN-6

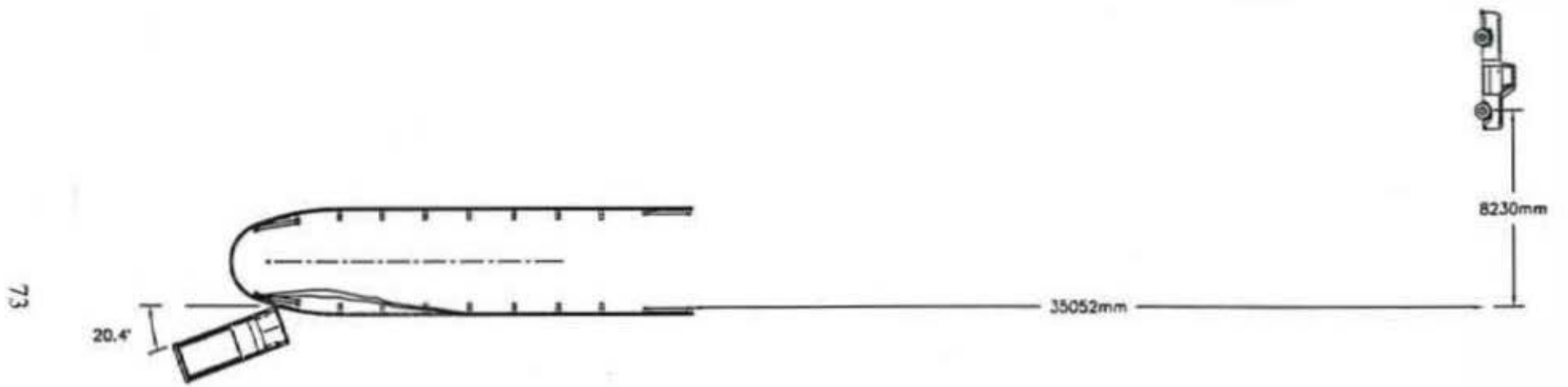


Figure 43. Vehicle Trajectory, Test MBN-6



Figure 44. Vehicle Damage, Test MBN-6



Figure 45. Barrier Damage, Test MBN-6



Figure 46. Barrier Damage, Test MBN-6



Figure 47. Barrier Damage, Test MBN-6

8 BARRIER MODIFICATIONS (DESIGN FOR MBN-7)

8.1 Modification of Bullnose Design

The bullnose barrier system was modified prior to conducting the third full-scale crash test of Phase III, test MBN-7. The full-scale test results of test MBN-6 demonstrated the importance of keeping the three beam rail upright and functional long enough in order to sufficiently capture the front of the impacting vehicle and prevent vehicle climbing and vaulting over the system. The failure of the guardrail in test MBN-6 to remain upright and functional can be attributed to a lack of sufficient tension in the guardrail upstream of the impact and a lack of lateral resistance in the barrier system. These factors were believed to have allowed the guardrail to deform and rotate excessively, and therefore design changes in the bullnose barrier were deemed necessary prior to performing test MBN-7.

Four modifications were made to the bullnose median barrier prior to conducting test MBN-7. These changes were intended to strengthen the guardrail in the area of the critical impact point without sacrificing the ability of the nose of the system to safely bring the previously tested head-on impacts to a controlled stop. First, the third post on each side of the system was changed from a BCT post to a CRT post. Second, two CRT posts were also added to each side of the system. The two new posts were placed midway between post nos. 2 and 3 and midway between post nos. 3 and 4 in the previous design. These posts were added in order to increase the lateral resistance in the barrier system, thus increasing the rails ability to capture and contain the impacting vehicle. Thirdly, the SKT soil tubes used with post nos. 1 and 2 were changed to standard, non-proprietary foundation tubes to eliminate any perceived conflicts in their use in the final design. The final modification was made to the second section of three beam rail. The addition of new posts to the system made it necessary to change the slot pattern in rail section no. 2 in order to allow for proper connection of the rail to the posts. The modified design is shown in Figures 48 through 50.

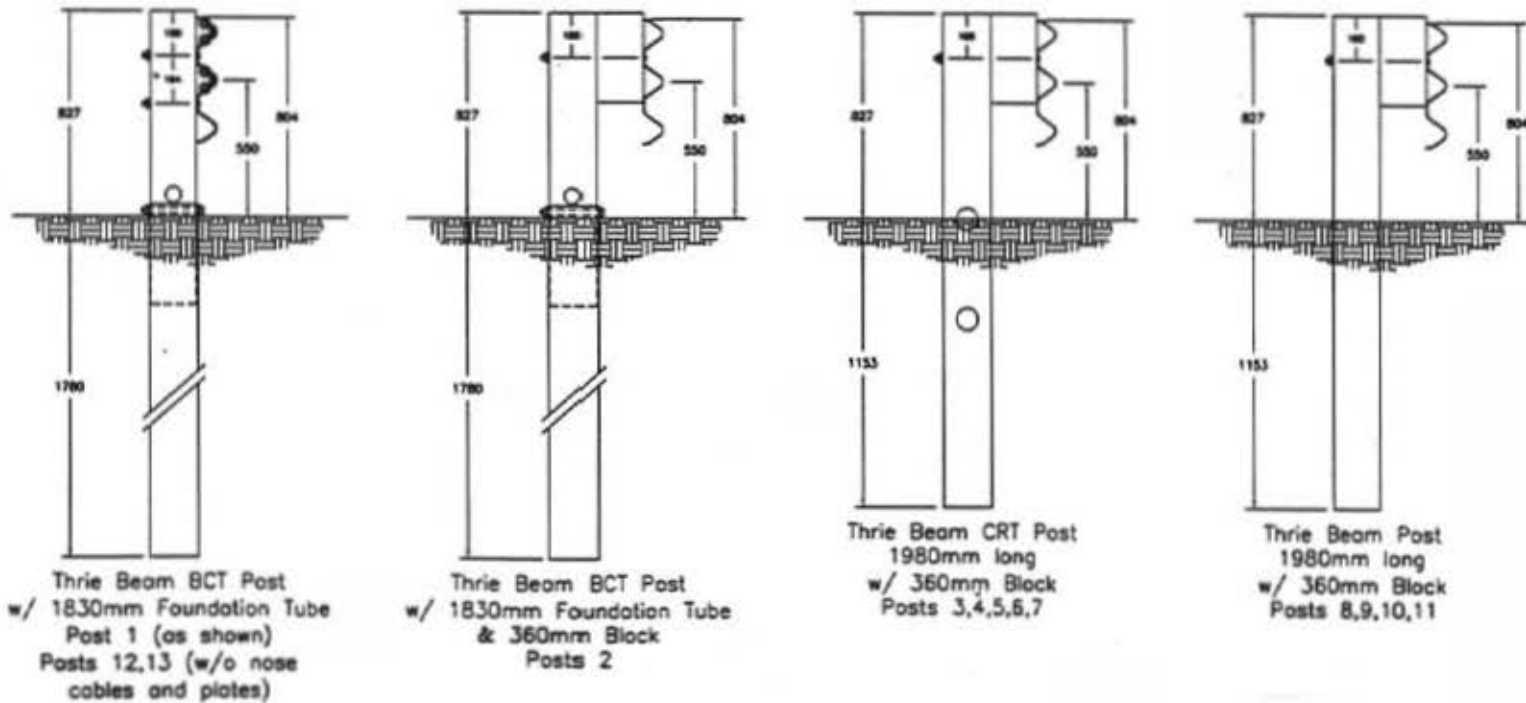
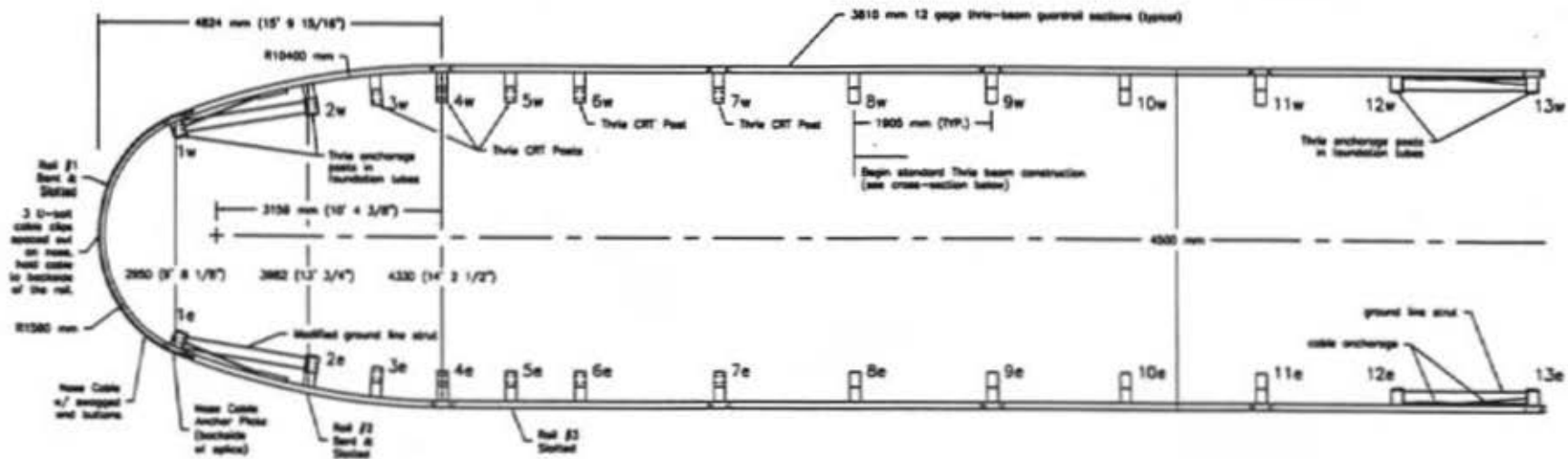
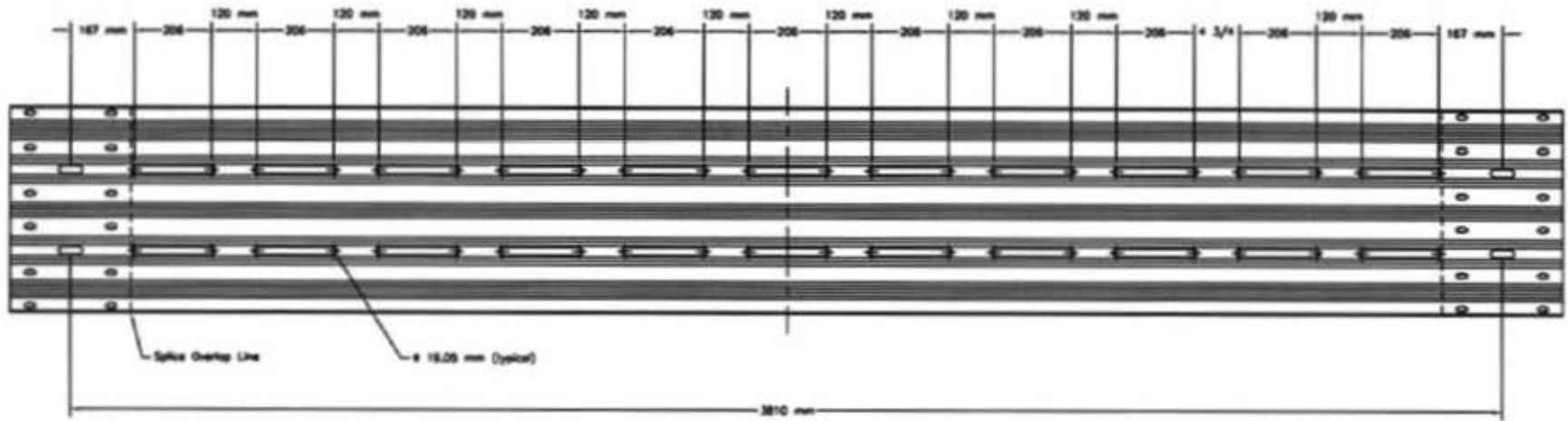
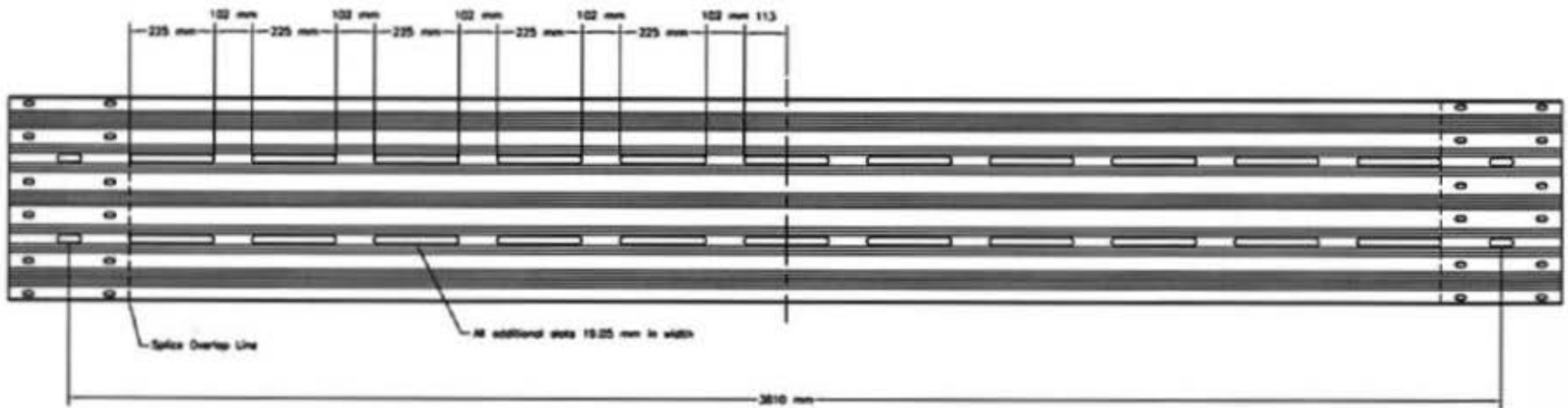


Figure 48. Bullnose Barrier Design, Test MBN-7



Rail Section 2

80



Rail Section 2

Figure 49. Modified Rail Section No. 2, Test MBN-7



Figure 50. Bullnose Design, Test MBN-7

9 CRASH TEST MBN-7

9.1 Test MBN-7

Test MBN-7 was conducted according to the NCHRP 350 test 3-38 impact conditions which are the same conditions used in test MBN-6. The 2,036-kg pickup truck impacted the bullnose barrier with the left-front corner of the vehicle aligned midway between post nos. 1 and 2, as shown in Figure 51, and at a speed of 100.0 km/h and at an angle of 24.9 degrees. A summary of the test results and the sequential photographs are shown in Figure 52. Additional sequential photographs are shown in Figure 53. Full-scale crash documentary photographs are shown in Figure 54.

9.2 Test Description

Following the initial impact with the pickup truck, the three beam rail immediately began to deform inward. At 0.026 sec after impact, the left front of the pickup truck impacted post no. 2 on the right side, causing it to deflect backward. The middle front of the pickup hit post no. 3 just as post no. 2 fractured at 0.052 sec. As the pickup penetrated farther into the barrier, post no. 4 on the right side was fractured as the front of the pickup truck impacted it at 0.104 sec. At 0.123 sec, post no. 1 on the right side fractured due to the lateral loading exerted from the vehicle onto the rail. This post fracture eliminated the cable anchor as well as any rail tension provided by the cable on that side. These post failures allowed the three beam to move longitudinally with the truck instead of providing the adequate resistance needed to capture the vehicle. This longitudinal movement allowed the three beam to lay down and rotate backward, thus creating a ramp for the vehicle to climb up and over the rail instead of capturing and redirecting the vehicle. The left-front wheel of the pickup truck began to travel over the three beam near post no. 5 at 0.152 sec. Subsequently, the right-front wheel traveled over the rail which pulled the truck toward the right. The truck continued to travel up and

over the rail until 0.597 sec after impact when the right-rear wheel of the pickup truck snagged on the guardrail while passing over it. This wheel snagging caused the front of the pickup to rotate down and toward the right. At 0.771 sec, the right-front side of the pickup contacted the ground after the right-rear tire disengaged from the rail. The momentum of the truck continued forward, rotating the back of the pickup forward over the right front of the truck, causing the vehicle to cartwheel across the system. The pickup truck then impacted the left side of the system as it continued to cartwheel, striking the top of the rail between post nos. 11 and 12 before coming to rest on its side approximately 5.5 m to the left of the system. The trajectory of the pickup truck during the crash test and the final position of the vehicle are provided in Figure 55.

9.3 Vehicle Damage

The moderate vehicle damage, occurring as a result of the vehicle vaulting over the system and rolling over upon impact, is shown in Figure 56. Minor undercarriage damage was observed on the vehicle. The right side of the front bumper was bent inward and around the frame rails. Minor buckling of the right-front fender was also found. The right front of the frame was bent significantly; however, it was believed that this damage occurred during the rollover event and not during the impact with the guardrail. There was no crushing or damage to the pickup truck's interior occupant compartment. It is noted that it is difficult to determine the amount and extent of the damage caused by interaction with the guardrail as opposed to damage caused with vehicle vaulting and subsequent rollover of the vehicle.

9.4 Barrier Damage

Barrier damage was extensive, as shown in Figures 57 through 59. All of the post damage occurred to the right side of the system. The first seven posts on the right side of the system were

fractured. BCT post nos. 1 and 2 fractured through the hole at ground level. CRT post no. 3 broke at the bottom hole, while CRT post no. 4 was fractured cleanly at the top hole. The fracture of post no. 5 was observed near the bottom hole in the post, while CRT post nos. 6 and 7 broke through the top hole near ground level.

The damage to the three beam guardrail in the system was more significant than was observed in test MBN-6 due to the improved vehicle interaction with the guardrail. Buckling of the rail on the right side occurred at three locations - 254-mm upstream of post no. 1, midway between post nos. 6 and 7, and near post no. 8. Buckling of the rail on the left side occurred at post no. 1. Tearing of the guardrail was observed upstream of post no. 1 on the right side of the barrier as well as in the top hump of the rail at two locations 381-mm upstream and 127-mm downstream of post no. 2. Major tearing of all three humps occurred 381-mm downstream of post no. 6 on the right side. The top of the guardrail was dented between post nos. 11 and 12 on the left side of the barrier when the vehicle rolled over. No damage to the cables or the cable plates was found.

9.5 Occupant Risk Values

The longitudinal and lateral occupant impact velocities (OIV) were determined to be 7.44 m/s and -1.38 m/s, respectively. The maximum 0.010-sec average occupant ridedown deceleration (ORD) in the longitudinal and lateral directions was 7.01 g's and 5.79/-5.57 g's, respectively. It is noted that the occupant impact velocities and occupant ridedown decelerations, as only determined by the vehicle contact with the barrier before rollover, were within the suggested limits provided in NCHRP Report No. 350. The results of the occupant risk data are summarized in Figure 52. Results are shown graphically in Appendix C. The results from the rate transducer are also shown graphically in Appendix C.

9.6 Discussion

Following test MBN-7, a safety performance evaluation was conducted, and the bullnose barrier design was determined to be unacceptable for the test 3-38 impact conditions according to the NCHRP Report No. 350 criteria. The bullnose barrier failed to contain and stop the test vehicle in a controlled manner due to the vehicle override and vaulting. Detached elements and debris from the test article did not penetrate or show potential for penetrating the occupant compartment. There was no significant deformation of, or intrusion into, the occupant compartment that could have caused serious injury. The vehicle did not remain upright during and after collision, and the vehicle's trajectory likely intruded into adjacent traffic lanes. Vehicle trajectory behind the test article was unacceptable as the test vehicle vaulted and became airborne in the median area behind the bullnose.

The failure of test MBN-7 to meet all of the safety performance criteria was directly attributed to the vaulting of the pickup truck. The pickup truck rode up the guardrail near post no. 5 on the right side of the system. The cause of the vaulting of the pickup truck in test MBN-7 was similar to what was observed during test MBN-6. Two factors were believed to have attributed to the vehicle climbing and vaulting over the system. The first contributing factor which led to the failure of the system was a lack of sufficient guardrail tension developed upstream of the impact point. After the failure of post no. 1 and the accompanying loss of the cable anchorage, there was not sufficient tension in the guardrail to safely redirect and contain the vehicle. A second factor was that insufficient lateral resistance was provided by the fractured posts fractured on the right side of the barrier. The lack of tension and lateral resistance allowed the pickup truck to penetrate into the guardrail with increased rail deflection and rotation and without the vehicle being captured or redirected. This combination turned the guardrail into an effective ramp for the impacting pickup

truck to climb up and vault over.

As a result of the failed test, design changes were necessary to allow the successful containment or redirection the pickup truck. This meant that the thrie beam rail would need to remain upright and functional long enough in order to capture the front of the impacting vehicle, thus preventing vehicle climbing, vaulting, and rollover. These changes required that the rail tension and lateral stiffness be increased without adversely affecting the head-on impact performance of either the pickup truck or small car impacts. Subsequently, computer simulation modeling of the previous two failures was performed in order to investigate the design flaws in the bullnose system as well as to investigate potential solutions.

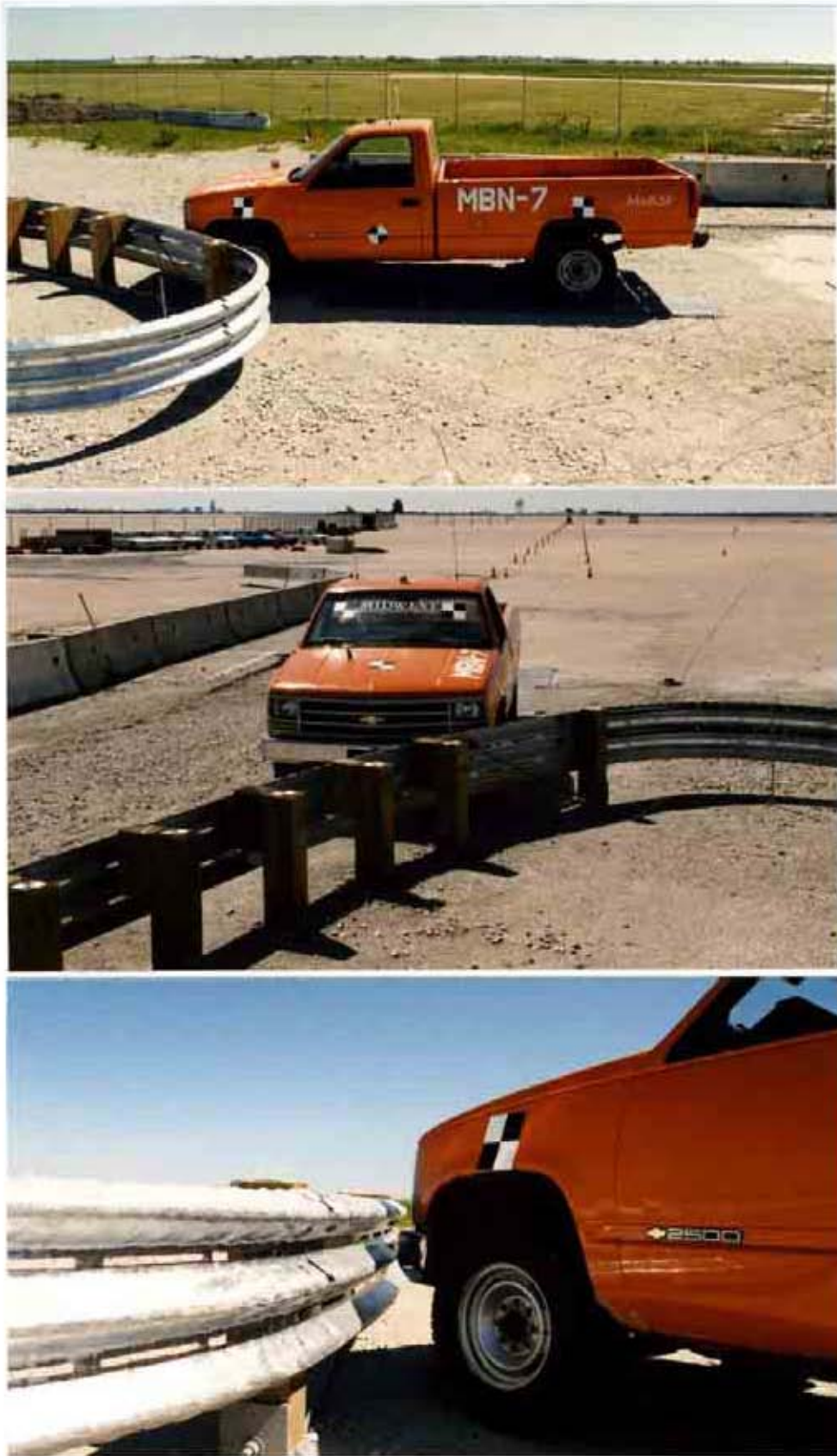
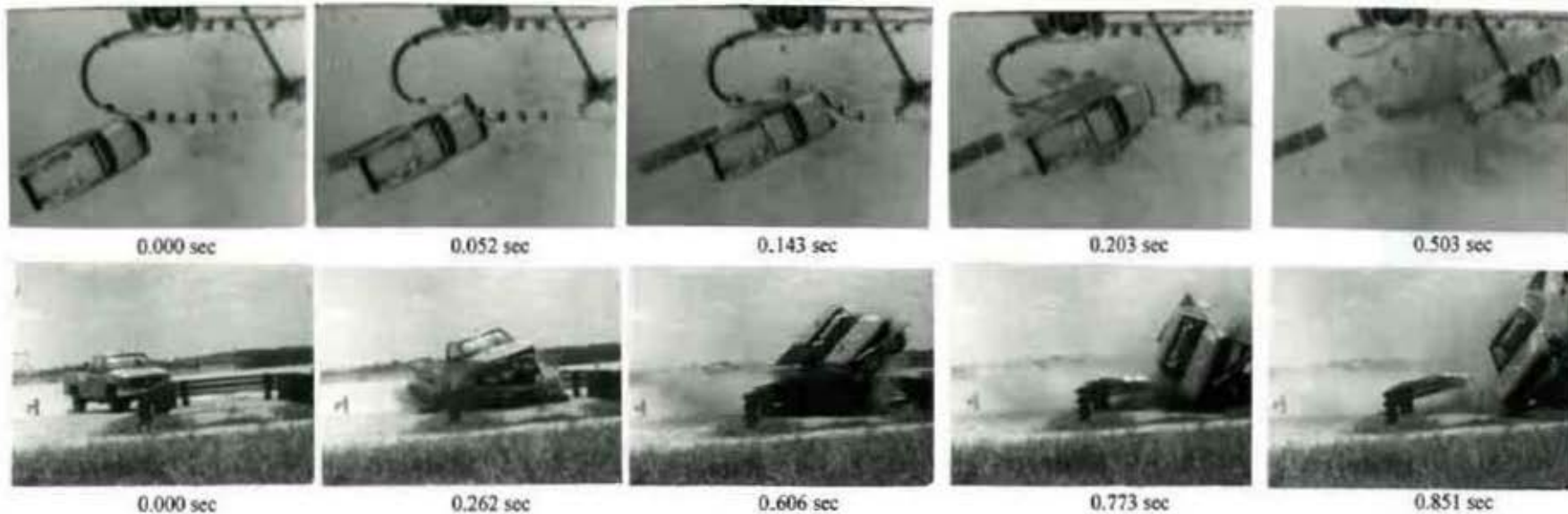


Figure 51. Impact Location, Test MBN-7



88

- Test Number MBN-7
- Date 5/24/99
- Appurtenance Bullnose Median Barrier
- Total Length 20,144 mm
- Steel Thrie Beam
 - Thickness 12 gauge (2.66 mm)
 - Top Mounting Height 804 mm
- Wood Posts
 - Post Nos. 1 - 2, 12 - 13 140 mm x 190.5 mm x 1080-mm long BCT
 - Post Nos. 3 - 7 150 mm x 200 mm x 1980-mm long CRT
 - Post Nos. 8 - 11 150 mm x 200 mm x 1980-mm long
- Wood Spacer Blocks
 - Post Nos. 2 - 11 150 mm x 200 mm x 360-mm long
- Soil Type Grading B - AASHTO M 147-65 (1990)
- Vehicle Model 1992 Chevy 2500 2WD
 - Curb 2,142 kg
 - Test Inertial 2,036 kg
 - Gross Static 2,036 kg
- Vehicle Speed
 - Impact 100.0 km/hr
 - Exit NA

- Vehicle Angle
 - Impact 24.9 deg
 - Exit NA
- Vehicle Snagging None
- Vehicle Stability Unsatisfactory/Rollover
- Occupant Ridedown Deceleration (10 msec avg.)
 - Longitudinal 7.01 g's
 - Lateral (not required) 5.79/-5.57 g's
- Occupant Impact Velocity
 - Longitudinal 7.44 m/s
 - Lateral (not required) -1.38 m/s
- Vehicle Damage Moderate (Rollover)
 - TAD[Ⓢ] NA
 - SAE[Ⓢ] NA
- Vehicle Stopping Distance 16.35 m downstream
7.74 m left of centerline
- Barrier Damage Extensive rail damage and seven fractured posts
- Maximum Deflections
 - Permanent Set NA
 - Dynamic NA

Figure 52. Summary and Sequential Photographs, Test MBN-7



0.000 sec



0.050 sec



0.107 sec



0.143 sec



0.250 sec

Figure 53. Additional Sequential Photographs, Test MBN-7



Figure 54. Full-Scale Crash Test, Test MBN-7

MBN-7

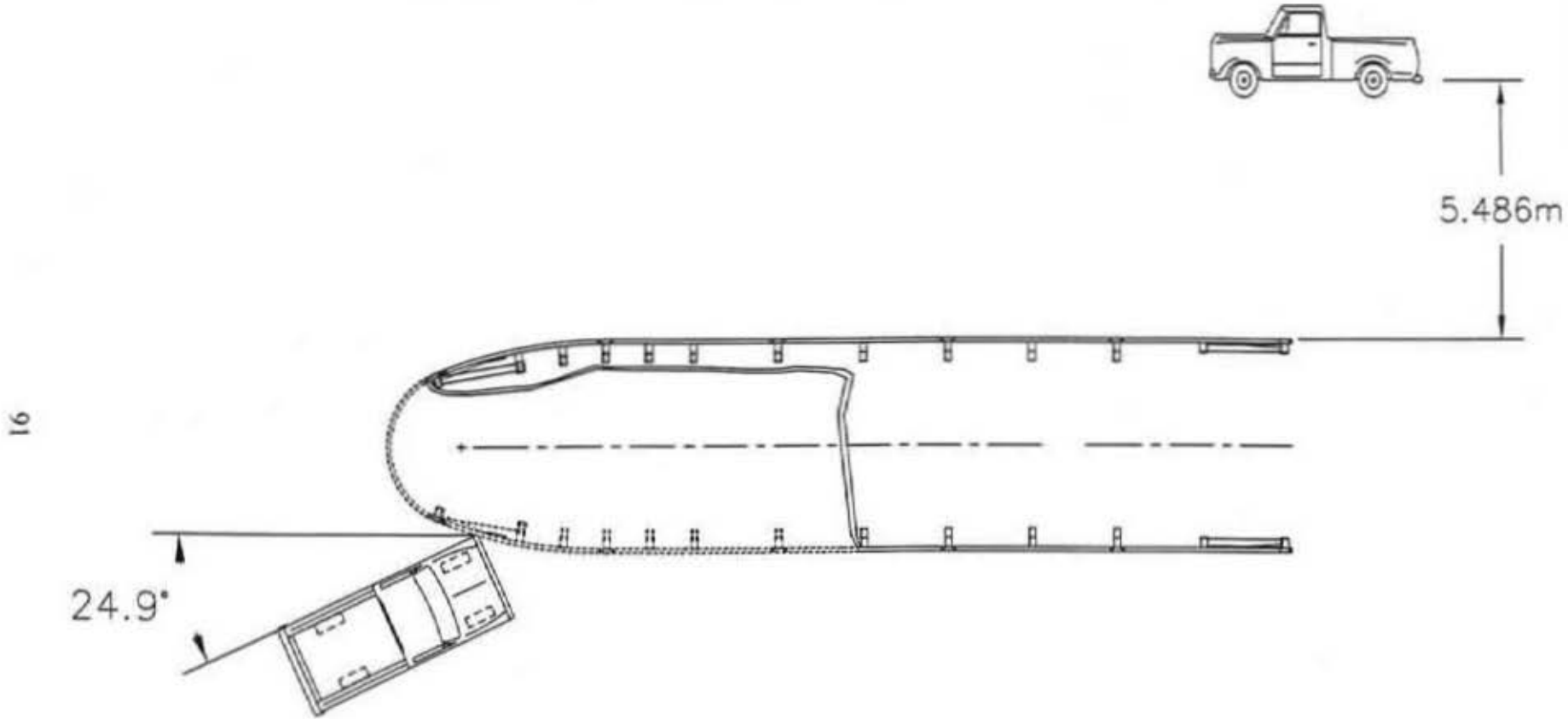


Figure 55. Vehicle Trajectory, Test MBN-7



Figure 56. Vehicle Damage, Test MBN-7



Figure 57. Barrier Damage, Test MBN-7



Figure 58. Barrier Damage, Test MBN-7



Figure 59. Barrier Damage, Test MBN-7

10 COMPUTER SIMULATION

10.1 Introduction

Nonlinear finite element analysis (FEA) using LS-DYNA (19) was performed to analyze and evaluate the bullnose system throughout its development. Previously, the FEA application for the frontal impact scenario was described in the Phase II report (3). This section describes the FEA application for the critical impact point (CIP) scenario. The previous failures of test nos. MBN-6 and MBN-7 had established the difficulty of impacting the CIP, and it was hoped that simulation could aid the search for a possible solution.

10.2 Transition from Frontal to CIP

To simulate the CIP scenario, the frontal impact model had to be converted to a model suitable for impacts along the side of the bullnose. This transition required a considerable amount of modeling effort. Since this modeling effort did not directly contribute to the analysis and design, it will not be documented in this section. However, from a modeling viewpoint, there was much gained by this transition modeling effort and thus, a conference paper was published documenting the work (20). A copy of that conference paper is attached as Appendix D.

10.3 MBN-6 Simulation and Analysis

MBN-6 was the CIP impact with a 2000-kg truck at 100 km/h and at 20 degrees. During the test, the rail began to roll over, forming a ramp which caused the truck to ride up and over the system. Simulating this event was the first step in the analysis. The CIP model and MBN-6 simulation of the event is shown in Figure 60. From the front-end view, it can be seen that the rail has rolled over, and the truck begins to climb up the rail.

By careful inspection of the simulation results, it was determined that the tire/suspension



Figure 60. MBN-6 Simulation

system influenced the truck ride up the rail due to the tire impacting the ground line strut. A cut away view of this behavior is shown in Figure 61. Examination and comparison of overhead views of both the MBN-6 simulation and full-scale testing showed that when the vehicle reaches post no. 3 the rail rollover becomes evident, as shown in Figure 62. When the baseline model is modified by removing the ground line strut and replacing post nos. 1 and 2 with longer posts, the tire-strut interaction is eliminated. Simulation results of this modified model shows noticeable improvement in the rail behavior, as shown in Figure 63.

10.4 Design Modifications

In addition to the ground line strut being removed, three additional modifications were made to the bullnose system model to improve its performance for the CIP impact. First, half-post spacing was used between original post nos. 1 and 4. This change added three new posts to each side of the system. Second, chamfered blockouts were used to improve the ability of the rail to wrap around the top of the tire and thus, get improved interlocking between the rail and the vehicle, as shown in Figure 64. Finally, double blockouts were used to reduce tire snag as well as to hold the rail higher for longer time as the post rotates during the impact. This is shown in Figure 65.

10.5 Final Design Simulation

Before running full-scale test MBN-8, the design modifications were made to the LS-DYNA model. The modified model is shown in Figure 66. Results indicated that the new design would safely capture the truck, as shown in Figure 67. Recall that the CIP test is defined as the impact condition where it was not known whether the bullnose would capture or redirect the vehicle. Physical testing later verified these results.

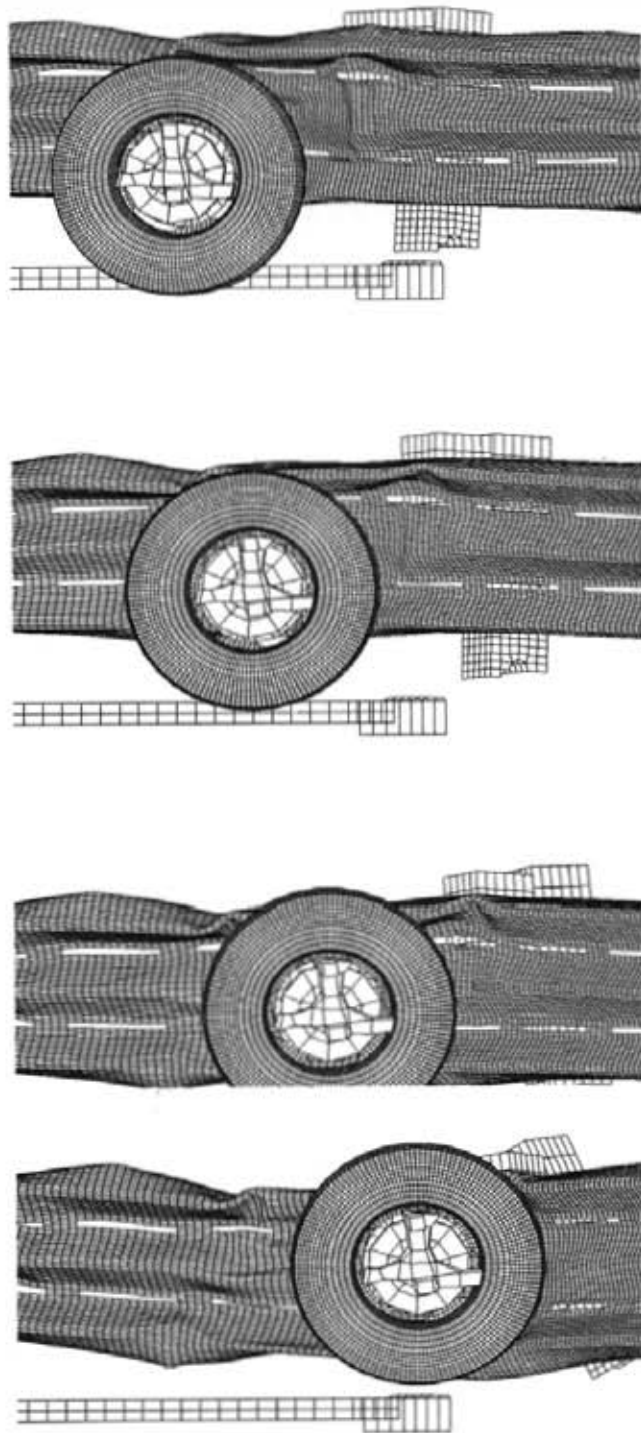


Figure 61. Ground Strut Influences Tire Behavior



Figure 62. MBN-6 Top View - Test and Simulation



Figure 63. No Strut Simulation - Rail Does Not Roll Over

Time - 35

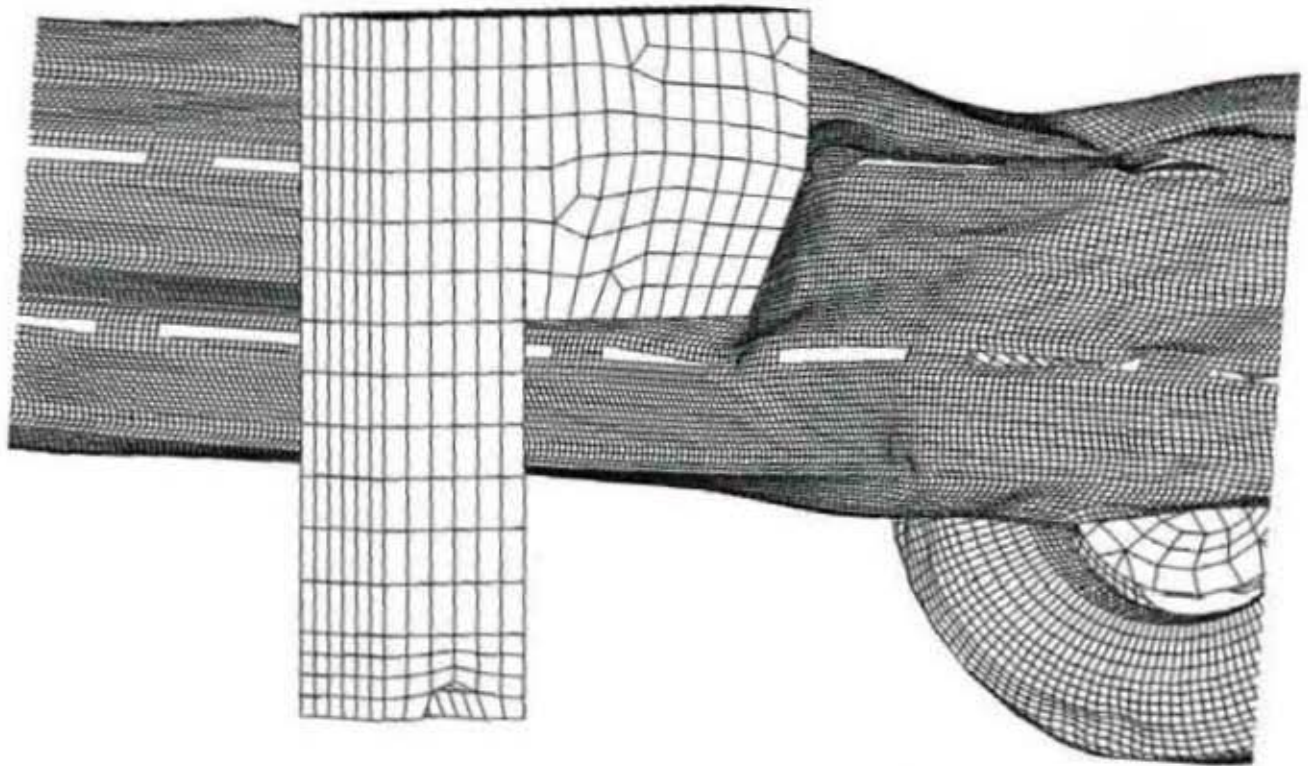


Figure 64. Chamfered Blockout Allows Rail to Wrap Around Tire

Time - 65

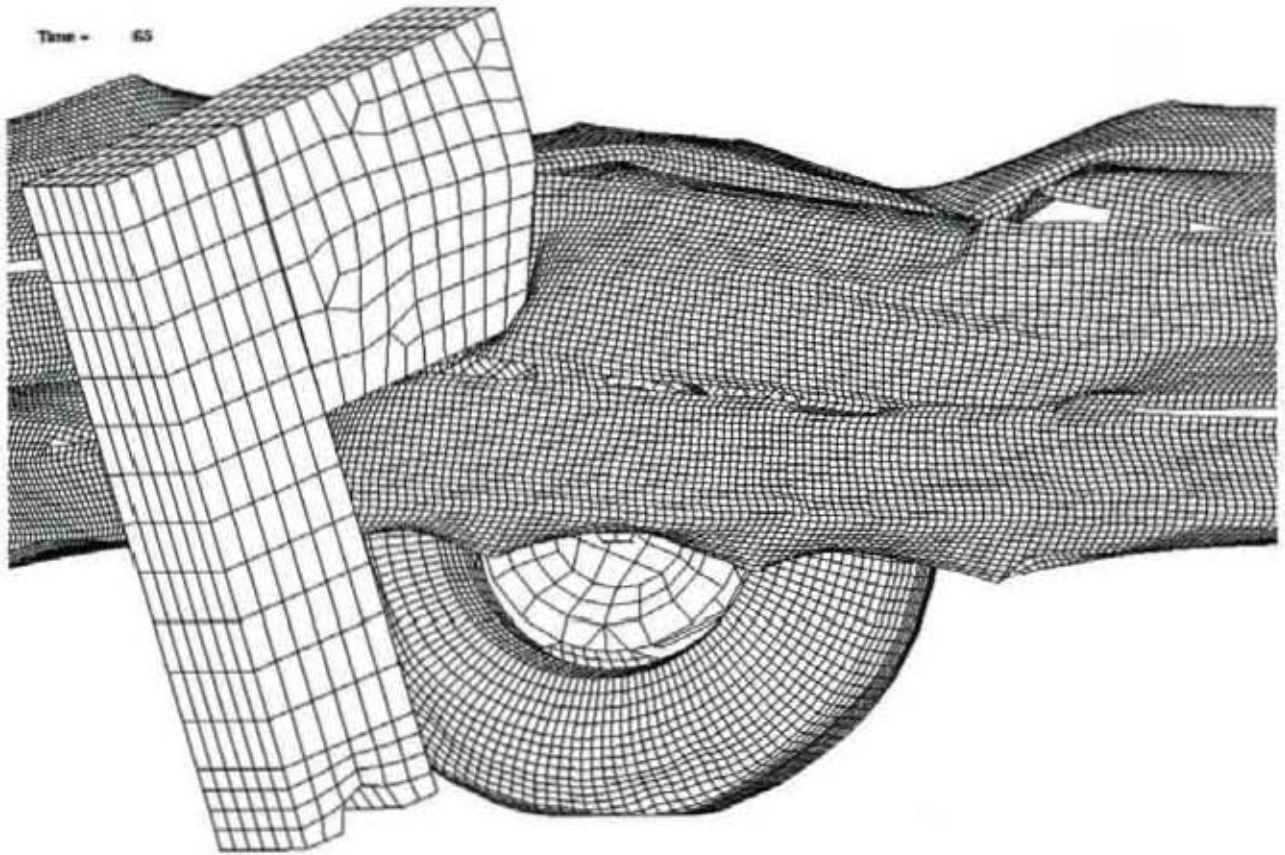


Figure 65. Double Blockout Reduces Tire Snag

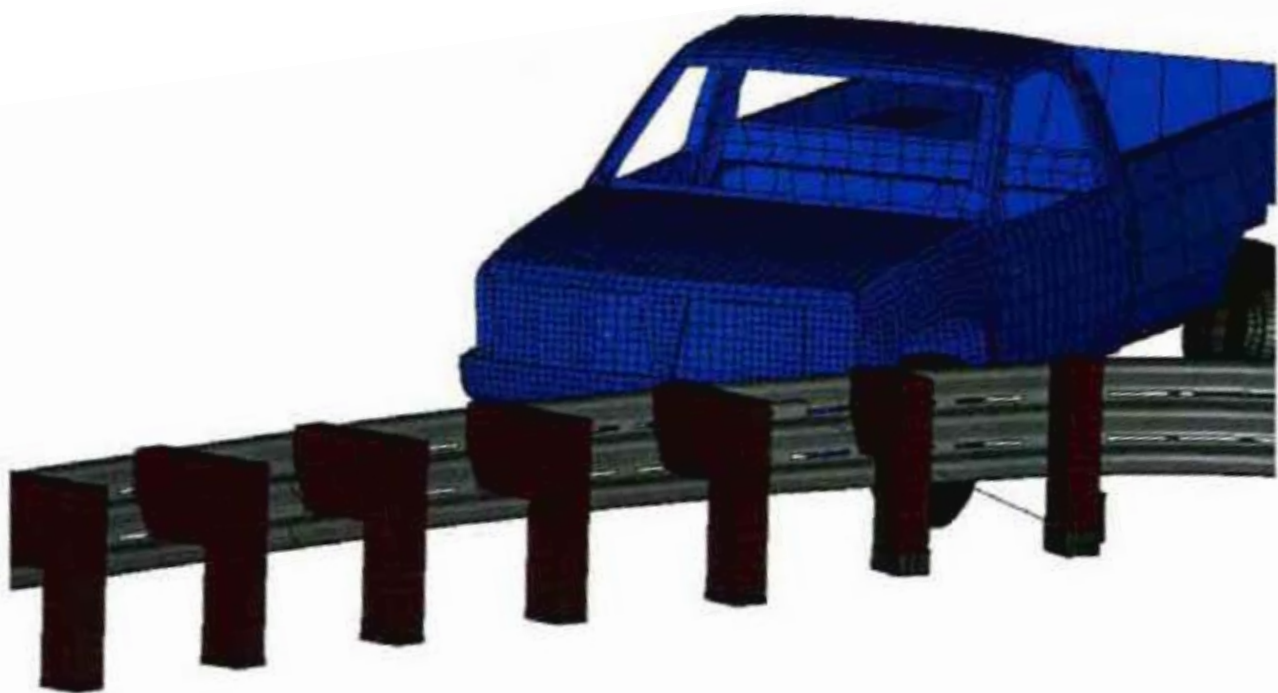


Figure 66. Model of Modified Design for Test MBN-8

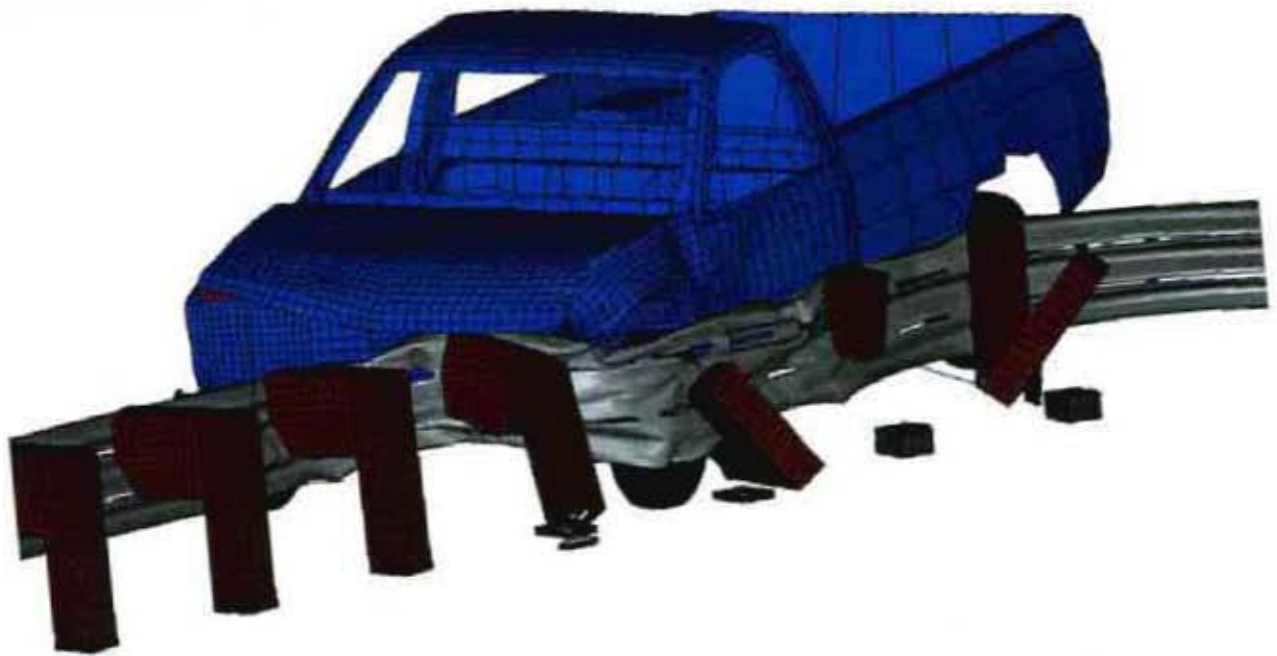


Figure 67. Modified Design Indicates Capture of Vehicle

11 BARRIER MODIFICATIONS (DESIGN FOR MBN-8)

11.1 Modification of Bullnose Design

The bullnose barrier system was modified prior to conducting the fourth full-scale crash test of Phase III, test MBN-8. The full-scale test results of test MBN-7 and the computer simulation discussed in the previous section led to several modifications to the bullnose barrier design that were aimed at improving its safety performance in the CIP impact test.

Four modifications were made to the bullnose median barrier for test MBN-8. First, the second post on each side of the system was changed from a CRT post to a BCT post. Second, an additional BCT post with a single blockout was also added to each side of the system. The new post was placed midway between post nos. 1 and 2 in the previous design. These two posts were added in order to increase the lateral resistance in the barrier system, thus increasing the rail's ability to capture and contain the impacting vehicle. Changes were also made to the blockouts used in the design. Post nos. 3 through 8 on both sides of the barrier were fitted with double blockouts in order to reduce wheel snag. In addition, the outside blockout on post nos. 2 through 8 were chamfered 25 degrees on the front face, beginning at the post bolt hole and continuing to the bottom. The purpose of the chamfered blockouts was to allow the thrie beam to fold back and wrap around the front tire of the impacting vehicle, thus aiding in vehicle capture. The final modification to the bullnose design was the removal of the ground line strut between post nos. 1 and 2 in the previous design. The ground line strut removal eliminated the interaction between the left-front vehicle tire and the ground line strut, thus reducing the potential for the vehicle to climb and vault the rail. The modified design is shown in Figures 68 through 70.

It was decided that the fourth test of Phase III would be a repeat of test nos. MBN-6 and

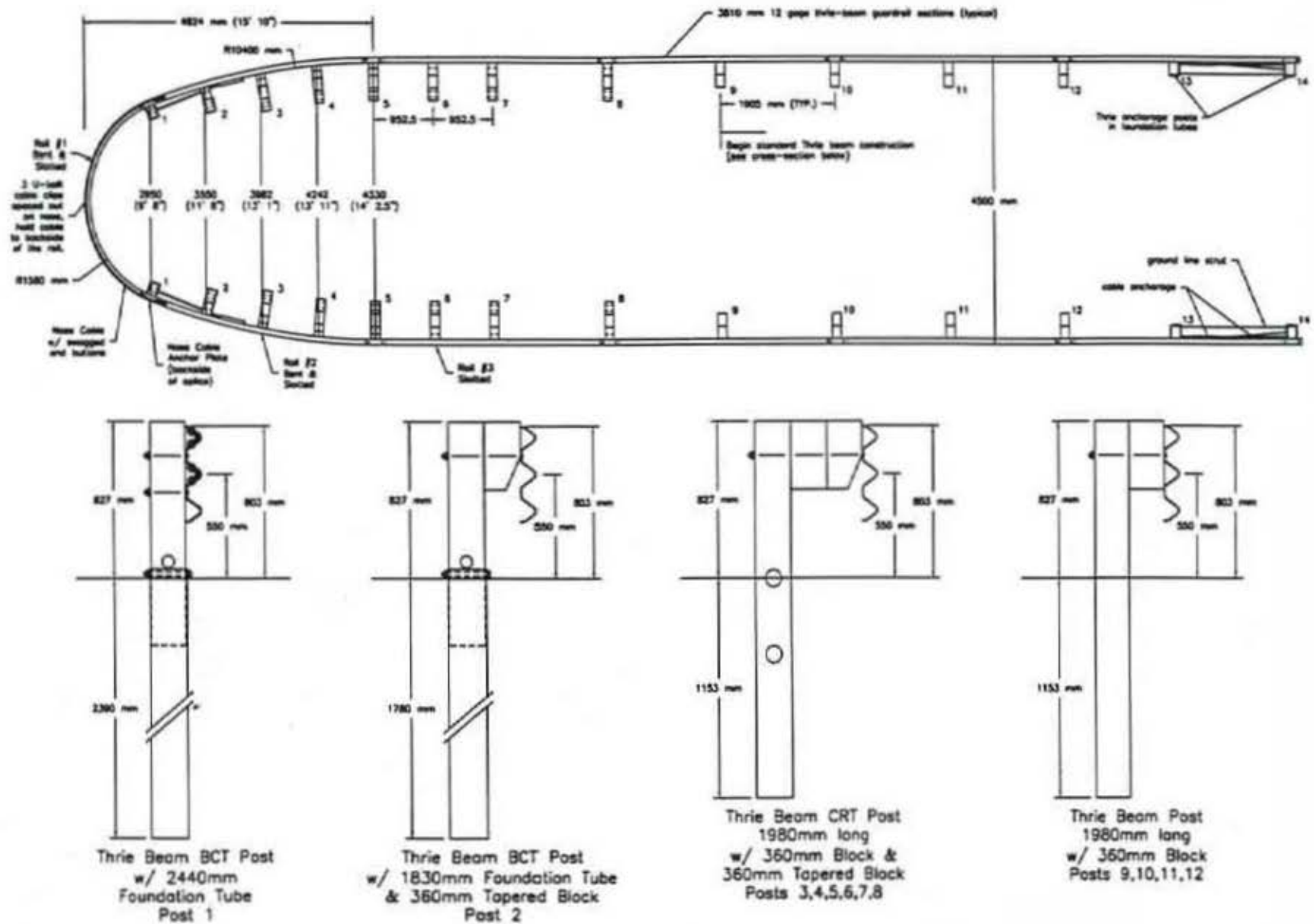


Figure 68. Bullnose Barrier Design, Test MBN-8



Figure 69. Bullnose Design, Test MBN-8



Figure 70. Bullnose Design, Test MBN-8

MBN-7 in order to prove that the modified design was capable of capturing a 2000-kg pickup truck impact occurring at the critical impact point.

12 CRASH TEST MBN-8

12.1 Test MBN-8

Test MBN-8 was conducted as a rerun of test nos. MBN-6 and MBN-7 with the design modifications specified in Section 11. The 2,033-kg pickup truck impacted the bullnose barrier, as shown in Figure 71, at a speed of 99.8 km/h and at an angle of 21.5 degrees in a similar location to that used in test nos. MBN-6 and MBN-7. A summary of the test results and the sequential photographs are shown in Figure 72. Additional sequential photographs are shown in Figure 73. Full-scale crash documentary photographs are shown in Figures 74 and 75.

12.2 Test Description

Following the initial impact with the pickup truck, the three beam rail immediately began to deform inward. At 0.031 sec after impact, the left front of the pickup truck impacted CRT post no. 3 on the right side, causing it to fracture. At 0.066 sec after impact, post nos. 2 through 4 on the right side had broken. As the pickup penetrated farther into the barrier, post nos. 5 and 6 on the right side broke due to the impact with the front of the pickup truck. At 0.143 sec, post no. 1 on the right side fractured as the rail wrapped around it, thus eliminating the cable anchor at post no.1 as well. However, unlike in tests MBN-6 and MBN-7, the guardrail system had adequate lateral stiffness and tension to allow the capture of the bumper and front wheels of the pickup truck prior to the loss of the cable anchor and upstream posts. As a result, the guardrail did not drop nor rotate backward as much as was observed in the previous two tests. As the pickup truck continued its rapid deceleration, the back wheels started to rise off of the ground at 0.296 sec. At 0.371 sec, the guardrail wrapped around post no. 1 on the left side of the barrier and broke it on the right side of the barrier system. In addition, the guardrail formed a right angle at post no. 8, causing the front bumper and wheels of

the pickup truck to be completely captured. At 0.703 sec, the pickup truck was nearly stopped when post no. 2 on the left side broke. By approximately 0.801 sec, the guardrail, which had been pulled taut at post no. 3 on the left side and post no. 8 on the right side, brought the forward motion of the pickup to a complete stop and caused the back end of the pickup truck to pitch into the air. At 1.43 sec, the back of the vehicle returned to the ground. The pickup truck came to rest after traveling longitudinally 10.18 m into the system. The trajectory of the pickup truck during the crash test and the final position of the vehicle are provided in Figure 76.

12.3 Vehicle Damage

Vehicle damage was moderate, as shown in Figure 77. The majority of the damage to the pickup truck occurred below the hood line. The front bumper and front end of the pickup truck were crushed inward across the entire width of the vehicle. The engine radiator was also flattened. The pickup truck's engine was shifted and twisted due to deformations to the front of the frame. The drive shaft was disengaged during the impact. The left-front fender of the pickup truck was bent down and inward around the left tire. The left-front tire was turned outward and pushed back into the wheel well. The tie rod on the left side was sheared off, and the front frame horn on the left side was bent almost 90-degrees downward. The front wheel on the right side was tore off during impact with the barrier. The right-front fender was crushed inward and downward due to the barrier impact. Minor cracking and chipping of the frame behind the right-front wheel was also observed. There was no crushing of the pickup truck's interior occupant compartment.

12.4 Barrier Damage

Barrier damage was extensive, as shown in Figures 78 through 80. Most of the post damage occurred to the right side of the system. Nine posts in the system were fractured. BCT post no. 1 on

the left side broke through the hole at ground line, while post no. 2 partially fractured but did not break off completely. On the right side, BCT post nos. 1 and 2 and CRT post nos. 3 and 4 were broken at the hole at ground level. CRT post nos. 5 through 7 on the right side fractured through the bottom hole. Post no. 6 was partially pulled out of the ground. No other posts in the system were fractured; however, post no. 8 on the right side had over 305 mm of permanent set deflection, as measured at ground line.

The damage to the three beam guardrail in the system consisted of buckling and tearing of the guardrail. Rail buckling was found on both sides of post no. 2 on the left side of the barrier. The rail on the right side of the barrier buckled into a 90-degree bend at a location 305-mm upstream of post no. 8 and again at post no. 9. Tearing of the tabs for the lower slots on the nose section of guardrail occurred 381 mm on each side of centerline. The middle hump of guardrail was torn 457-mm downstream of post no. 7 on the right side of the system and beginning at the slot tab. No damage to the cables or the cable plates was found. The maximum longitudinal permanent set deflection of the rail was 10.2-m downstream from the nose of the barrier.

Finally, it should be noted that several large pieces of barrier debris were dislodged during impact and deposited a significant distance from the barrier. A large piece of BCT post no. 1 on the right side of the barrier fractured off and was sent into the air, landing approximately 12.2-m to the left of post no. 7 on the left side of the system. Two pieces of wood blockouts from unidentified posts were also dislodged during impact, landing 57.9-m to the left of post no. 14 on the left side of the system.

12.5 Occupant Risk Values

The longitudinal and lateral occupant impact velocities (OIV) were determined to be 8.90

m/s and 2.39 m/s, respectively. The maximum 0.010-sec average occupant ridedown deceleration (ORD) in the longitudinal and lateral directions was 10.90 g's and 3.05/-7.82 g's, respectively. It is noted that the occupant impact velocities and occupant ridedown decelerations were within the suggested limits provided in NCHRP Report No. 350. The results of the occupant risk data are summarized in Figure 72. Results are shown graphically in Appendix E. The results from the rate transducer are also shown graphically in Appendix E.

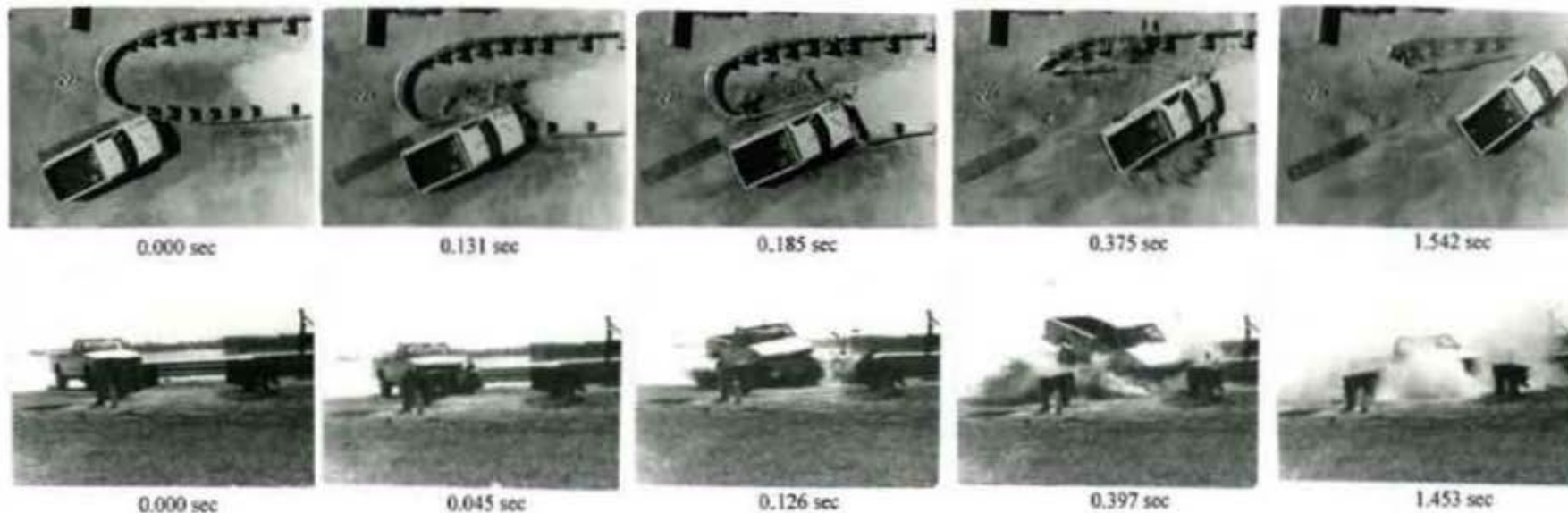
12.6 Discussion

Following test MBN-8, a safety performance evaluation was conducted, and the bullnose barrier design was determined to be acceptable for the test 3-38 impact conditions according to the NCHRP Report No. 350 criteria. The bullnose barrier successfully contained and stopped the test vehicle in a controlled manner. Detached elements and debris from the test article did not penetrate or show potential for penetrating the occupant compartment; however, several sizeable pieces of debris were detached and may have intruded on opposing traffic lanes. There was no deformation of, or intrusion into, the occupant compartment that could have caused serious injury. The vehicle remained upright during and after collision, and the vehicle's trajectory did not intrude into adjacent traffic lanes. Vehicle trajectory behind the test article was acceptable as the test vehicle was captured in the median area behind the bullnose. The occupant impact velocities and ridedown accelerations were within the suggested limits imposed by NCHRP Report No. 350.

The next full-scale test of the bullnose median barrier, test MBN-9, was chosen in order to evaluate the NCHRP Report No. 350 impact conditions of test 3-32. This test consists of a 820-kg small car impacting at a speed of 100 km/h and at an angle of 15-degrees on the nose of the system. No changes were made to the design of the bullnose median barrier for this test.



Figure 71. Impact Location, Test MBN-8



- Test Number MBN-8
- Date 9/24/99
- Appurtenance Bullnose Median Barrier
- Total Length 20,144 m
- Steel Thrie Beam
 - Thickness 12 gauge (2.66 mm)
 - Top Mounting Height 804 mm
- Wood Posts
 - Post Nos. 1 - 2, 13 - 14 140 mm x 190.5 mm x 1080-mm long BCT
 - Post Nos. 3 - 8 150 mm x 200 mm x 1980-mm long CRT
 - Post Nos. 9 - 12 150 mm x 200 mm x 1980-mm long
- Wood Spacer Blocks
 - Post Nos. 2 150 mm x 200 mm x 360-mm long tapered
 - Post Nos. 3 - 8 150 mm x 200 mm x 360-mm long tapered, single full size, single tapered
 - Post Nos. 9 - 12 150 mm x 200 mm x 360-mm long
- Soil Type Grading B - AASHTO M 147-65 (1990)
- Vehicle Model 1992 GMC 2500 2WD
 - Curb 2,106 kg
 - Test Inertial 2,033 kg
 - Gross Static 2,033 kg
- Vehicle Speed
 - Impact 99.8 km/hr
 - Exit 0.0 km/hr
- Vehicle Angle
 - Impact 21.5 deg
 - Exit NA
- Vehicle Snagging None
- Vehicle Stability Satisfactory
- Occupant Ridedown Deceleration (10 msec avg.)
 - Longitudinal 10.90 g's
 - Lateral (not required) 3.05/-7.82 g's
- Occupant Impact Velocity
 - Longitudinal 8.90 m/s
 - Lateral (not required) 2.39 m/s
- Vehicle Damage Moderate
 - TAD⁽¹⁾ 11FDEW3
 - SAE⁽²⁾ 11-FD-4
- Vehicle Stopping Distance 8.04 m downstream
0.08 m right of centerline
- Barrier Damage Extensive rail damage and nine fractured posts
- Maximum Deflections
 - Permanent Set 10.18 m downstream
 - Dynamic NA

Figure 72. Summary and Sequential Photos, Test MBN-8



0.000 sec



0.056 sec



0.133 sec



0.258 sec



0.411 sec

Figure 73. Additional Sequential Photographs, Test MBN-8



Figure 74. Full-Scale Crash Test MBN-8



Figure 75. Full-Scale Crash Test MBN-8

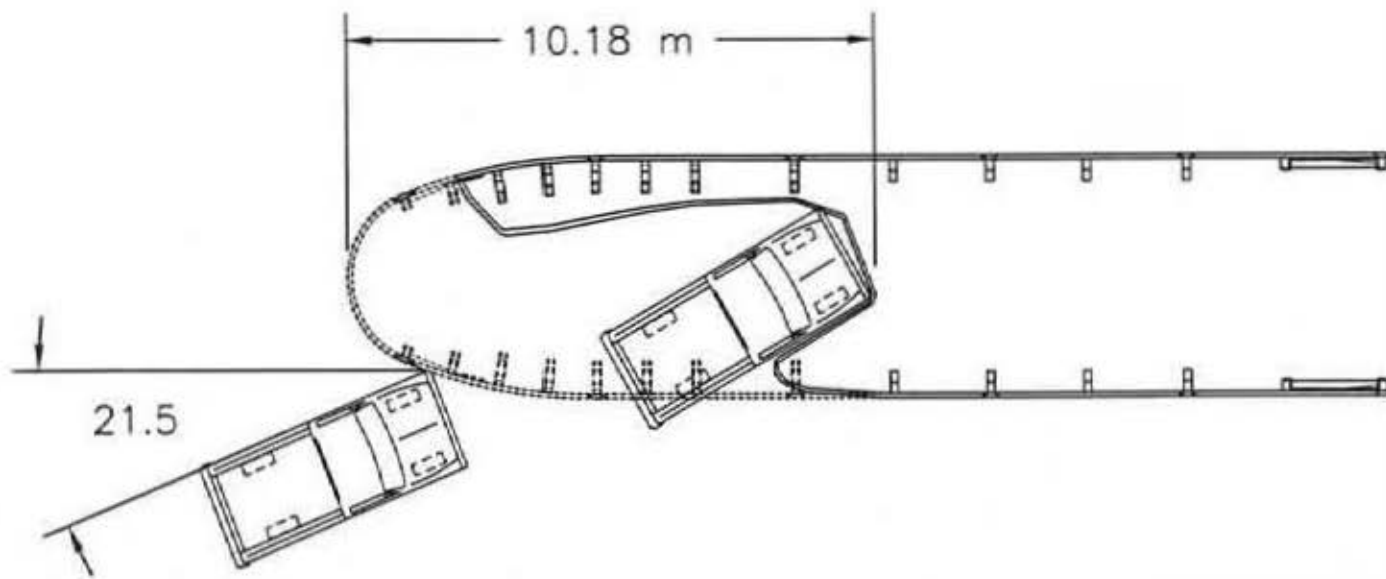


Figure 76. Vehicle Trajectory, MBN-8



Figure 77. Vehicle Damage, Test MBN-8



Figure 78. Barrier Damage, Test MBN-8



Figure 79. Barrier Damage, Test MBN-8



Figure 80. Barrier Damage, Test MBN-8

13 CRASH TEST MBN-9

13.1 Test MBN-9

Test MBN-9 was conducted according to the requirements of NCHRP Report No. 350 test 3-32. The 904-kg small car impacted the nose of the bullnose barrier, as shown in Figure 81, at a speed of 105.0 km/h and at an angle of 15.7 degrees. A summary of the test results and the sequential photographs are shown in Figure 82. Additional sequential photographs are shown in Figure 83. Full-scale crash documentary photographs are shown in Figures 84 and 85. No changes were made to the design of the bullnose median barrier for this test.

13.2 Test Description

Following the initial impact with the small car, the thrie beam rail immediately began to deform around the front of the vehicle with the middle and bottom humps capturing the front bumper and the top hump moving onto the hood. At 0.037 sec after impact, the thrie beam continued to deform inward as the top hump impacted the hood, dented it, and pushed it backward, causing the hood to buckle. The top hump of the thrie beam continued to be pushed up underneath the hood, bending it significantly. As the small car penetrated farther into the barrier, post no. 1 on the right side was fractured as the beam wrapped around it at 0.076 sec. At 0.111 sec, post no. 1 on the left side fractured as the rail loaded the post. The rail on the left side of the system bowed outward and pulled away from post nos. 2 and 3. Shortly thereafter, a buckle in the guardrail near post no. 1 on the left side was pulled back into the small car, impacting the front-left door and shattering the window. By 0.163 sec into the impact, post no. 2 on the right side fractured as the rail wrapped around the post, and post no. 3 on the left side was fractured as it was impacted by the small car. Post no. 2 on the left side fractured soon afterward as the rail from the opposite side contacted it at 0.204

sec after impact. At 0.302 sec, post no. 3 on the right side was broken and the vehicle began decelerating rapidly. The rapid deceleration of the vehicle forced the vehicle to yaw counter clockwise, causing the back tires to lift off the ground slightly. The guardrail formed a right angle at post no. 4 on the right side at 0.471 sec. At the same time, the small car continued to slow down as the guardrail was pulled taut at post no. 4 on both sides of the system. By 0.861 sec after impact, the small car had been stopped completely 6.50 m into the system. The trajectory of the small car during the crash test and the final position of the vehicle are provided in Figure 86.

13.3 Vehicle Damage

Vehicle damage was moderate, as shown in Figure 87. The engine hood was pushed back and upward, causing it to bend and fold at several locations. The front end of the small car was crushed inward across the entire width of the vehicle. The radiator was flattened along with other engine components near the engine block. Minor bending of the front of the frame was also observed. The right-front fender was crushed all along its length and pushed back toward the door. The left-front tire was turned outward and pushed back into the wheel well. The left-front fender was also severely deformed inward. The left-side door buckled near the front region when it contacted the fender and was pushed backward. This door buckling caused the left-front window to shatter. Scratching and denting of the left-side door due to contact with the rail was evident as well. There was no crushing of the small car's interior occupant compartment.

13.4 Barrier Damage

Barrier damage was extensive, as shown in Figures 88 through 89. A total of six posts in the system were fractured. BCT post nos. 1 and 2 on both sides of the system fractured through the hole at ground level. CRT post no. 3 on the left side broke at the top hole and was trapped between the

end of the rail and post no. 4. CRT post no. 3 on the right side fractured at the bottom hole. No other posts in the system were fractured.

The damage to the thrie beam guardrail in the system consisted of buckled and torn guardrail. Buckling of the rail on the left side occurred 762-mm upstream of post no. 3. On the right side, the barrier buckled at post nos. 3 and 4. All of the slot tabs in the nose section of thrie beam guardrail were torn apart, allowing all three humps of rail to separate. No other significant tearing of the rail was observed. No damage to the cables or the cable plates was found. The permanent set deflection of the rail was 6.50-m downstream from the nose of the barrier.

13.5 Occupant Risk Values

The longitudinal and lateral occupant impact velocities (OIV) were determined to be 9.94 m/s and 0.796 m/s, respectively. The maximum 0.010-sec average occupant ridedown deceleration (ORD) in the longitudinal and lateral directions was 13.86 g's and 10.55/-11.04 g's, respectively. It is noted that the occupant impact velocities and occupant ridedown decelerations were within the suggested limits provided in NCHRP Report No. 350. The results of the occupant risk data are summarized in Figure 82. Results are shown graphically in Appendix F. The results from the rate transducer are also shown graphically in Appendix F.

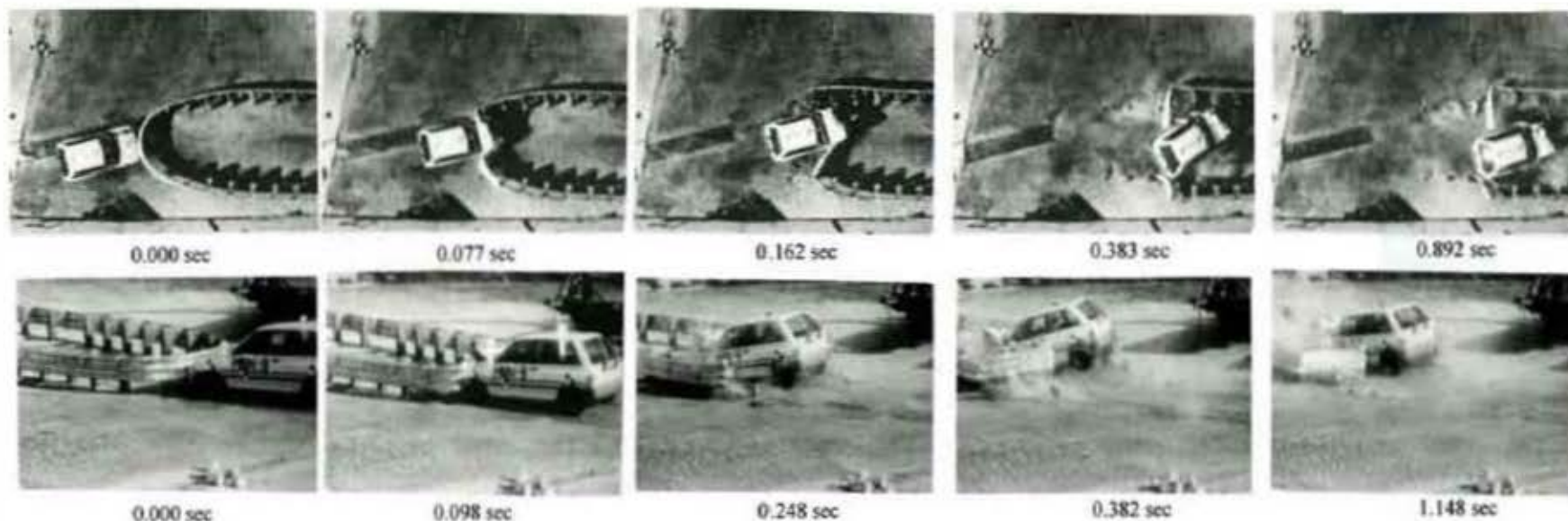
13.6 Discussion

Following test MBN-9, a safety performance evaluation was conducted, and the bullnose barrier design was determined to be acceptable for the test 3-32 impact conditions according to the NCHRP Report No. 350 criteria. The bullnose barrier successfully contained and stopped the test vehicle in a controlled manner. Detached elements and debris from the test article did not penetrate or show potential for penetrating the occupant compartment. There was no deformation of, or

intrusion into, the occupant compartment that could have caused serious injury. The vehicle remained upright during and after collision, and the vehicle's trajectory did not intrude into adjacent traffic lanes. Vehicle trajectory behind the test article was acceptable as the test vehicle was captured in the median area behind the bullnose. The occupant impact velocities and ridedown accelerations were within the suggested limits imposed by NCHRP Report No. 350.



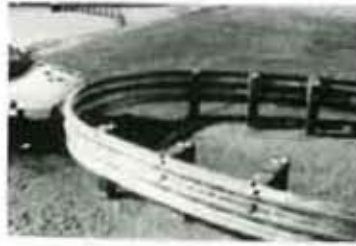
Figure 81. Impact Location, Test MBN-9



- Test Number MBN-9
- Date 10/29/99
- Appurtenance Bullnose Median Barrier
- Total Length 20,144 m
- Steel Thrie Beam
 - Thickness 12 gauge (2.66 mm)
 - Top Mounting Height 804 mm
- Wood Posts
 - Post Nos. 1 - 2, 13 - 14 140 mm x 190.5 mm x 1080-mm long BCT
 - Post Nos. 3 - 8 150 mm x 200 mm x 1980-mm long CRT
 - Post Nos. 9 - 12 150 mm x 200 mm x 1980-mm long
- Wood Spacer Blocks
 - Post Nos. 2 150 mm x 200 mm x 360-mm long tapered
 - Post Nos. 3 - 8 150 mm x 200 mm x 360-mm long tapered, single full size, single tapered
 - Post Nos. 9 - 12 150 mm x 200 mm x 360-mm long
- Soil Type Grading B - AASHTO M 147-65 (1990)
- Vehicle Model 1990 Ford
 - Curb 856 kg
 - Test Inertial 829 kg
 - Gross Static 904 kg
- Vehicle Speed
 - Impact 105.0 km/hr
 - Exit 0.0 km/hr

- Vehicle Angle
 - Impact 15.7 deg
 - Exit NA
- Vehicle Snagging None
- Vehicle Stability Satisfactory
- Occupant Ridedown Deceleration (10 msec avg.)
 - Longitudinal 13.86 g's
 - Lateral (not required) 10.55/-11.04 g's
- Occupant Impact Velocity
 - Longitudinal 9.94 m/s
 - Lateral (not required) 0.796 m/s
- Vehicle Damage Moderate
 - TAD⁽¹⁾ 11FDEW3
 - SAE⁽²⁾ 11-FD-5
- Vehicle Stopping Distance 6.17 m downstream
0.59 m left of centerline
- Barrier Damage Extensive rail damage and six fractured posts
- Maximum Deflections
 - Permanent Set 6.50 downstream
 - Dynamic NA

Figure 82. Summary and Sequential Photos, Test MBN-9



0.000 sec



0.037 sec



0.157 sec



0.339 sec



0.442 sec

Figure 83. Additional Sequential Photographs, Test MBN-9



Figure 84. Full-Scale Crash Test, Test MBN-9



Figure 85. Full-Scale Crash Test, Test MBN-9

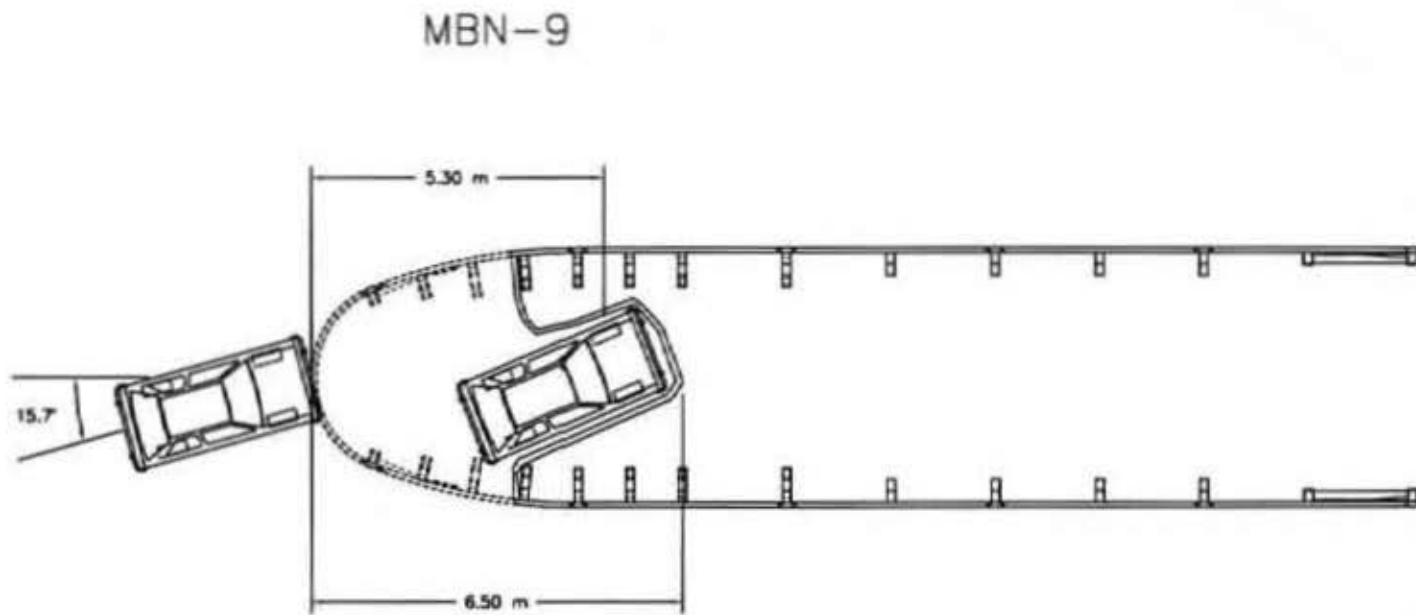


Figure 86. Vehicle Trajectory, Test MBN-9



Figure 87. Vehicle Damage, Test MBN-9



Figure 88. Barrier Damage, Test MBN-9



Figure 89. Barrier Damage, Test MBN-9

14 SUMMARY AND CONCLUSIONS

A bullnose median barrier was developed and full-scale crash tested to further develop the design concept and to provide compliance testing according to federal impact safety standards. Five crash tests were performed according to Test Level 3 (TL-3) of NCHRP Report No. 350. The results of the tests are summarized in Table 5. The first test, test MBN-5, was conducted according to the NCHRP Report No. 350 impact conditions for test 3-33. The test consisted of a 2,039-kg pickup truck impacting the nose of the barrier at a speed of 103.0 km/h and at an angle of 13.4 degrees. This test was judged acceptable as the bullnose system successfully captured the pickup truck. Originally, the bullnose barrier system was believed to be a gating system, and the test matrix was configured accordingly. However, test MBN-5 showed that the bullnose system was actually a non-gating terminal since it contained the vehicle when impacted on the nose of the device and at an angle. This change in classification required that the test matrix be revised in order to reflect its non-gating status.

The second test, test MBN-6, was conducted according to the NCHRP Report No. 350 test 3-38 impact conditions for non-gating terminals. The test consisted of a 2,031-kg truck impacting the CIP of the system at a speed of 101.5 km/h and at an angle of 20.4 degrees. Test MBN-6 failed to meet the NCHRP safety requirements as the pickup truck vaulted over the system and rolled over. The vaulting of the pickup truck was directly attributed to a lack of tension and lateral stiffness in the system making the guardrail unable to remain upright and functional long enough to allow the successful capture of the vehicle. The test results were used to make design changes to the bullnose barrier which were aimed at increasing rail tension and lateral stiffness. These changes were necessary to effectively capture the front of the vehicle. Modifications consisted of adding two posts

Table 5. Summary of Safety Performance Evaluation

Evaluation Factors	Evaluation Criteria	Test MBN-5	Test MBN-6	Test MBN-7	Test MBN-8	Test MBN-9
Structural Adequacy	A. Test article should contain and redirect the vehicle the vehicle should not penetrate, underride, or override the installation although controlled lateral deflection of the test article is acceptable.	S	U	U	S	S
	C. Acceptable test article performance may be by redirection, controlled penetration, or controlled stopping of the vehicle.	S	U	U	S	S
Occupant Risk	D. Detached elements, fragments or other debris from the test article should not penetrate or show potential for penetrating the occupant compartment, or present an undue hazard to other traffic, pedestrians, or personnel in a work zone. Deformations of, or intrusions into, the occupant compartment that could cause serious injuries should not be permitted.	S	S	S	M	S
	F. The vehicle should remain upright during and after collision although moderate roll, pitching, and yawing are acceptable.	S	U	U	S	S
	H. Occupant impact velocities should satisfy the following: Occupant Impact Velocity Limits (m/s) <u>Component</u> Preferred Maximum Longitudinal and Lateral 9 12	S	S	S	S	S
	I. Occupant ride down accelerations should satisfy the following: Occupant Ride down Acceleration Limits (G's) <u>Component</u> Preferred Maximum Longitudinal and Lateral 15 20	S	S	S	S	S
Vehicle Trajectory	K. After collision it is preferable that the vehicle's trajectory not intrude into adjacent traffic lanes.	S	U	U	S	S
	L. The occupant impact velocity in the longitudinal direction should not exceed 12 m/s and the occupant ridedown acceleration in the longitudinal direction should not exceed 20 G's.	S	S	S	S	S
	M. The exit angle from the test article preferably should be less than 60 percent of the test impact angle, measured at the time the vehicle lost contact with the device.	S	S	S	S	S
	N. Vehicle trajectory behind the test article is acceptable.	S	U	U	S	S

S - (Satisfactory)

M - (Marginal)

U - (Unsatisfactory)

to each side of the system between post nos. 2 and 4 and changing post no. 3 from a BCT post to a CRT post.

Test MBN-7 consisted of a retest of test MBN-6 on the modified design using a 2,036-kg pickup truck. The pickup truck impacted the barrier system at a speed of 100.0 km/h and at an angle of 24.9 degrees. This test also failed as the pickup truck vaulted over the guardrail and rolled over. However, it should be noted that the design modifications showed promise as the pickup truck was contained and redirected much farther into the system prior to vaulting than was observed in the previous test. Consequently, there still was not adequate tension and lateral stiffness in the guardrail system to allow the vehicle to be safely captured.

Computer simulation modeling using LS-DYNA was then used to analyze the failures of test nos. MBN-6 and MBN-7 as well as to investigate possible solutions to the problems being encountered. An investigation of the simulated test results showed that the tire interaction with the ground line strut could increase the potential for the vehicle and tire to climb up the guardrail and vault over the system. Simulation of the barrier system with the ground line strut removed showed a reduced tendency for vehicle climbing and vaulting over the rail. Computer simulation was also used to examine whether modified blockouts could improve performance. The analysis showed that double chamfered blockouts reduced tire snag and allowed the lower thrie corrugation to fold back, thus increasing wheel capture.

Based on the simulation analysis and results from the previous tests, the bullnose barrier was modified to include the removal of the ground line strut and the addition of doubled chamfered blockouts at post nos. 2 through 8. A BCT post was also placed at the half-post spacing downstream from post no. 1 on each side of the system. A simulation of the modified bullnose system indicated

that the new design would be capable of capturing the impacting pickup truck.

Testing of the modified design was then continued with test MBN-8, a retest of test nos. MBN-6 and MBN-7. Test MBN-8 passed the NCHRP Report No. 350 safety requirements for the test 3-38 impact conditions as the pickup truck was safely captured and contained by the bullnose barrier.

The final test of the bullnose barrier, test MBN-9, was conducted according to the NCHRP Report No. 350 test 3-32 impact conditions. For this test, a small car impacted on the nose of the barrier at a speed of 105.0 km/h and at an angle of 15.7 degrees. No changes were made to the bullnose design for this test. Test MBN-9 successfully met the NCHRP 350 requirements as the small car was safely captured and contained by the bullnose barrier.

Throughout the course of the development of the bullnose barrier, a host of modifications and design changes were made to improve the performance of the system. It was important to consider the effect that the design changes would have on the behavior of the system with respect to previously run full-scale compliance tests. A total of three full-scale compliance tests for the bullnose barrier were not rerun since it was believed that the design changes would not adversely effect the results from the previous successful tests. These successful tests were test nos. MBN-2, MBN-4, and MBN-5, which were performed according to the NCHRP Report No. 350 impact conditions for test nos. 3-30, 3-31, 3-33, respectively.

Test 3-30, which was previously run as test MBN-2, was a $\frac{1}{4}$ -offset small car impact on the nose of the barrier at a speed of 100 km/h and an angle of 0 degrees. Based on the success of test MBN-9, a successful test of a small car impact on the nose of the barrier at a speed of 100 km/h and at an angle of 15 degrees, it is believed that the design changes would not degrade the performance

of the barrier for test 3-30. Therefore, the researchers believe that it does not need to be rerun.

Test nos. 3-31 and 3-33 were 2000-kg pickup truck impacts that were previously run successfully as test nos. MBN-4 and MBN-5, respectively. Consideration was given to the possibility of rerunning those tests after several modifications were made to the barrier design in the course of subsequent testing. After deliberation, the researchers believed that there was no need to rerun these tests, because the changes made to the system in order to stiffen the barrier for the C.I.P. impact would not degrade the performance of the barrier for the head on impacts. It was noted that the additional posts added to the system in test nos. MBN-8 and MBN-9 stiffened the system; however, they did not hinder the system performance in test MBN-9, a successful small car impact at an angle on the nose of the system. The increased stiffness of the system should have even less of an effect on the pickup truck in test nos. 3-31, and 3-33 than in the small car test no. MBN-9. The use of the additional modified blockouts should also pose no problem for these tests.

It should also be noted that three of the tests listed in the NCHRP Report No. 350 test matrix for the bullnose barrier were not conducted. These are the length-of need tests, test nos. 3-36 and 3-37, and the reverse direction test, test 3-39. The two length of need tests were not conducted because previous testing has shown that three beam guardrail is capable of meeting the length of need requirements found in the NCHRP 350 impact safety standards. Similarly, the reverse direction impact test was also left untested. Test 3-39 calls for a reverse direction impact of a 2000-kg pickup truck on a point at the length of the terminal divided by two. In the case of the bullnose barrier system, this impact would have been placed near the middle of the straight three beam section of the barrier between post nos. 5 through 14. Thus, based on previous experience with straight three beam guardrail testing, it was believed that test 3-39 was unnecessary.

The Phase III development of the bullnose barrier end terminal was successfully completed. The initial design concept was further developed and successfully tested for all of the necessary NCHRP Report No. 350 compliance tests.

15 RECOMMENDATIONS

A bullnose median barrier designed for use in the protection of errant vehicles from median hazards was successfully crash tested according to the criteria found in NCHRP Report No. 350. The results of these tests suggest that this design is suitable for Federal-aid highways. However, it should be noted that any design modifications made to the bullnose barrier require verification through full-scale vehicle crash testing.

The bullnose barrier system, as shown in Figures G-1 through G-6 in Appendix G, was tested with a 4,500-mm width to represent a configuration with the minimum system width. As mentioned previously, a narrow bullnose installation requires tighter guardrail radii and induces much greater stresses and strains in the guardrail when an impacting vehicle penetrates into the system. The tighter guardrail radii and higher stresses and strains should lead to greater likelihood of rail rupture and higher decelerations on impacting vehicles. Therefore, the narrow design was selected for testing as a worst case installation.

While the focus of this research has been the development of the bullnose barrier for protection of narrow median hazards such as bridge piers and overhead sign support structures, other possible applications for the design exist. There are two additional foreseeable field applications for the bullnose barrier system: (1) the protection of the gap between twin bridges; and (2) gore area protection. For each of the three bullnose applications, there are installation and design factors that must be addressed before the design can properly be used in these situations. These additional considerations will be addressed for each application.

The narrow median hazard situation is the most basic application for the bullnose barrier. An example of a typical, narrow bullnose barrier used for the protection of bridge piers is shown in

Figure 90. During the crash testing program, the maximum longitudinal vehicle penetration and barrier deflection was approximately 15.4-m downstream from post no. 1, as observed in test MBN-4. In the test, the front of the pickup truck came to rest about one quarter of the way down rail section no. 6 of the bullnose system. Based on this test deformation, a minimum of 19.125-m of guardrail, as measured longitudinally, or five sections of guardrail downstream of post no. 1 of the system is recommended in front of any hazard. The recommended distance is slightly higher than the maximum observed deflection to provide a factor of safety for the design. It also allows for a whole number of guardrail sections in front of the hazard.

An additional consideration for the application of the bullnose barrier to a narrow median hazard situation is the lateral clearance between the tangent segments of the bullnose barrier system and the face of the hazard. Previous testing conducted by TTI on a three beam longitudinal barrier system found a maximum dynamic deflection of 680 mm (21). Based on this data, the minimum recommended lateral clearance between the back of the posts and the face of the hazard is 700 mm.

The second major application for the bullnose median barrier is the protection of the gap between twin bridges on divided highways. This application is more complex than the narrow median hazard application due to the need to flare the guardrail away from the bridge rail. Since the width of the bullnose barrier system may be narrower than the width of the median, long sections of guardrail may be required in order to move the face of the guardrail closer to the roadway edge. In many instances, the guardrail adjacent to the roadway is within the driver's shy distance. In this case, flare rates must be severely limited to avoid affecting vehicle lane placement as traffic approaches the bridge. Further, although recent research indicates that higher flare rates are actually more cost beneficial (22), the *Roadside Design Guide* (23) still recommends very flare rates for high-

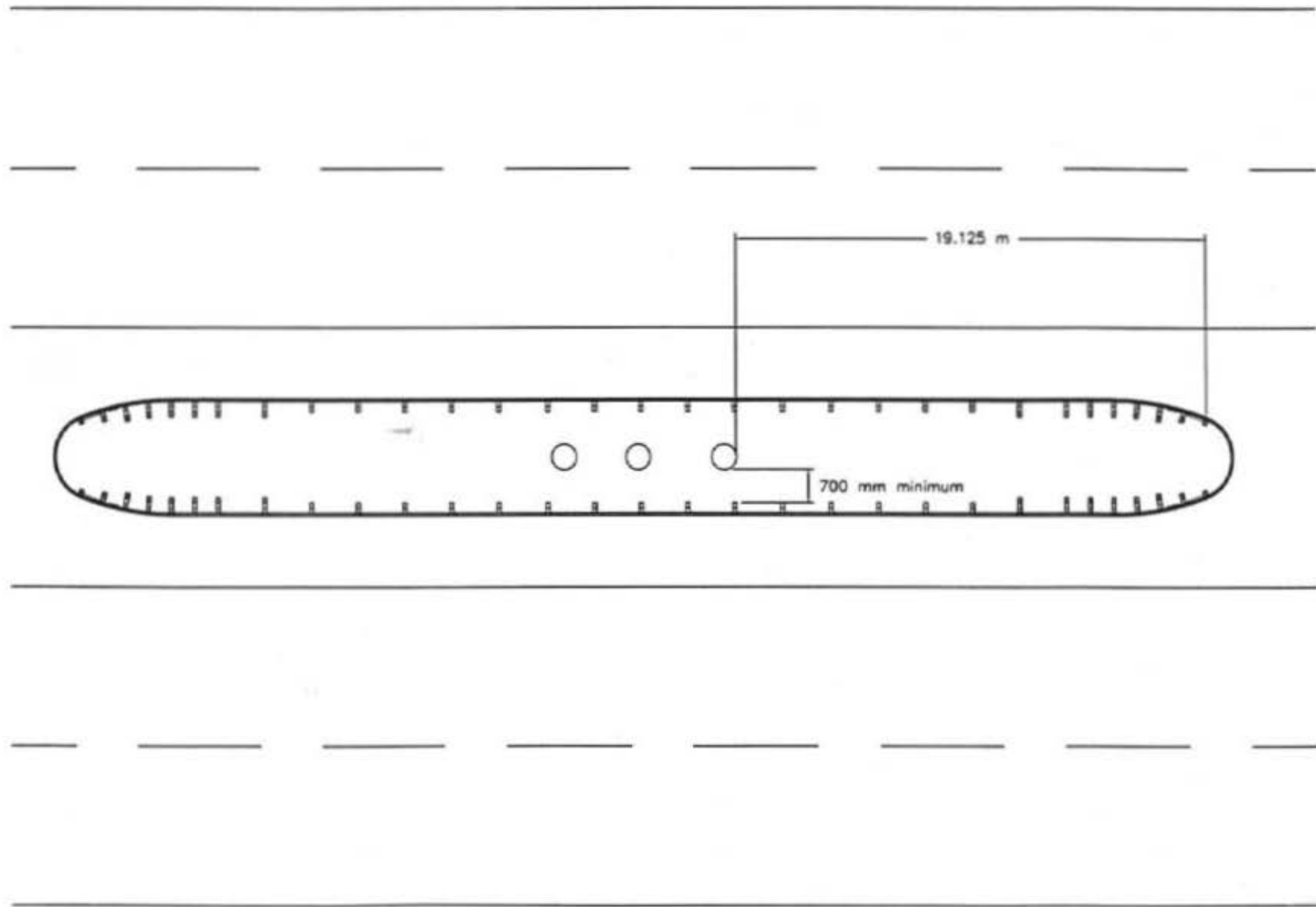


Figure 90. Typical Bullnose Installation for Protection of Median Hazards

speed roadways, even when the guardrail is outside of the driver's shy distance.

The median area used to separate divided highways is often 9 m or more wide. Therefore, this median width may not be easily protected by the 4.5-m wide version of the bullnose median barrier that was tested. In order to better accommodate larger widths, two wider bullnose barrier designs were developed, as shown in Figures H-1 through H-3 of Appendix H and Figures I-1 through I-3 of Appendix I. The two wider bullnose designs were created by laterally pushing out the sides of the system and then modifying the size of the nose section. It is noted that the geometry and slot patterns of rail section nos. 2 and 3 remained unchanged. For the two new configurations, a 5715-mm long and 7620-mm long section of three beam guardrail was bent to form the 2370-mm and 3160-mm radii, respectively. A 3810-mm long section of guardrail was used for the nose section of the system that was crash tested. While the size of the nose section was increased, it was simply scaled upwards to account for the longer section length and did not change in shape. The new widths for the widened bullnose designs are 5807 mm and 7283 mm. It is suggested that these widened systems be used for attachment to twin bridges on a divided highway. The wider bullnose systems offer economy over the narrow, crash tested design as the potential exists for reduced lengths of flared guardrail between the bullnose barrier and the bridge rail and transition systems.

No wider designs were developed at this time. The current designs are as wide as the bullnose can be made without modifying any rail sections other than the nose or using a nose section of guardrail that is longer than 7620 mm. It is currently unknown how further widening of the system would effect the performance of the system. Modification of rail section no. 2 is not advisable due to the unforeseen effects this would have on the system. This curved section aids in the buckling of the guardrail and may require further testing if modified. Using an even longer section of guardrail

in the nose potentially presents other problems as well, with the most obvious being the issue of the added cantilever weight from the additional guardrail. It is also believed that as the bullnose system is widened the energy absorption of the system changes. The wider systems do not bend the guardrail through as severe an angle as a narrow system, and the rail loading on the posts as the guardrail system deforms changes as well. These differences could be significant if the bullnose is widened further than the alternatives described above.

While the widened bullnose median barrier designs improve the adaptability of the system to applications across wide medians, an appropriate flare will likely be required in most installations in order to meet existing bridge rails. The flare rates used for these installations should be obtained based on guidelines set forth in the *AASHTO Roadside Design Guide*, or other applicable research. As mentioned above, crash tests of temporary concrete barriers have shown that the flare rates presented in the *Roadside Design Guide* appear to be very conservative. The use of slightly higher flare rates can greatly reduce the length of the bullnose system without creating a significantly higher impact angle on the flared sections. It is recommended that the flare begin no sooner than the start of rail section no. 3. It is believed that flaring the guardrail prior to this first straight section could adversely affect the performance of the barrier. While the shape of rail section no. 2 should not be changed, it should be allowable to straighten the end of the section to meet the specified flare rate. Such a configuration would facilitate a smooth transition from the curved guardrail to the flare. A schematic of the three bullnose designs applied to a 10-m wide median with twin bridges is shown in Figure 91.

Another consideration in the twin bridge rail application of the bullnose median barrier is the length of system required before the attachment of bridge or guardrail transitions. The results from

Protection of dual bridges separated by a median

- Allowable taper angle and the corresponding system length (15:1 taper allowable)
- Application of taper to existing design (beginning at start of section 3 as shown)

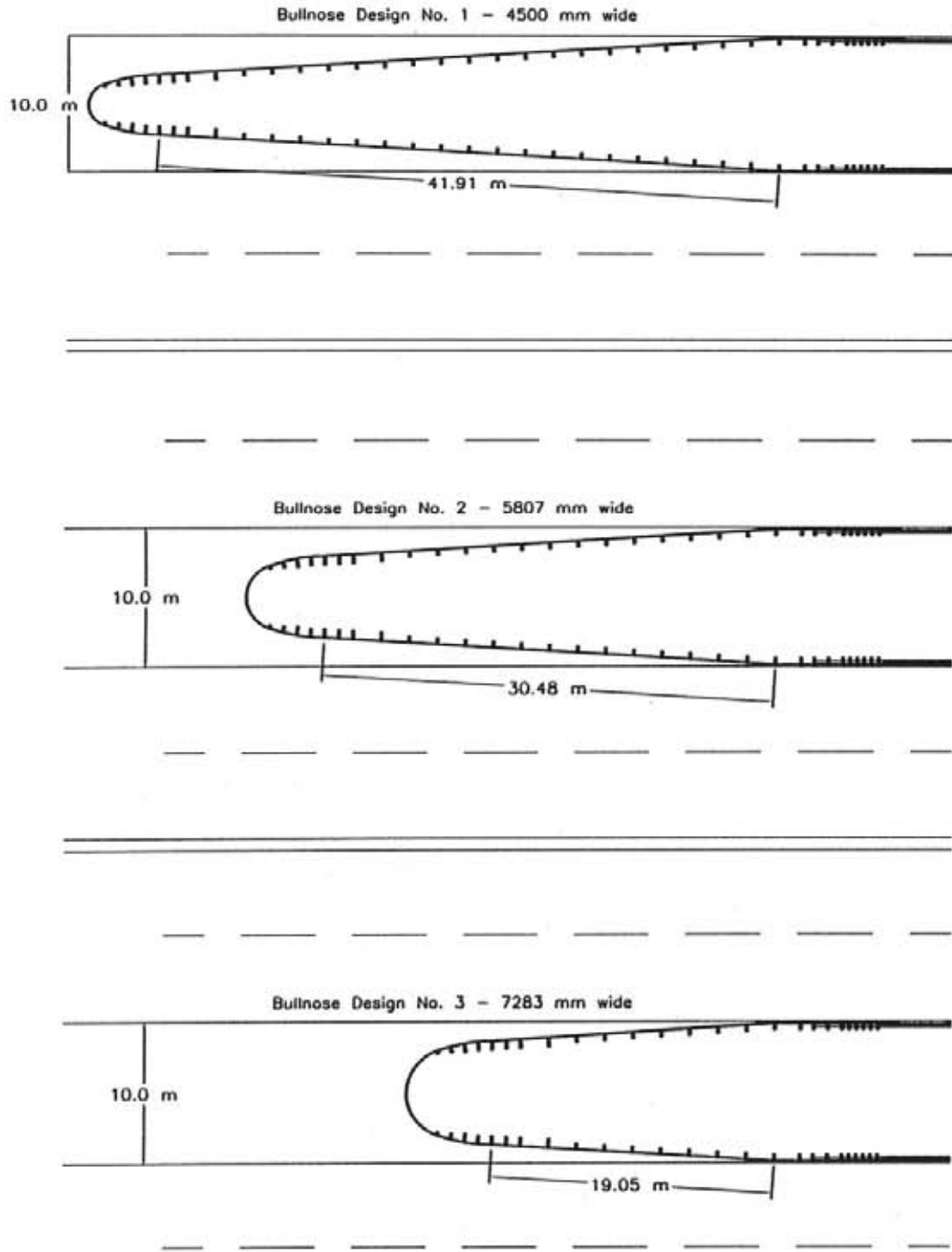


Figure 91. Schematic of Double Bridge Rail Installation

test MBN-8 showed deformation of the three beam guardrail as far as the middle of rail section no. 4. This was the farthest distance from the nose of the barrier that deformation of guardrail was observed in any of the bullnose tests. Due to the importance of guardrail deformation in the proper energy absorption and performance of the bullnose, it is believed that attachment of any transition prior to the areas where the three beam guardrail deformed in testing could prove detrimental to the behavior of the system. Therefore, it is recommended that any transitions used in conjunction with the bullnose median barrier should be placed no closer than the end of rail section no. 4 or 15.17-m downstream of post no. 1. This should allow for the necessary deformation of the three beam guardrail prior to any transition attached to the system.

The final application of the bullnose barrier system is the protection of gore areas. Similar design considerations exist for the gore area installations as described in the two previous applications. The length of the barrier required prior to a hazard or transition section should follow the guidelines for the double bridge rail and median hazard installations described previously. Flare guidelines for gore area installations should be the same as those referenced for the twin bridge application described above.

16 REFERENCES

1. Ross, H.E., Sicking, D.E., Zimmer, R.A. and Michie, J.D., *Recommended Procedures for the Safety Performance Evaluation of Highway Features*, National Cooperative Highway Research Program (NCHRP) Report No. 350, Transportation Research Board, Washington, D.C., 1993.
2. Bielenberg, B. W., Faller, R. K., Reid, J. D., Rohde, J. R., Sicking, D.L., Keller, E.A., *Concept Development of a Bullnose Guardrail System for Median Applications*, MwRSF Report No. TRP-03-73-98, Final Report, Submitted to the Missouri Department of Transportation, Midwest Roadside Safety Facility, May 22, 1998.
3. Bielenberg, B. W., Faller, R. K., Reid, J. D., Rohde, J. R., Sicking, D.L., Keller, E.A., Holloway, J. C., *Phase II Development of a Bullnose Guardrail System for Median Applications*, MwRSF Report No. TRP-03-78-98, Final Report, Submitted to the Midwest States Regional Pooled Fund Program, Midwest Roadside Safety Facility, December 18, 1998.
4. Button, J.W., Buth, E. and Olson, R.M., *Crash Tests of Five Foot Radius Plate Beam Guardrail*, Submitted to the Department of Highways, State of Minnesota, Performed by Texas Transportation Institute, Texas A & M University, June 1975.
5. Task Force 13, *A Guide to Standardized Highway Barrier Hardware*, AASHTO-AGC-ARTBA Joint Cooperative Committee Subcommittee on New Highway Materials, Task force 13, 1995.
6. Robertson, R.G. and Ross, H.E. Jr., *Colorado Median Barrier End Treatment Tests*, TTI Research Report No. 4179-1F, Submitted to the Colorado Department of Highways, Performed by Texas Transportation Institute, Texas A&M University, May 1981.
7. Bronstad, M.E., Ray, M.H., Mayer, J.B. Jr. and Brauer, S.K., *Median Barrier Terminals and Median Treatments. Volume 1 Research Reports and Appendix A*, Report No. FHWA/RD-088/004, Final Report to the Federal Highway Administration, Southwest Research Institute, October 1987.
8. Bronstad, M.E., Ray, M.H., Mayer, J.B. Jr. and Brauer, S.K., *Median Barrier Terminals and Median Treatments. Volume 2 Appendices B and C*, Report No. FHWA/RD-088/005, Final Report to the Federal Highway Administration, Southwest Research Institute, October 1987.
9. Bronstad, M.E., Calcote, L.R., Ray, M.H., and Mayer, J.B., *Guardrail-Bridge Rail Transition Designs - Volume 1 - Research Report*, Report No. FHWA/RD-86/178, Final Report to the Safety Design Division, Federal Highway Administration, Performed by Southwest Research Institute, April 1988.

10. Bronstad, M.E., Ray, M.H., Mayer, J.B., Jr., and McDevitt, C.F., *W-Beam Approach Treatment at Bridge Rail Ends Near Intersecting Roadways*, Transportation Research Record No. 1133, Transportation Research Board, National Research Council, Washington, D.C., 1987.
11. Mayer, J.B., *Full-Scale Crash Testing of Approach Guardrail for Yuma County Public Works Department*, Final Report, Project No. 06-2111, Southwest Research Institute, San Antonio Texas, 1989.
12. *Curved W-Beam Guardrail Installations at Minor Roadway Intersections*, Federal Highway Administration (FHWA), U.S. Department of Transportation, Technical Advisory T 5040.32, April 13, 1992.
13. Ross, H.E., Jr., Bligh, R.P., and Parnell, C.B., *Bridge Railing End Treatments at Intersecting Streets and Drives*, Report No. FHWA TX-91/92-1263-1F, Final Report to the Texas Department of Transportation, Performed by Texas Transportation Institute, Texas A&M University, November 1992.
14. Bligh, R.P., Ross, H.E., Jr., and Alberson, D.C., *Short-Radius Thrie Beam Treatment for Intersecting Streets and Drives*, Report No. FHWA/TX-95/1442-1F, Final Report to the Texas Department of Transportation, Performed by Texas Transportation Institute, Texas A&M University, November 1994.
15. Sicking, D. L., Reid, J. D., and Rohde, J. R., *Development of a Sequential Kinking Terminal for W-Beam Guardrails*, TRB Paper 980614, Transportation Research Board, January 1998.
16. Hinch, J., Yang, T-L, and Owings, R., *Guidance Systems for Vehicle Testing*, ENSCO, Inc., Springfield, VA, 1986.
17. *Vehicle Damage Scale for Traffic Investigators*, Second Addition, Technical Bulletin No. 1, Traffic Accident Data (TAD) Project, National Safety Council, Chicago, Illinois, 1971.
18. *Collision Deformation Classification - Recommended Practice J224 March 1980*, Handbook Volume 4, Society of Automotive Engineers (SAE), Warrendale, Pennsylvania, 1985.
19. Hallquist, J.O., *LS-DYNA Keyword User's Manual*, Livermore Software Technology Corporation, California, 1997.
20. J.D. Reid, *Transition from a Frontal Impact to a Redirection Impact on a New Bullnose Guardrail System Design, Crashworthiness, Occupant Protection and Biomechanics in Transportation Systems - 1999*, ASME, AMD-Vol. 237, November 1999, pp. 303-317.
21. Buth, C.E. and Menges, W.L., "NCHRP Report 350 Test 3-11 of the Strong Wood Post

Thrie Beam Guardrail," Test Report No. 404211-11, Contract No. DTFH61-97-C-00039, TTI, Texas A&M University, July 1998.

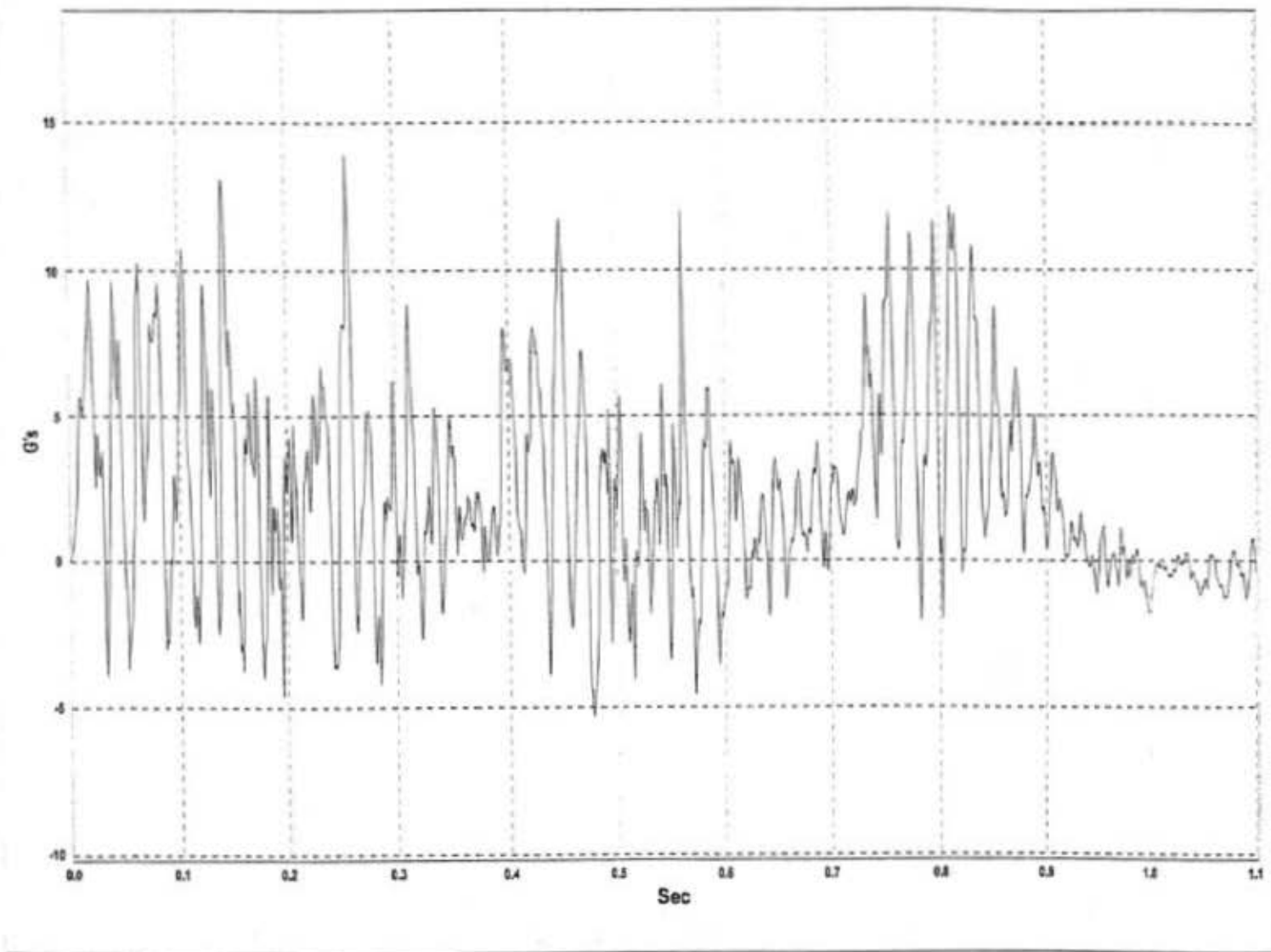
22. Ross, H.E., Krammes, R.A., Sicking, D.L., Tyer, K.D., and Perera, H.S., *Recommended Practices for Use of Traffic Barrier and Control Treatments for Restricted Work Zones*, National Cooperative Highway Research Program (NCHRP) Report No. 358, Transportation Research Board, Washington, D.C., 1994.
23. *Roadside Design Guide*, American Association of State Highway and Transportation Officials (AASHTO), Washington D.C., January 1996.

17 APPENDICES

APPENDIX A

ACCELEROMETER DATA ANALYSIS TEST MBN-5

- Figure A-1. Graph of Longitudinal Deceleration - Filtered Data, Test MBN-5
- Figure A-2 Graph of Longitudinal Occupant Impact Velocity - Filtered Data, Test MBN-5
- Figure A-3. Graph of Longitudinal Occupant Displacement - Filtered Data, Test MBN-5
- Figure A-4. Graph of Lateral Deceleration - Filtered Data, Test MBN-5
- Figure A-5. Graph of Lateral Occupant Impact Velocity - Filtered Data, Test MBN-5
- Figure A-6. Graph of Lateral Occupant Displacement - Filtered Data, Test MBN-5
- Figure A-7. Rate Transducer Data, Test MBN-5



156

Figure A-1. Graph of Longitudinal Deceleration - Filtered Data, Test MBN-5

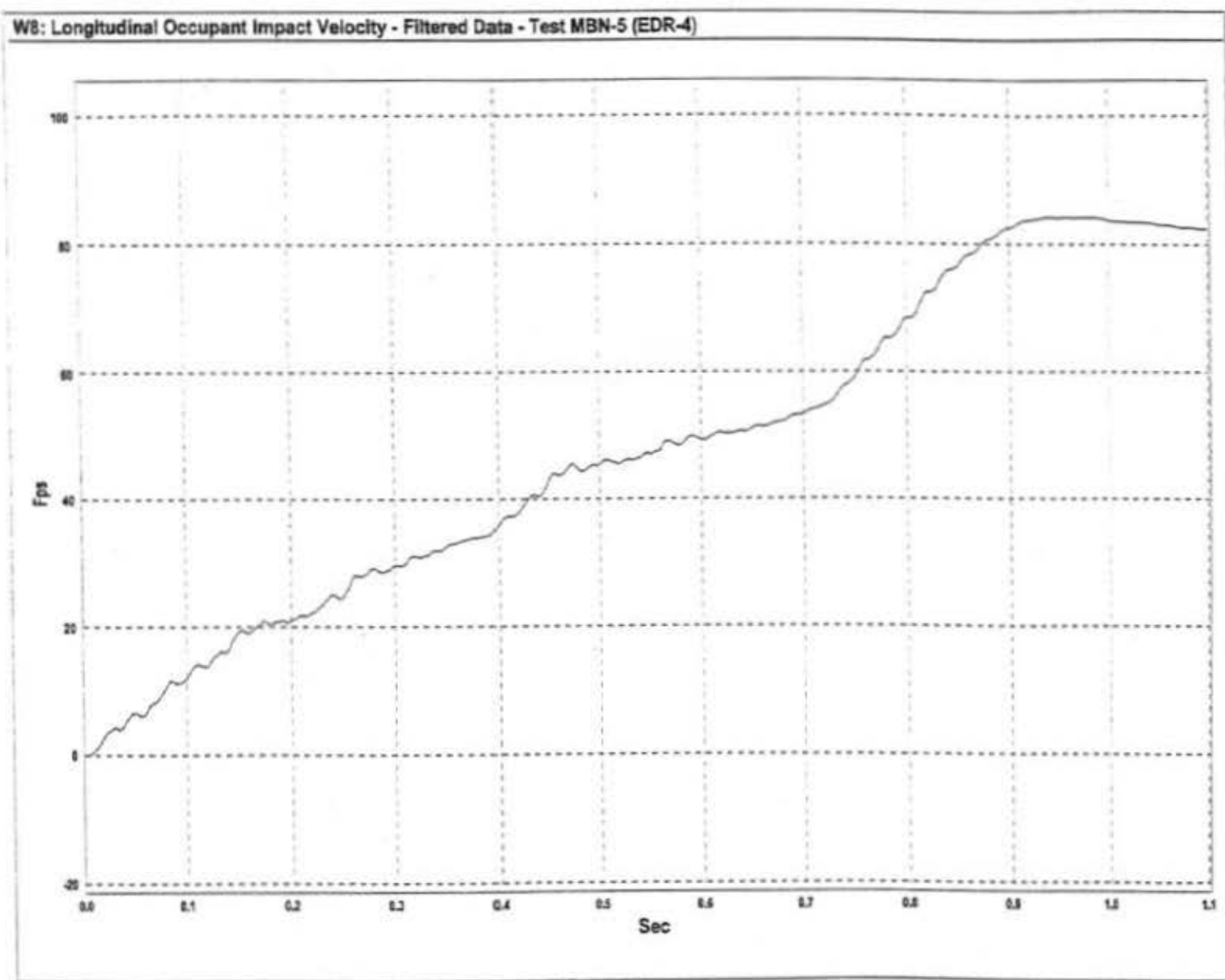


Figure A-2. Graph of Longitudinal Occupant Impact Velocity - Filtered Data, Test MBN-5

W9: Longitudinal Occupant Displacement - Filtered Data - Test MBN-5 (EDR-4)

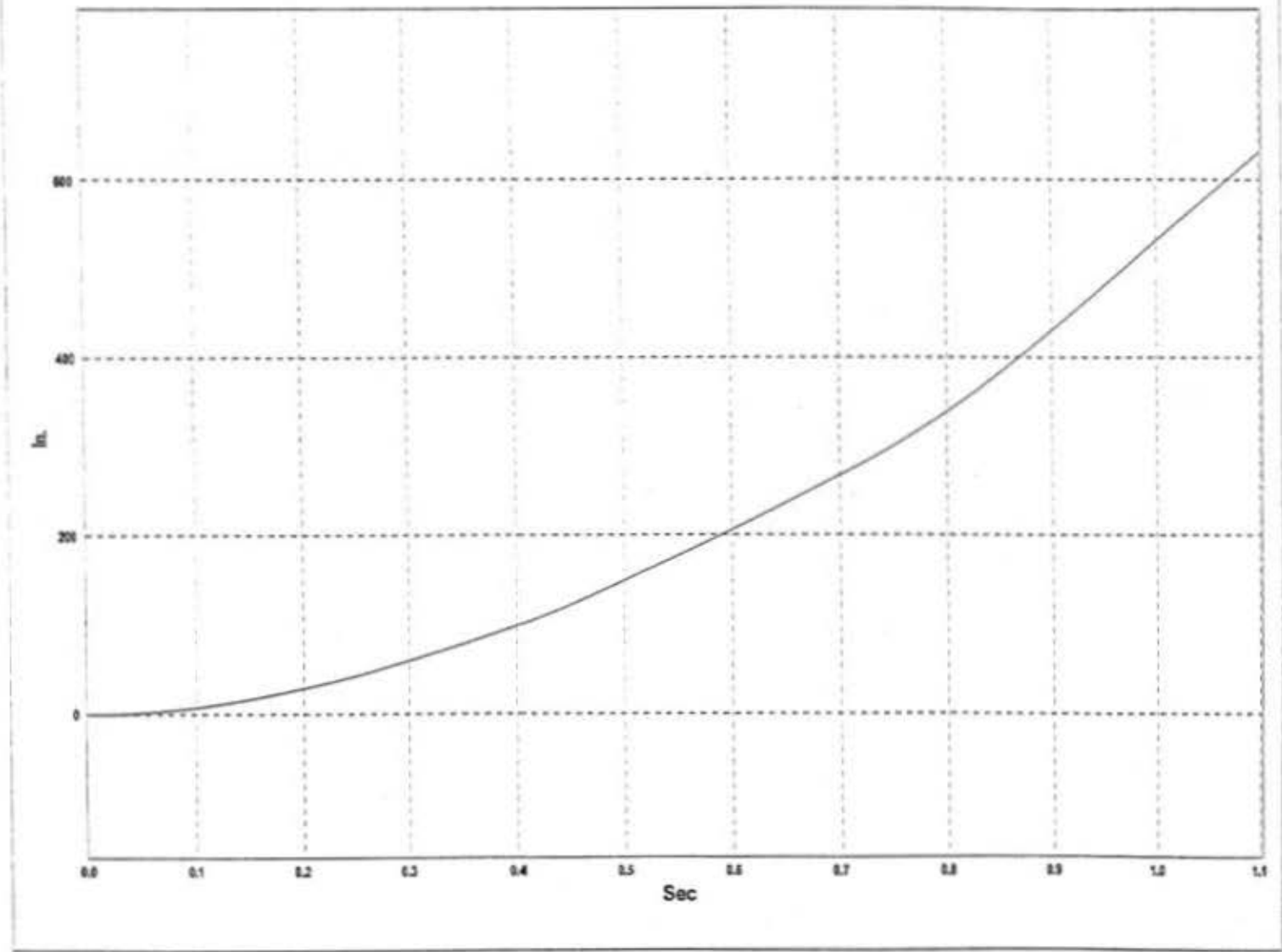


Figure A-3. Graph of Longitudinal Occupant Displacement - Filtered Data, Test MBN-5

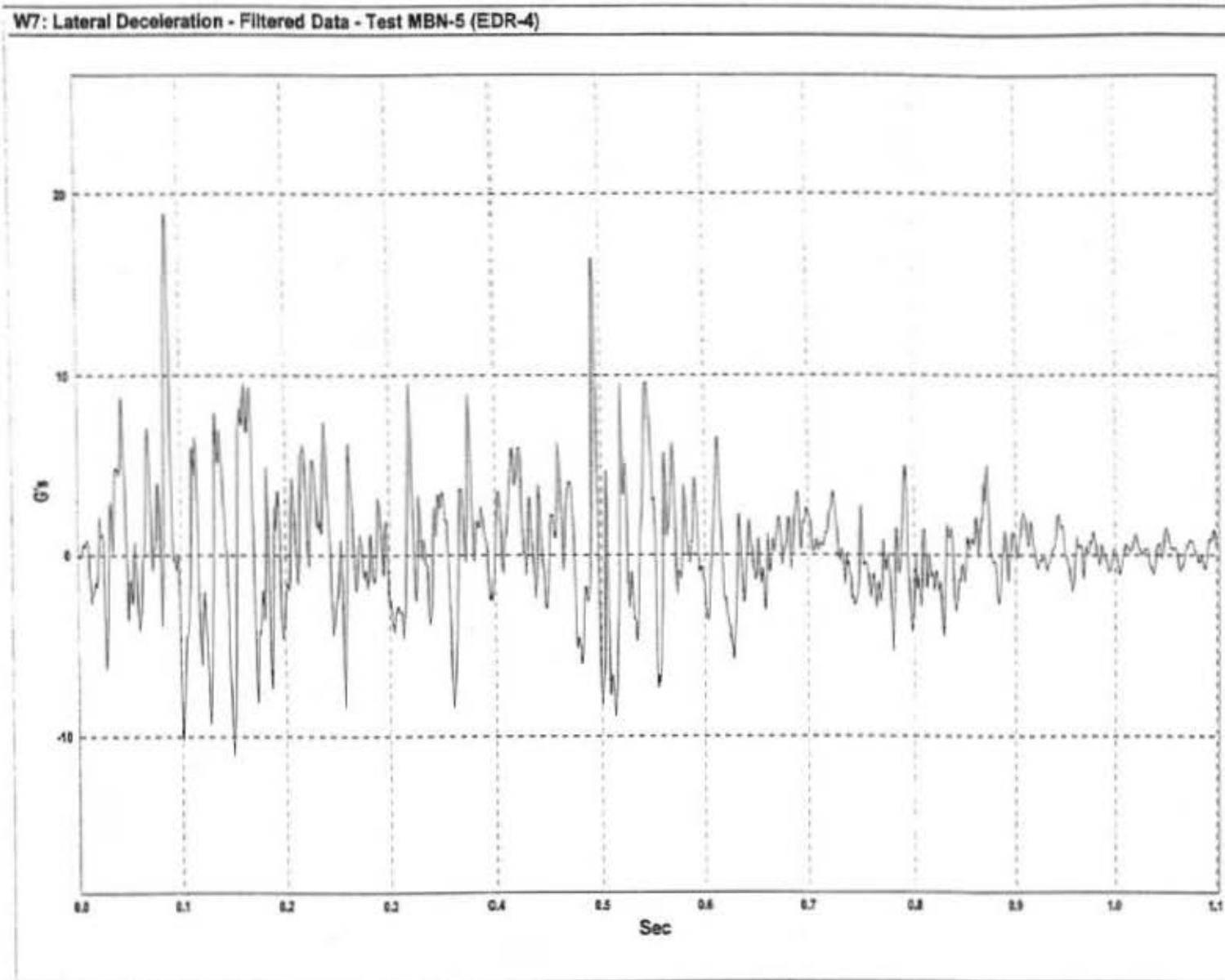


Figure A-4. Graph of Lateral Deceleration - Filtered Data, Test MBN-5

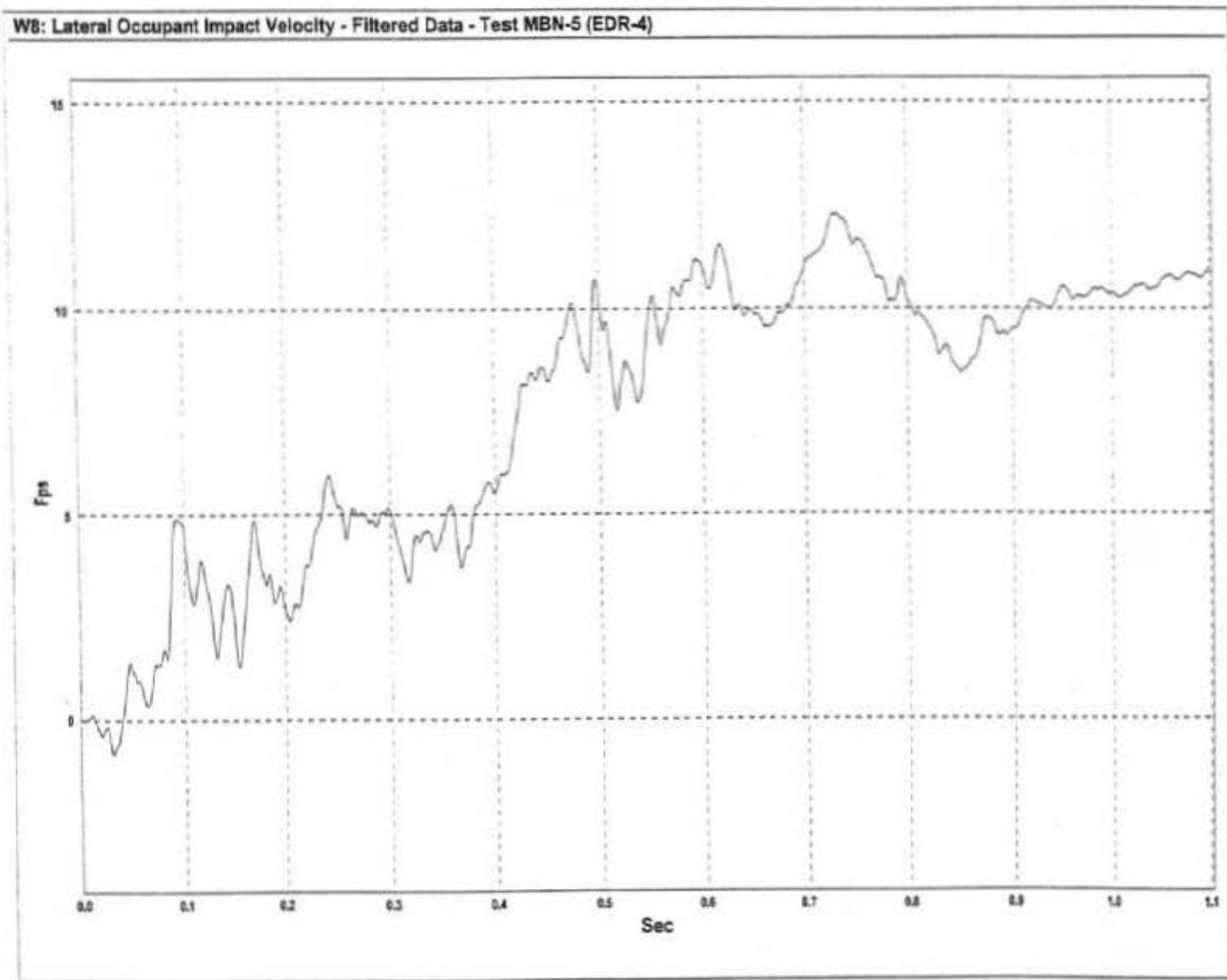


Figure A-5. Graph of Lateral Occupant Impact Velocity - Filtered Data, Test MBN-5

W9: Lateral Occupant Displacement - Filtered Data - Test MBN-5 (EDR-4)

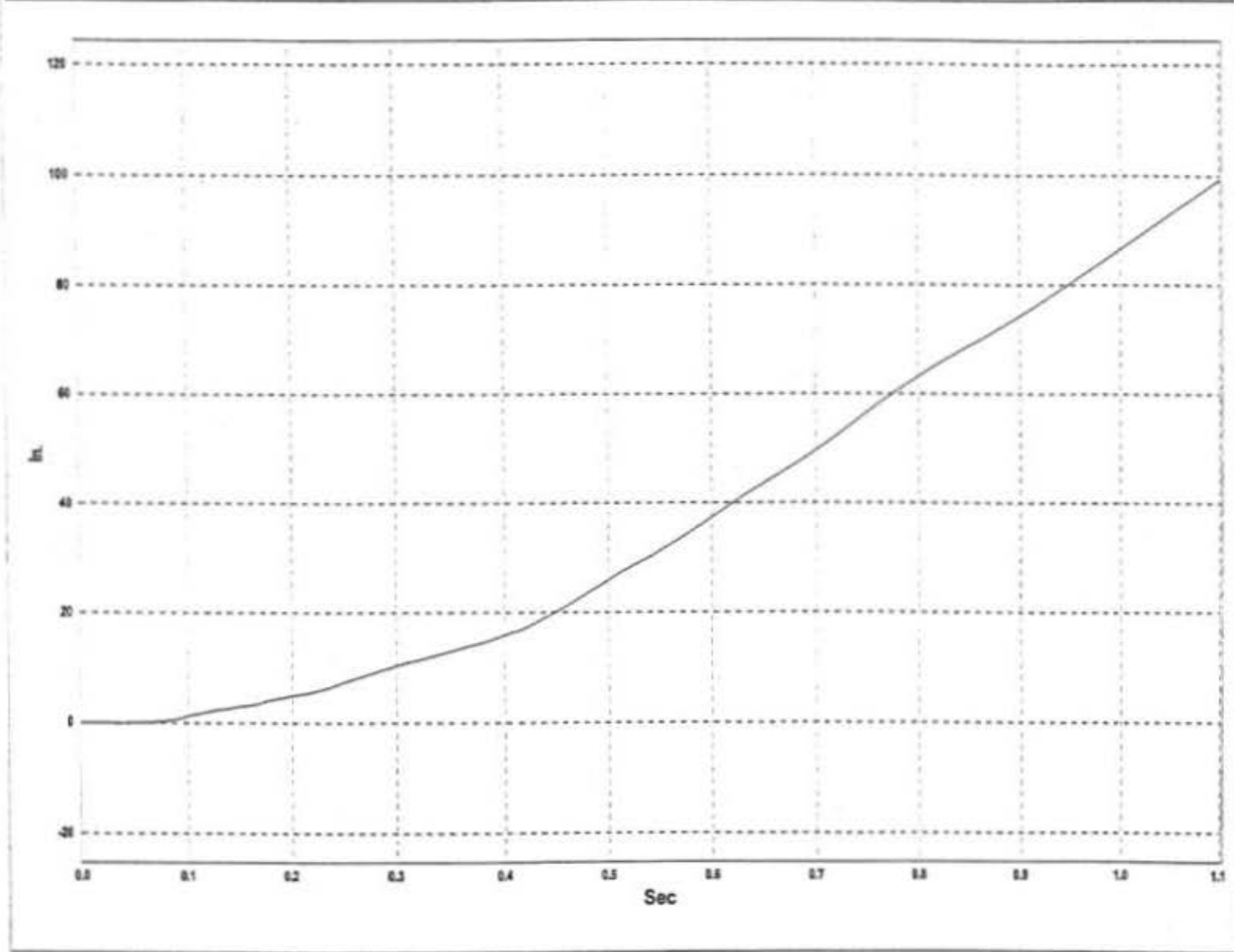


Figure A-6. Graph of Lateral Occupant Displacement - Filtered Data, Test MBN-5

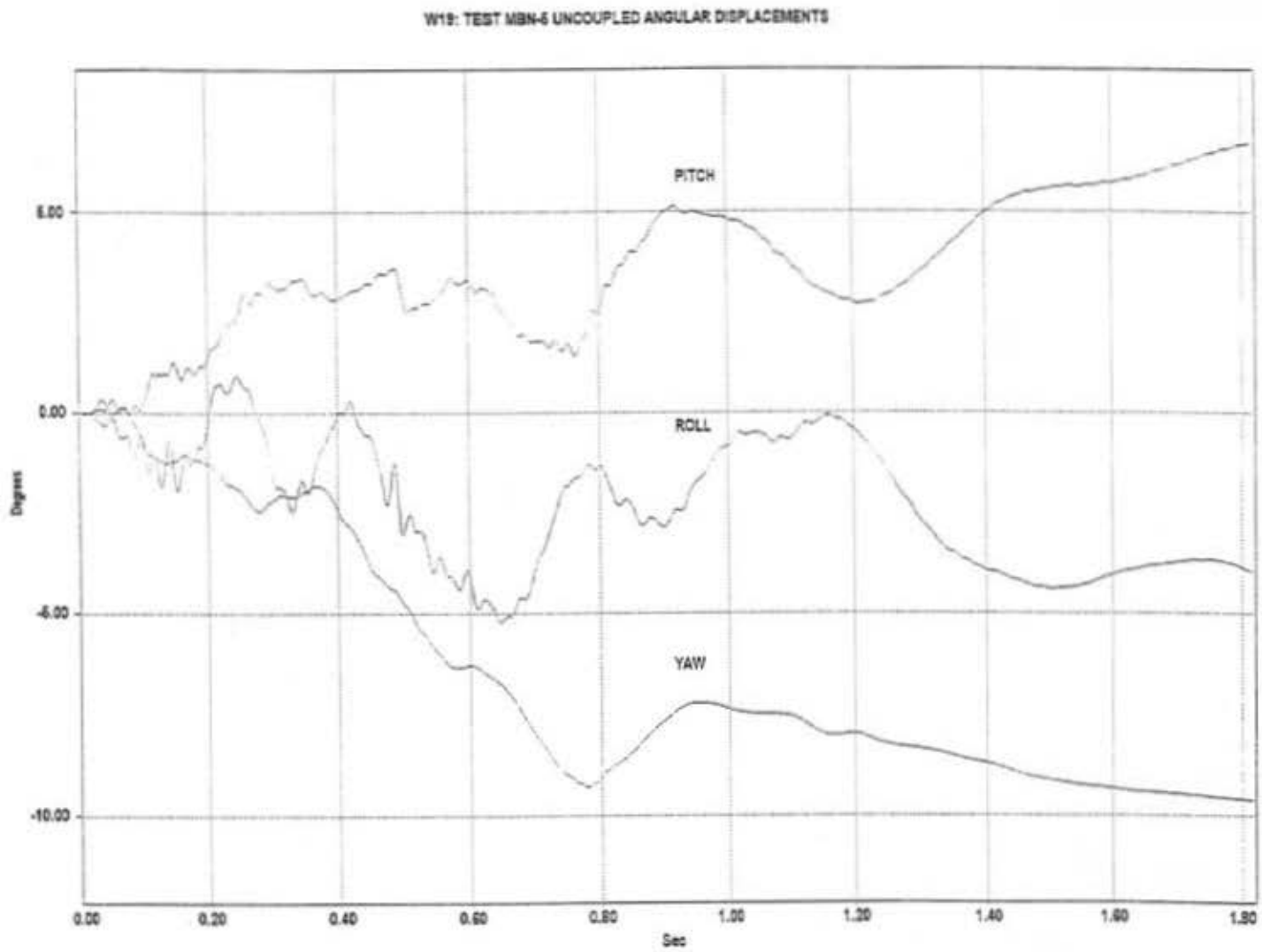


Figure A-7. Rate Transducer Data, Test MBN-5

APPENDIX B

ACCELEROMETER DATA ANALYSIS TEST MBN-6

- Figure B-1. Graph of Longitudinal Deceleration - Filtered Data, Test MBN-6
- Figure B-2. Graph of Longitudinal Occupant Impact Velocity - Filtered Data, Test MBN-6
- Figure B-3. Graph of Longitudinal Occupant Displacement - Filtered Data, Test MBN-6
- Figure B-4. Graph of Lateral Deceleration - Filtered Data, Test MBN-6
- Figure B-5. Graph of Lateral Occupant Impact Velocity - Filtered Data, Test MBN-6
- Figure B-6. Graph of Lateral Occupant Displacement - Filtered Data, Test MBN-6

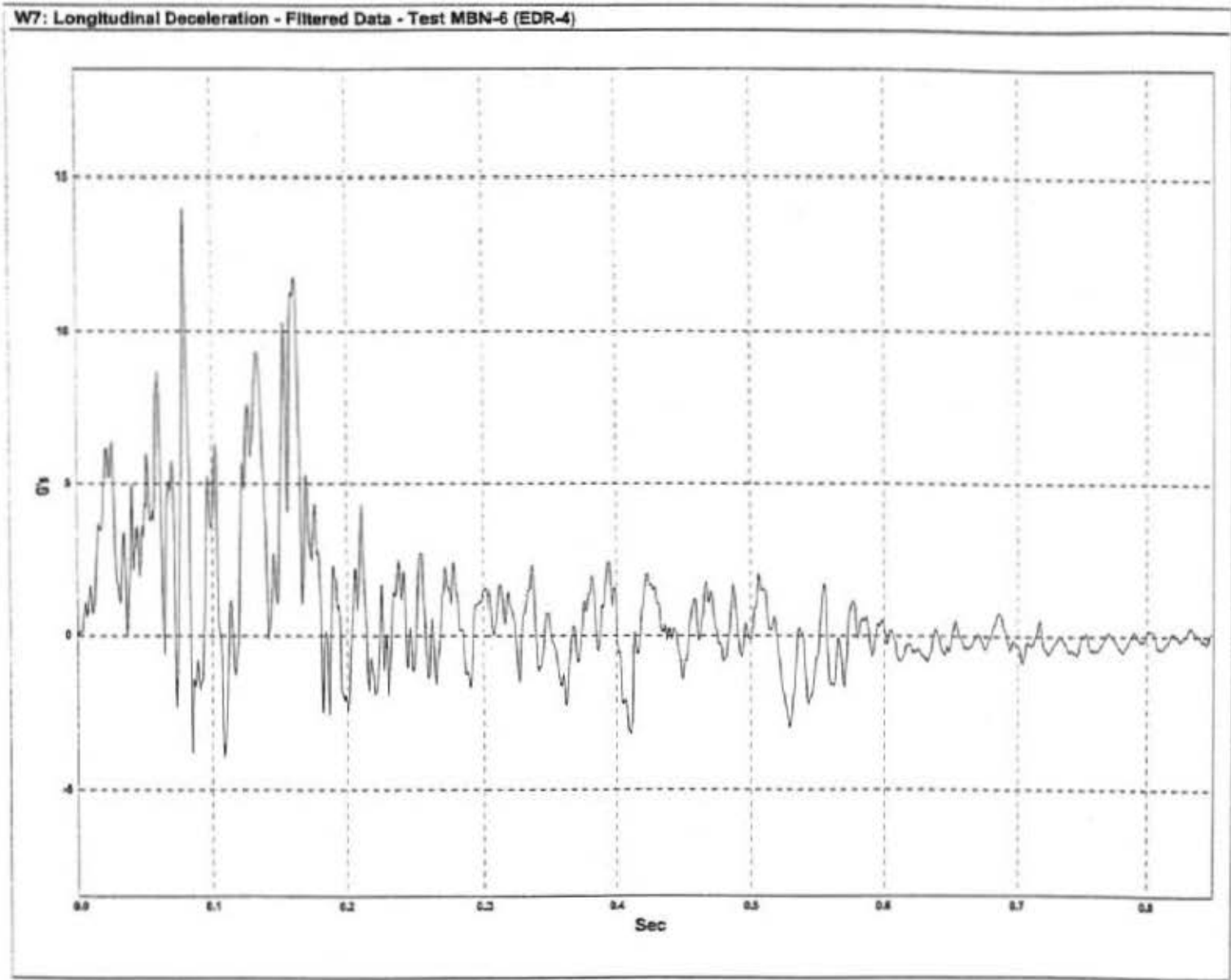


Figure B-1. Graph of Longitudinal Deceleration - Filtered Data, Test MBN-6

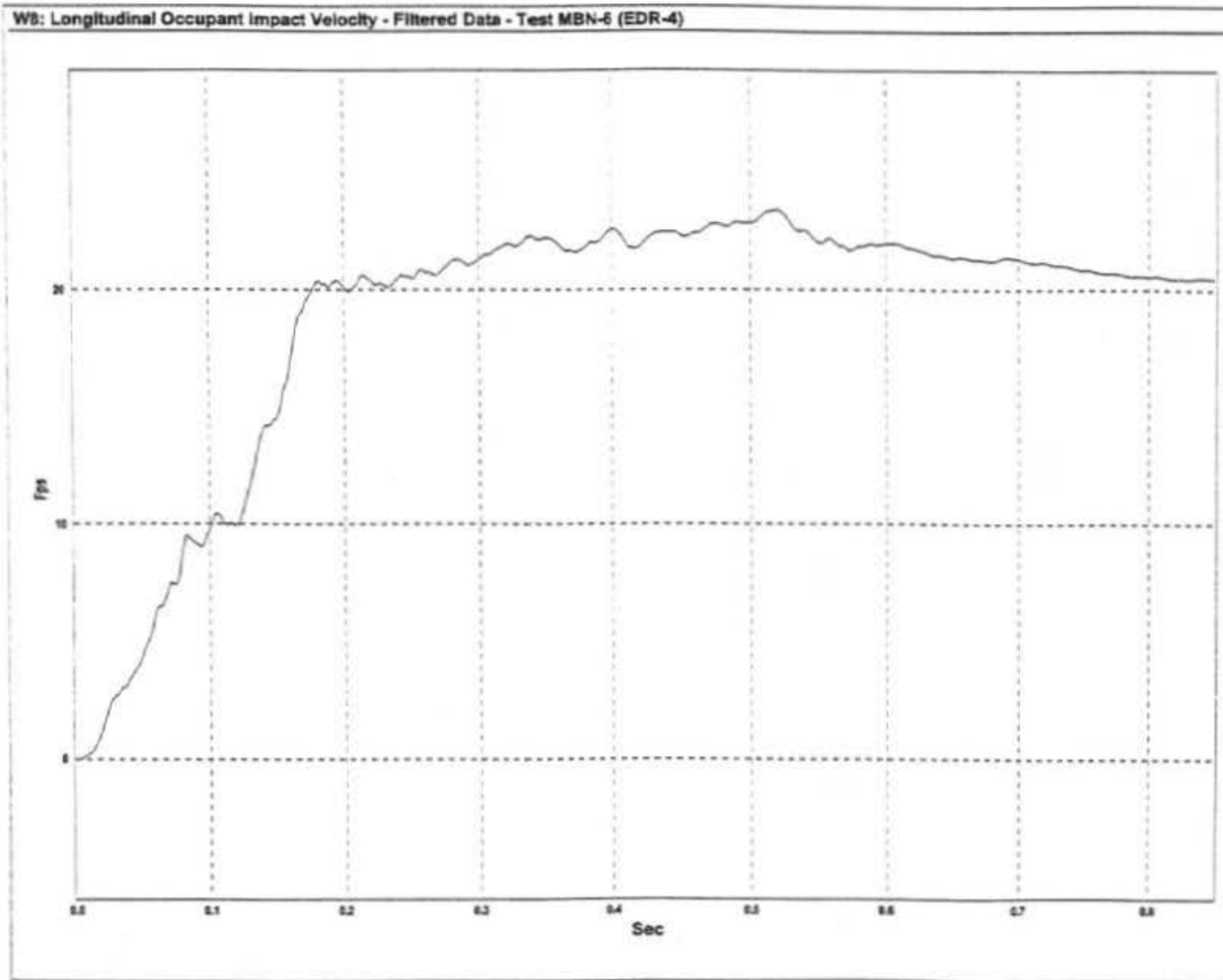


Figure B-2. Graph of Longitudinal Occupant Impact Velocity - Filtered Data, Test MBN-6

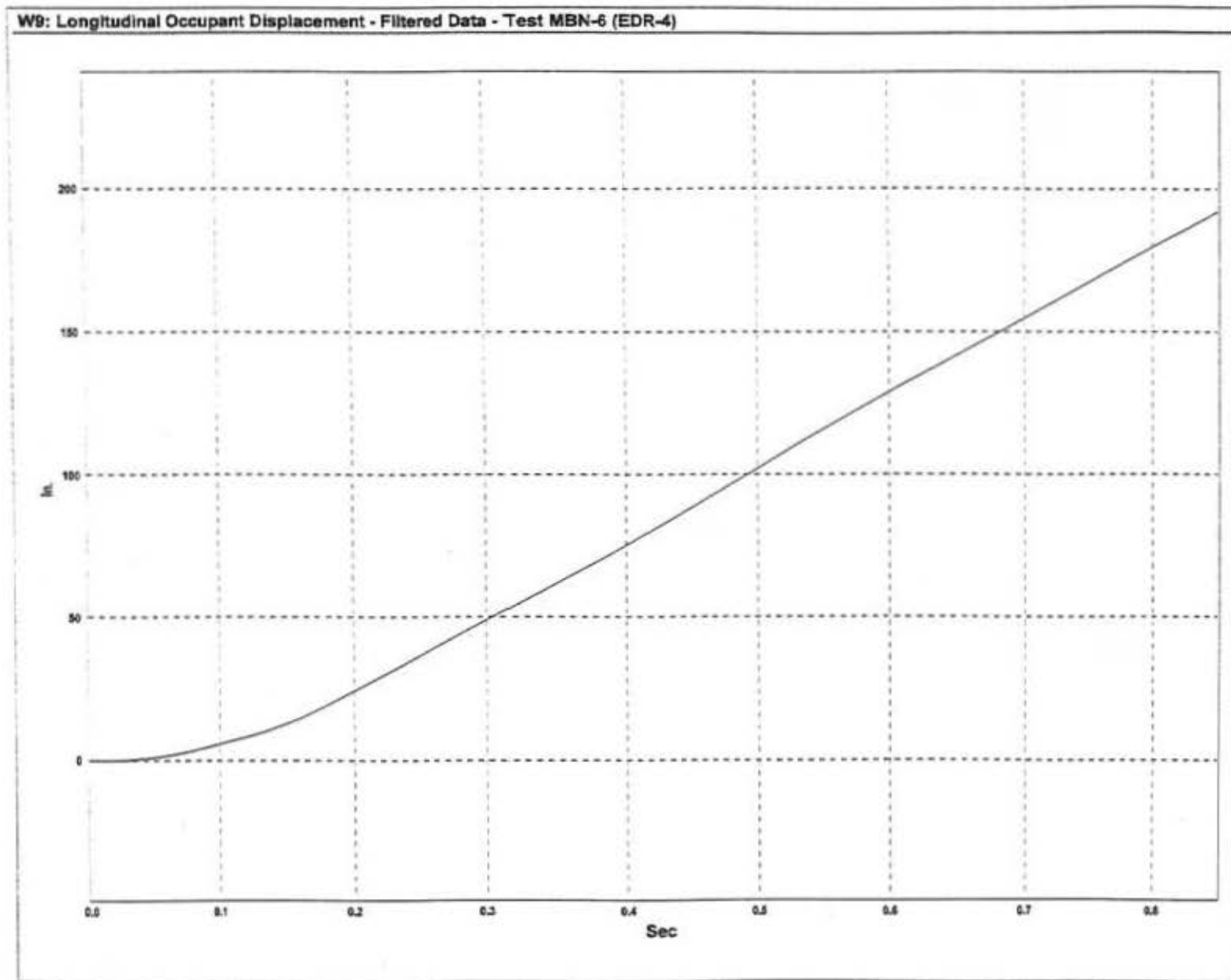


Figure B-3. Graph of Longitudinal Occupant Displacement - Filtered Data, Test MBN-6

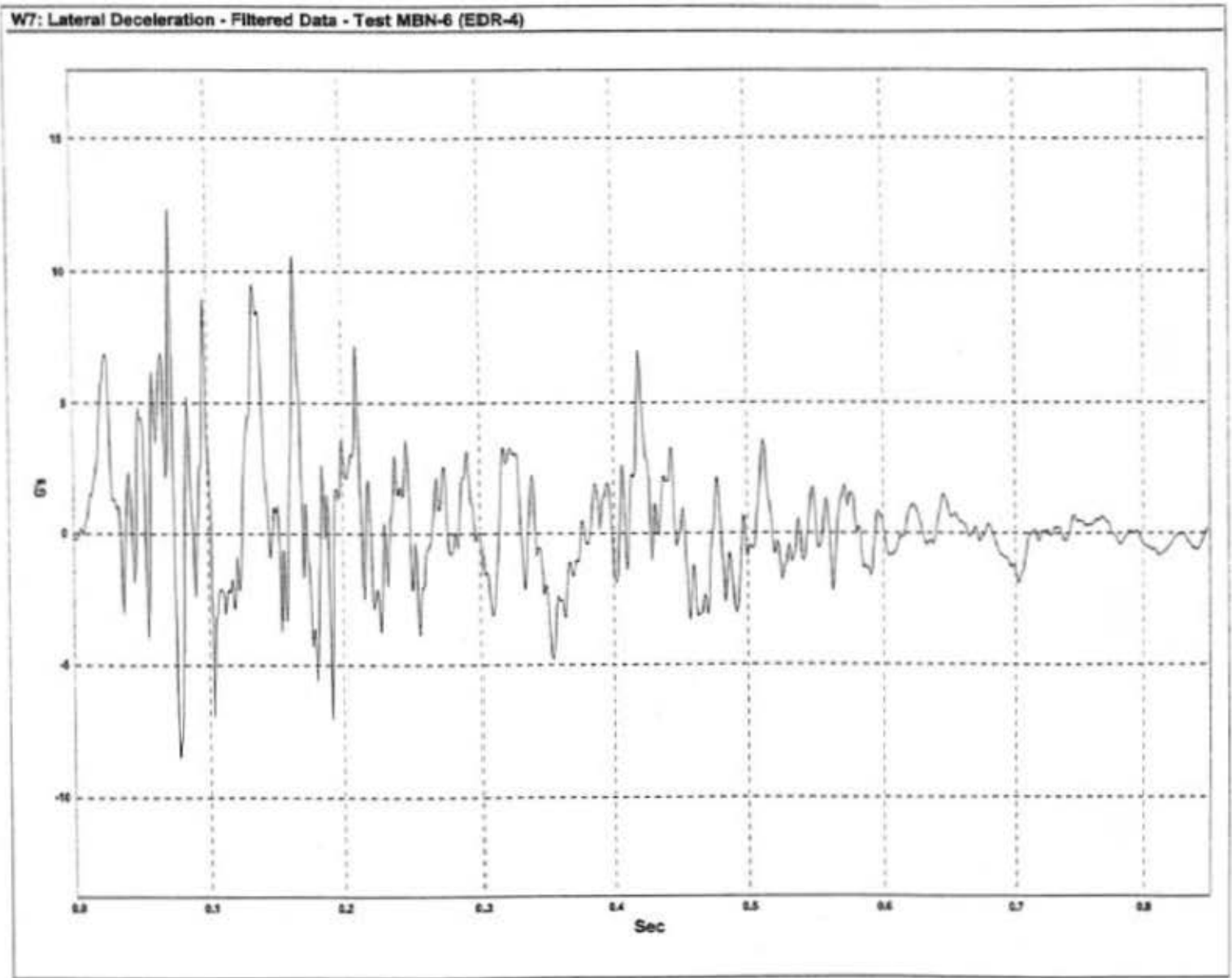


Figure B-4. Graph of Lateral Deceleration - Filtered Data, Test MBN-6

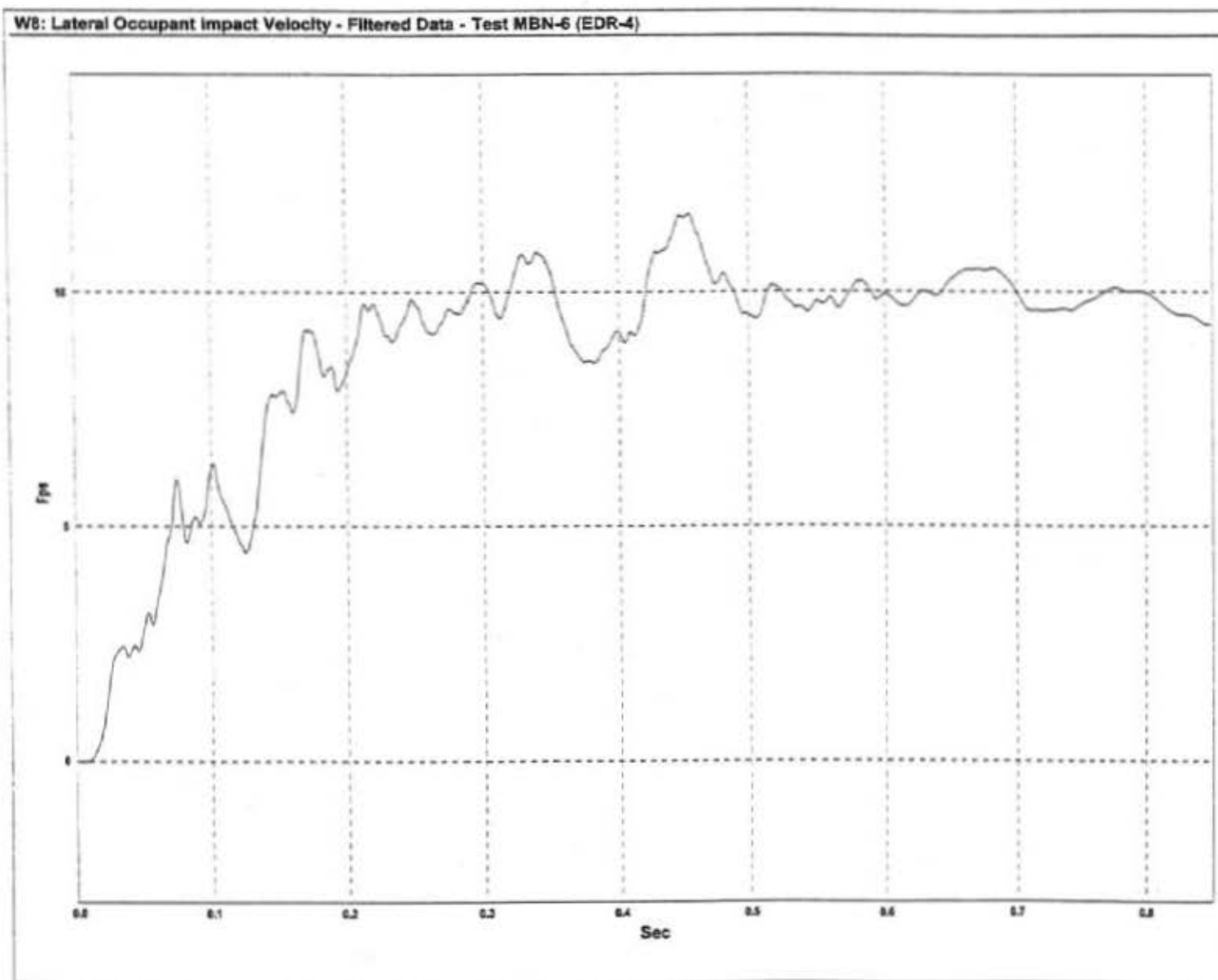


Figure B-5. Graph of Lateral Occupant Impact Velocity - Filtered Data, Test MBN-6

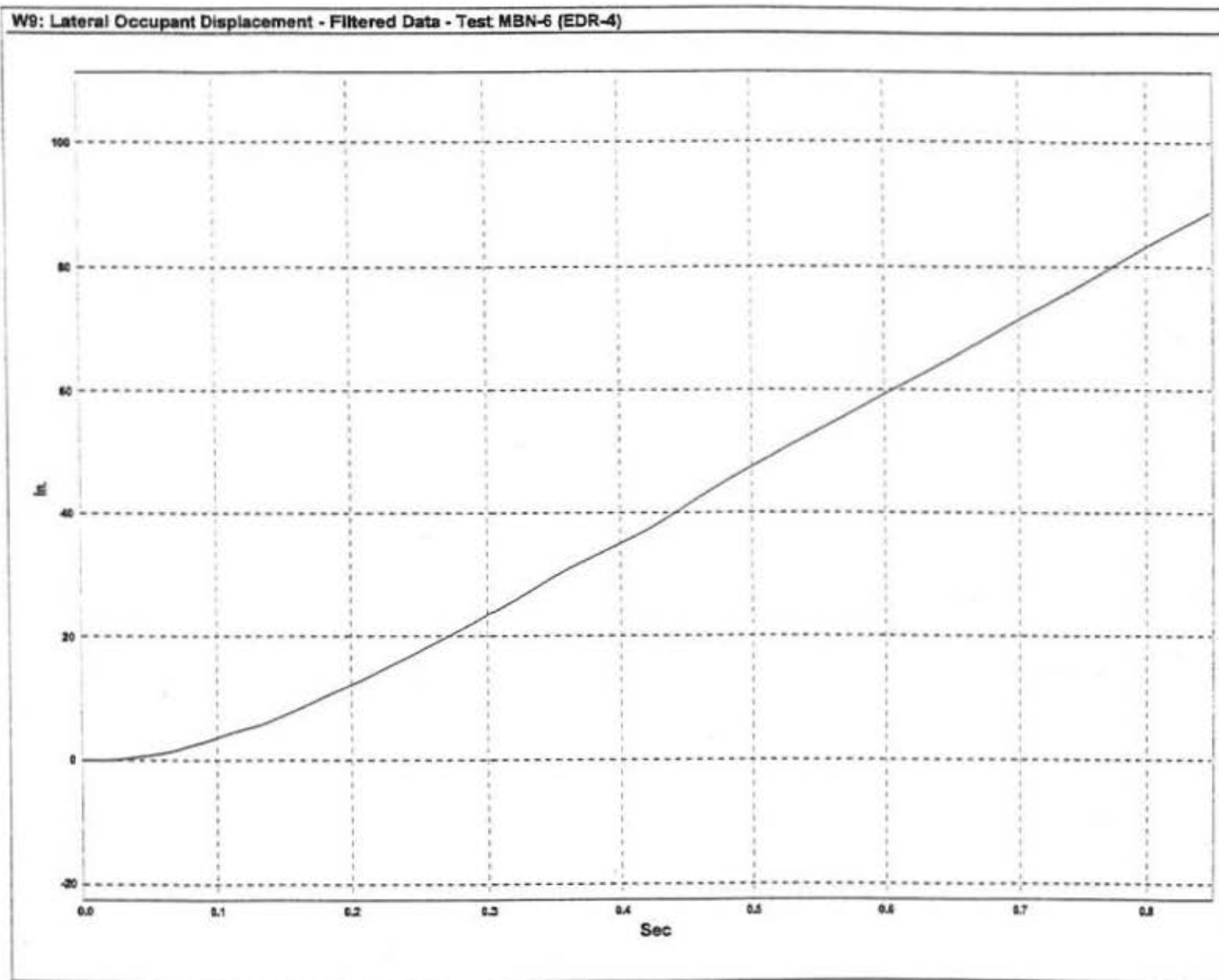


Figure B-6. Graph of Lateral Occupant Displacement - Filtered Data, Test MBN-6

APPENDIX C

ACCELEROMETER DATA ANALYSIS TEST MBN-7

- Figure C-1. Graph of Longitudinal Deceleration - Filtered Data, Test MBN-7
- Figure C-2. Graph of Longitudinal Occupant Impact Velocity - Filtered Data, Test MBN-7
- Figure C-3. Graph of Longitudinal Occupant Displacement - Filtered Data, Test MBN-7
- Figure C-4. Graph of Lateral Deceleration - Filtered Data, Test MBN-7
- Figure C-5. Graph of Lateral Occupant Impact Velocity - Filtered Data, Test MBN-7
- Figure C-6. Graph of Lateral Occupant Displacement - Filtered Data, Test MBN-7
- Figure C-7. Rate Transducer Data, Test MBN-7

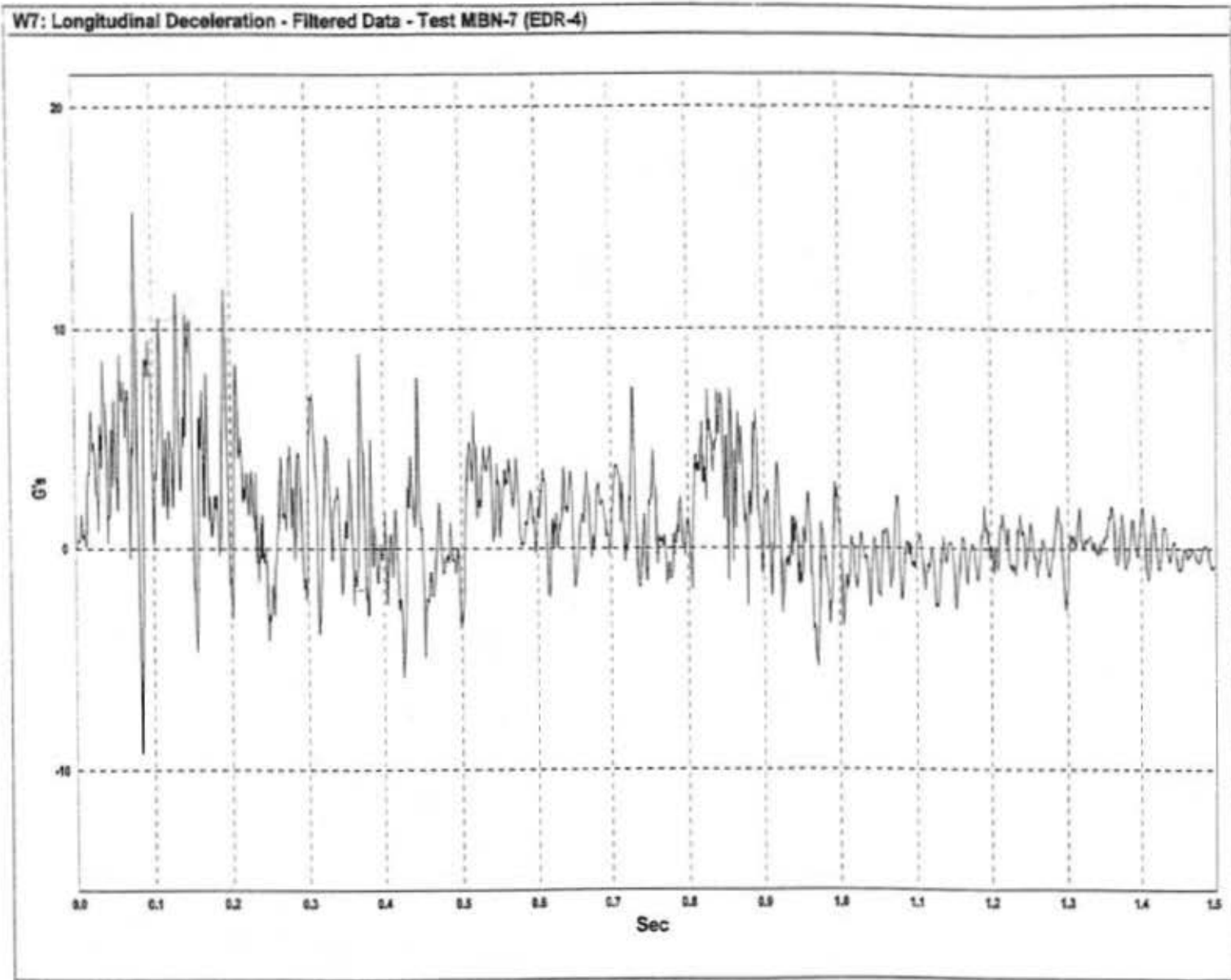


Figure C-1. Graph of Longitudinal Deceleration - Filtered Data, Test MBN-7

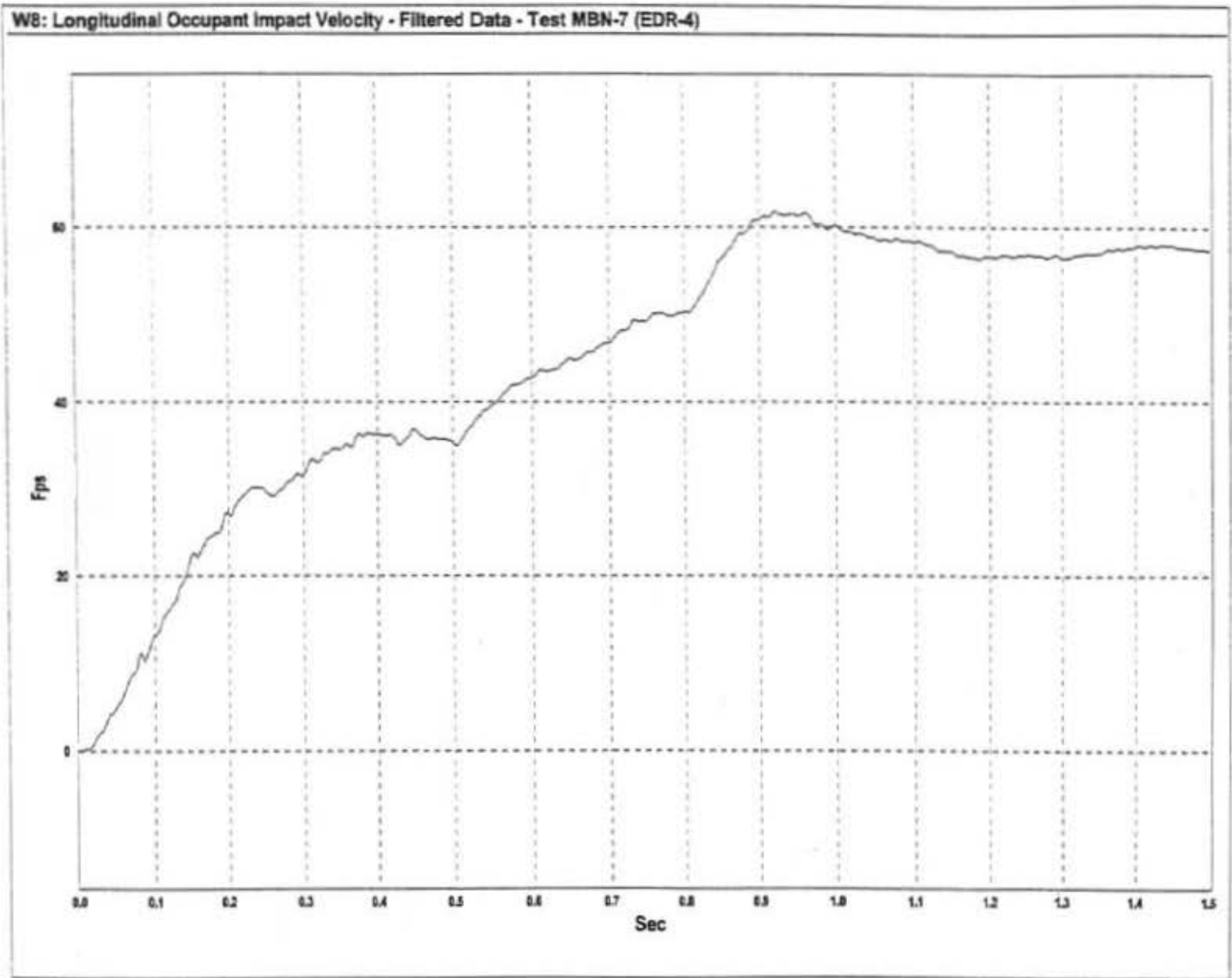


Figure C-2. Graph of Longitudinal Occupant Impact Velocity - Filtered Data, Test MBN-7

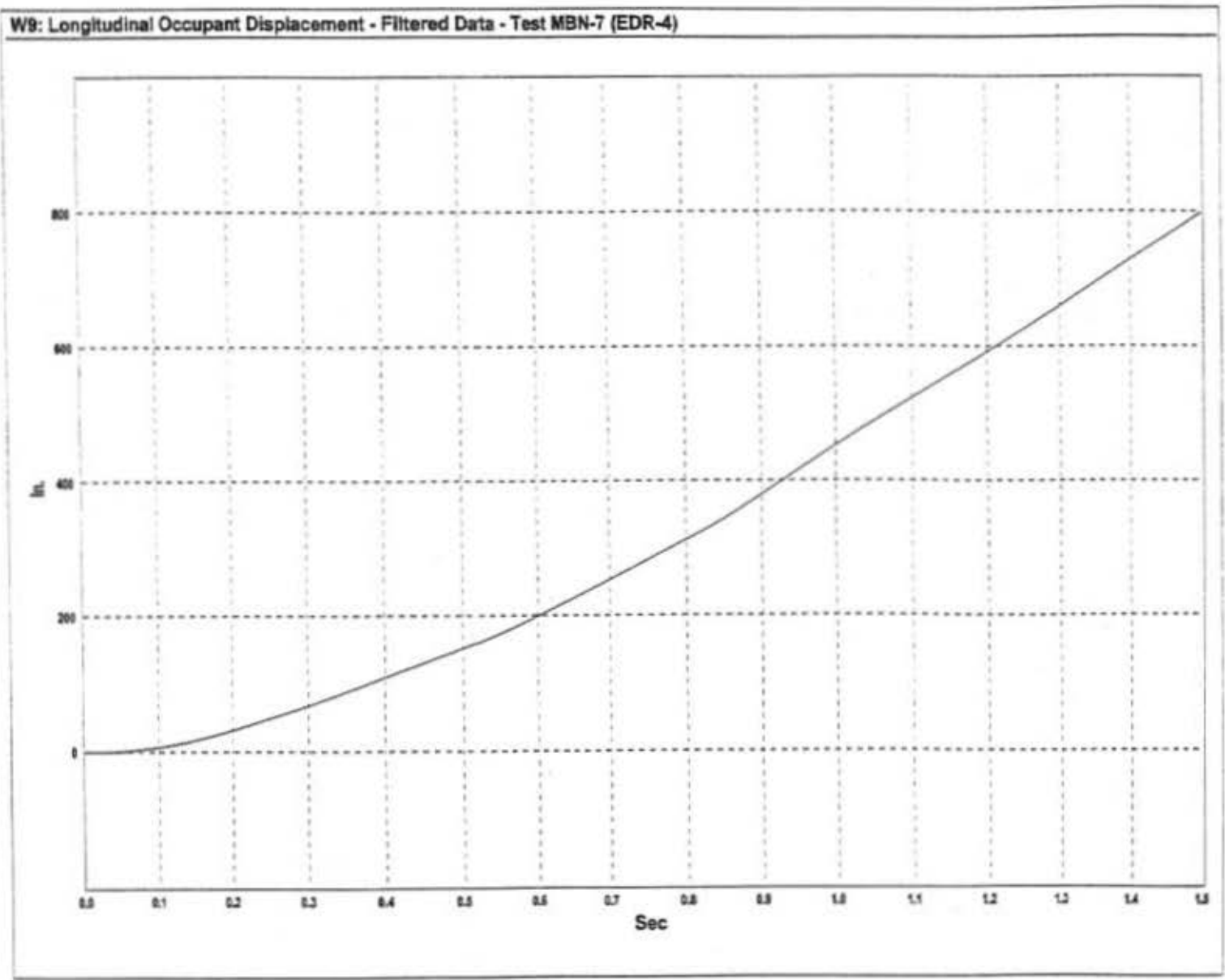


Figure C-3. Graph of Longitudinal Occupant Displacement - Filtered Data, Test MBN-7

W7: Lateral Deceleration - Filtered Data - Test MBN-7 (EDR-4)

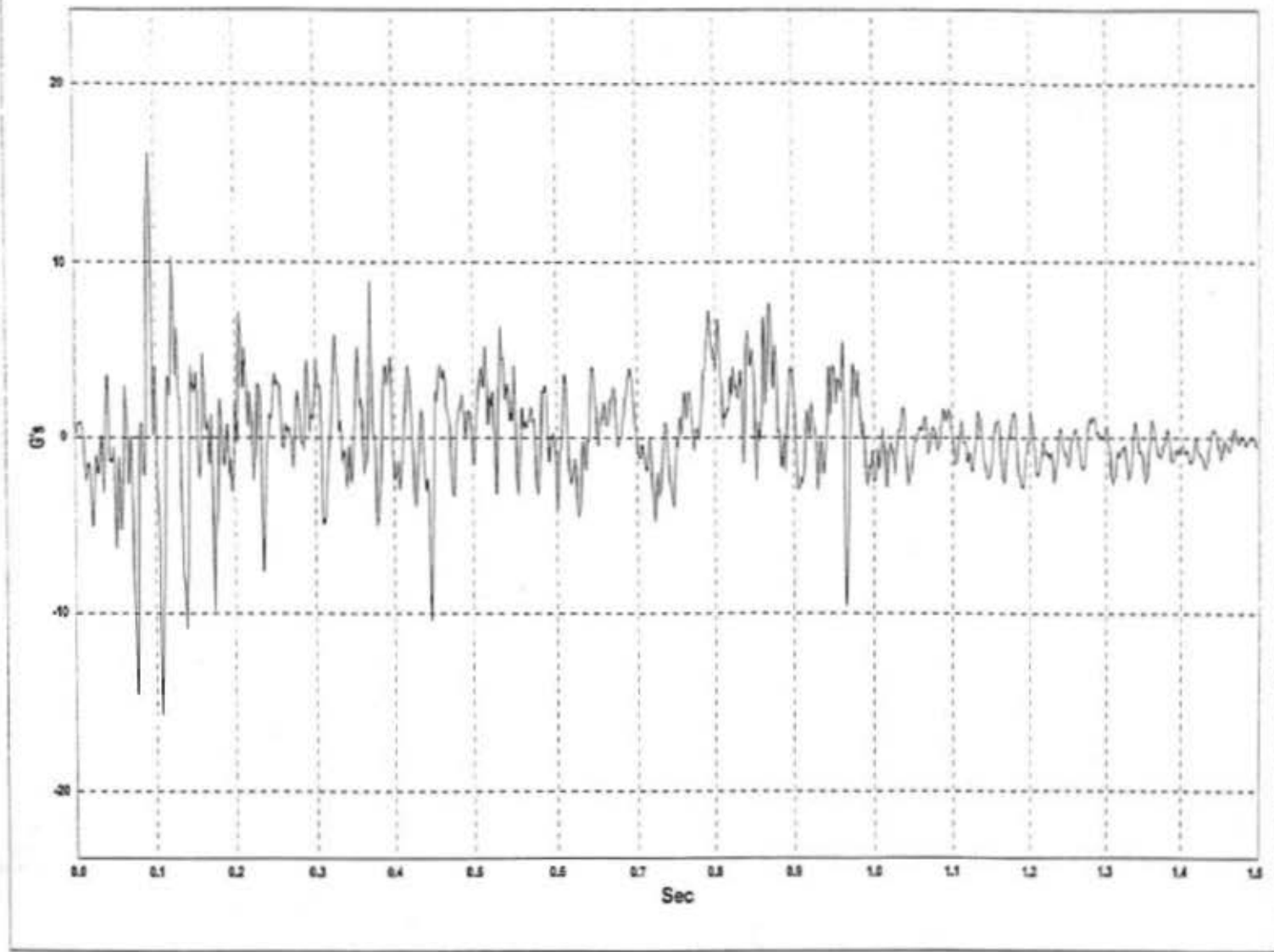


Figure C-4. Graph of Lateral Deceleration - Filtered Data, Test MBN-7

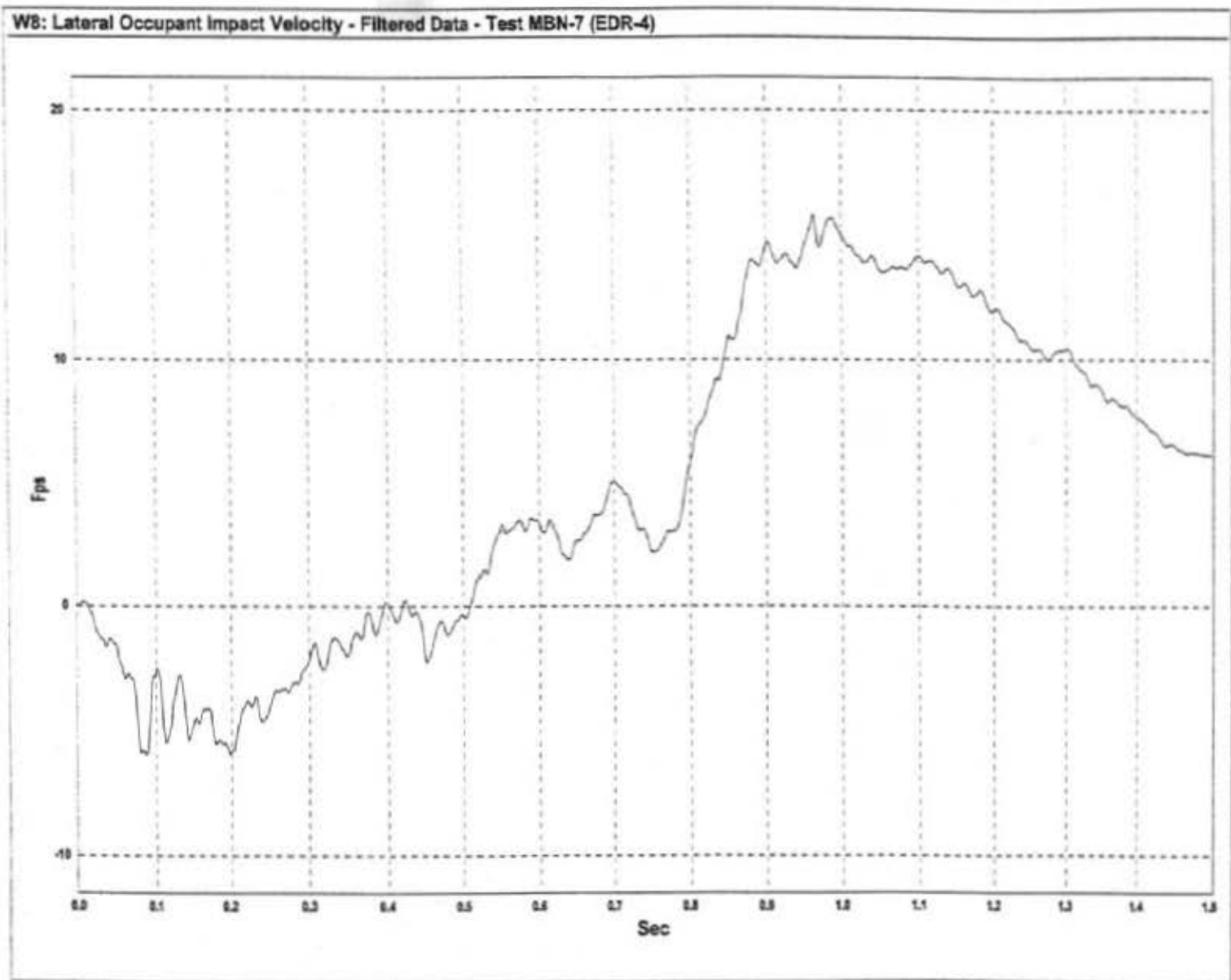


Figure C-5. Graph of Lateral Occupant Impact Velocity - Filtered Data, Test MBN-7

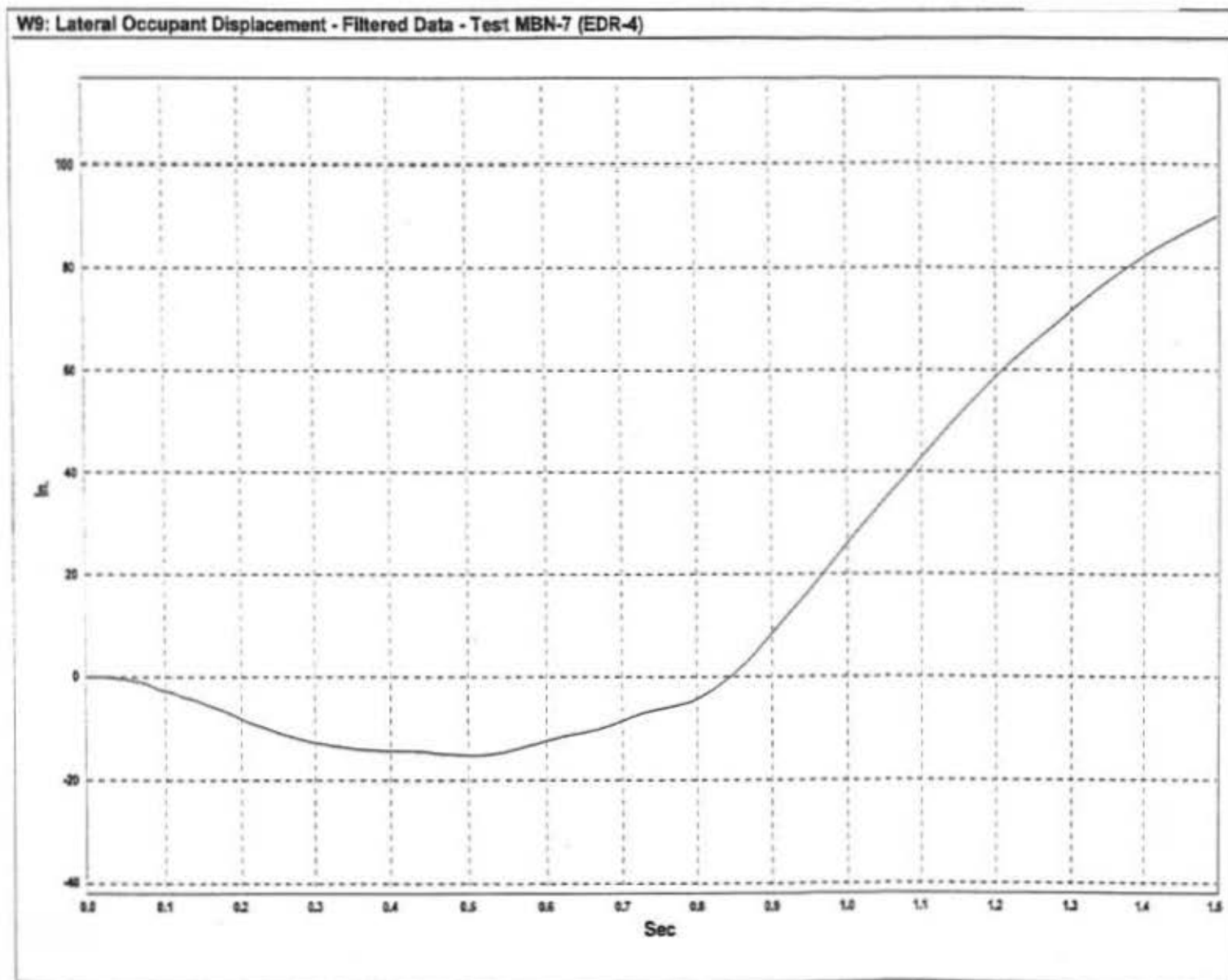
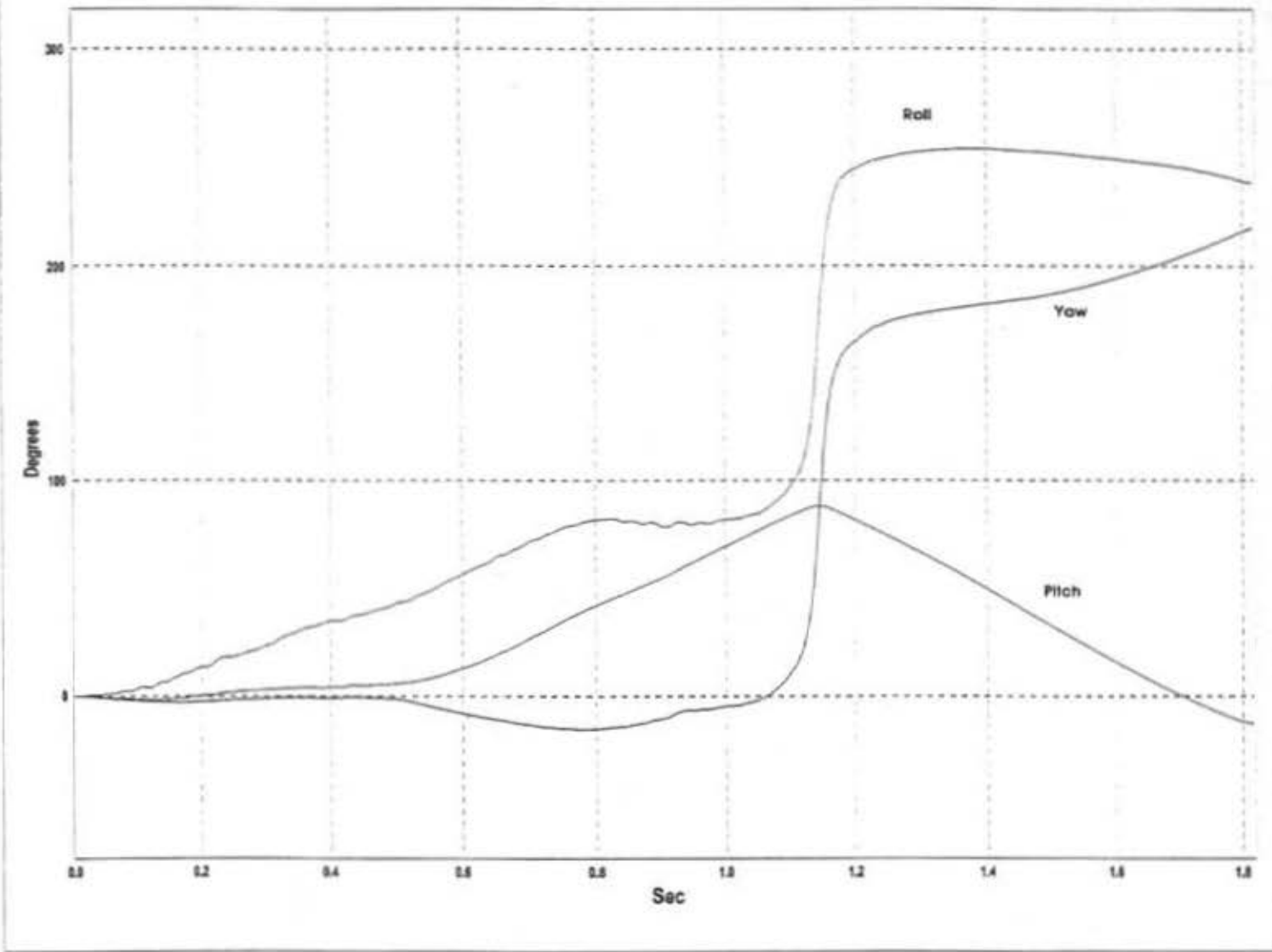


Figure C-6. Graph of Lateral Occupant Displacement - Filtered Data, Test MBN-7

W25: Test MBN-7 Uncoupled Angular Displacements



177

Figure C-7. Rate Transducer Data, Test MBN-7

APPENDIX D

ADDITIONAL COMPUTER SIMULATION DISCUSSION AND RESULTS

Transition from a Frontal Impact to a Redirection Impact on a New Bullnose Guardrail System Design

John D. Reid
University of Nebraska-Lincoln

ABSTRACT

Bullnose guardrail systems are used to protect vehicles from hazards in the median of divided highways. The Midwest Roadside Safety Facility is currently designing and testing a new bullnose system that will meet relatively new Federal safety performance specifications. After developing a system that successfully handled frontal impacts, attention was then focused on the redirection impacts required of such systems. Similar to vehicle design for frontal and side impact, there are many differences in the modeling and simulation requirements between frontal and redirection impacts for bullnose systems. Several complicated modeling problems were solved that only became evident when contacts became unstable during the simulations. The problems were mainly related to modeling issues such as course mesh sizes, contact penalty factors, contact thicknesses, edge-to-edge penetrations not being addressed in the model, and unstable element formulations after significant hourglassing had been induced. The resulting model can now be used to help re-design the bullnose system to meet the redirection requirements of such systems.

INTRODUCTION

Divided highways separated by a median area are a valuable safety feature in modern roadway design. However, many roadway structures are built in the median such as bridge supports, drainage structures, and large sign supports. These structures present hazards to vehicles in the median. There are three main treatments that have been used in the protection against median hazards such as crash cushions, open guardrails, and closed guardrail envelopes, called bullnose systems. Bullnose systems involve wrapping the guardrail completely around the hazards (see Figure 1).

In past years, several design studies were undertaken to improve and evaluate the performance of closed guardrail median barriers [1,2,3]. Results from these projects had varying degrees of success but none of the designs studied meet current safety standards as specified in the National Cooperative Highway Research Program (NCHRP) Report No. 350, *Recommended Procedures for the Safety Performance Evaluation of Highway Features* [4]. Seven different crash tests are required in order for a bullnose guardrail system to be approved to be installed on our Federal Highways. These tests fall under three categories, head-on impacts, redirection impacts, and reverse direction impacts. A schematic of the tests is shown in Figure 2. All tests are run at 100 km/h.

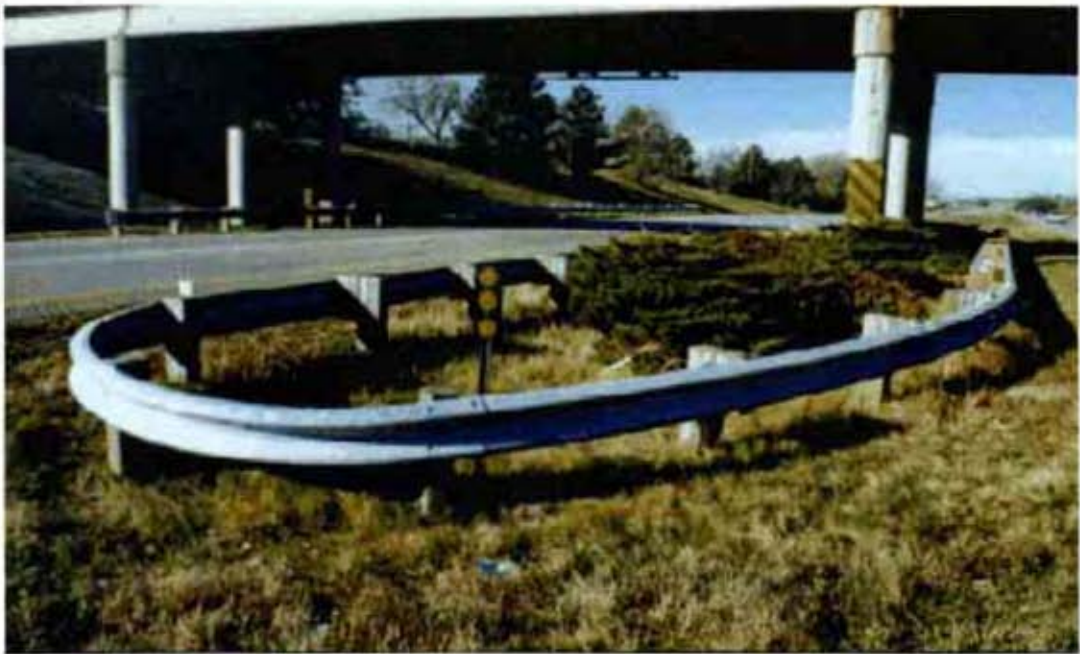


Figure 1. Typical W-Beam Bullnose Guardrail

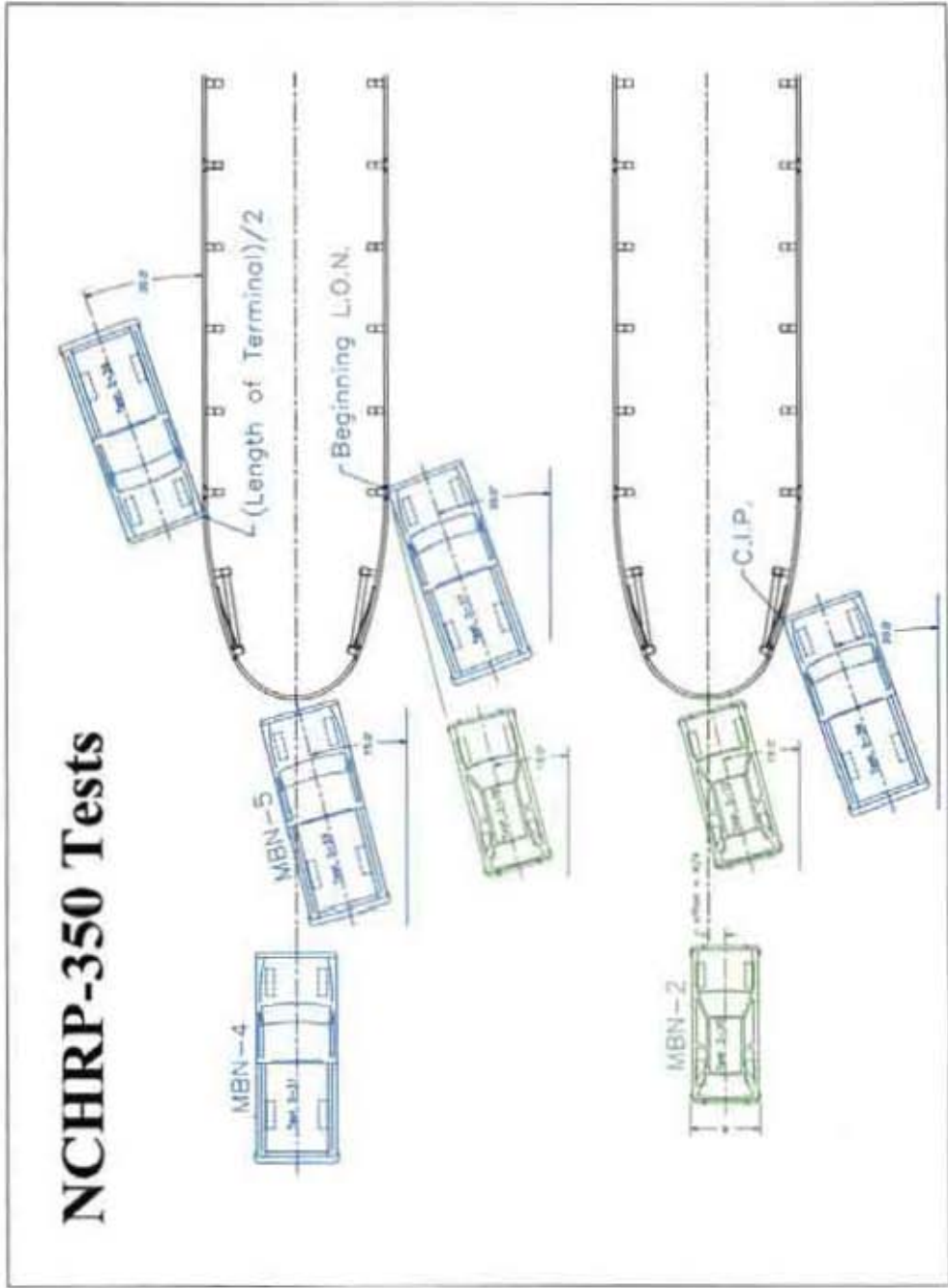


Figure 2. NCHRP Report 350 Crash Tests for a Bullnose System

In 1997, the Midwest Roadside Safety Facility (MwRSF) began a project to develop a new bullnose system that would meet NCHRP 350 requirements. This project is sponsored by the Midwest Pooled Fund States and by the Federal Highway Administration (FHWA).

The first phase of the project concentrated on the head-on impact conditions involving two tests with a 2000-kg pickup truck and one test with a 820-kg small car. In order to pass these three tests, two major design changes were required due to two failed crash tests. Throughout this effort, nonlinear, finite element simulation played a key roll in identifying the cause of failure and predicting the successful re-design. Results from both simulation and physical testing of the head-on impact with the 2000-kg truck are shown in Figure 3. Note that the simulation was completed prior to the physical test. Details of the first phase were documented by Reid and Bielenberg [5]

Researchers were then presented with a new challenge when the newly designed bullnose system failed the 100 km/h redirection test with a 2000-kg pickup. The bullnose failed to contain the pickup and instead rolled back and formed a ramp causing the truck to vault into the air and over the system (see Figure 4). To determine the cause of the failed test, researchers again turned to simulation. Unfortunately the transition from simulating the head-on impact to the redirection impact required an extensive modeling effort. Not only did the model require major modifications, a series of contact troubles delayed the project several months.

The bullnose project is still under development at the MwRSF. This paper documents the transition from testing and simulating the head-on impact condition to the testing and simulation of the redirection impact condition required to meet NCHRP 350 specifications. The software used for this effort was LS-DYNA, developed by Livermore Software Technology Corporation [6].

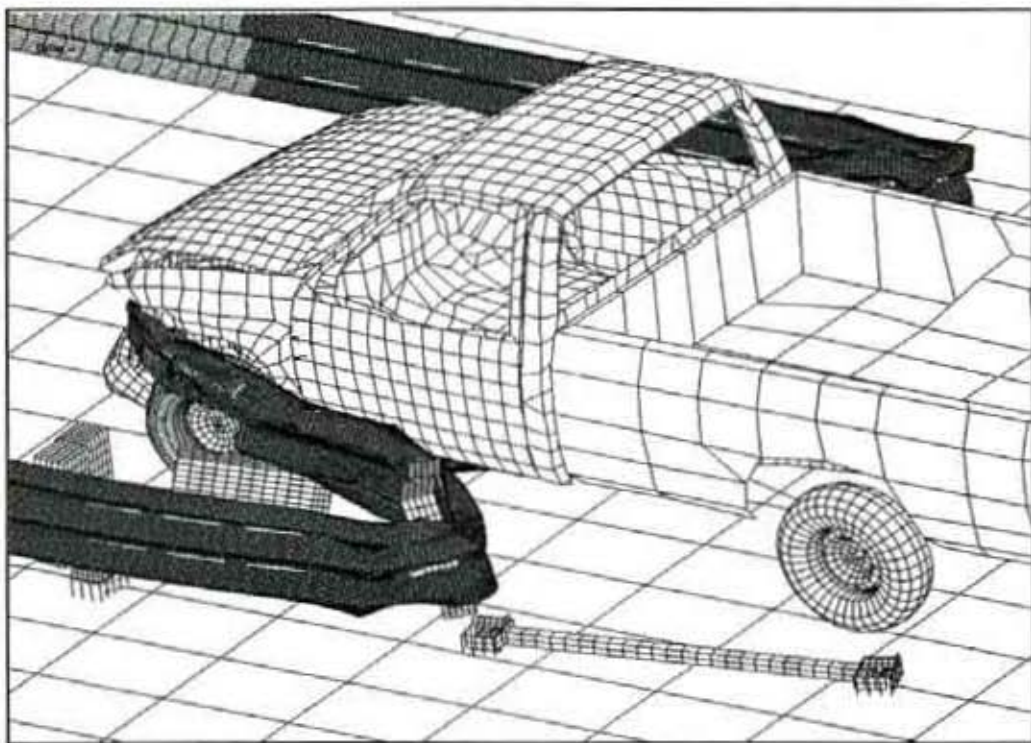


Figure 3. Frontal Impact - Bullnose Captures Vehicle

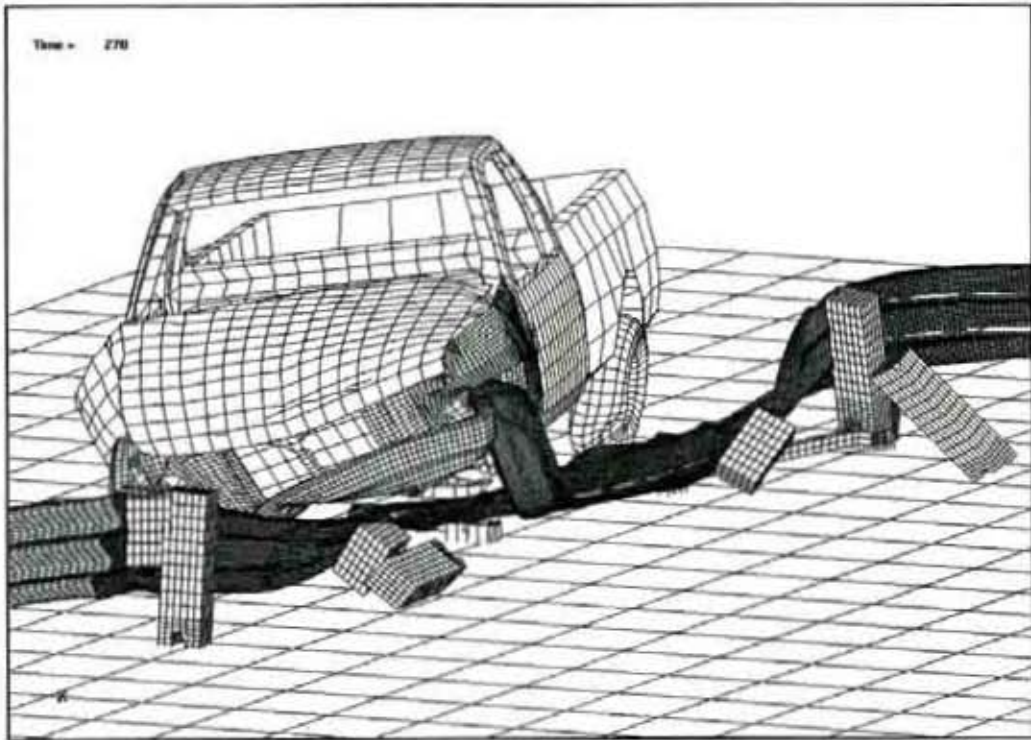


Figure 4. Redirection Impact - Truck Vaults Over Bullnose

BARRIER DESIGN

The front portion of the bullnose system is shown in Figures 5 and 6. The nose section was formed using one 1,580-mm radius curved section of 12-gauge steel thrie beam with one 10,400-mm radius curved section attached to each end of the center section. During a vehicle head-on impact with a bullnose, the rail element is forced to bend through an angle of 180 degrees as the vehicle progresses into the system. The bending strength of two thrie beams is relatively high and would result in high vehicle decelerations. Additionally, previous research had shown a tendency for a large vehicle or truck to over ride bullnose type systems and for a small car to under ride such a system [3]. To address these concerns, slots were cut in the valleys of the rail. The slots accomplish two tasks. First, they allow the front peaks to wrap around a vehicle to capture it and prevent over ride and under ride. Second, they weaken the rail to allow for lower force bending levels.

The system was symmetric with eleven posts positioned on each side. The first two posts on each side of the system were standard BCT (Breakaway Cable Terminal) posts set in foundation tubes with soil plates. The third post on each side of the system was a BCT post set in a foundation tube without a bearing plate. The fourth and fifth posts on each side of the barrier were CRT (Controlled Releasing Terminal) posts. The remaining posts of the bullnose barrier were standard 200-mm deep by 150-mm wide by 1830-mm long wood posts spaced 1905-mm apart. With the exception of post 1, a wood blockout was used to space the rail away from the posts. A cable anchor system was used between the first and second posts on each side of the system to develop the tensile strength of the thrie beam guardrail downstream of post no. 2.

MODELING

The bullnose is composed of many components, including wood posts, cable anchor bracket assembly, guardrail, ground strut, foundation tubes and various brackets and attachment bolts. Reid and Bielenberg described the simulation model for the frontal impact scenario previously in [5] (see Figure 5). Three important modeling features noted were the mesh size of the rail, the failure criteria of the rail and the modeling of the breakaway wood posts.

The redirection model of the bullnose is depicted in Figure 6. Many modifications to the frontal model were required in order to effectively simulate the redirection impact. The following list summarizes the major changes.

Bullnose Model Changes

- Add the cable anchor assembly.
- Remove everything beyond post 2 on the left side (impact is on right side).
- Update slot pattern to be more accurate.
- Add CRT posts and soil springs for posts 4 and 5.
- Add CRT post parts to the contact interior definition, which prevented negative volumes.

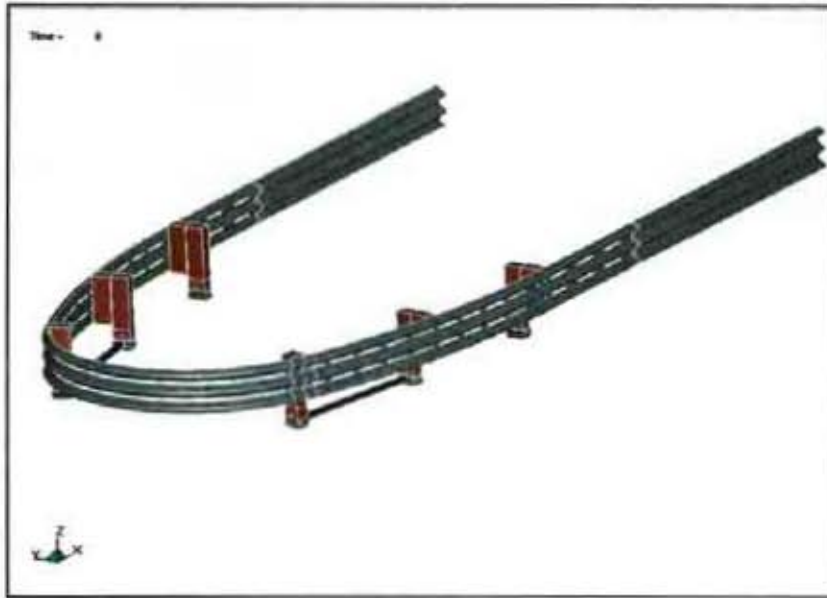


Figure 5. Overview of Frontal Impact Model

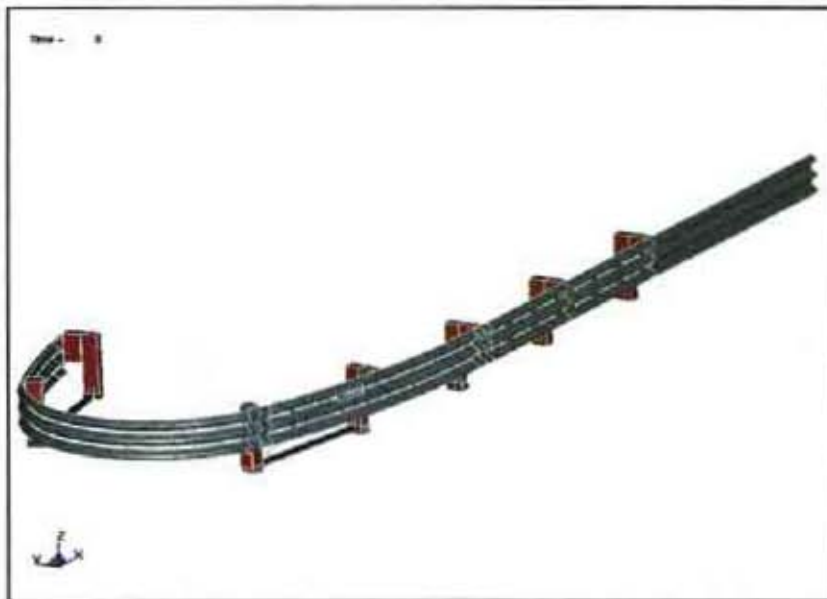


Figure 6. Overview of Redirection Impact Model

- Extend deformable rail to approximately post 7 location (previously extension was to post 5 location).
- Replace fix boundary condition on end of rail on impact side with a discrete spring to simulate rail flexibility.
- Add shell elements to cover the rail slots, use null material.
- Add control accuracy to the model - objective stress updates and invariant node numbering for shell elements.

Truck Model Changes

The FHWA had previously contracted model development of a C2500 pickup truck to the National Crash Analysis Center (NCAC) [7]. The NCAC subsequently developed a truck model with approximately 10,000 elements for frontal impact scenarios. Version 7 of the NCAC reduced truck model was downloaded from the NCAC web site and was modified for this study. When converting from the frontal impact scenario to the redirection impact, the following changes were made to the truck model.

- Truck was repositioned for a 20 degree impact at the critical impact location (which was half-way between posts 1 and 2). This also required an update of the direction for the initial velocity specification.
- A new part was added to fill in the light-holes on the radiator-tie bar to improve contacts.
- Refine the mesh of the left front tire, bumper, radiator-tie bar and left front mounting brackets by splitting the elements (1 element into 4 elements) to improve contacts.
- Doubly refine the mesh of the left front fender and wheel well by splitting the elements twice (1 element into 16 elements) to improve contacts.
- Switch element formulation for the left front tire, left front fender and radiator-tie bar to a fully integrated scheme (type 16) to prevent hourglassing.
- Stiffen the tire to prevent excessive, unrealistic deformations.

MODELING CHALLENGES

The transition from the frontal impact to what is believed a reasonable redirection simulation required a total of 24 separate simulation runs, each run making one or more modifications to the model. This section describes three of the problems encountered and the implemented solutions.

The majority of the challenges were related to contacts. Not in the contacts themselves, there were no instances where any contact algorithms were found to be in error. The problems were mainly related to modeling issues such as course mesh sizes, contact penalty factors, contact thicknesses, edge-to-edge penetrations not being addressed in the model, and unstable element formulations after significant hourglassing had been induced. Many different contacts and contact parameters were tried throughout the study. By monitoring contact forces with force transducers, it was possible to grasp a better understanding of the system behavior and come up with various fixes for the model.

Cable Anchor to Post Contact

Figure 7 demonstrates the problem and fix. The cable anchor assembly is used to provide tension anchorage for the guardrail during redirection. One end of a cable is attached to the rail, the other end is attached to bracket at the base of post one. The tension force in the cable during an

impact can reach around 180 kN (40 kips). This force is transmitted to the ground through the bracket and post base. During simulation these forces caused excessive deformations in the wood post and led to an unstable result. By decreasing the contact scale factor, the contact forces were stabilized and the problem was fixed.

Radiator-Tie Bar Interaction with Guardrail

After 145 ms of simulation time, the radiator-tie bar on the truck began contact with the guardrail. Due to the coarse mesh and shape of the rad-tie bar, a snag developed between the two parts and caused the solution to go unstable (see Figure 8). This could probably be attributed to an edge-to-edge penetration. Instead of investigating various contact changes, it was decided to make a more uniform contact surface between the parts. Changes to the truck model included filling in the holes of the radiator tie bar, refining the mesh of the tie bar and moving some of the nodes of the tie bar to smooth its surface. Simulation results showed that these changes stabilized the contacts in this area of the model.

Rolling Tire Nodes Through the Rail Slot

Slots are cut in the valleys of the guardrail in order to weaken the rail for the frontal impact, allowing it to wrap around a vehicle without excessive forces. (High forces would result in excessive decelerations on the passengers.) Because a three-beam rail is used, these slots do not significantly reduce the tensile capacity of the rail. During simulation, however, these slots provide an opening in the rail for portions of the vehicle to wedge through and cause contact troubles. An example of this is shown in Figure 9. As the tire of the truck hits the rail a portion of the tire goes through one of slots (marked by the arrow in Figure 9). In this case, the node penetrated far enough through the slot that it got trapped on the other side of the rail as the tire continued to rotate. For about 10 ms the tire happily rotated and moved forward along the rail with the node being trapped on the wrong side. Shortly thereafter the contact became unstable causing the tire to experience shooting nodes.

Physically, a real tire could not experience this type of behavior. Instead, a portion of the tire tread would be simply cut off by the edge of the rail slot. The details to model this phenomena would be excessive for this project. Thus, a cover was placed over the slots to provide a contact area to prevent such behavior. This was accomplished with a single row of shell elements using the null material. Slot covers proved to be an effective method for preventing vehicle parts from interlocking with the rail unrealistically through the slots.

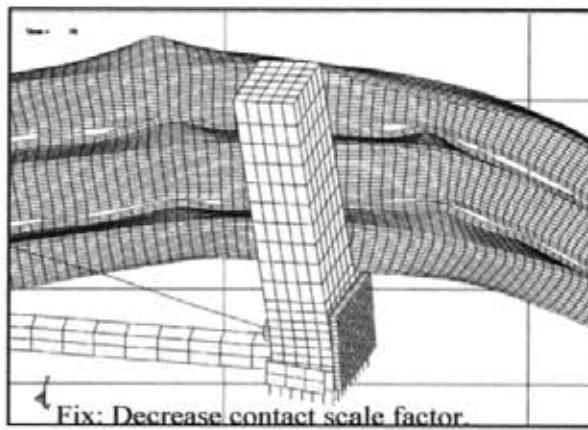
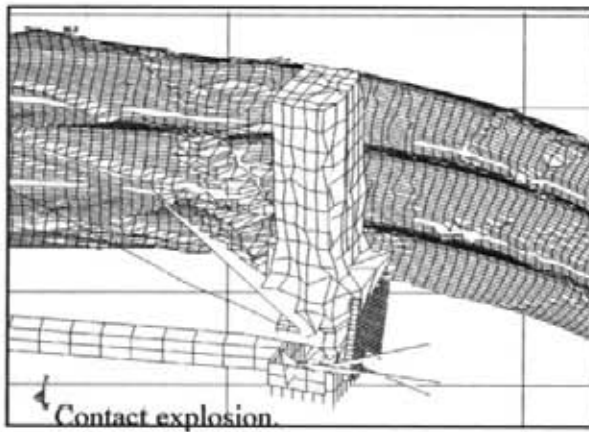
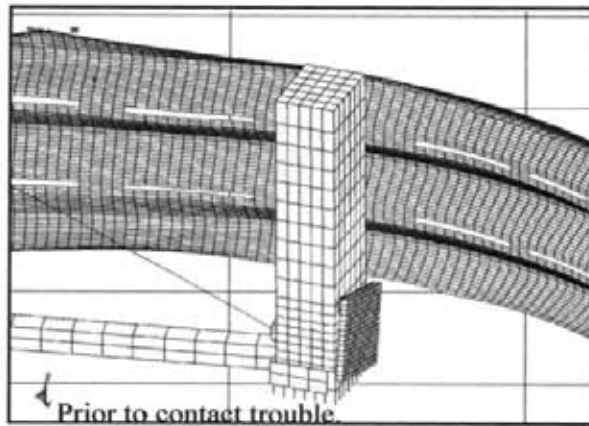


Figure 7. Cable Anchor - Post Contact

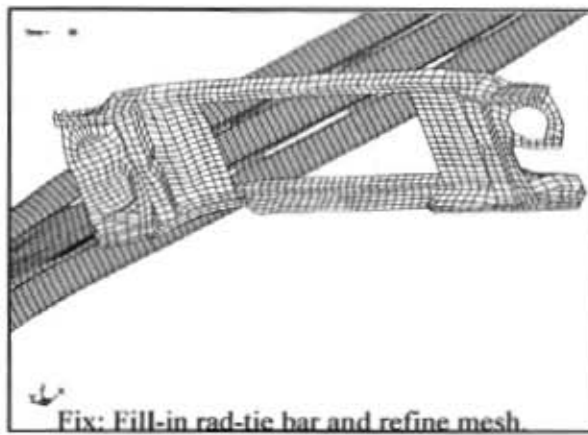
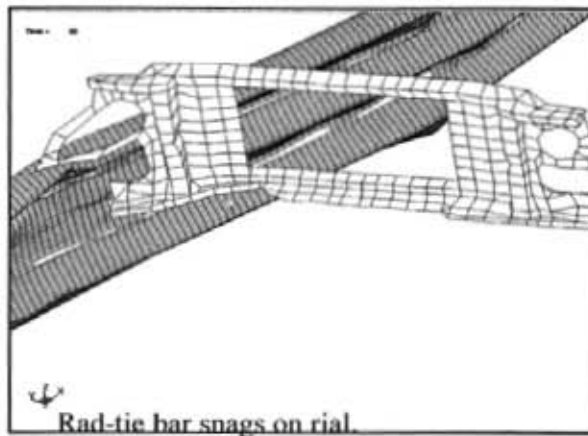
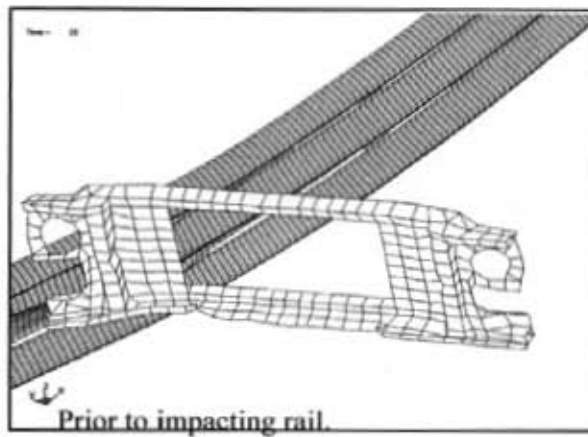
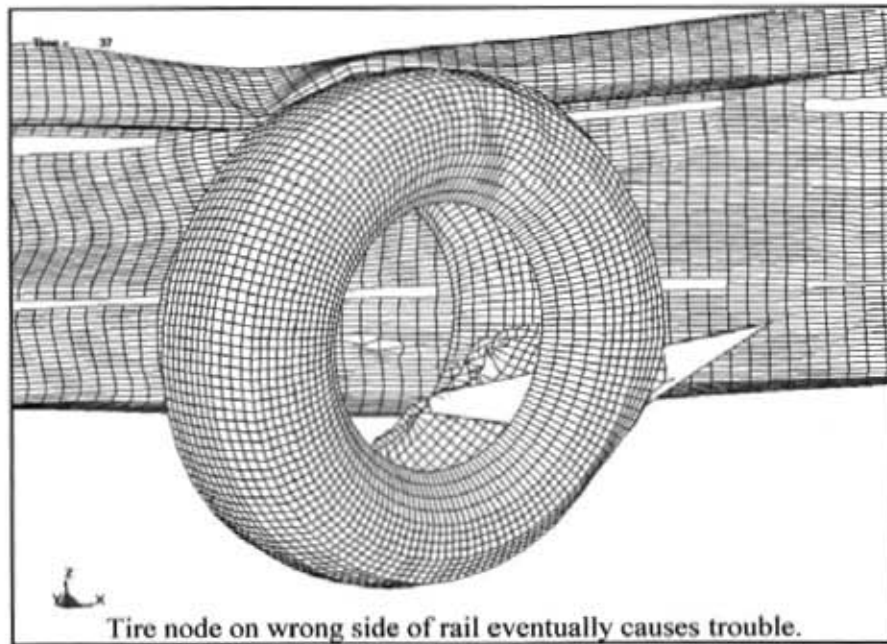
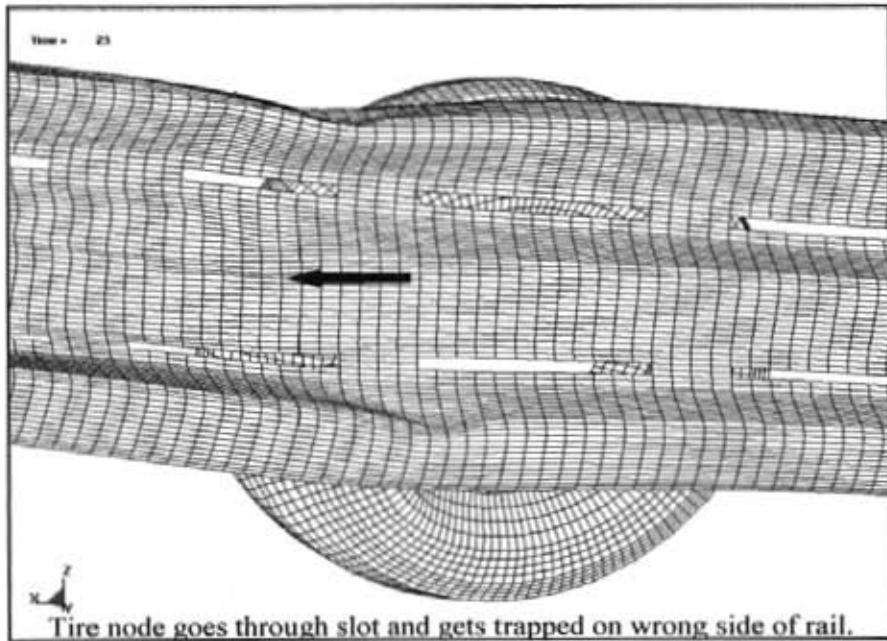


Figure 8. Radiator-Tie Bar Interaction with Guardrail



Fix: Add a single row of null-shells to cover slots, provide contact area.

Figure 9. Tire Through Rail Slot

REDIRECTION SIMULATION

After a series of modeling adjustments, the failed redirection test was reasonably simulated (see Figure 4). The simulation was ended at 278 ms due to another instability in the solution. However, because the failure phenomenon was clearly captured further simulation was deemed nonessential. Results showed posts 2 and 3 breaking early in the event, allowing the rail to roll back and form a ramp, which vaults the vehicle up and over the system.

The final simulation took 120 hours using 2 processors on an R10000 SGI Octane workstation. The model was composed of approximately 75,000 shell, 8,000 solid and 450 beam elements. Roughly 95% of these elements were deformable.

CONCLUSIONS

- Frontal impacts and redirection impacts of bullnose guardrail systems are significantly different and each require unique attention, similar to frontal and side impact design of a vehicle.
- What are sometimes referred to as “contact troubles,” are often signs of detailed modeling requirements. Areas where more modeling details might be required manifest themselves as unstable contacts during simulation.
- An LS-DYNA model of a bullnose system that fairly accurately simulates a failed redirection crash test was developed.

The bullnose project is still under development and is left for future work. The model described in this paper will be used to evaluate possible design alternatives.

ACKNOWLEDGMENTS

The author acknowledges the Midwest States Pooled Fund Program, the MwRSF personnel, and Livermore Software Technology Corporation. Acknowledgments to the NCAC for providing the C2500 vehicle model. This material is based upon work supported by the Federal Highway Administration under cooperative agreement number DTFH61-97-X-00028.

DISCLAIMER STATEMENT

Any opinions, findings, and conclusions or recommendations expressed in this publication are those of the authors and do not necessarily reflect the views of the Federal Highway Administration or the state highway departments participating in the Midwest States Pooled Fund Program.

REFERENCES

1. Button, J.W., Buth, E. and Olson, R.M., *Crash Tests of Five Foot Radius Plate Beam Guardrail*, Submitted to the Department of Highways, State of Minnesota, Texas Transportation Institute, June 1975.
2. Robertson, R.G. and Ross, H.E. Jr., *Colorado Median Barrier End Treatment Tests*, TTI Research Report No. 4179-1F, Texas Transportation Institute, May 1981.
3. Bronstad, M.E., Ray, M.H., Mayer, J.B. Jr. and Brauer, S.K., *Median Barrier Terminals and Median Treatments. Volume 1 Research Reports and Appendix A*, Report No. FHWA/RD-088/004, Southwest Research Institute, October 1987.
4. Ross, H.E., Sicking, D.E., Zimmer, R.A. and Michie, J.D., *Recommended Procedures for the Safety Performance Evaluation of Highway Features*, National Cooperative Highway Research Program Report No. 350, Transportation Research Board, Washington, DC, 1993.
5. Reid, J.D. and Bielenberg, B.W., "Using LS-DYNA Simulation to Solve a Design Problem: A Bullnose Guardrail Example," *Accepted for Transportation Research Record (number to be assigned)*, Washington, DC, 1999.
6. Hallquist, J.O., *LS-DYNA Keyword User's Manual*, Livermore Software Technology Corporation, California, 1997.
7. Zaouk, A., Bedewi, N. and Meczowski, L.. "Development and Validation of Detailed Chevrolet C-1500 Pickup Truck Model for Multiple Impact Applications," *TRB Paper 980419*, Transportation Research Board, Washington, DC, January 1998.

APPENDIX E

ACCELEROMETER DATA ANALYSIS TEST MBN-8

- Figure E-1. Graph of Longitudinal Deceleration - Filtered Data, Test MBN-8
- Figure E-2. Graph of Longitudinal Occupant Impact Velocity - Filtered Data, Test MBN-8
- Figure E-3. Graph of Longitudinal Occupant Displacement - Filtered Data, Test MBN-8
- Figure E-4. Graph of Lateral Deceleration - Filtered Data, Test MBN-8
- Figure E-5. Graph of Lateral Occupant Impact Velocity - Filtered Data, Test MBN-8
- Figure E-6. Graph of Lateral Occupant Displacement - Filtered Data, Test MBN-8
- Figure E-7. Rate Transducer Data, Test MBN-8

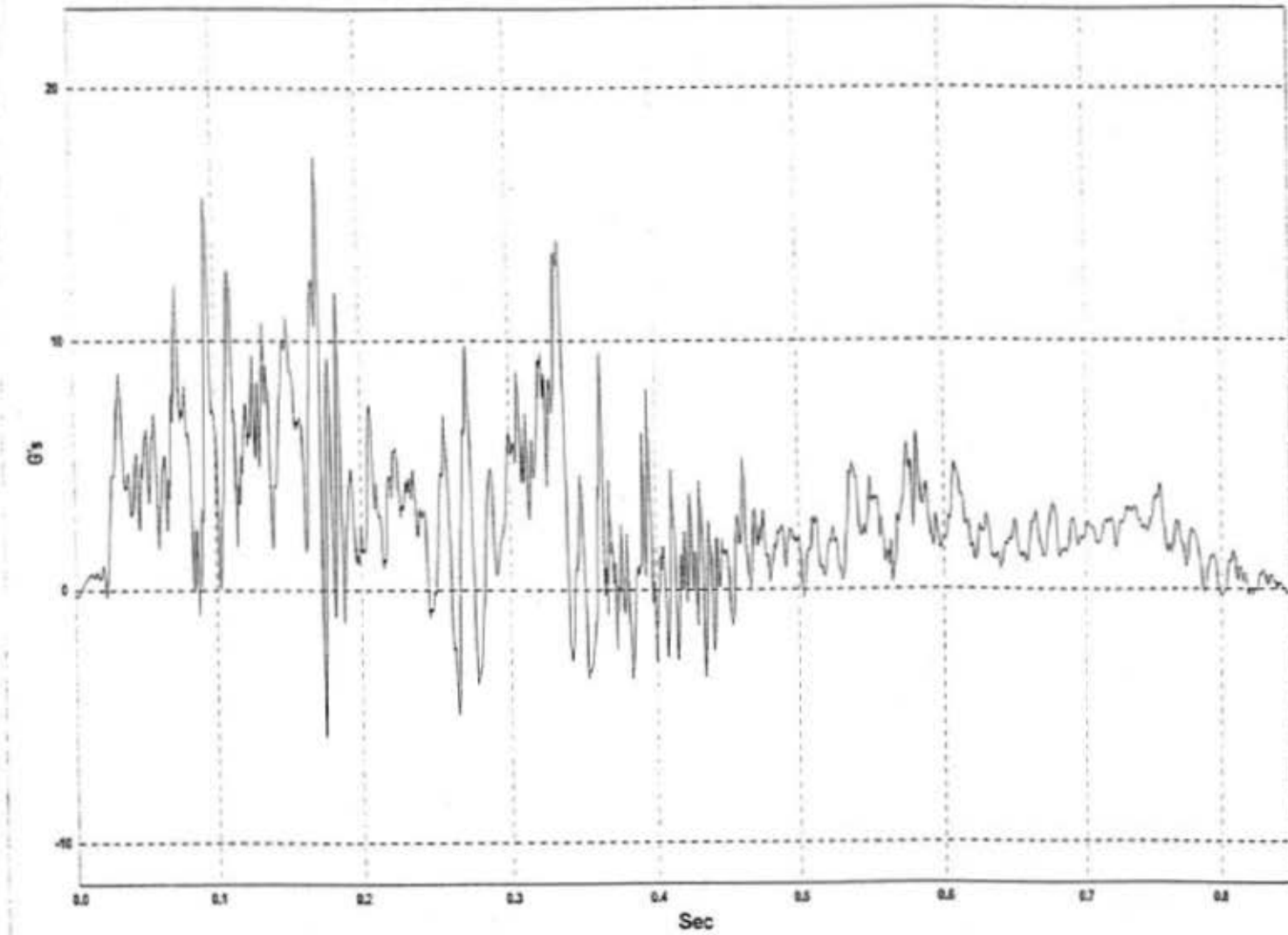


Figure E-1. Graph of Longitudinal Deceleration - Filtered Data, Test MBN-8

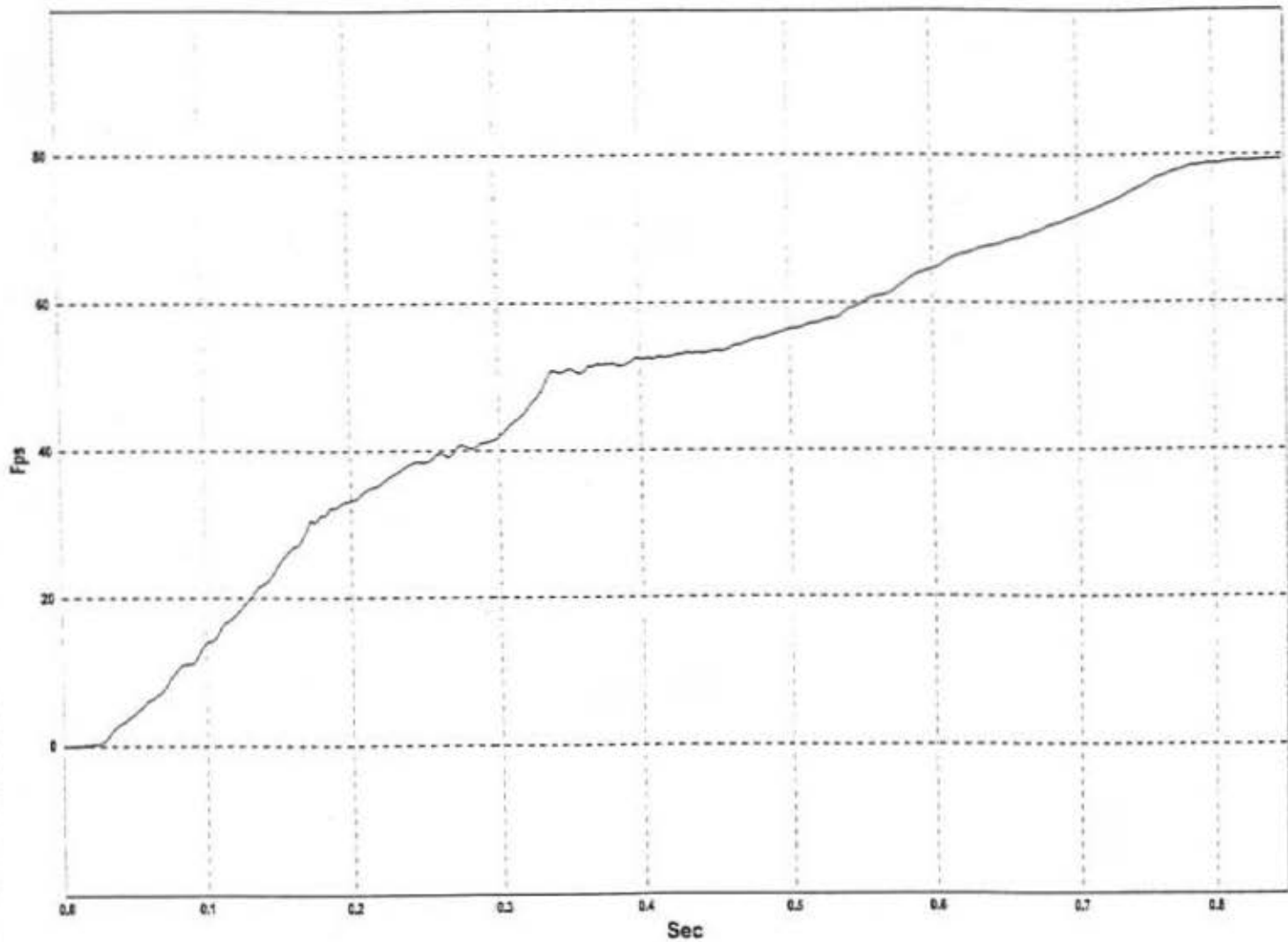


Figure E-2. Graph of Longitudinal Occupant Impact Velocity - Filtered Data, Test MBN-8

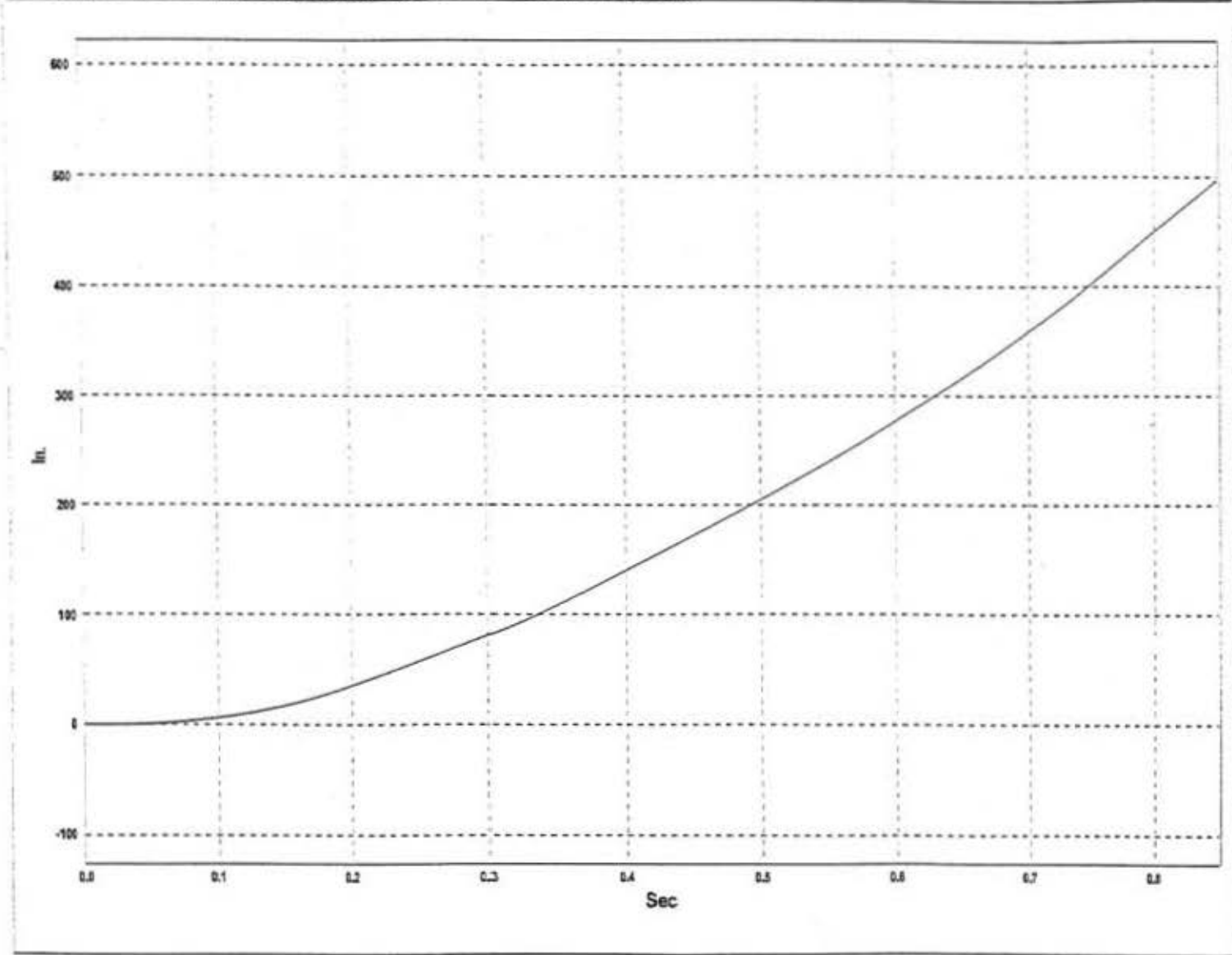


Figure E-3. Graph of Longitudinal Occupant Displacement - Filtered Data, Test MBN-8

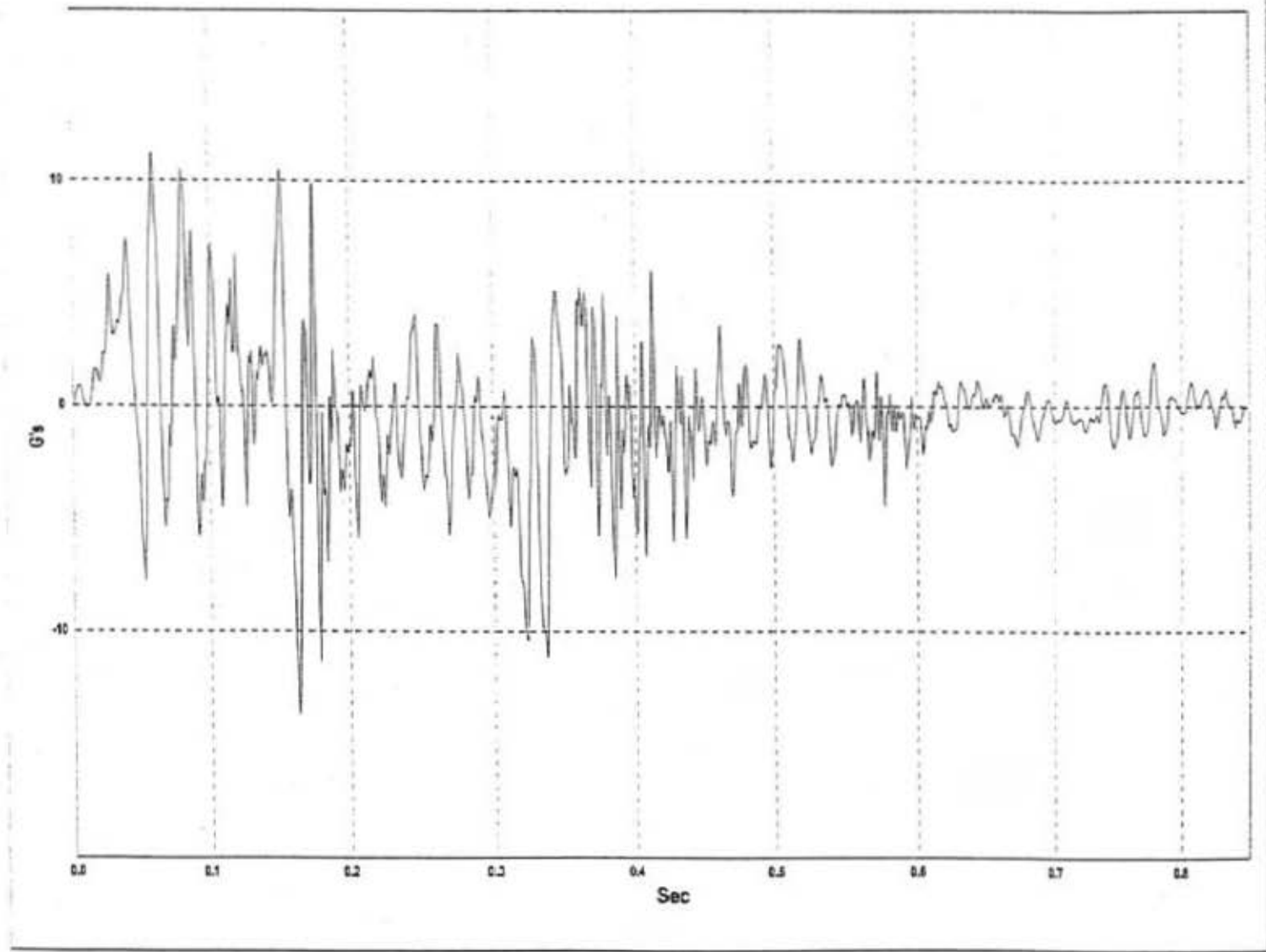


Figure E-4. Graph of Lateral Deceleration - Filtered Data, Test MBN-8

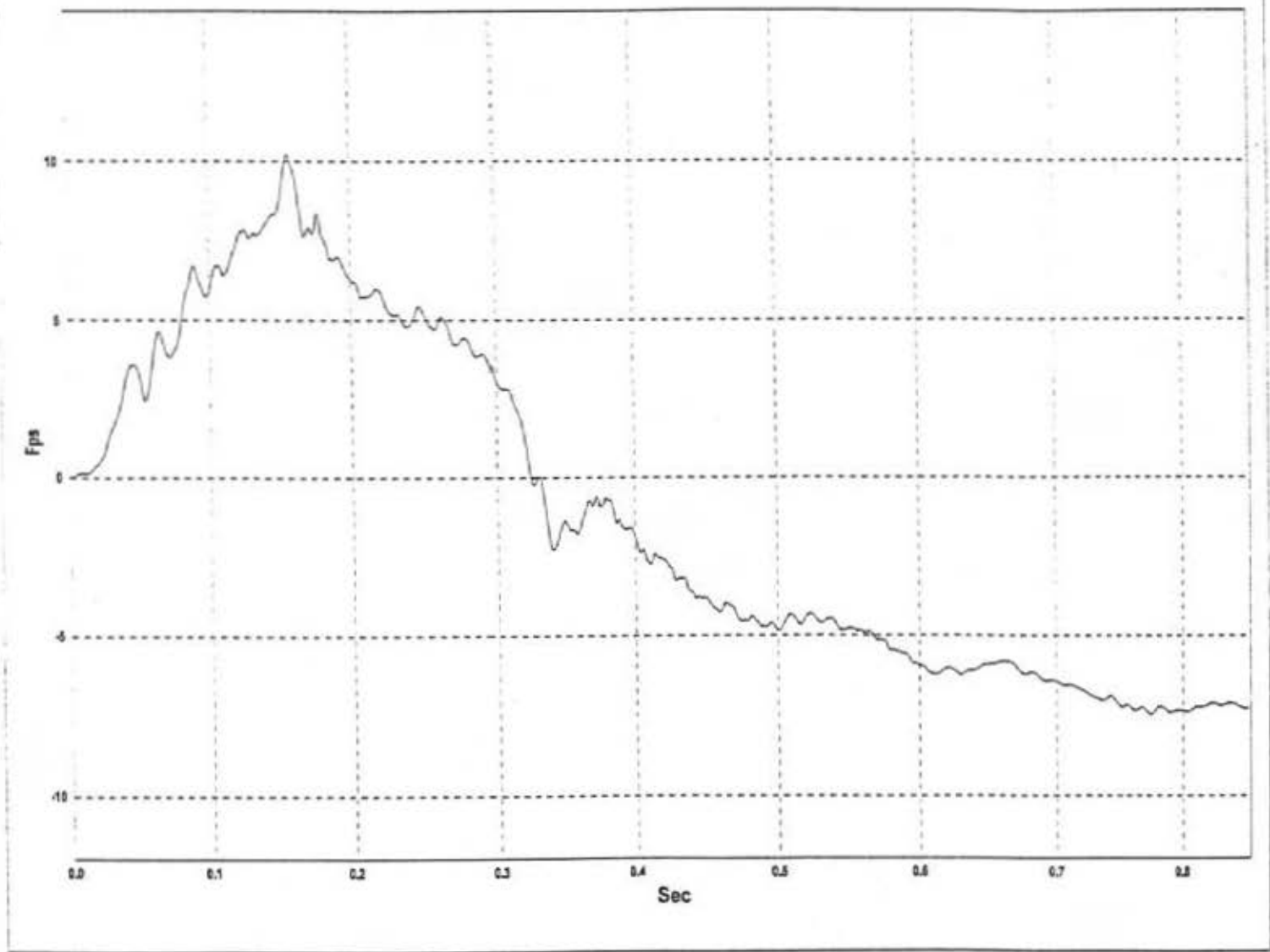
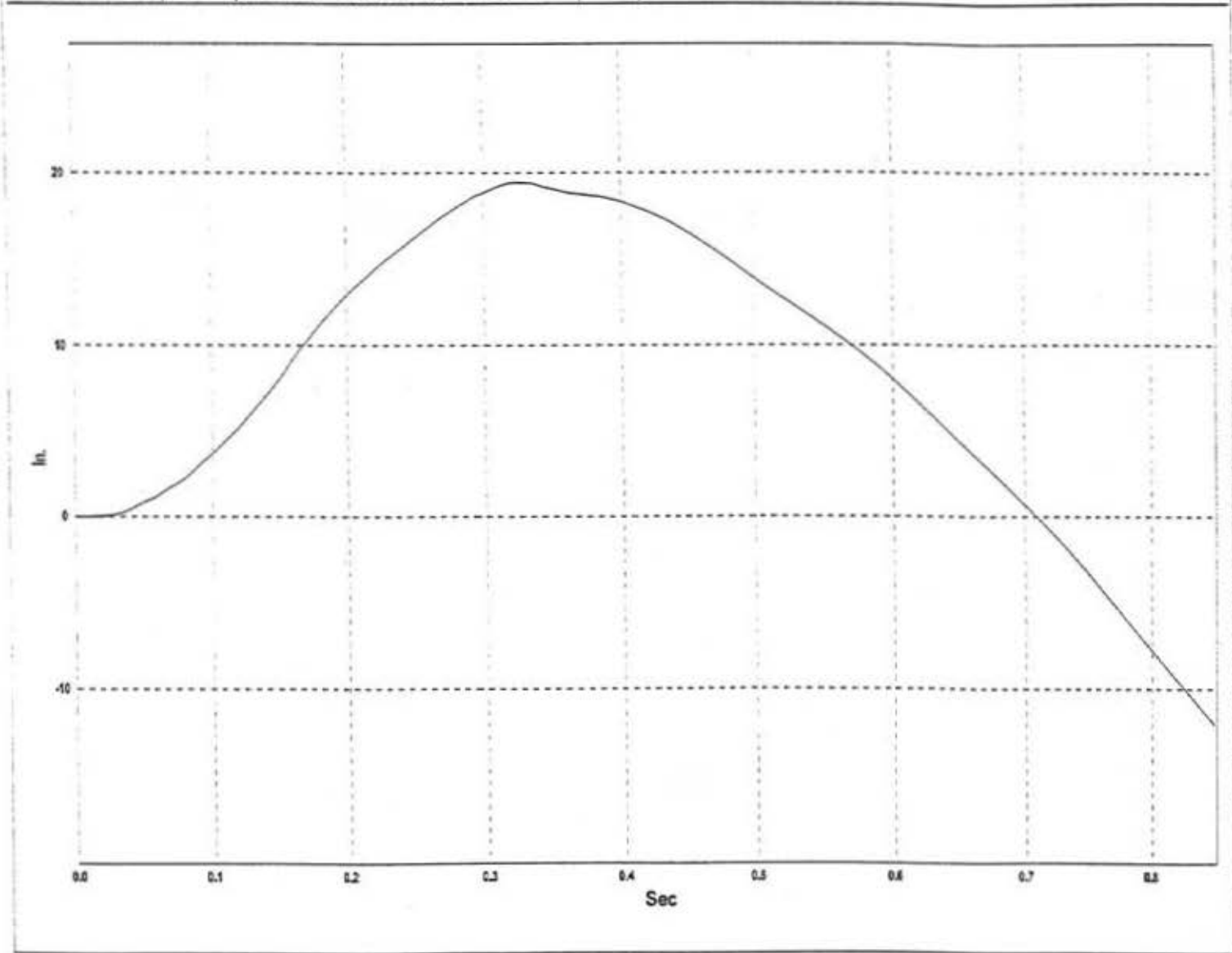


Figure E-5. Graph of Lateral Occupant Impact Velocity - Filtered Data, Test MBN-8

W9: Lateral Occupant Displacement - Filtered Data - Test MBN-8 (EDR-4)



200

Figure E-6. Graph of Lateral Occupant Displacement - Filtered Data, Test MBN-8

W24: TEST MBN-8 UNCOUPLED ANGULAR DISPLACEMENTS

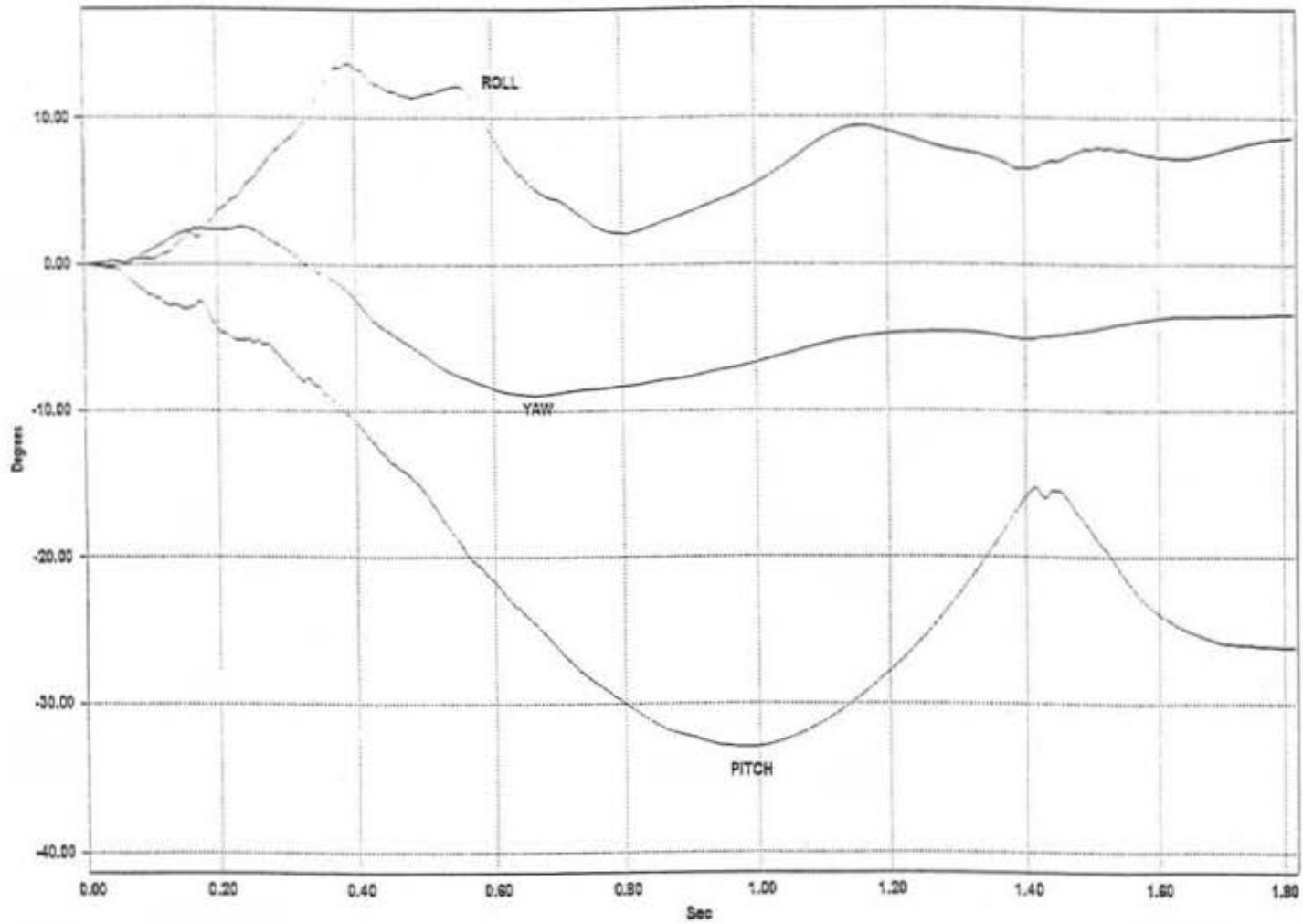


Figure E-7. Rate Transducer Data, Test MBN-8

APPENDIX F

ACCELEROMETER DATA ANALYSIS TEST MBN-9

Figure F-1. Graph of Longitudinal Deceleration - Filtered Data, Test MBN-9

Figure F-2. Graph of Longitudinal Occupant Impact Velocity - Filtered Data, Test MBN-9

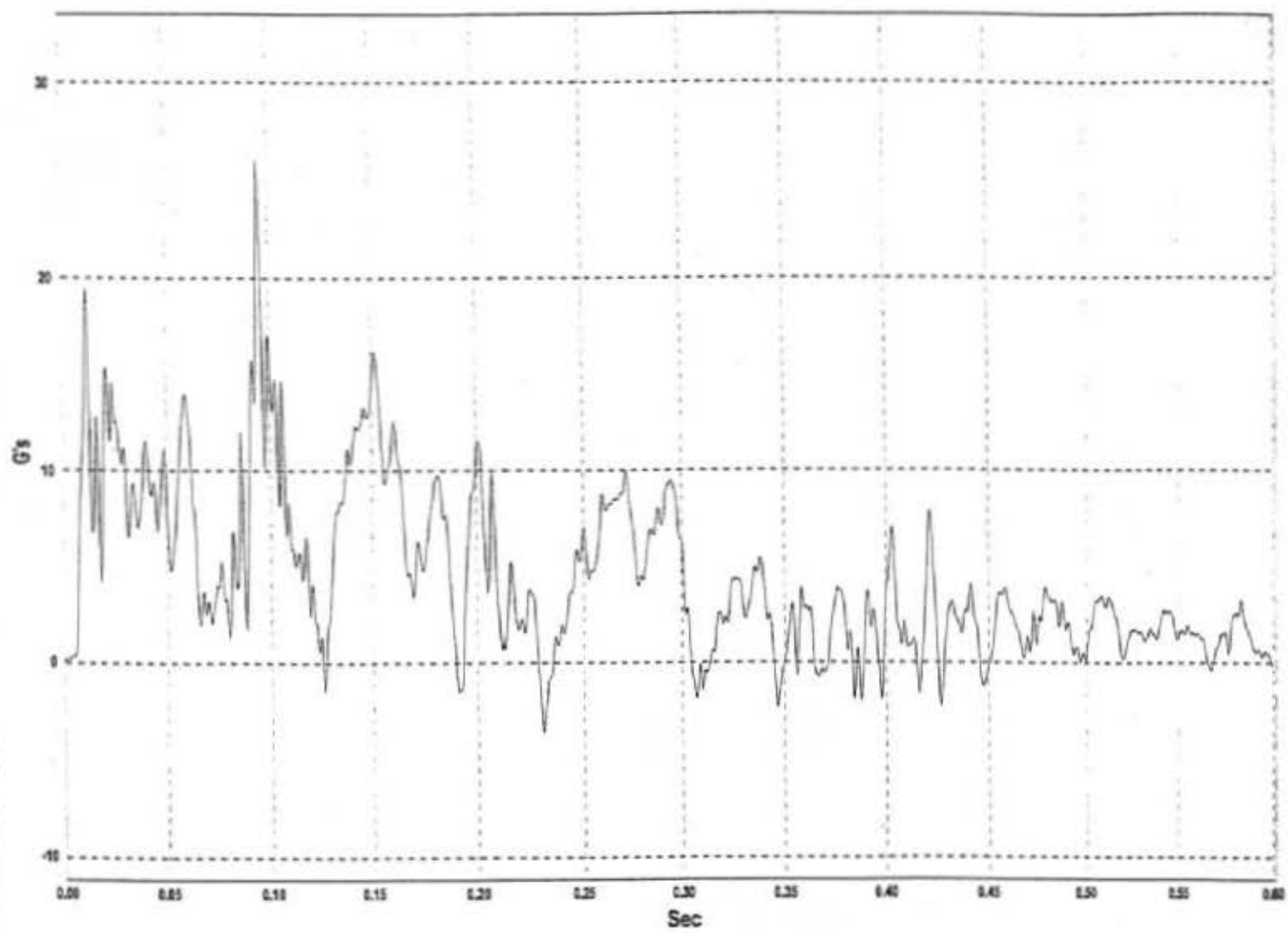
Figure F-3. Graph of Longitudinal Occupant Displacement - Filtered Data, Test MBN-9

Figure F-4. Graph of Lateral Deceleration - Filtered Data, Test MBN-9

Figure F-5. Graph of Lateral Occupant Impact Velocity - Filtered Data, Test MBN-9

Figure F-6. Graph of Lateral Occupant Displacement - Filtered Data, Test MBN-9

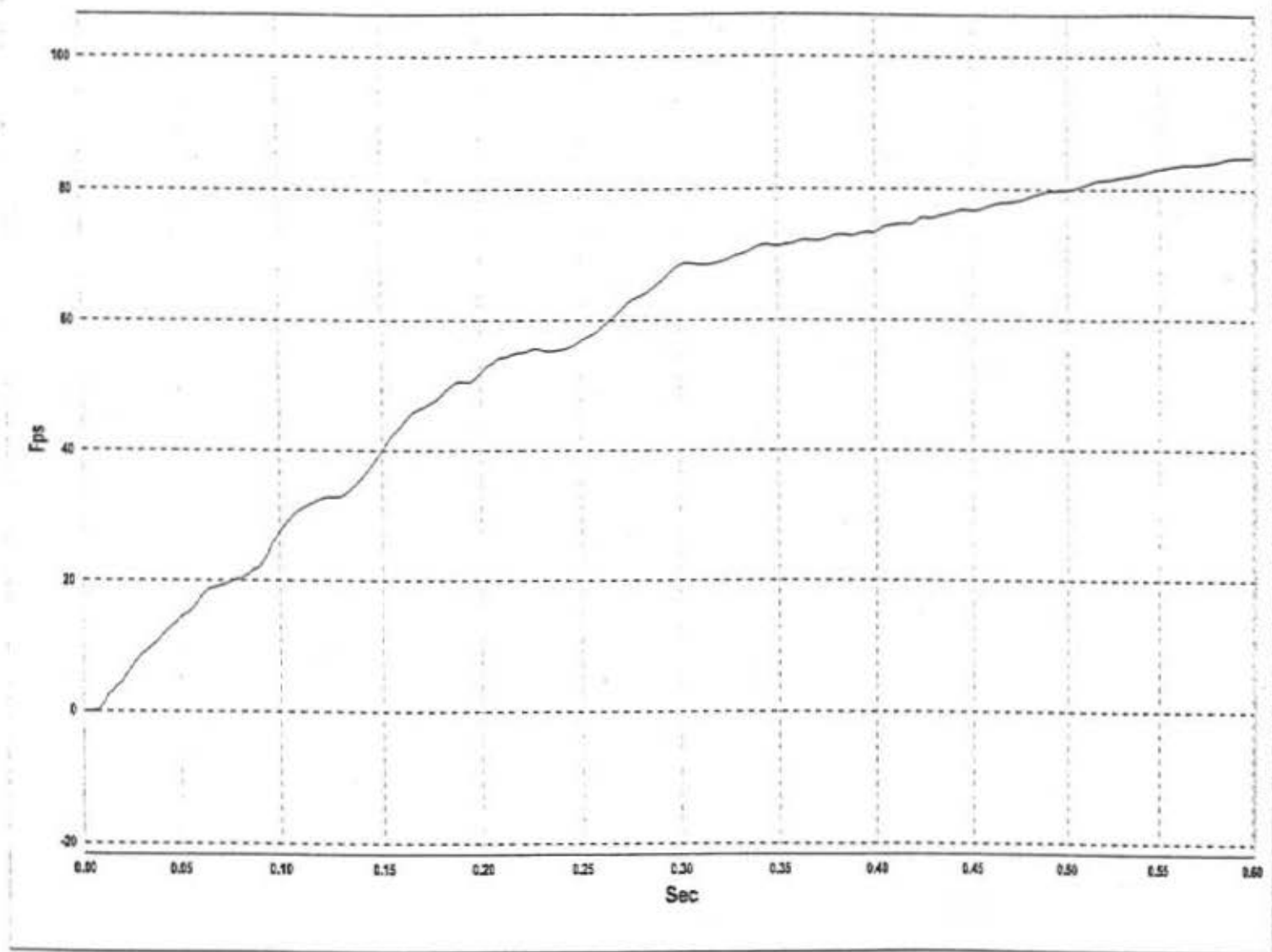
Figure F-7. Rate Transducer Data, Test MBN-9



203

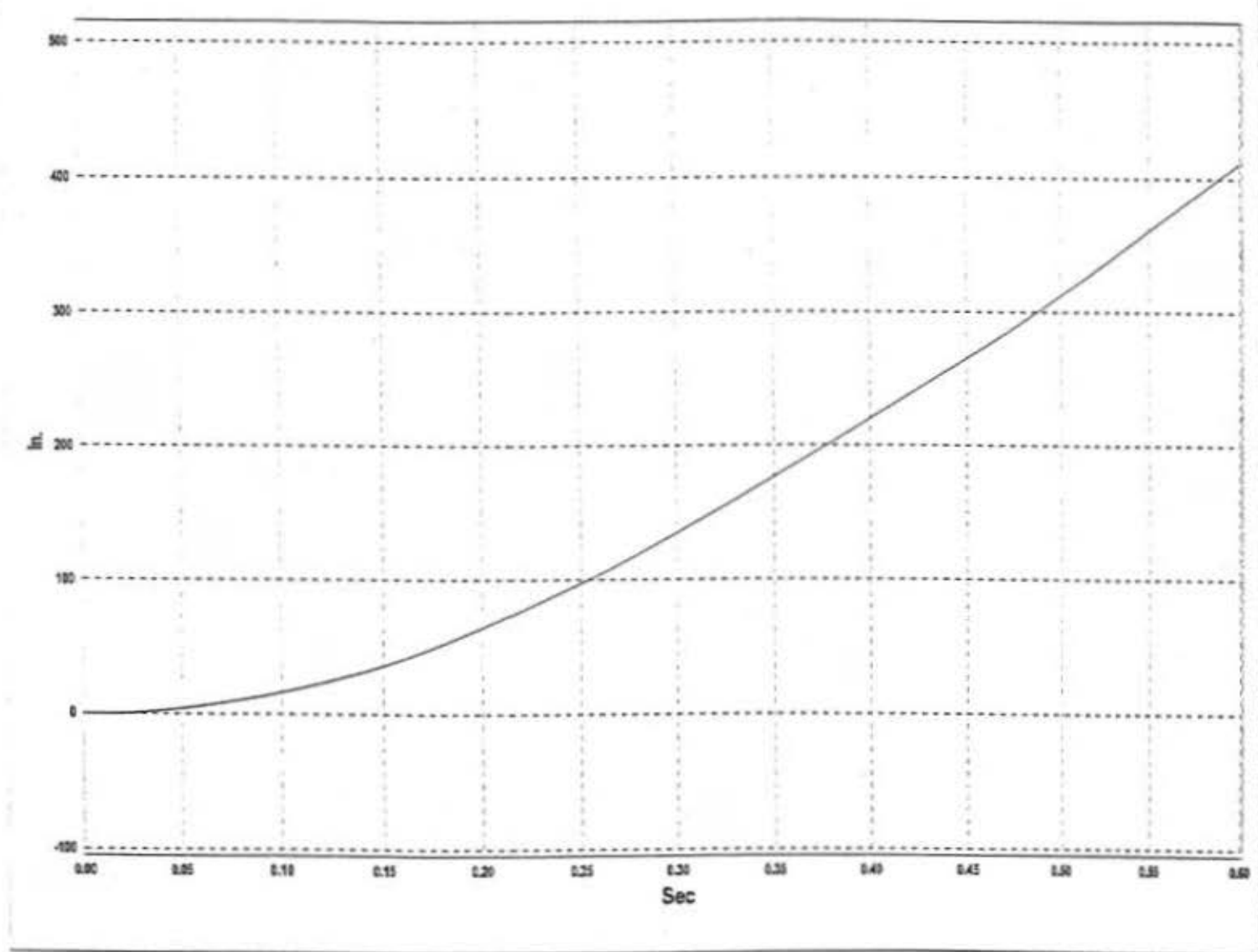
Figure F-1. Graph of Longitudinal Deceleration - Filtered Data, Test MBN-9

W8: Longitudinal Occupant Impact Velocity - Filtered Data - Test MBN-9 (EDR-4)



204

Figure F-2. Graph of Longitudinal Occupant Impact Velocity - Filtered Data, Test MBN-9



205

Figure F-3. Graph of Longitudinal Occupant Displacement - Filtered Data, Test MBN-9

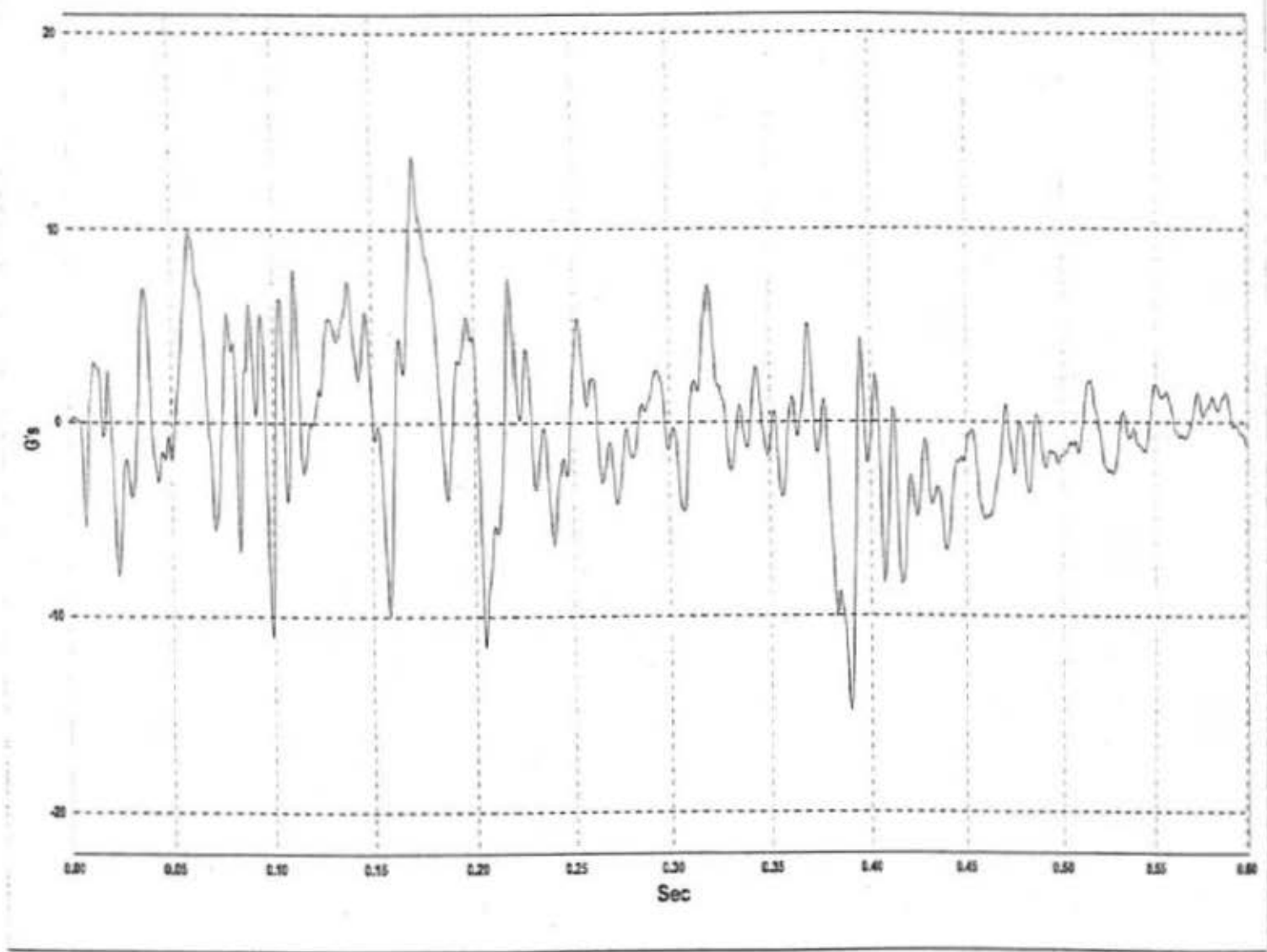


Figure F-4. Graph of Lateral Deceleration - Filtered Data, Test MBN-9

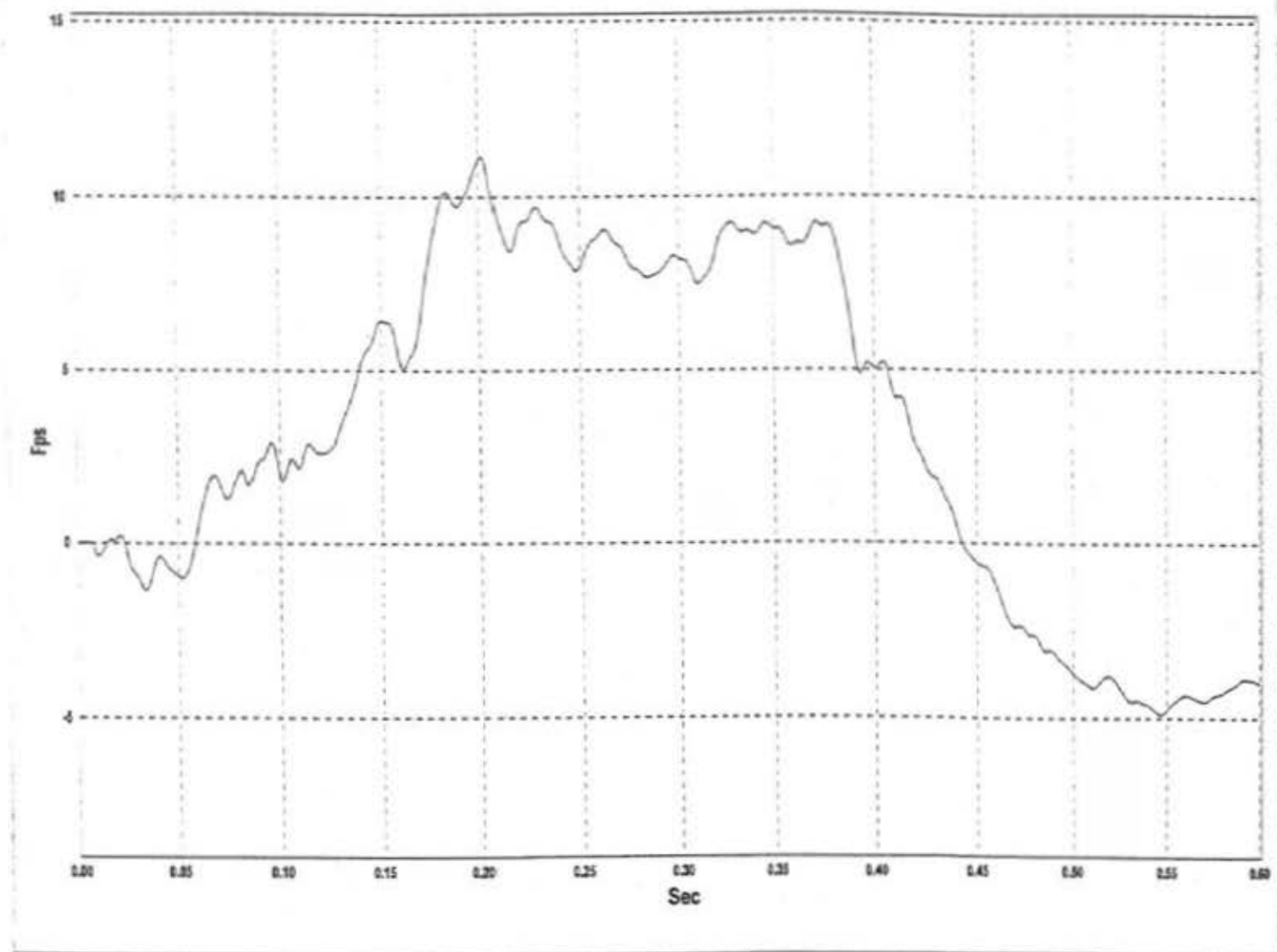


Figure F-5. Graph of Lateral Occupant Impact Velocity - Filtered Data, Test MBN-9

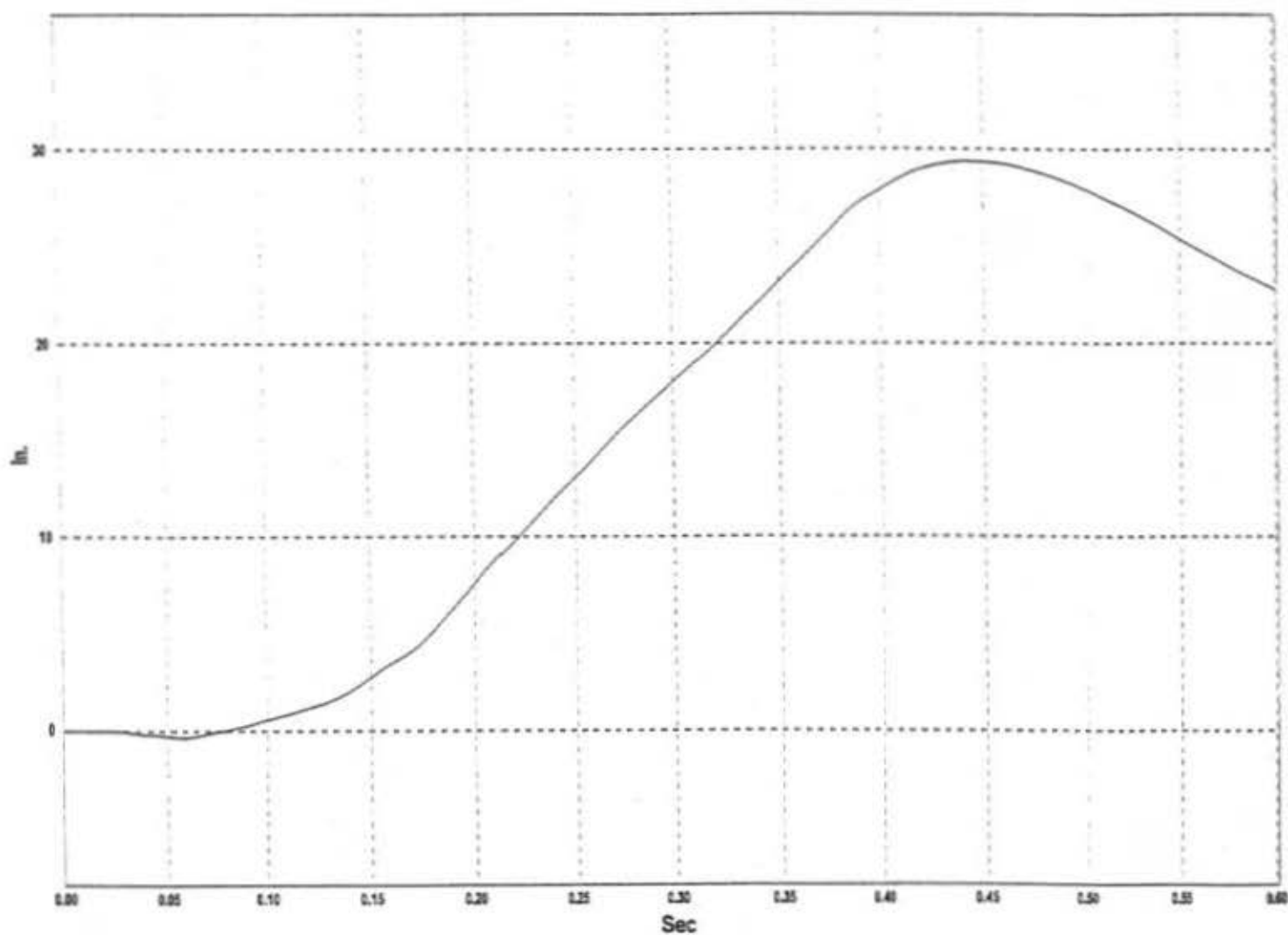


Figure F-6. Graph of Lateral Occupant Displacement - Filtered Data, Test MBN-9

W13: TEST MBN-9 UNCOUPLED ANGULAR DISPLACEMENTS

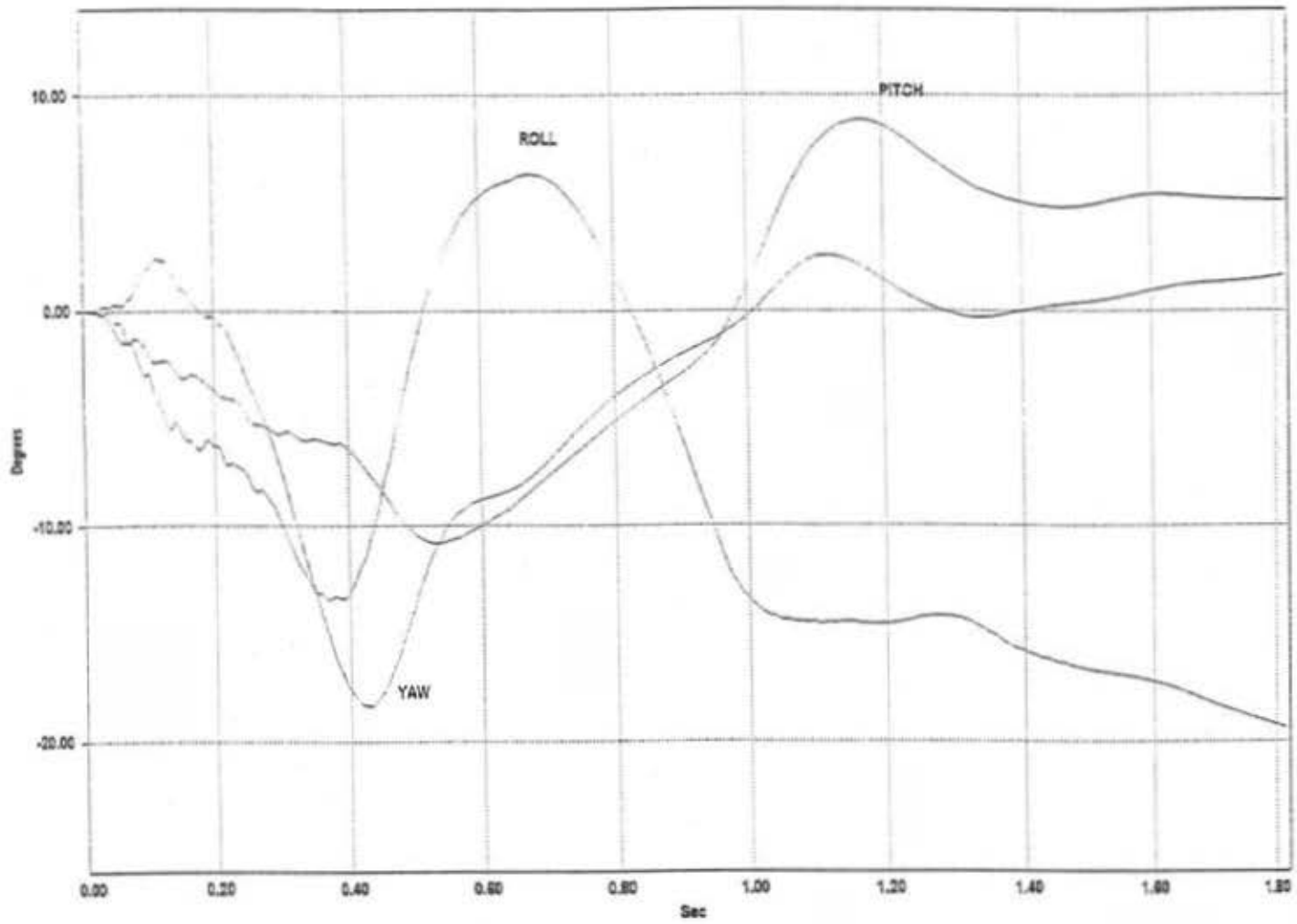


Figure F-7. Rate Transducer Data, Test MBN-9

APPENDIX G

FINAL PHASE III BULLNOSE MEDIAN BARRIER DESIGN DETAILS

- Figure G-1. Final Bullnose Barrier Design
- Figure G-2. Layout of Bullnose Rails No. 1 and 2
- Figure G-3. Rail Section No. 1 Detail
- Figure G-4. Rail Section No. 2 Detail
- Figure G-5. Rail Section No. 3 Detail
- Figure G-6. Post Details
- Figure G-7. Bullnose Cable Assembly
- Figure G-8. Cable Detail and Cable Plate
- Figure G-9. Final Bullnose Barrier Design , English Units
- Figure G-10. Layout of Bullnose Rails No. 1 and 2, English Units
- Figure G-11. Rail Section No. 1 Detail, English Units
- Figure G-12. Rail Section No. 2 Detail, English Units
- Figure G-13. Rail Section No. 3 Detail, English Units
- Figure G-14. Post Details, English Units Bullnose Cable Assembly, English Units
- Figure G-15. Bullnose Cable Assembly, English Units
- Figure G-16. Cable Detail and Cable Plate, English Units

Bullnose 350 Test Layout
MBN-8 Test

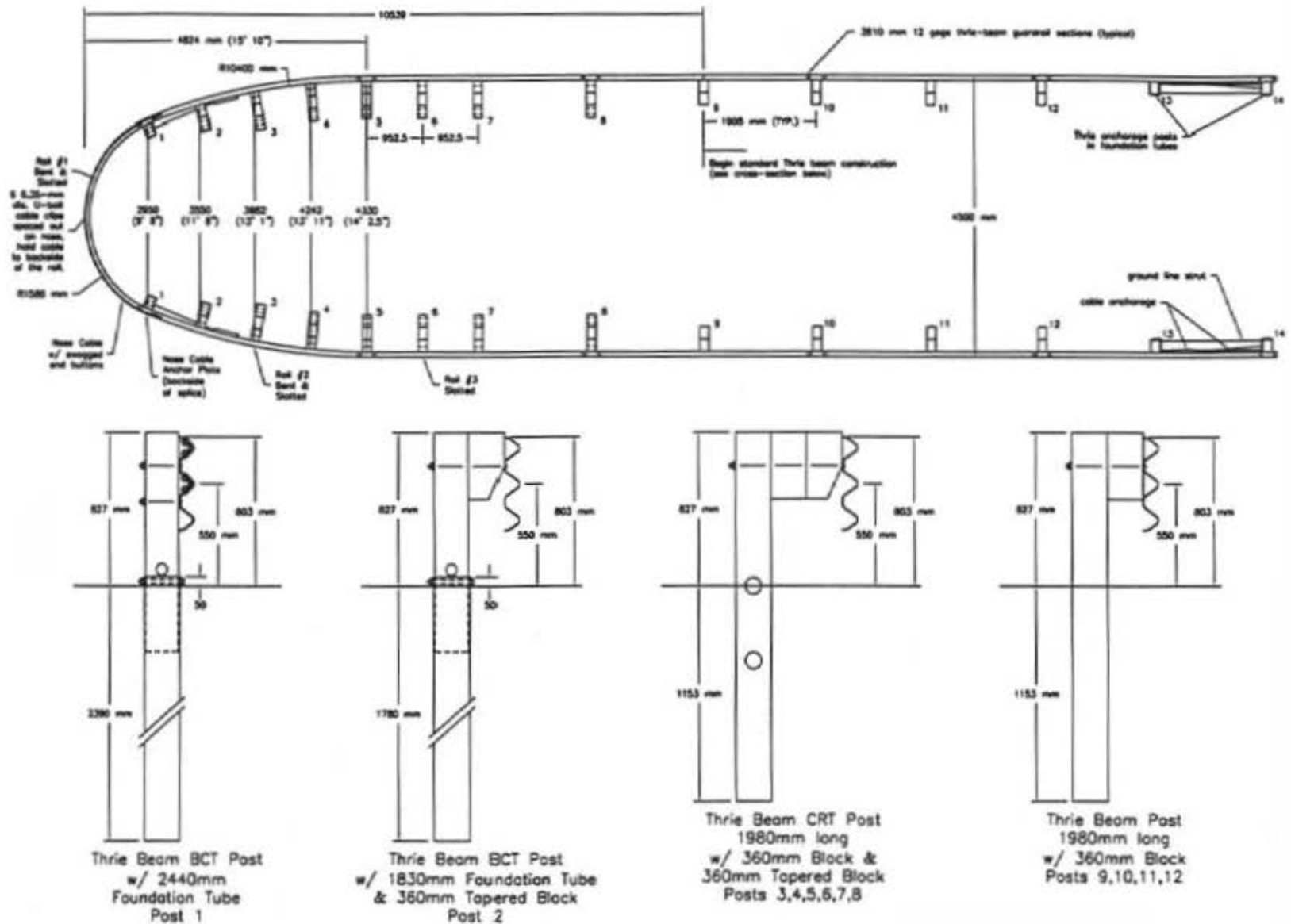


Figure G-1. Final Bullnose Barrier Design

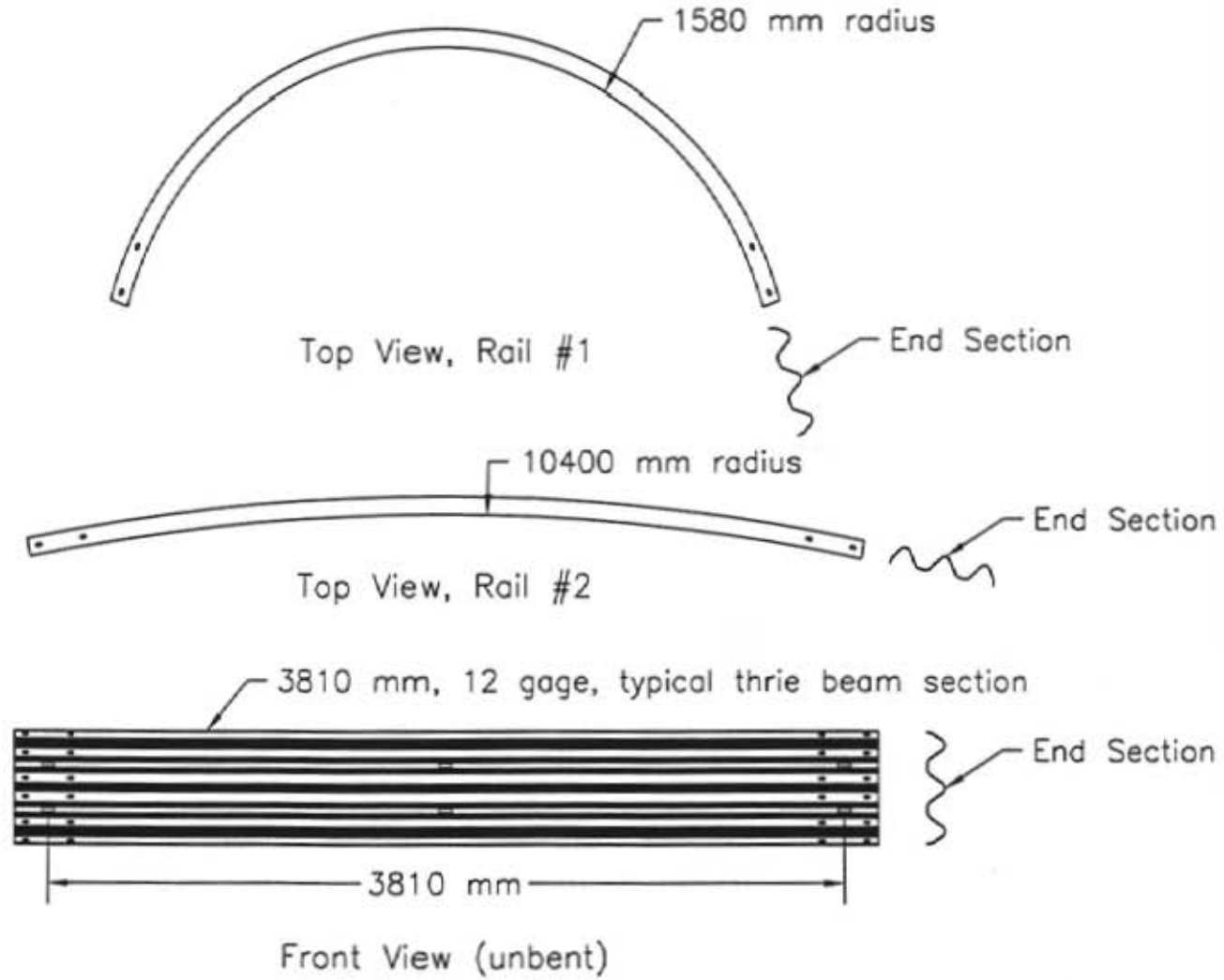
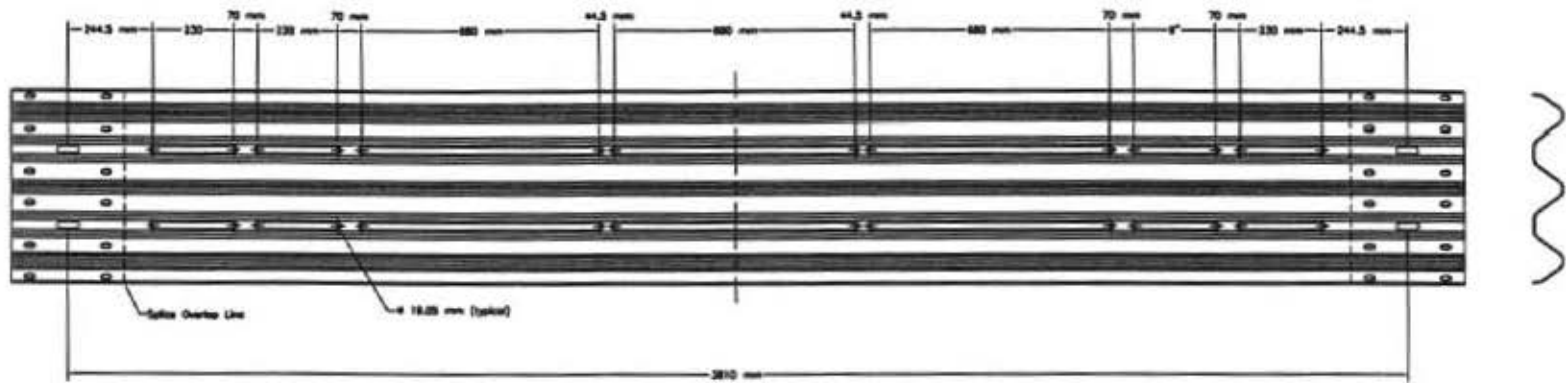
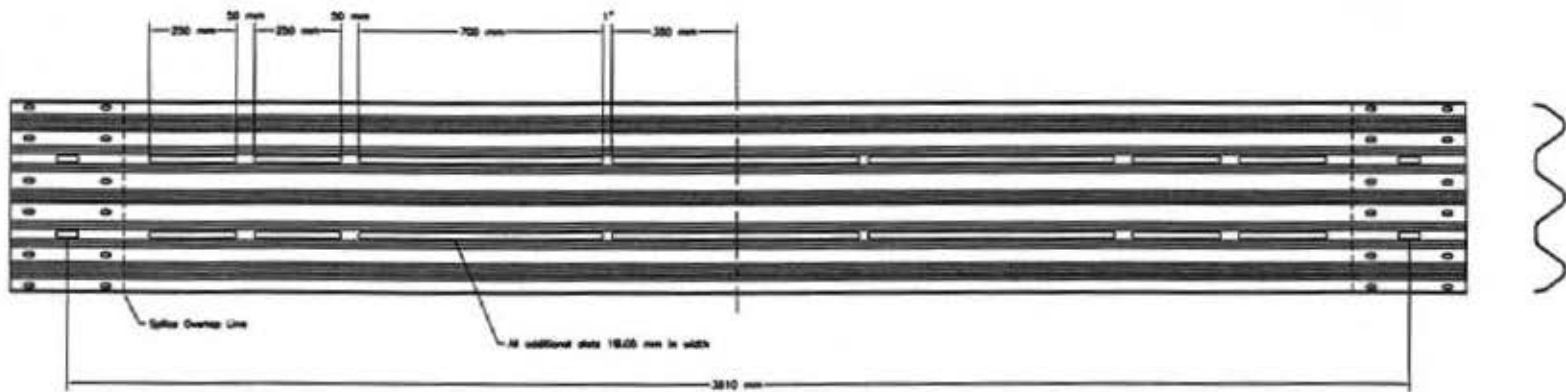


Figure G-2. Layout of Bullnose Rails No. 1 and 2

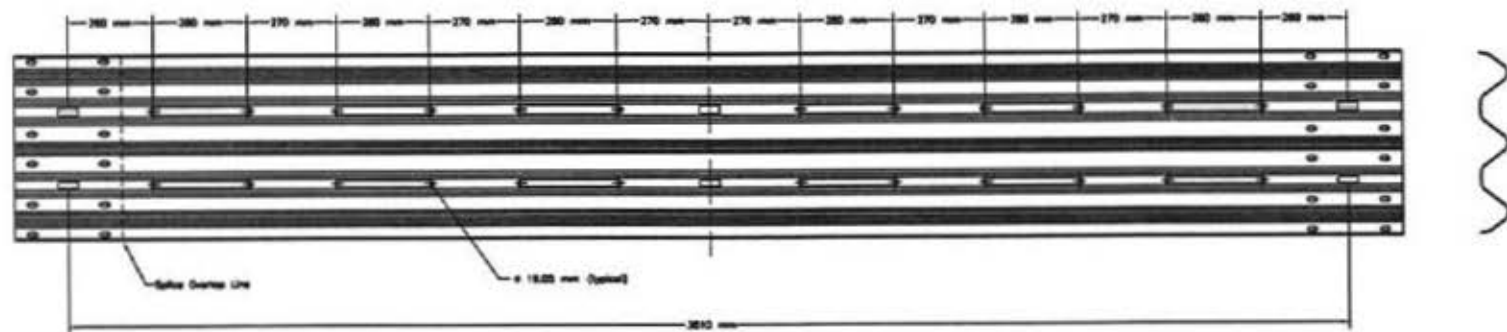


Rail Section 1 ("Nose" Section)

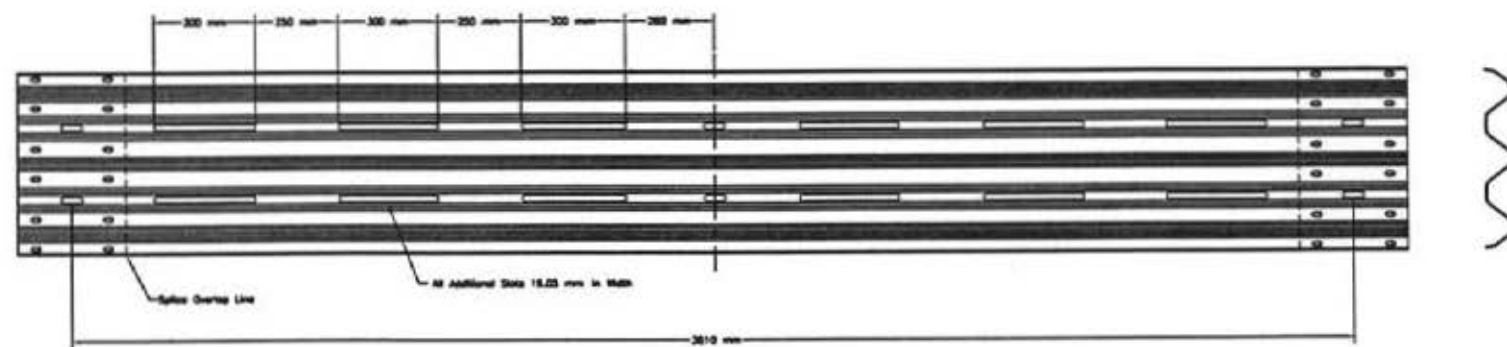


Rail Section 1 ("Nose" Section)

Figure G-3. Rail Section No. 1 Detail

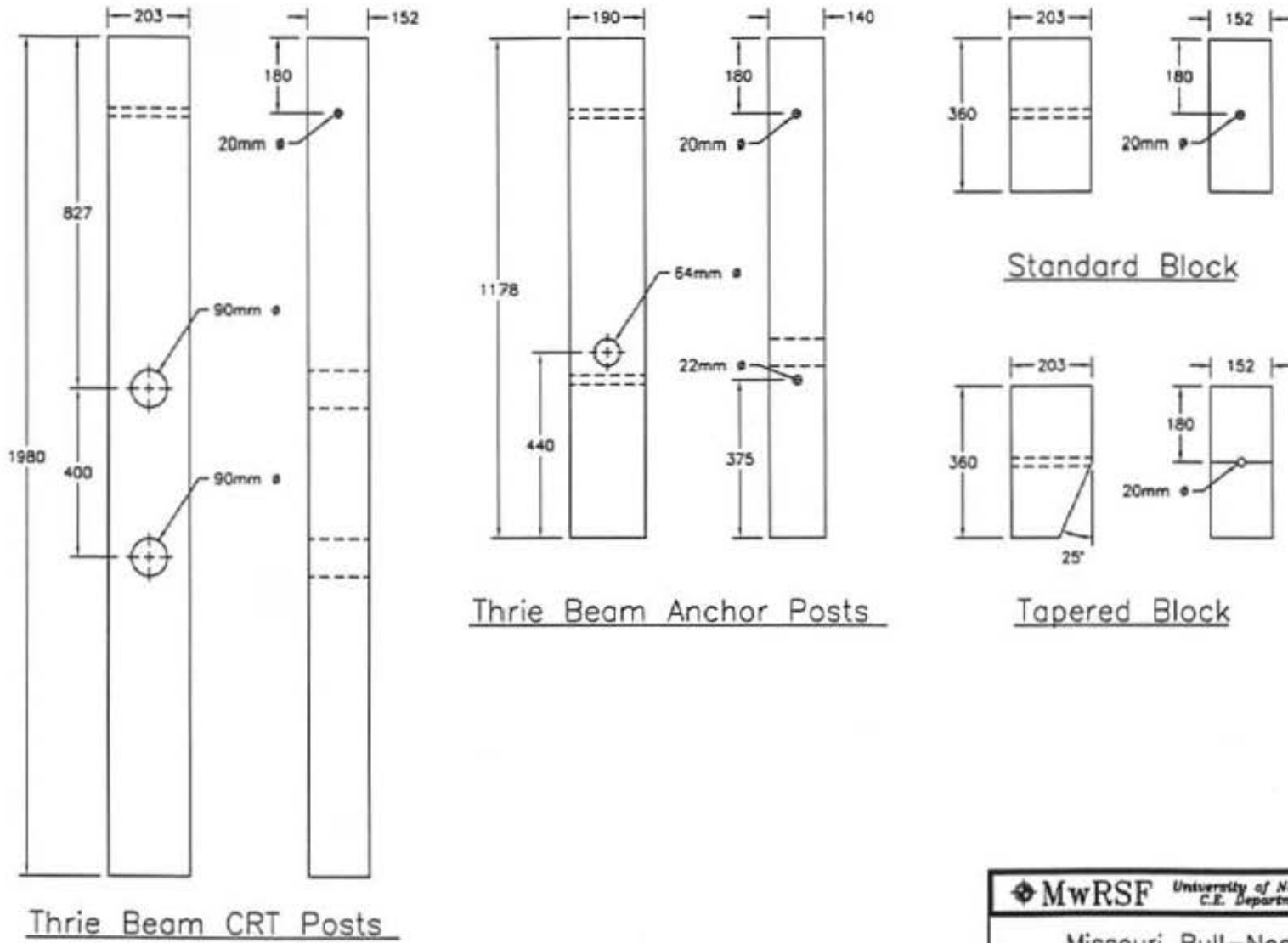


Rail Section 3



Rail Section 3

Figure G-5. Rail Section No. 3 Detail



MwRSF University of Nebraska C.E. Department	
Missouri Bull-Nose	
DATE: 7/15/99	
SCALE: none	
DRN: EAK	bnposts8

Figure G-6. Post Details

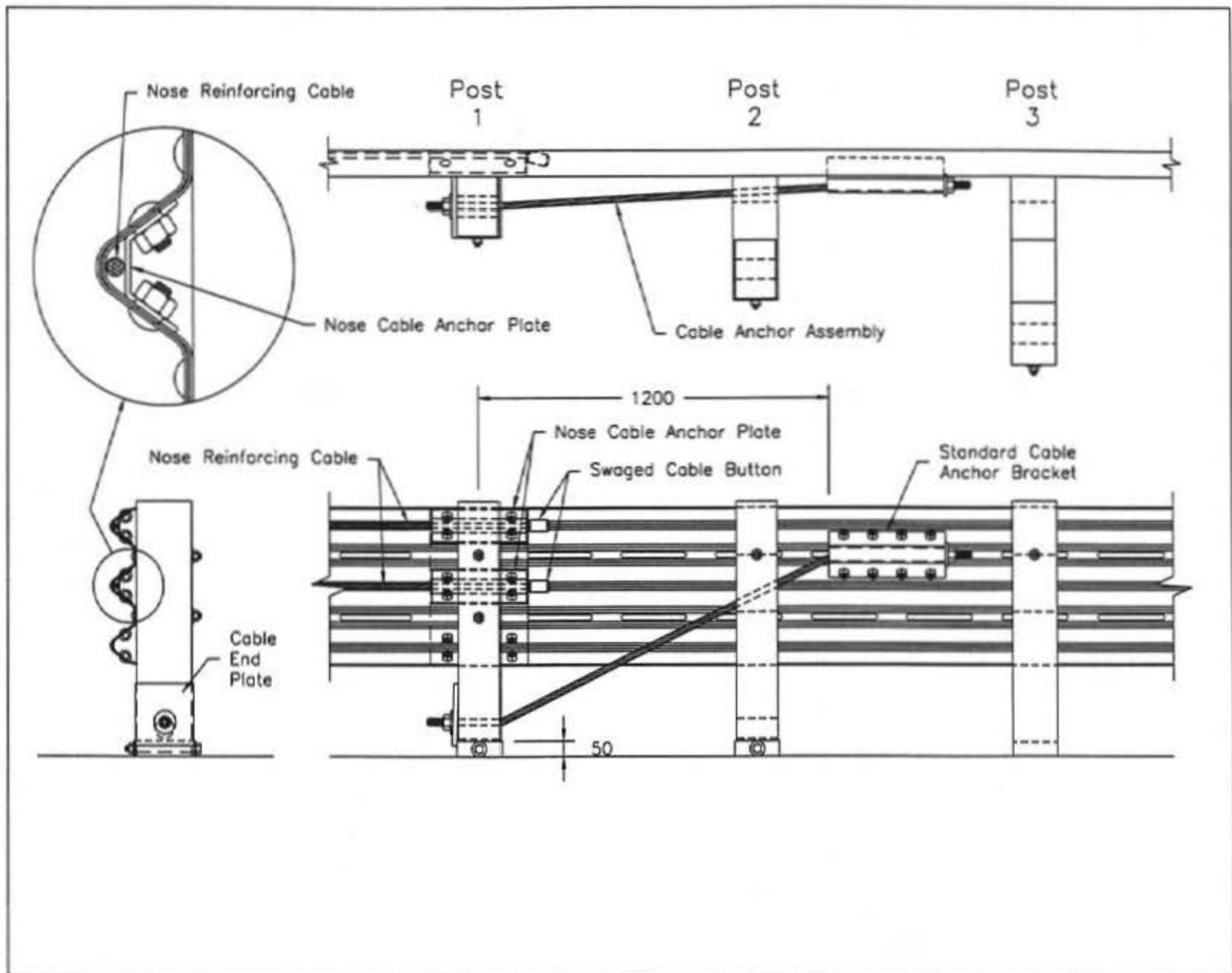
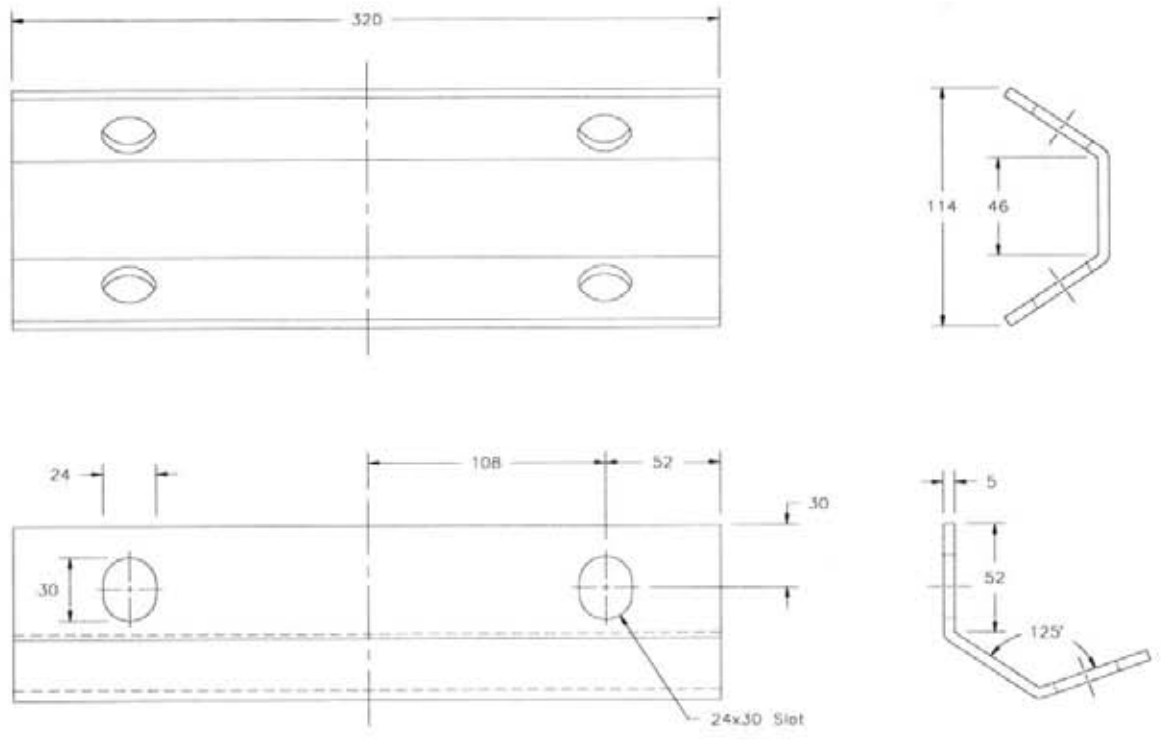
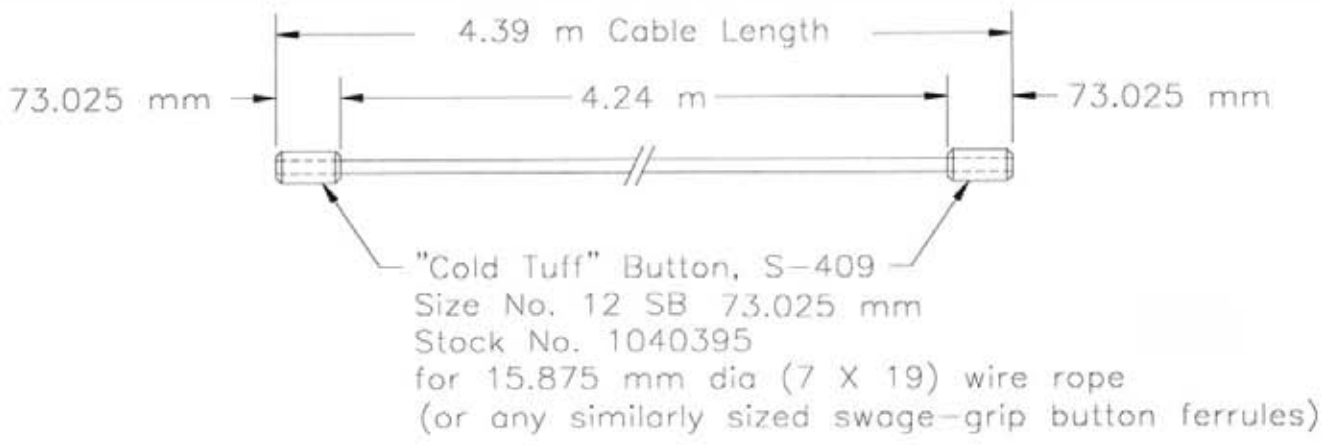


Figure G-7. Bullnose Cable Assembly



Steel Plate, A306
 320mm x 150mm x 5mm

Figure G-8. Cable Detail and Cable Plate

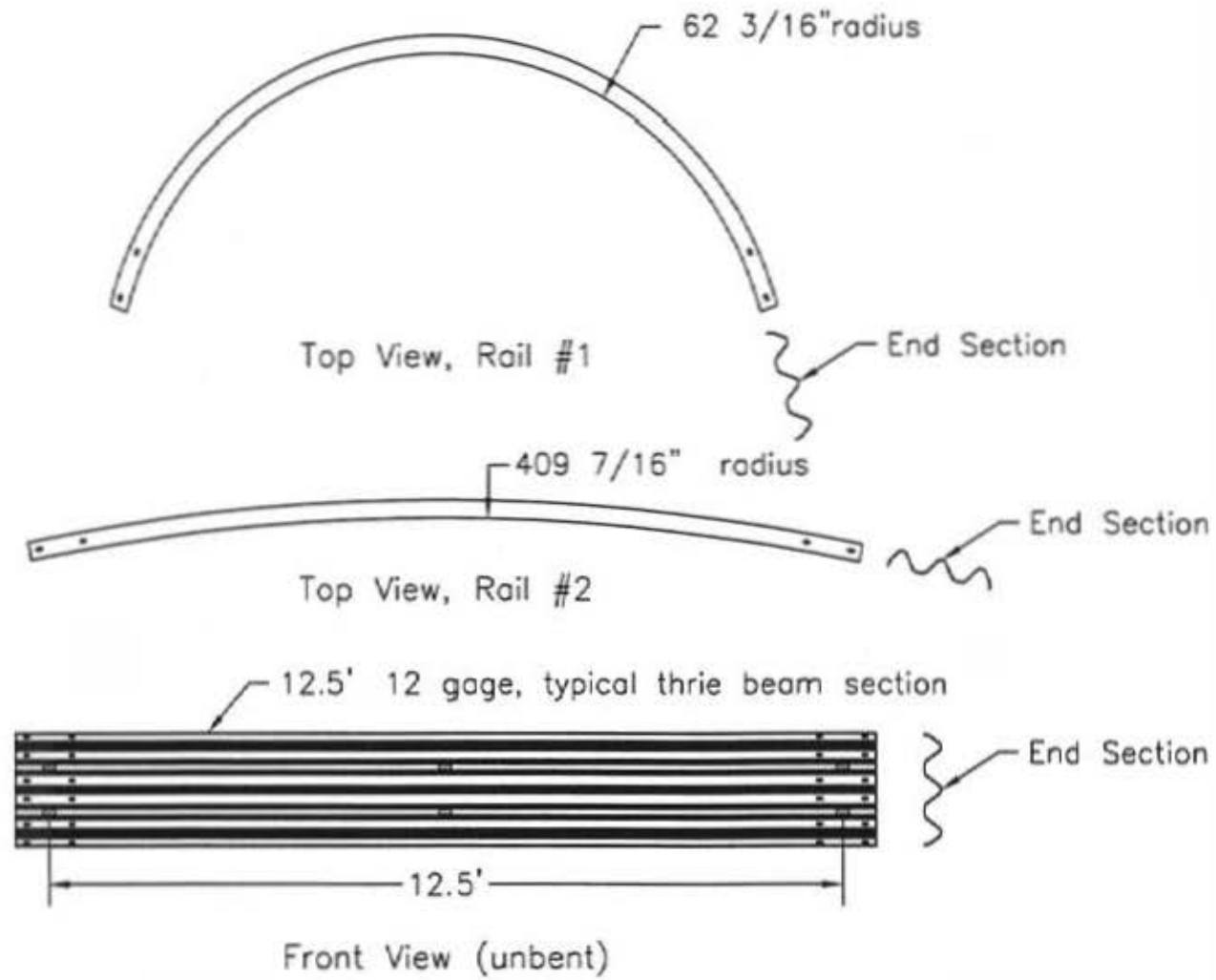


Figure G-10. Layout of Bullnose Rails No. 1 and 2, English Units

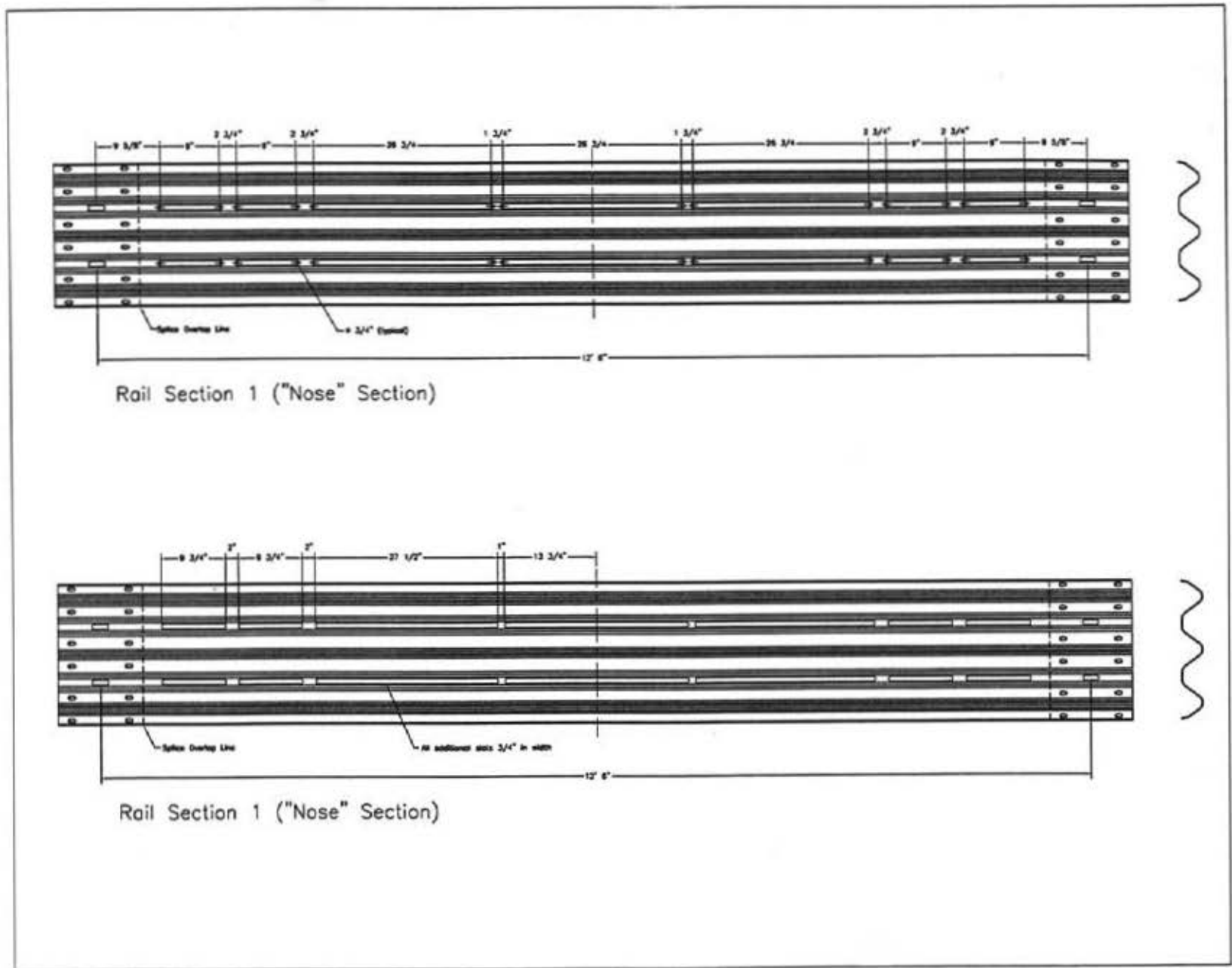


Figure G-1. Rail Section No. 1 Detail, English Units

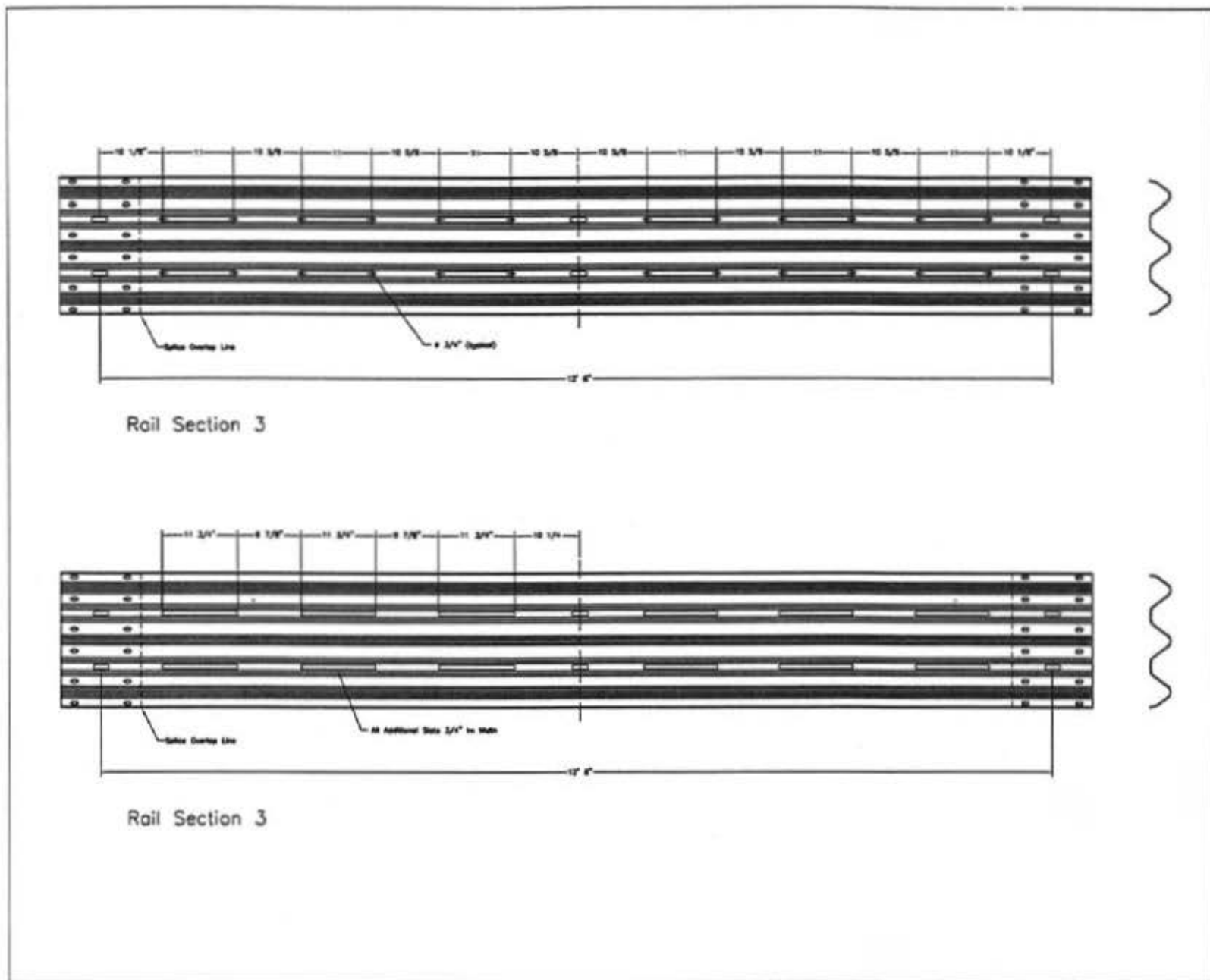


Figure G-13. Rail Section No. 3 Detail, English Units

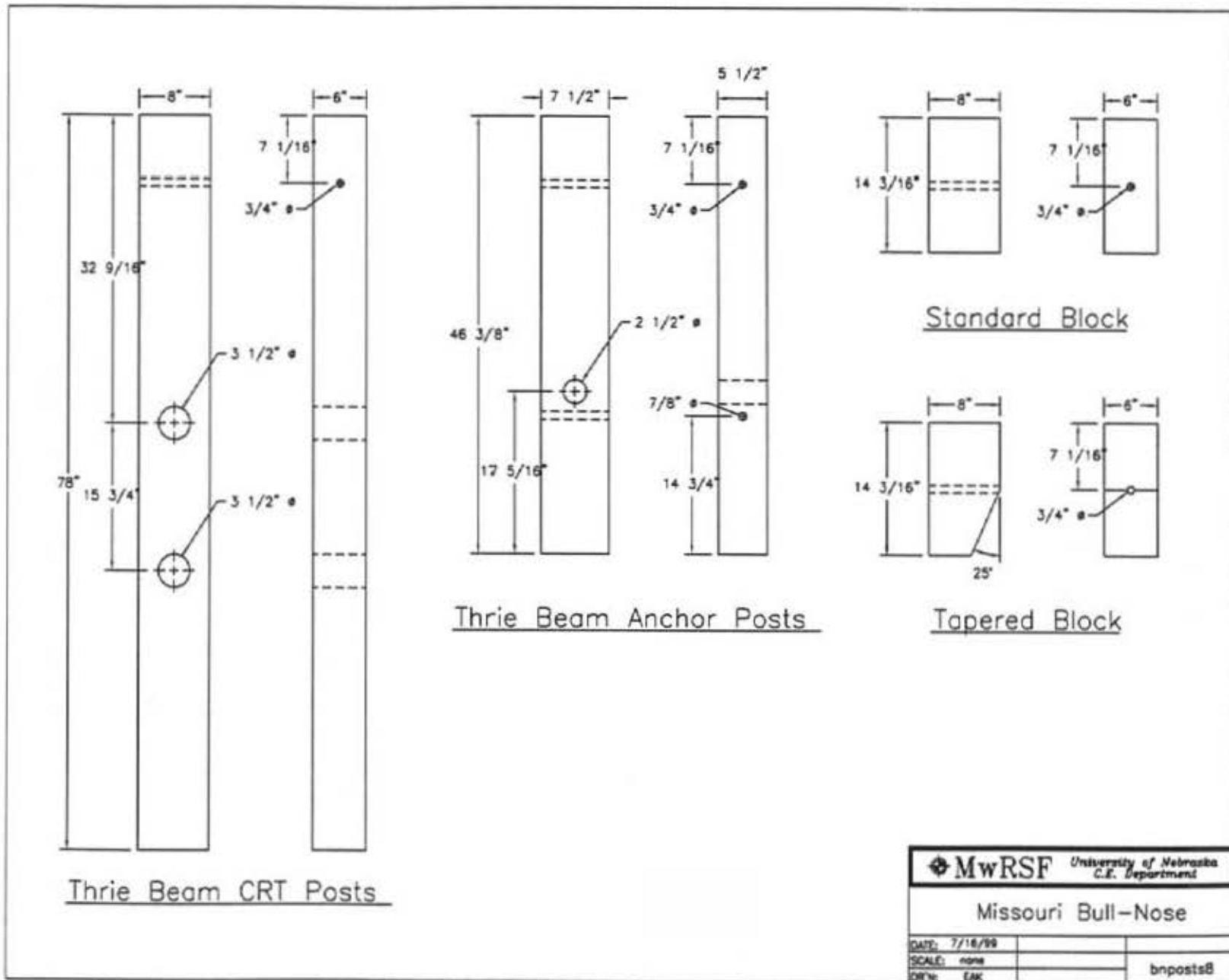


Figure G-14. Post Details, English Units

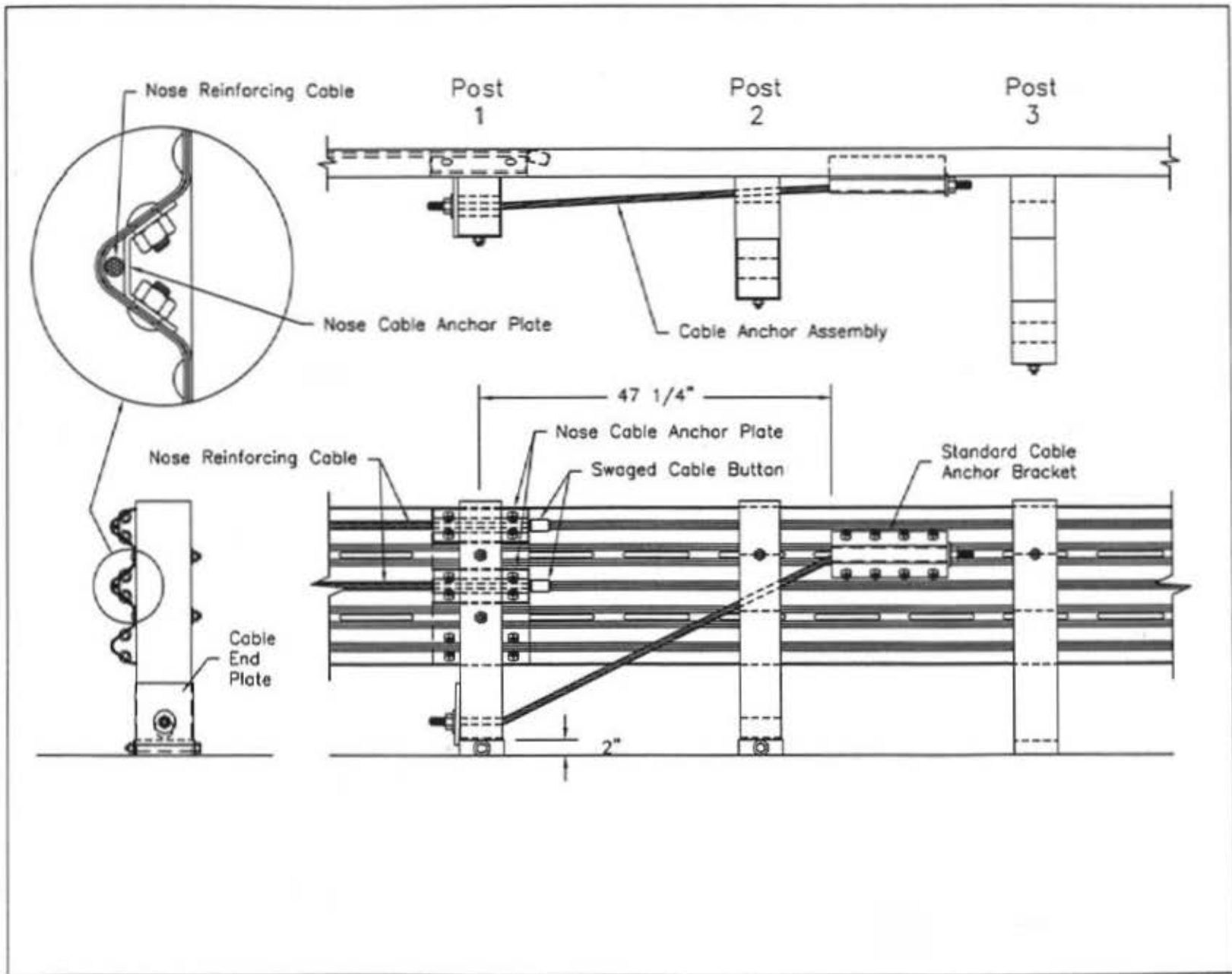


Figure G-15. Bullnose Cable Assembly, English Units

APPENDIX H

BULLNOSE MEDIAN BARRIER DESIGN NO. 2 DETAILS

Figure H-1. Bullnose Design No. 2

Figure H-2. Rail Section No. 1, Bullnose Design No. 2

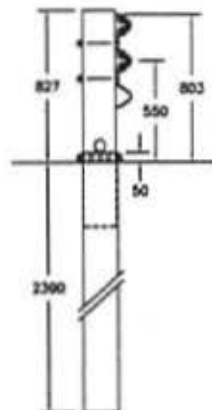
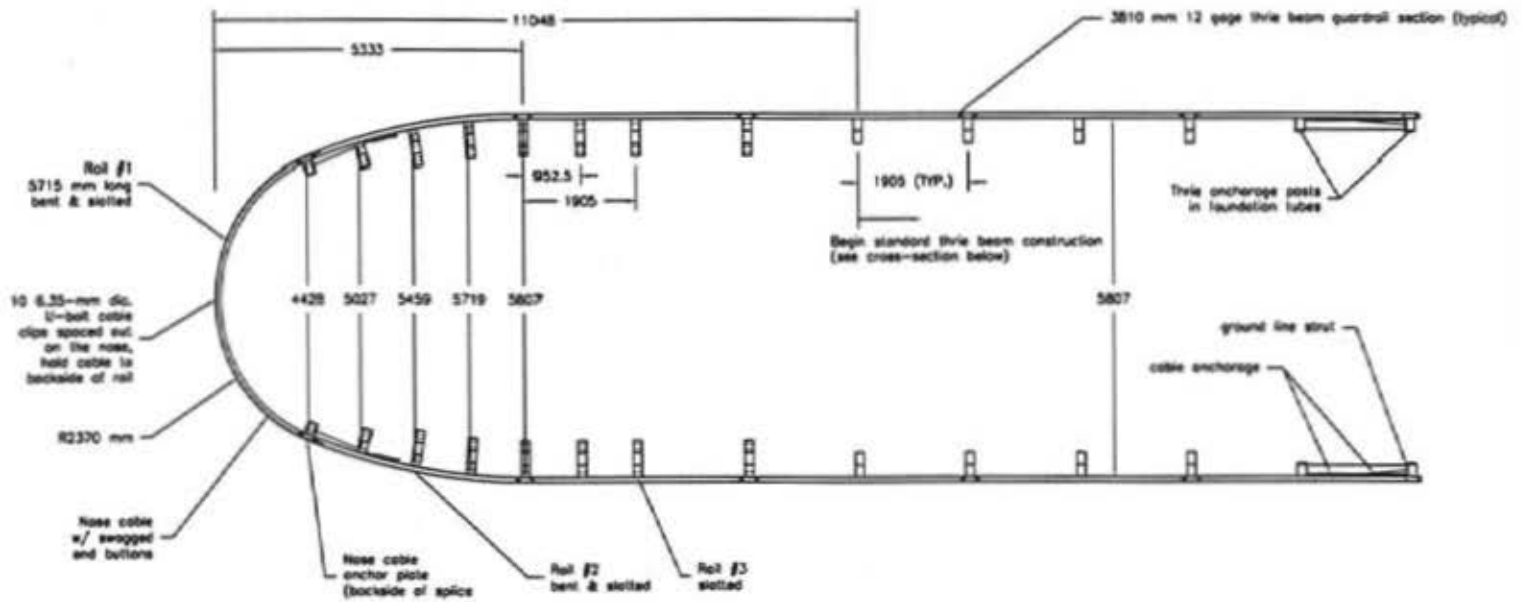
Figure H-3. Nose Cable, Bullnose Design No. 2

Figure H-4. Bullnose Design No. 2, English Units

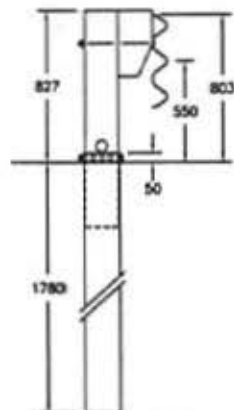
Figure H-5. Rail Section No. 1, Bullnose Design No. 2, English Units

Figure H-6. Nose Cable, Bullnose Design No. 2, English Units

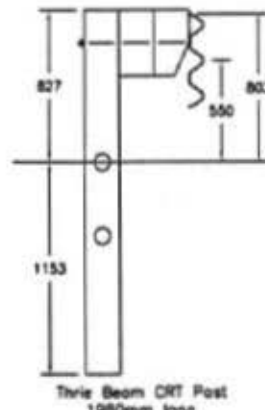
Widened Bullnose Median Barrier Design No. 2
 Rail Section No. 1 = 5715 mm long



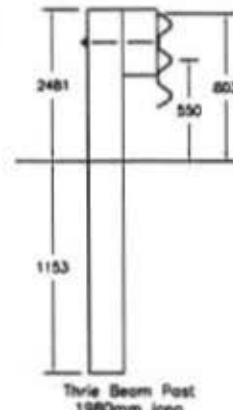
Thrie Beam BCT Post
 w/ 2440mm
 Foundation Tube
 Post 1



Thrie Beam BCT Post
 w/ 1830mm Foundation Tube
 & 360mm Tapered Block
 Post 2



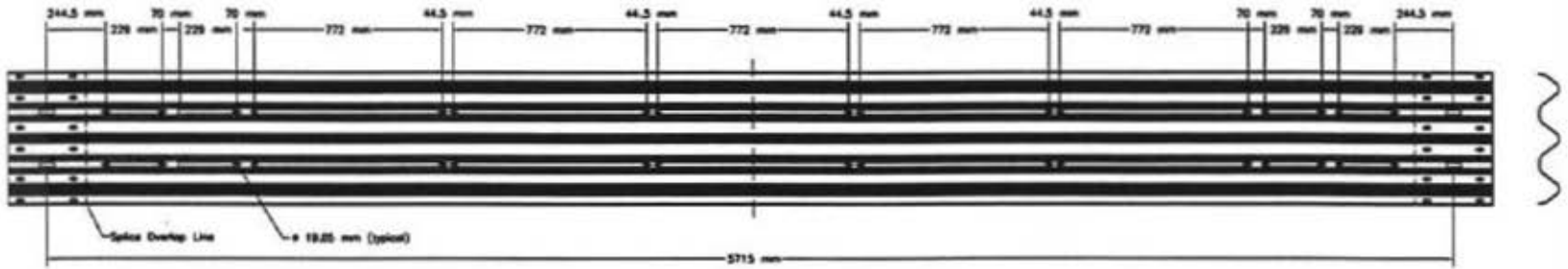
Thrie Beam CRT Post
 1980mm long
 w/ 360mm Block &
 360mm Tapered Block
 Posts 3,4,5,6,7,8



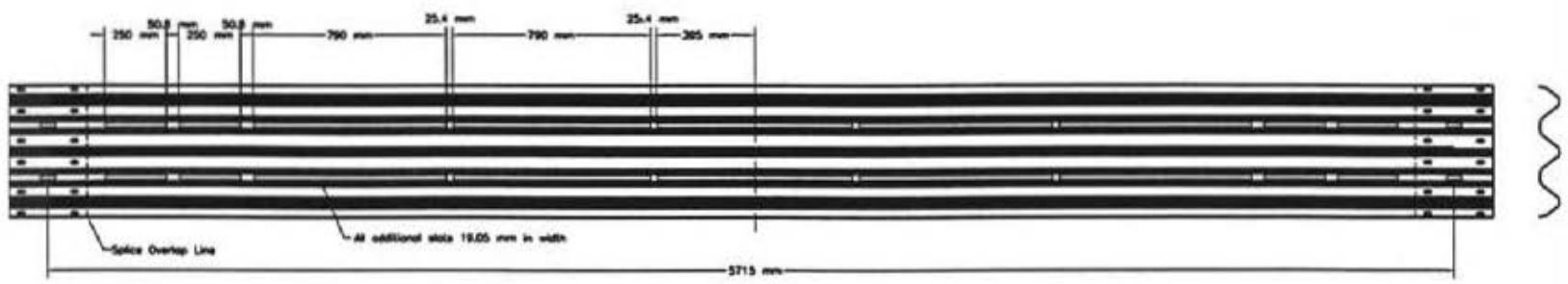
Thrie Beam Post
 1980mm long
 w/ 360mm Block
 Posts 9,10,11,12

Note: All units are mm unless otherwise indicated.

Figure H-1. Bullnose Design No. 2



Rail Section 1 ("Nose" Section)



Rail Section 1 ("Nose" Section)

Figure H-2. Rail Section No. 1, Bullnose Design No. 2

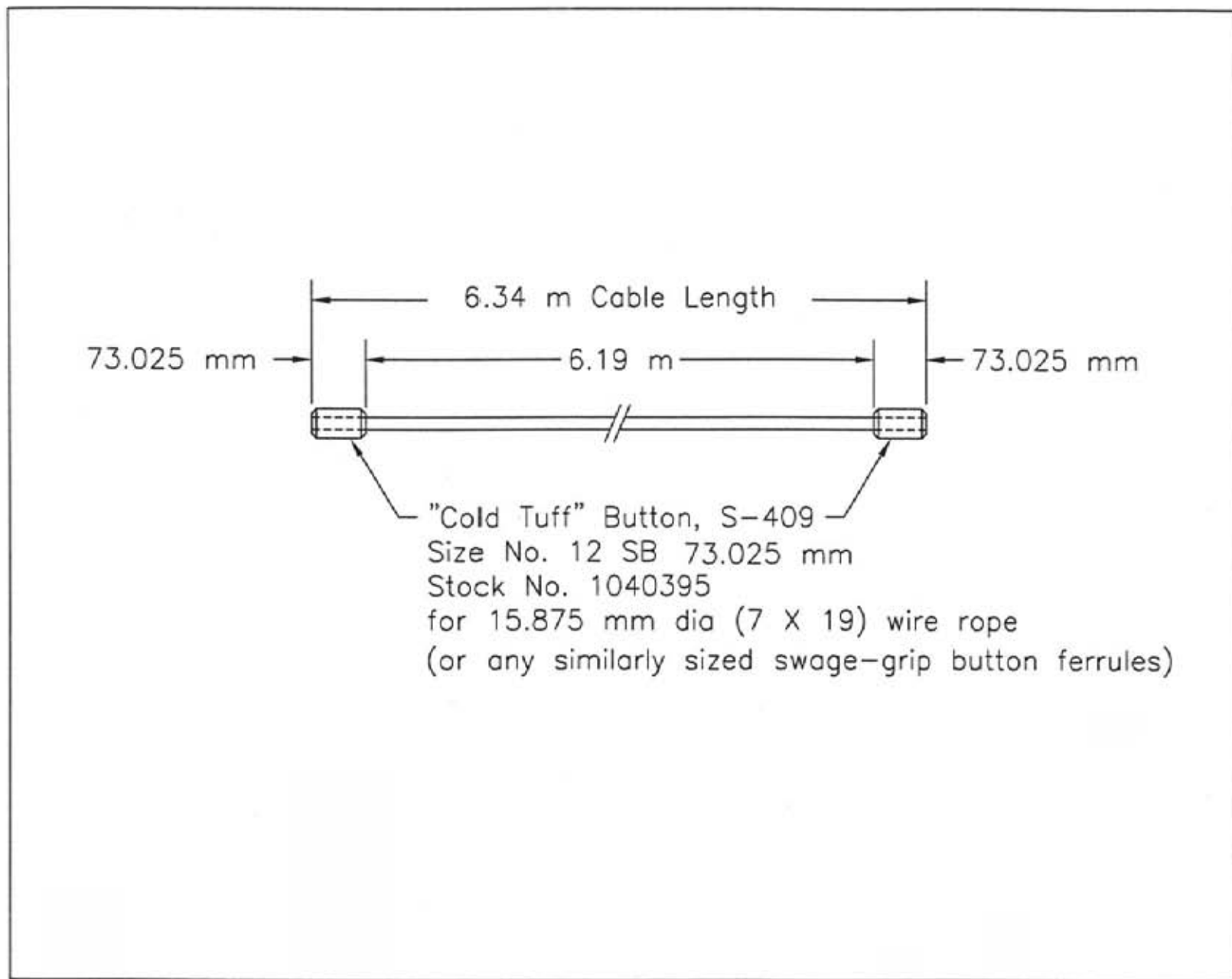


Figure H-3. Nose Cable, Bullnose Design No. 2

Widened Bullnose Median Barrier Design No. 2
 Roll Section No. 1 = 18' 9" long

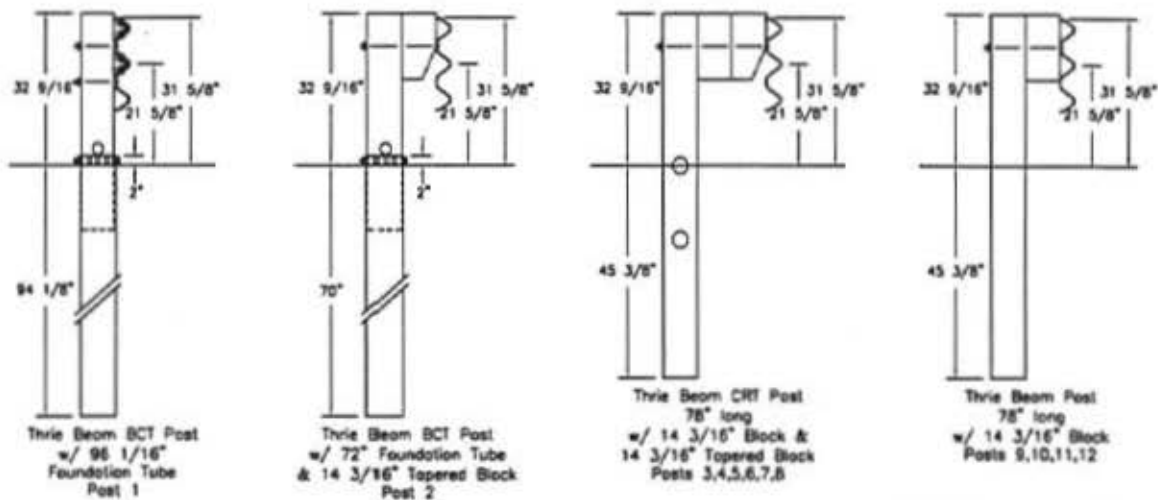
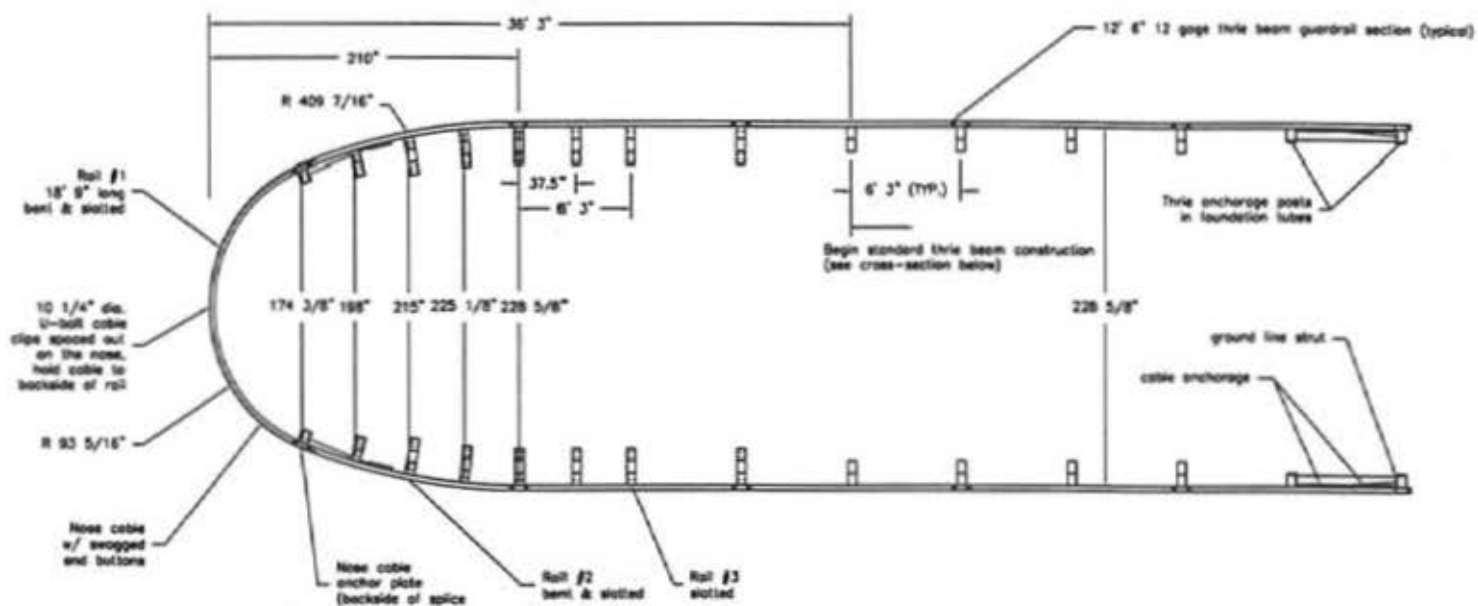


Figure H-4. Bullnose Design No. 2, English Units

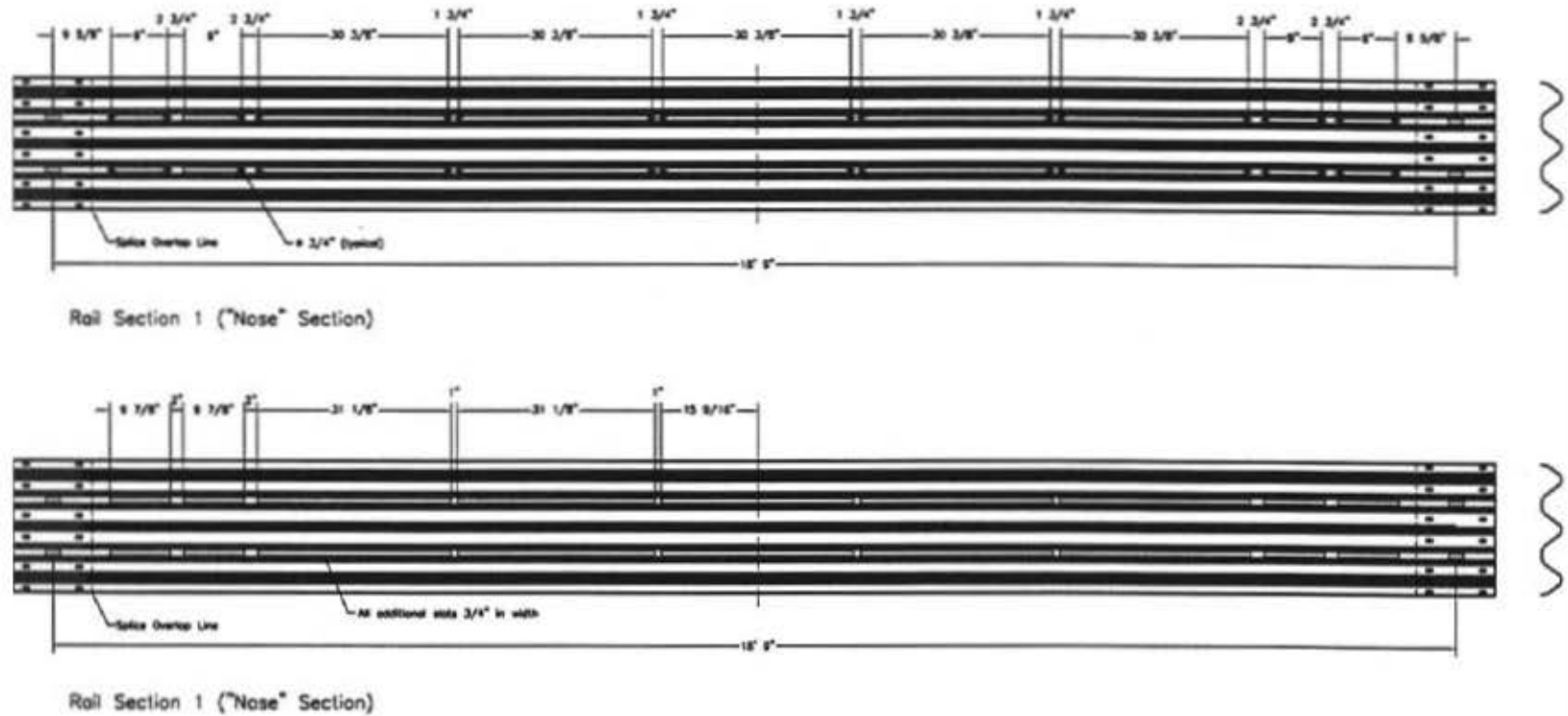


Figure H-5. Rail Section No. 1, Bullnose Design No. 2, English Units

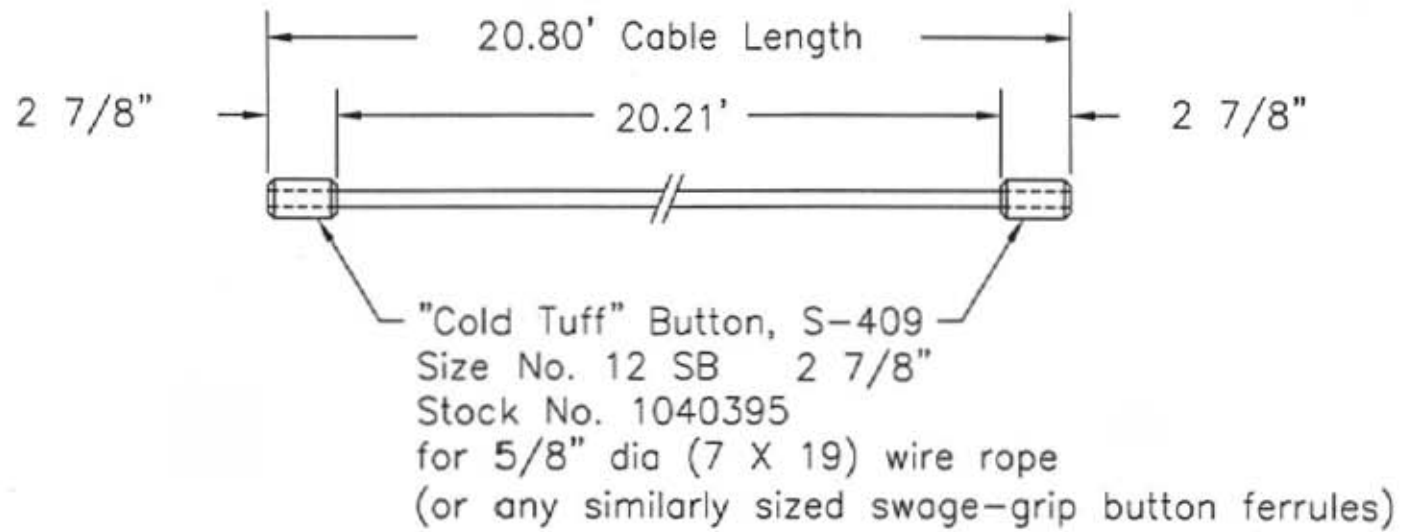


Figure H-6. Nose Cable, Bullnose Design No. 2, English Units

APPENDIX I

BULLNOSE MEDIAN BARRIER DESIGN NO. 3 DETAILS

Figure I-1. Bullnose Design No. 3

Figure I-2. Rail Section No. 1, Bullnose Design No. 3

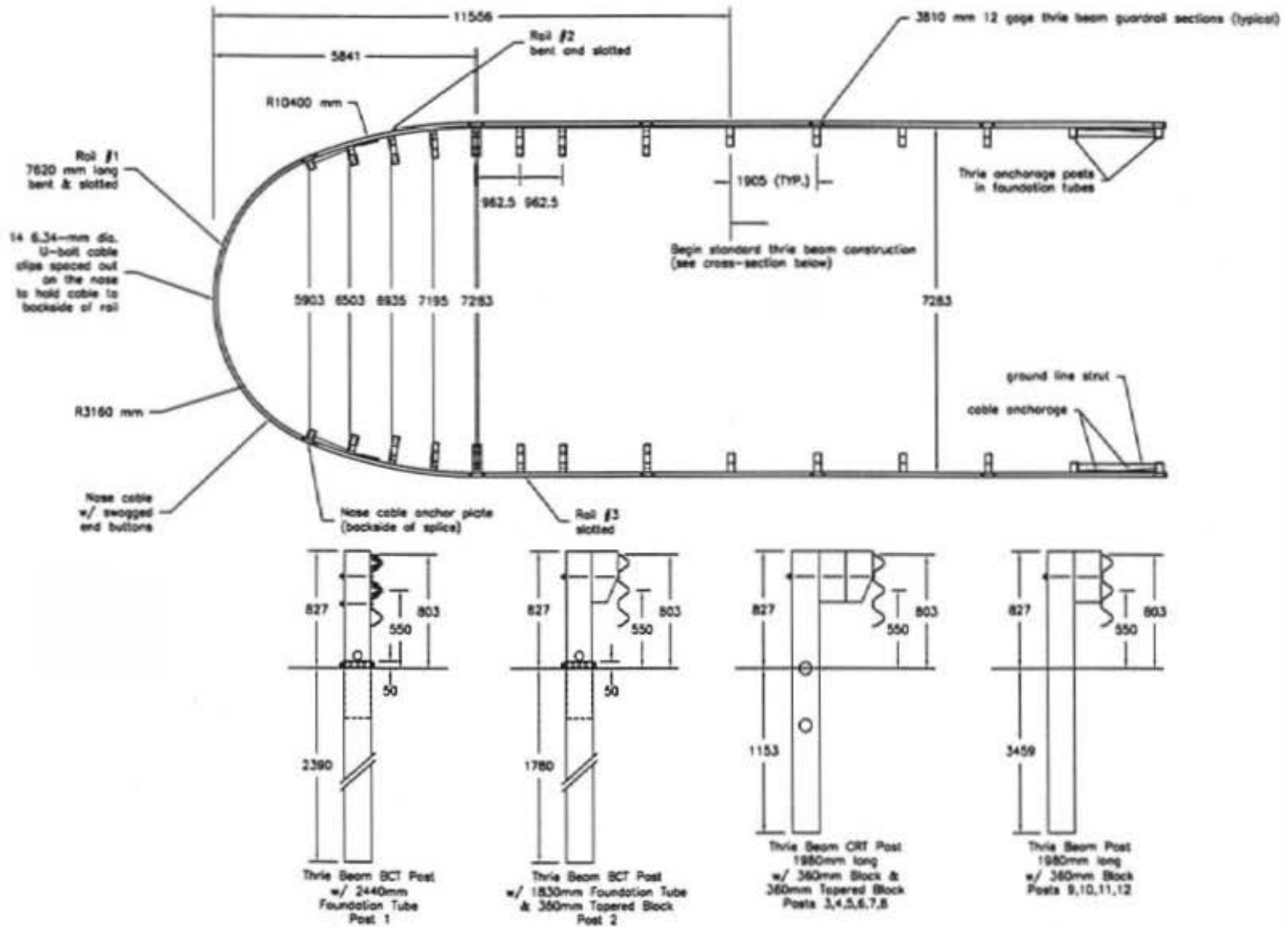
Figure I-3. Nose Cable, Bullnose Design No. 3

Figure I-4. Bullnose Design No. 3, English Units

Figure I-5. Rail Section No. 1, Bullnose Design No. 3, English Units

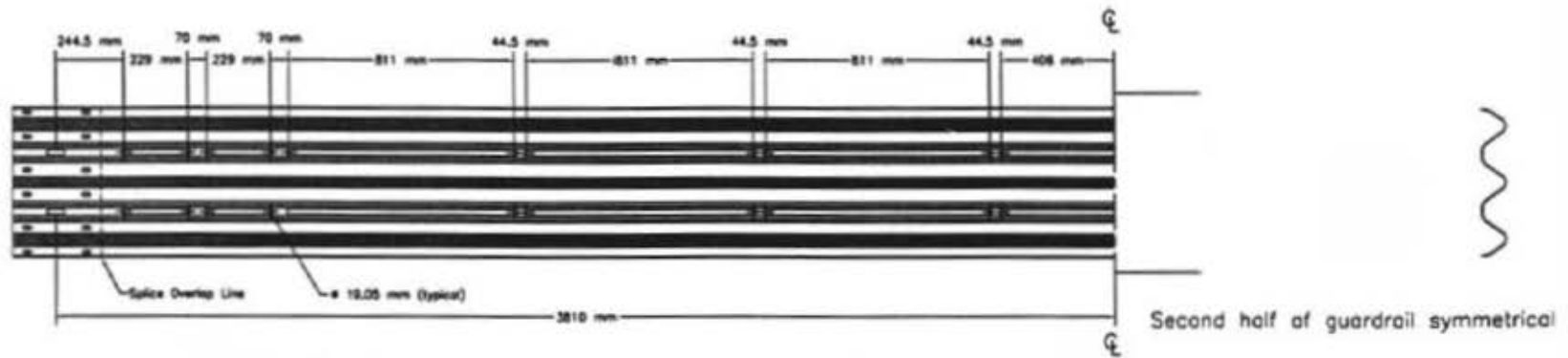
Figure I-6. Nose Cable, Bullnose Design No. 3, English Units

Widened Bullnose Median Barrier Design No. 3
 Rail Section No.1 = 7620 mm long

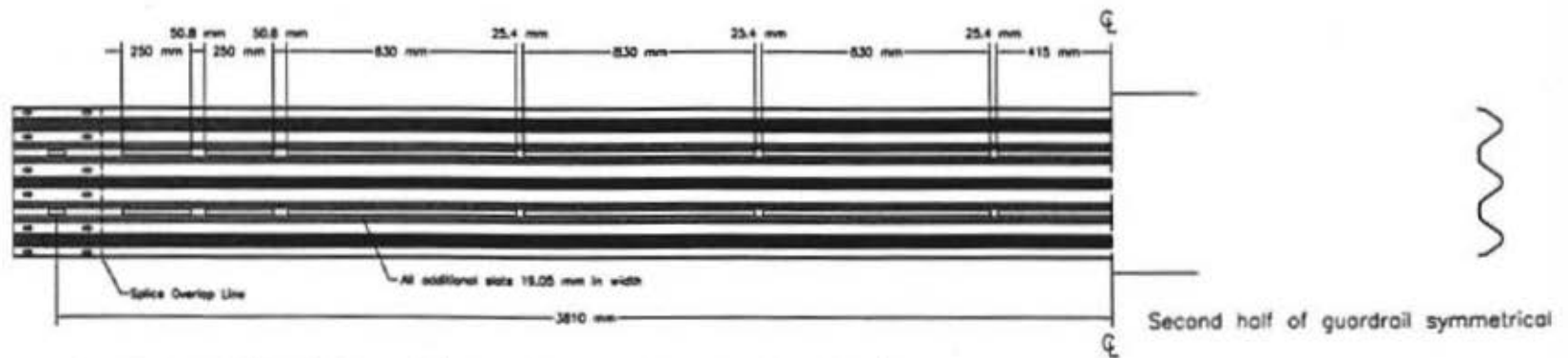


Note : All units are mm unless otherwise indicated

Figure I-1. Bullnose Design No. 3



Rail Section 1 ("Nose" Section) (only half shown, total length 7620mm)



Rail Section 1 ("Nose" Section) (only half shown, total length 7620 mm)

Figure I-2. Rail Section No. 1, Bullnose Design No. 3

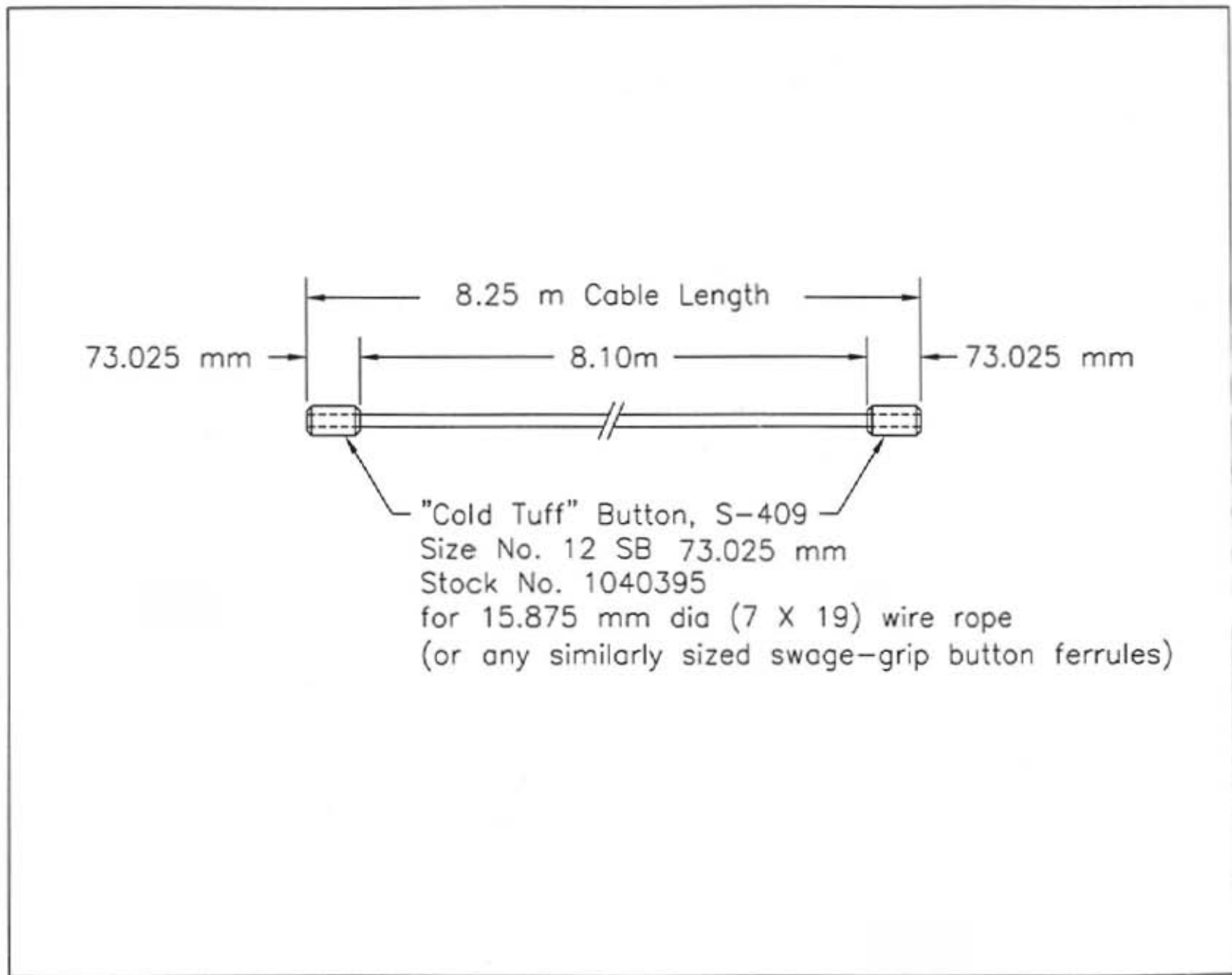


Figure I-3. Nose Cable, Bullnose Design No. 3

Widened Bullnose Median Barrier Design No. 3
 Rail Section No.1 = 25' long

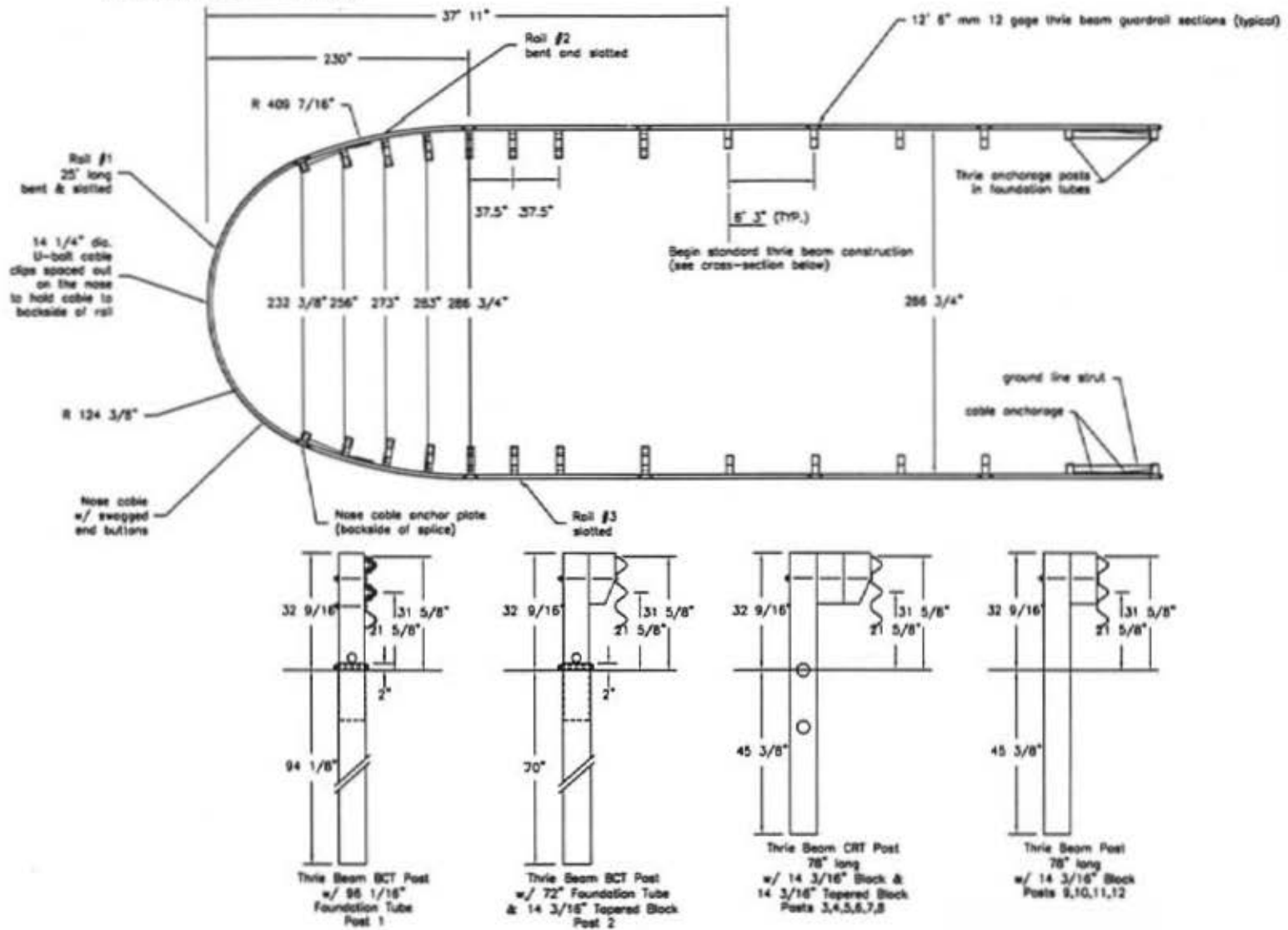
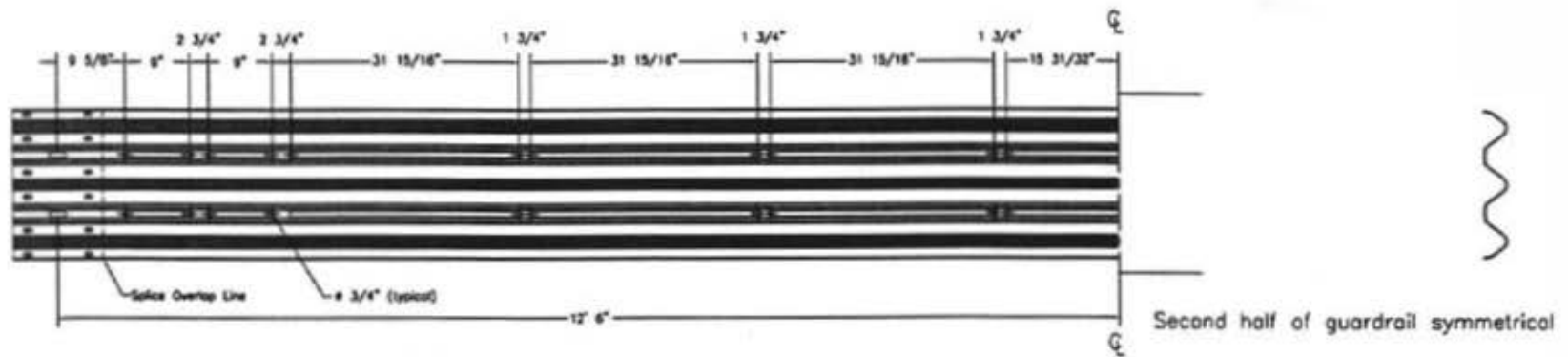
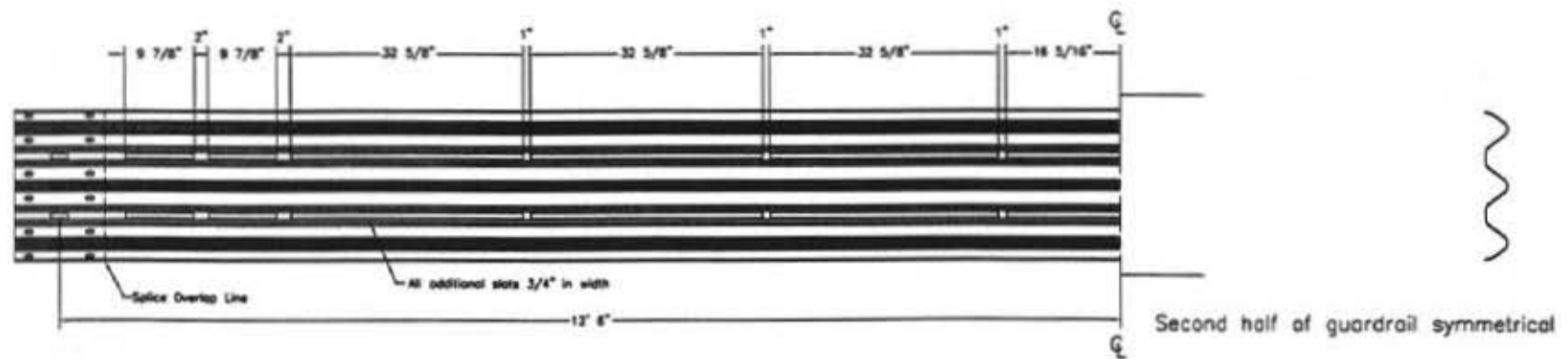


Figure I-4. Bullnose Design No. 3, English Units



Rail Section 1 ("Nose" Section) (only half shown, total length 7620mm)



Rail Section 1 ("Nose" Section) (only half shown, total length 25')

Figure I-5. Rail Section No. 1, Bullnose Design No. 3, English Units

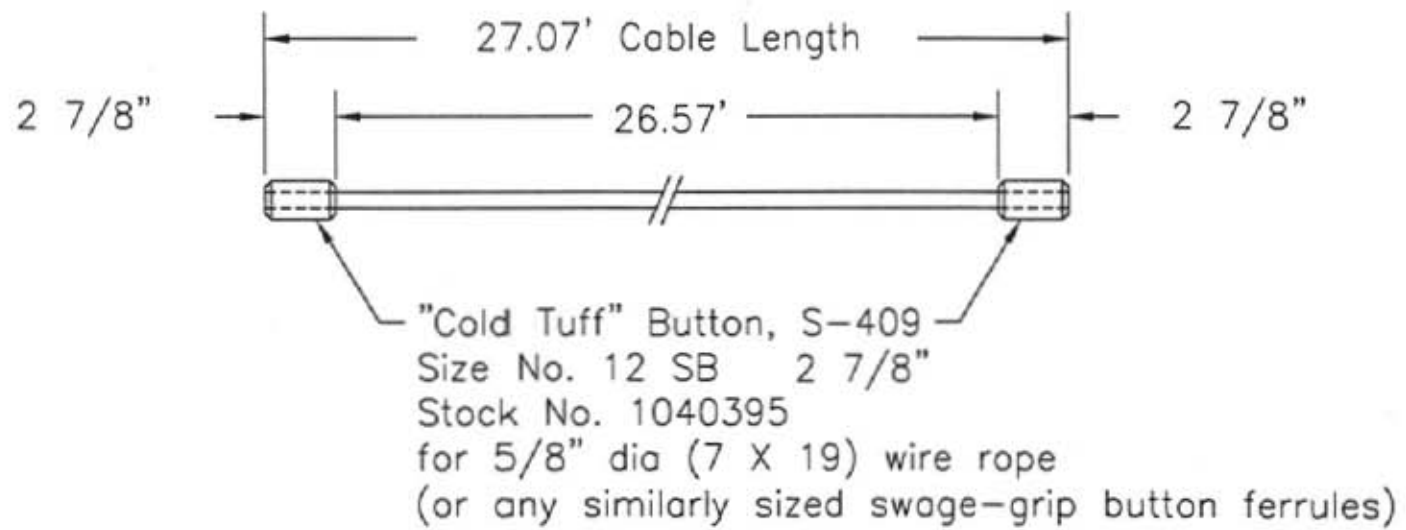


Figure I-6. Nose Cable, Bullnose Design No. 3, English Units